SORPTION KINETICS OF Co, Sr, Ru AND Cs IN FRESHWATER SYSTEMS

A thesis submitted to the University of Manchester

for the degree of Ph.D. in the Faculty of Science, 1997

Deborah Joy Bunker

Department of Chemistry

ProQuest LLC.
789 East Eisenhower Parkway
P.O. Box 1346
Ann Arbor, MI 48106 – 1346

CONTENTS

List of figures presented in this thesis

List of tables presented in this thesis

Abstract

Samples of sediment and water were collected from two freshwater sites; Botany Pond in Dorset and Esthwaite Water in Cumbria. Using the batch method, the adsorption behaviour of four radionuclides - ^{57}Co, ^{85}Sr, ^{103}Ru and ^{134}Cs - was studied as a function of time in these systems using adsorption times ranging from 0.5-1700 hours. Different behaviour was observed for the radionuclides in each freshwater system, reflecting a dependence upon solid and solution composition. Unexpected trends which were sometimes observed at longer contact times, in which sorption was greatly reduced, were ascribed to biological activity in the samples. Adsorption data were then used to test the applicability of a kinetic box model to describe sorption in these systems. Generally, a 2-box model was needed in order to describe radionuclide sorption adequately and the appropriate rate and equilibrium constants were obtained.

Desorption behaviour was studied using several techniques. Complete exchangeability was only observed for ^{85}Sr. Sequential extraction experiments provided additional information concerning the distribution and extractability of the four radionuclides in each system. Following an increase in adsorption time, these experiments revealed a redistribution and an increasing degree of fixation for all four radionuclides in both systems.

Declaration

No portion of the work referred to in this thesis has been submitted in support of an application for another degree or qualification of this or any other university or other institute of learning.

Copyright

For my parents and grandparents.

Acknowledgements

I would like to thank the following people for their help throughout the course of this work.

My supervisors, Francis Livens and John Hilton, for their continual advice and encouragement.

The staff at IFE (Windermere and Wareham) for taking the time to help me on my numerous visits. Particularly;

Liam Nolan (IFE Windermere) for his assistance with fieldwork and Jim Smith (IFE Wareham) for his help with the modelling work.

The NERC Institute of Freshwater Ecology for financial support of this project.

The Manchester Radiochemistry Research Group members (past and present); Alex, Nick, Rick, Anna, Kath, Jane, Leigh, Paul, Ying-Jie, Tahera, Ben, Jun, Lesley and Miranda.

And last, but by no means least, my mum, dad and sister, Suzanne.

The Author

The Author graduated from the University of Manchester in 1993 with an upper second class honours degree in Chemistry. Between 1993 and 1996, she has been a member of the Radiochemistry Group at the University of Manchester. Under the joint supervision of Francis Livens and John Hilton (IFE), she has carried out research in the field of Environmental Radiochemistry. She is currently working in the aromachemicals industry.

"Science is a first-rate piece of furniture for a man's upper-chamber, if he has common-sense on the ground floor." Oliver Wendell Holmes (The Poet at the Breakfast Table, 1871).

CHAPTER 1 - INTRODUCTION

CHAPTER 1 - INTRODUCTION

1.1 Introduction

The release of radionuclides into the environment inevitably leads to concerns for public health. These concerns highlight the importance of improving our understanding of the environmental behaviour and eventual fate of such radionuclides. Radionuclides can be present in the environment as part of naturally occurring processes or they can enter the environment as a result of atomic bomb tests and also from the release of material from sites such as nuclear reactors and hospitals. These releases can be controlled, such as the regular discharges from the plant at Sellafield, Cumbria, to the Irish Sea, or accidental, such as the nuclear accident which occurred at Chernobyl in 1986 (Santschi and Honeyman, 1989).

The behaviour of radionuclides in the aquatic environment is of particular interest because of the importance of water. Not only is water crucial to all life forms but it is also important in moving and distributing elements on Earth. On entering the aquatic environment, the radionuclide may remain in solution and be transported throughout the water column or it may become fixed by sorbing to particulate matter or bottom sediments, thus removing it from the water column and reducing its mobility. Sorption to, or the formation of, colloids will also reduce the mobility of the radionuclide within the environment.

The ability of radionuclides to sorb to a solid phase has been the subject of much study (e.g. Nishita et al, 1956; Abdel Gawad et al, 1977; Li et al, 1984; Berry et al, 1988; Robbins et al, 1992) and the ability of certain mineralogical components present

in the solid phase to retain particular radionuclides has been identified. For example, a positive correlation has been found between the hydrous Mn oxide content in the solid phase and the amount of ^{60}Co sorbed (Means et al, 1978a), and micaceous clays, such as illite, are known to retain radiocaesium effectively for long periods of time (Sawhney, 1972; Comans et al, 1991). The role that individual components play in sorption is therefore important and information acquired in studies of this kind allows both the mechanism of sorption to be examined in more detail and also the importance of the role played by different mineralogical phases in the sorption of particular radionuclides to be assessed. It also means that some predictions about radionuclide behaviour and reactivity in a freshwater system can be made, given mineralogical information about the freshwater sediment. However, although some quantitative relationships can be observed, e.g. the % illite in sediment correlates with the % Cs sorbed (Aston and Duursma, 1973), due to the complex nature of a bulk sediment and the interactions which occur between different mineralogical phases, sorption data obtained from individual mineralogical components cannot be extrapolated to predict accurately the behaviour of the bulk sediment (Torstenfelt et al, 1982; Ohnuki, 1994). Hence it is still important to continue to study and compare the sorption of radionuclides on to different bulk sediments in addition to investigating individual mineralogical phase - radionuclide interactions.

Other physical and chemical parameters, in addition to the composition of the solid phase, are also important in controlling radionuclide sorption. These include solution composition, temperature, pH, redox potential and the length of adsorption time (Elprince et al, 1977; Torstenfelt et al, 1982; Benes et al, 1989; Cornell, 1993). It is often difficult to study sorption behaviour in field situations however, particularly in freshwater systems, because of the imperfect mixing of the reacting species, the

impossibility of controlling biological behaviour and also because the system is continually undergoing both mechanical and thermal disturbances. It is therefore more practical to use laboratory studies as conditions within the system can be controlled more precisely. These studies can then be used to provide useful and informative indications of likely sorption behaviour when applied to similar conditions in the field.

1.2 Project outline

Using laboratory experiments, this project investigates the sorption kinetics (short-term and long-term) of four radionuclides - ^{57}Co, ^{85}Sr, ^{103}Ru and ^{134}Cs - in two freshwater systems. These elements were chosen because they each have radioisotopes which may represent serious hazards to the environment if released, and also because each radionuclide displays very different sorption behaviour. The freshwater systems studied were chosen because of their different sediment and water chemistries, and sediment and water from both systems were also mixed to allow further comparisons to be made. Adsorption reactions were studied in each system, and these provided data which were then used in a kinetic box model to determine whether this model could be used successfully to predict radionuclide behaviour in certain freshwater systems, and if so, to obtain sorption rates. Desorption reactions were also studied, using a variety of approaches, to determine the degree of radionuclide fixation within each system.

1.3 Thesis presentation

Before any interpretation of the experimental data can occur, it is necessary to understand the sorption process, and also the chemical and environmental properties

of the four radionuclides being studied. Chapter 1 contains this background information, providing an introduction to the work which has been carried out during the project. Chapter 2 provides details of the two field sites and results of the characterisation of the sediments and lake waters are presented.

The adsorption studies are presented in Chapter 3. Details of the adsorption experiments are given and the results are presented and discussed. Similarly, desorption studies are presented in Chapter 4. Due to the large volume of data and the limitations of time and space, the results from both the adsorption and desorption experiments have been discussed by isotope, and the emphasis has been on providing an inter-sediment comparison (as this was one of the primary objectives of the project). However, a brief inter-element discussion has also been included at the end of each chapter, together with a short summary listing the main points. The data from Chapter 3 have been used in a kinetic box model, and a discussion of this model and presentation of these results is given in Chapter 5.

Conclusions from the project and a brief discussion of the possible future work which has arisen from these studies is contained in Chapter 6. References are provided in full at the end of the thesis and all raw data reported in Chapters 3 and 4 are listed in the Appendices.

1.4 The sorption process

Sorption is the general term used to describe the fixation of a radionuclide to a sediment or any solid phase. More specifically, sorption occurs via either adsorption or absorption although it is often not possible or necessary to distinguish between the

two.

The term absorption is used when the chemical species moves from the solution and actually penetrates into the structure of the solid phase, thereby causing the structure of the solid to become altered. The process of adsorption however (the opposite of which is desorption), involves transfer of the chemical species from the solution phase to the surface of the solid phase, but as no penetration of the solid occurs the structure of the bulk solid is left unaltered (Greenland and Hayes, 1981).

There are two different types of adsorption: adsorption which involves a chemical interaction (called chemisorption), and adsorption in which only a physical interaction is involved (called physisorption). Chemisorption often needs an activation energy in order to proceed and strong bonds, covalent or ionic, are formed between the surface of the solid and the sorbed species. Very often, distinct chemical compounds are then formed which can make desorption difficult unless a sufficient energy input occurs. Physisorption, however, does not need an activation energy to proceed. It is fast, and although strong chemical bonds are not formed between the surface of the solid and the sorbing species, weaker interactions such as hydrogen bonding and Van der Waal's forces can occur, which cause changes in the electronic configuration of the sorbing species (Greenland and Hayes, 1981).

1.5 Methods of sorption

The mechanism by which sorption proceeds will depend on the nature of the radionuclide being studied and the environmental conditions, such as pH, Eh, sediment and solution composition. This section describes the different mechanisms which can

occur, and a schematic representation of these mechanisms is shown in Figure 1.1.

1.5.1 Cation exchange

Probably the simplest type of reaction, cation exchange involves the replacement of a cation at the surface of the mineral, with a cation of like charge from the solution. Divalent cations should compete more strongly in ion exchange than monovalent cations. Although all of the mineralogical components of a sediment will participate in cation exchange, the extent and quality of the contribution made by each component to the cation exchange capacity will vary. In addition to the mineralogical phases present in the sediment, the cation exchange process is also dependent upon pH and the ionic strength of the solution. A higher ionic strength means that there is a greater concentration of potentially competing cations in solution.

The various mineralogical phases in a sediment which can contribute to the overall cation exchange capacity can be classified as inorganic, organic or a mixture of both inorganic and organic material (Greenland and Hayes, 1981).

(i) Inorganic

Inorganic materials include hydrous metal oxide phases, such as Fe, Al, Si, Ti and Mn oxides, and clay minerals, which are produced as a result of weathering processes. Both of these play an important role in ion exchange reactions.

Hydrous metal oxides are solids which consist of a metal cation combined with water, hydrogen and oxygen. Iron and manganese oxides are particularly recognised for

Figure 1.1 Schematic representation of retardation mechanisms (McKinley and Alexander, 1992)

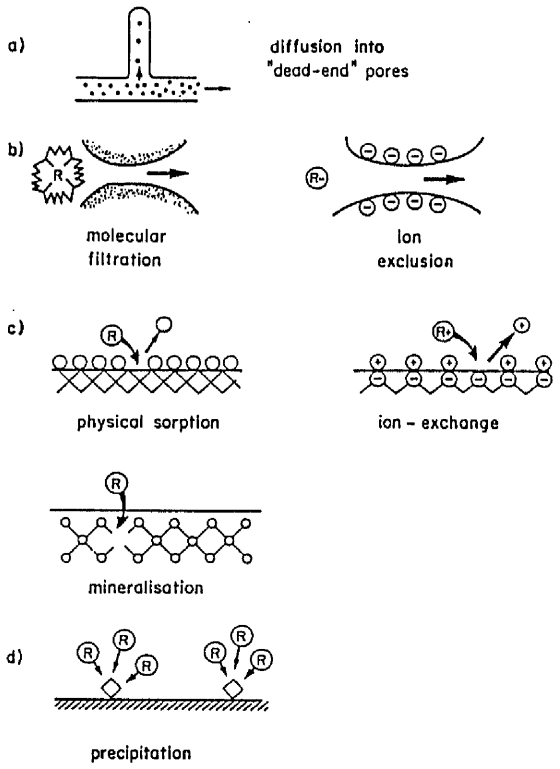

playing an important part in controlling trace element cycling (Krauskopf, 1956; Jenne, 1968; Erel et al, 1991) and the sorption of radionuclides (Means et al, 1978a). In addition to their high natural abundance, their role in sorption is ascribed to their unusually high negative surface charge and cation exchange capacity over the pH range of most natural waters (Means et al, 1978a). These properties are dependent upon both pH and redox conditions however, and Mn oxide solubility has been found to be greatest at low pH and/or low Eh (Crerar et al, 1972). Acidic, anaerobic and also high carbonate conditions (high carbonate content together with low Eh may induce Mn oxide conversion to rhodochrosite) must therefore be avoided to ensure the stability of Mn oxides and the retention of sorbed trace elements.

The crystal structures of manganese (IV) oxides consist of edge-shared $[MnO_6]$ octahedra which are linked in varying degrees of complexity. Figure 1.2 shows a structural model of chalcophanite, which is a manganese (IV) oxide with a sheet structure. Chalcophanite consists of single layers of water molecules between layers of edge-shared $[MnO_6]$ octahedra. Zn^{2+} ions exist between the water layer and the oxygen atoms in the $[MnO_6]$ layer. Vacancies in the layer of $[MnO_6]$ octahedra occur so that six out of every seven octahedral sites are occupied by Mn atoms. Divalent cations in solution, such as Ni^{2+} and Cu^{2+}, can be adsorbed initially on to the surfaces of these particles close to these vacancies (Burns, 1976).

Clay minerals are the products of weathering processes and are significant components of most soils and sediments. Clays are extremely fine-grained and are best described as hydrous alumino-silicates, although many clay minerals contain other metals, such as Mg and Fe. All clay minerals consist of a combination of two types of layers or sheet structures - the octahedral layer and the tetrahedral layer (Krauskopf, 1979).

Figure 1.2 Chalcophanite crystal structure (Burns, 1976); (a) projection along b axis; (b) edge-shared [MnO_6] layer viewed normal to the basal plane

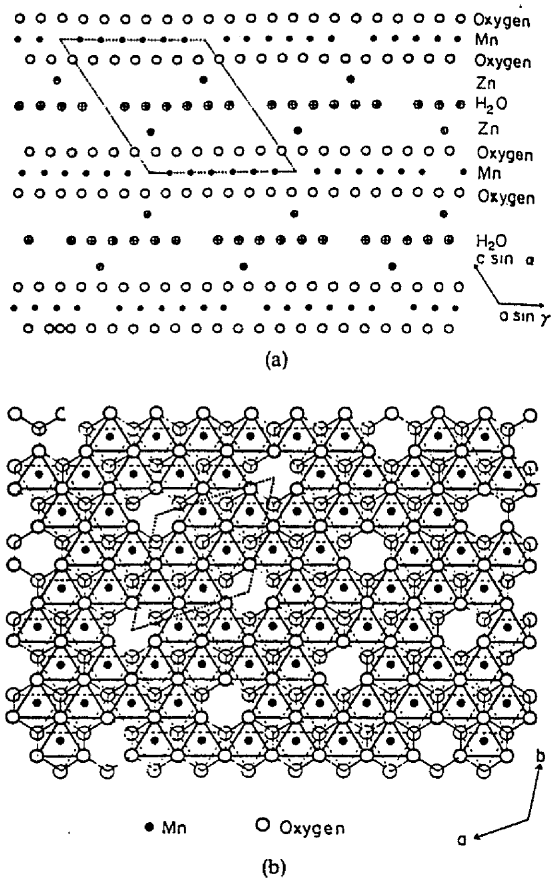

The octahedral sheet is made up of a gibbsite [$Al(OH)_6$] type structure, in which Al^{3+} is surrounded by O^{2-} and OH^- ions in an octahedron. The O^{2-} and OH^- ions are shared with the adjacent octahedra so that a continuous structure is formed. The tetrahedral sheet is the silica layer, with Si^{4+} in the centres of a tetrahedra of O^{2-} and OH^- ions. The oxygen ions at the bases of these tetrahedra are shared. The simplest combination of layers is to have a single octahedral sheet linked to a single tetrahedral sheet through the sharing of some oxygen ions and this is the structure of the clay kaolinite (a 1:1 structure). Clays such as montmorillonite, however, consist of an octahedral sheet sandwiched between two tetrahedral sheets (a 2:1 structure). Isomorphous substitution, in which the Al^{3+} and Si^{4+} ions are replaced by ions such as Mg^{2+} and Fe^{3+}, can occur in clay minerals. As the replacement ions have a lower charge, isomorphous substitution results in an overall negative charge in the clay. This can be reduced by either replacing O^{2-} with OH^- ions, by introducing excess cations into the octahedral layer or by the adsorption of cations on to the surfaces of individual layers, thereby giving rise to a cation exchange capacity. The ions on the surfaces are held loosely by the clay and are readily replaced by other cations.

Table 1.1 Comparison of cation exchange capacities

MINERAL	CEC ($mol_c kg^{-1}$)
kaolinite	0.01-0.1
chlorite	0.1-0.4
illite	0.2-0.4
montmorillonite	0.8-1.2
vermiculite	1.2-1.5
hydrous Mn oxides	15 (at pH 8.3)

Structural differences between clay minerals will be reflected in the magnitude of their

cation exchange capacities. For example, kaolinite type clays have their layers bound together more tightly, therefore these clays have lower cation exchange capacities than other clays (Krauskopf, 1979). Typical CEC values are shown in Table 1.1.

(ii) Organic matter

Organic matter is present in soils and sediments as a result of a series of biological and chemical reactions on plant and animal debris. These reactions are known as humification and they transform the debris into humic material, which is resistant to any further degradation processes. Each humic molecule is different, with respect to functional group composition, and their molecular weights vary, but organic material overall will have a pH-dependent net negative charge which results primarily from the dissociation of hydrogen ions from carboxyl groups (Greenland and Hayes, 1981).

The placing of the functional groups within the humic material determines the cation selectivity because of the effect that the functional groups have on each other in terms of the electron density distribution. In general, two or three carboxyl groups which are attached to nearby carbon atoms are more selective towards multivalent cations than when they are more widely spaced. Cation selectivity decreases in the order: carboxylic > carboxyl-phenolic hydroxyls > phenolic hydroxyls. In addition to its dependence upon functional groups, sorption is also dependent upon the identity of the cation. For example, multivalent cations are preferred to monovalent cations, and d-block metals are preferred to metals from Groups 1 and 2 of the Periodic Table (Greenland and Hayes, 1981).

A positive correlation between the amount of organic material present and the

retention of heavy metals has been recorded (e.g. Hodgson, 1963). In addition to providing cation exchange sites, humic molecules have a strong affinity for heavy metals, such as Cu^{2+}, Fe^{2+} and Pb^{2+}, due to the functional groups also being capable of forming chelates and/or complexes with the metals (Greenland and Hayes, 1981).

(iii) Organo-mineral complexes

As well as occurring separately within a soil or sediment, organic and inorganic phases can also combine to form complexes. Once combined in an organo-mineral complex, the cation exchange capacity and also the cation selectivity of each mineralogical component will change from that described previously. The cation exchange capacity of the complex will always be lower than the sum of the individual cation exchange capacities of the phases which combined to make the complex. As organic matter can block exchange sites in minerals and also because organic matter has a preference for multivalent cations, the exchange of alkali metals, such as potassium is considerably reduced. The presence of these organo-mineral complexes in a soil or sediment therefore has important consequences in the sorption of trace elements (Greenland and Hayes, 1981).

1.5.2 Anion exchange

Although there is an overall negative charge on a soil or sediment, which gives rise to the cation exchange capacity, the negative charge arises from a combination of both negative and positive charges. These positive charges can result from the uptake of protons from the solution on to suitable sites, such as,

$-NH_2 \leftrightharpoons -NH_3^+$

$-OH \leftrightharpoons -OH_2^+$

Positive charges are therefore dependent upon pH, and as pH falls to between 4 and 7 some positive charges usually exist to which anions in solution can be electrostatically attracted (Greenland and Hayes, 1981).

Anions can be split into two groups. (1) Non-specifically adsorbed anions (eg. Cl^-, NO_3^-). These ions are always monovalent and are electrostatically attracted to any positive surface site. (2) Specifically adsorbed anions. This group consists of all other anions, which behave as ligands. Attracted only to specific surface sites, these anions form chemical bonds with the surface, making them harder to desorb (Greenland and Hayes, 1981).

Anion exchange can occur on any positive site on any mineralogical component within the soil or sediment, such as hydrous metal oxides and at the edges of 1:1 clay minerals (particularly the sulphate and phosphate anions). Illite clays also have a small anion exchange capacity although this is sometimes due to contamination of clay particles with hydrous oxide coatings. Organic material can remove anions from solution (such as phosphate or nitrate) by incorporating them into the structure biologically or by forming chelates (Greenland and Hayes, 1981).

1.5.3 Precipitation - dissolution reactions

Although not strictly "sorption" processes, precipitation and dissolution reactions are also important for governing the distribution of a trace element between the solid and

the solution phase. As environmental conditions will determine the solubility of chemical species, any changes which occur in these conditions can induce the precipitation of solid phases and the coprecipitation of trace metals, or alternatively cause the dissolution of solid phases, thereby releasing ions back into solution.

The solubility of calcium and magnesium carbonates in soils, for example, is determined by the solubility of the carbonate ion, which is controlled by the partial pressure of carbon dioxide in the soil atmosphere, pH, soil temperature and the concentration of dissolved ions in solution (Greenland and Hayes, 1981). In addition to providing sites for adsorption, incorporation of uranium into the solid structures of carbonates has been observed (Meece and Benninger, 1993), as well as the nucleation and precipitation of sorbing cations (for example, Mn^{2+}) on the surface of carbonate (McBride, 1979). Similar reactions result in the formation of sulphates, phosphates and alumino-silicates.

The concentration of iron and manganese ions in solution in freshwater sediments will be determined by the solubility of their oxides as, in freshwater sediments, these are the dominant Fe and Mn phases. The solubility of these oxides is controlled mainly by the redox conditions. Iron (III) oxides will be reduced under anoxic conditions, causing concentrations of dissolved iron to increase as the more soluble Fe^{2+} is produced (Krauskopf, 1979).

1.5.4 Oxidation and reduction

The redox potential of a system is important in determining the speciation of many trace elements. Speciation, along with other parameters, is of primary importance in

determining the behaviour of trace elements and radionuclides such as U, Pu (Krauskopf, 1979; Sharpe, 1986) and Ru (see Section 1.7.3) in the environment.

Redox conditions in freshwater systems can change as a result of thermal stratification which can take place in freshwater lakes as temperatures increase during summer months. Conditions at the sediment-water interface can become reducing in biologically productive lakes, such as Esthwaite Water, leading to the production of NH_4^+ ions and the dissolution of hydrous iron and manganese oxide phases (Mortimer, 1941, 1942; Sholkovitz and Copland, 1982).

Thermal stratification

During the spring, the lake is approximately the same temperature from top to bottom. When the wind blows from one direction, it can set the whole lake in circulation, mixing the dissolved salts and gases so that they become uniformly distributed in the water. As the temperature increases, the surface waters of the lake start to warm up, reducing the density of the water. A temperature gradient soon becomes established and the lake becomes stratified, with a distinct upper layer of warm water (called the epilimnion) sitting on a deeper, cooler layer (called the hypolimnion). The zone between these layers in which there is a rapid change of temperature is called the thermocline or metalimnion. The epilimnion can now circulate independently of the hypolimnion.

During the summer, the epilimnion is well supplied with oxygen. The hypolimnion, however, has to rely on the store of oxygen it contained before stratification occurred and, as the summer proceeds, demands are made on this store of oxygen from

decomposition reactions. In a biologically productive lake, such as Esthwaite Water, where oxygen demands are high, the store of oxygen in the hypolimnion can become depleted. Microbial activity in the sediment uses up the oxygen causing conditions at the sediment surface to become anaerobic. A layer of anoxic water can then build up at the bottom of the lake.

When the temperature of the epilimnion starts to fall again at the start of autumn, the temperature difference between the surface and the deeper waters starts to decrease until, eventually, the wind can overcome the small density difference and the lake waters become mixed. Stores of oxygen are then replenished in the hypolimnion and conditions at the sediment surface become aerobic again. This is called the autumnal overturn (Mortimer, 1941).

1.6 Quantitative measurement of sorption

The extent of sorption - both adsorption and desorption - which has taken place can be estimated by measuring the distribution of a radionuclide between the solution and solid phase. The data can be presented as the fraction of radionuclide remaining in solution or the fraction sorbed on to the solid phase, but it is often more useful and more common to present sorption data in the form of a Kd value, which is referred to as the distribution coefficient.

1.6.1 The distribution coefficient

The distribution coefficient is commonly used to describe the solid-solution partitioning of a trace element (Comans et al, 1991; Lima and Mazzilli, 1994; Ohnuki,

1994; Hsu and Chang, 1995) and it is defined as the ratio of the activity concentration of radionuclide sorbed on to the solid phase (Bq kg^{-1}) to the activity concentration of radionuclide remaining in solution (Bq l^{-1}).

As the distribution coefficient is a ratio, it is a more sensitive means of displaying sorption data than, for example, a fraction or percentage (Jannasch et al, 1988), particularly when extreme changes in sorption are being measured, i.e. measurements below 10% and above 90%.

Once calculated, distribution coefficients can be used in safety assessment models, particularly those models which are concerned with the transport of radionuclides throughout the environment. However, problems arise due to the rather simplistic definition of Kd and misuse of this important parameter. The subject of sorption nomenclature and the associated problems have been discussed by McKinley and Alexander (1992) who recommended that the term Kd only be used for sorption which is demonstrated to be fast, reversible and independent of the solute concentration. In addition to this, they also stress the importance of defining the phases, as Kd is only applicable to a two phase system. Colloidal matter in a system will result in the addition of a third phase and will cause overestimation of the "dissolved" concentration and hence underestimation of the distribution coefficient. This is a problem particularly when studying elements such as Th and Pa which are readily hydrolysed and are known to form colloids. As many of the systems studied in this project can be seen not to have reached an equilibrium and therefore do not fit the description above, the term Rd - distribution ratio - has been adopted in this work to describe the solid-solution partitioning in order to avoid any confusion.

1.7 Chemical properties and environmental behaviour of the radionuclides

To explain the sorption behaviour of the four radionuclides during the experimental work (results are presented in Chapters 3 and 4) and to understand further the mechanisms by which sorption proceeds for these radionuclides, it is necessary to have some knowledge of their chemistries. The following section describes in detail the chemical and nuclear properties of each radionuclide used in this project, and also discusses studies performed prior to this work with relation to the environmental behaviour of these radionuclides (particularly within the marine environment).

1.7.1 Cobalt

Geochemistry

Classified mainly as a chalcophile element (which means it has an affinity for sulphur), cobalt is often associated in the environment with nickel, silver, lead, copper and iron. It occurs naturally in arsenide and sulphide ores, such as cobaltite and smaltite, with the main ore deposits in Zaire, Morocco and Canada. It has an average crustal rock abundance of approximately 25 ppm and an average freshwater concentration of 0.1 ppb (Rose et al, 1979).

Chemical properties

Cobalt was first discovered in 1735 by Brandt. It is in the first row of the d-block elements of the periodic table, between iron and nickel, and has an atomic number of 27. It is a bluish-white, hard and brittle metal, resembling both iron and nickel in

appearance. The metal is used mainly with other metals such as chromium and tungsten to form a wide range of hard, non-corroding, non-ferrous alloys and it is also used in special steels and magnetic materials. It is used in electroplating because of its appearance, hardness and resistance to oxidation, and for centuries compounds of cobalt have been used in the production of blue dyes which are used in porcelain and glass.

Less reactive than iron, cobalt will dissolve slowly in dilute mineral acid whilst the action of concentrated nitric acid makes it passive. There is no reaction with alkalis. Unless heated, or very finely divided, cobalt does not react with oxygen.

Although cobalt is known in valence states 1 - 4, the continuing decrease in high oxidation state stability which occurs between iron and cobalt means that cobalt (IV) only occurs in a few rare compounds, (eg. $Cs_2[CoF_6]$). Very few binary Co(III) compounds are known, and the blue diamagnetic cation $[Co(H_2O)_6]^{3+}$ is a powerful oxidant. This oxidation state can be stabilised by complex formation with ammonia, amines or cyanide and there is an extensive chemistry of low-spin Co(III) (d^6) complexes. Co(II) usually forms simple, stable compounds, and many Co(II) complexes (octahedral and tetrahedral) are known. In aqueous solution it occurs as the high spin $[Co(H_2O)_6]^{2+}$ ion. Lower valency compounds usually contain ligands such as carbonyl groups, for example, $Co_2(CO)_8$ and $HCo(CO)_4$ although the Co(I) oxidation state is generally unstable and will readily oxidise.

There are several important biological complexes which contain cobalt, for example Vitamin B_{12}, and various compounds of cobalt, when carefully used, have been found to be effective in correcting certain mineral deficiency diseases in animals. Hence any

unstable isotopes of cobalt entering the body, whilst causing damage to cells and organs, would also be hard to remove (Sharpe, 1986; Cotton and Wilkinson, 1988).

Nuclear properties

There are many unstable isotopes of cobalt, mainly beta emitters, with half-lives ranging from 10^{-1} seconds to over 5 years. Produced and released into the environment by the nuclear industry, there are also many uses for cobalt radioisotopes. ^{60}Co particularly, is an important gamma source, and is used as a tracer and in therapeutic systems. The isotope used in this work, ^{57}Co, has a half-life of 271.8 days and emits gamma rays with principal energies of 122 and 136 keV.

Behaviour in the environment

For the last forty years it has been demonstrated that cobalt, along with other elements such as nickel, copper and zinc, is greatly enriched in manganese-containing environments. In deep-sea ferromanganese nodules for example, chemical analyses have shown that cobalt is always present in much greater concentrations than the concentrations of cobalt which have been measured in sea water, pelagic clays and "average" igneous rock (Goldberg, 1954; Cronan and Tooms, 1969), so much so that these marine nodules are regarded as a potentially important ore deposit (Morganstein, 1973). In the terrestrial environment, studies have revealed that almost all of the cobalt content of soils is contained within the manganese minerals present, e.g. birnessite, lithiophorite and hollandite (Taylor and McKenzie, 1966; Taylor, 1968). More recently, Means et al (1978a) found a positive correlation between the concentrations of Mn oxide present in a contaminated soil and the quantity of

anthropegenic ^{60}Co present, and studies of cobalt sorption on to marine sediments have revealed higher Kd values (by up to two orders of magnitude) for those which are enriched in manganese oxides (Nyffeler et al, 1984). It is therefore not surprising that much of the work carried out with cobalt focusses primarily on its association with these manganese oxide minerals and the mechanism by which the observed enrichment of cobalt in manganese oxide minerals occurs.

It was first proposed by Goldberg (1954) that cobalt was adsorbing on to the surface of deep sea ferromanganese nodules, thereby causing its enrichment. Investigation by McKenzie (1967) into cobalt sorption on to the manganese oxides which are present in soils concluded that once cobalt is sorbed on to these minerals it becomes increasingly fixed over time, eventually becoming non-extractable after several months. This fixation has important agricultural consequences and the importance of manganese in limiting cobalt contamination of crops was further shown by Adams et al (1969) and Tiller et al (1969) who found that the uptake of cobalt by clover is in fact inversely proportional to the manganese content of soils. This observed fixation of cobalt by manganese oxides implies a strong mechanism of adsorption, with processes in addition to ion exchange occurring.

Loganathan and Burau (1973) found that large concentrations of Mn ions were released into solution as Co sorbed on to MnO_2 phases and they also found evidence to suggest that Co was in fact exchanging at three different sites: (1) surface bound H^+, (2) structural Mn^{2+}, and (3) a Mn bearing site which was believed to accommodate Mn^{3+} ions, thereby suggesting that cobalt was somehow able to penetrate into the solid phase. Since cobalt and nickel are geochemically similar and their solution chemistries are virtually identical it would be expected that similar sorption properties would be

displayed with hydrous manganese oxides. It was therefore surprising when Murray (1975a) reported that Co (II) adsorbs much more strongly than Ni (II) on hydrous MnO_2. It was proposed that the difference in sorption behaviour could be due to oxidation of Co (II) to Co(III) at the manganese oxide surface.

In order to understand the proposed mechanism of cobalt sorption on to hydrous manganese oxides, it is necessary to know a little about the electronic configuration and ionic radii of both cobalt and manganese. These are shown in Figures 1.3 and 1.4 respectively. On the Earth's surface, only the high spin species of Mn^{2+} and Mn^{3+} ions and the low spin species of Mn^{4+} ions exist in minerals and, as in most oxide structures (particularly manganese (IV) oxides), only high spin Co^{2+} and low spin Co^{3+} cations occur in octahedral sites. Examining the ionic radii, it can be seen that there is a large difference between that of octahedrally coordinated low spin Co^{3+} (0.53 Å) and high spin Mn^{2+} (0.82 Å) and Mn^{3+} (0.65 Å) which makes it unlikely that Co^{3+} could substitute for these manganese cations. There is however close agreement between the ionic radius of Co^{3+} and Mn^{4+} (0.54 Å) and this led Burns (1976) to suggest that some cobalt substitutes for Mn^{4+} in the edge-shared $[MnO_6]$ octahedra on which the structures of manganese (IV) oxides are based (refer to Section 1.5.1). As this site would not be accessible for Ni^{2+} (0.69 Å) this would also account for the strong specific adsorption of Co (III) and the greater adsorption capacity of hydrous MnO_2 for Co (II) over Ni (II).

Murray (1975b) and Tewari and Lee (1975) found that adsorption of cobalt on to hydrous manganese oxides increased with increasing pH until all of the cobalt was removed from solution. Between pH 6 and 8 there was a particularly marked increase in sorption but, beyond pH 8, adsorption became increasingly masked by the

Figure 1.3 Electronic configuration and ionic radii of cobalt (Burns, 1976)

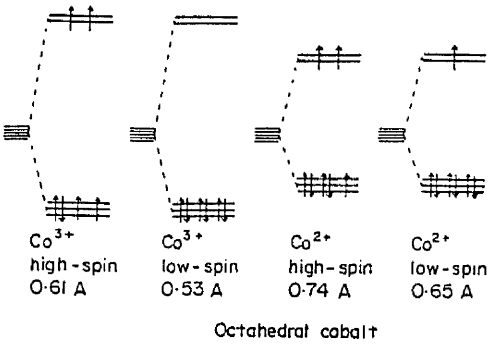

Figure 1.4 Electronic configuration and ionic radii of manganese (Burns, 1976)

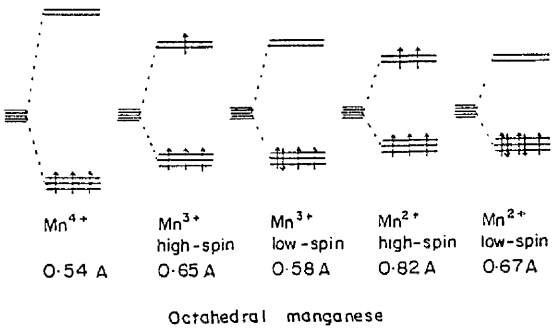

precipitation of $Co(OH)_2$. The marked increase between pH 6 and 8 was ascribed to two possible causes. An increase in pH would cause the surface charge of the oxide to become increasingly negative, therefore increasing its capacity to sorb positive ions. Secondly, the proportion of hydrolysed ions in solution also increases with pH, and hydrolysed multivalent ions are usually adsorbed more readily than non-hydrolysed ions. An increase in cobalt sorption with increasing pH was also observed with canal sediment (Abdel Gawad et al, 1977).

In addition to the pronounced association between cobalt and manganese oxides, a smaller degree of association has also been observed with iron oxides (Jenne and Wahlberg, 1965) and organic material (Jenne and Wahlberg, 1965; McClaren et al, 1986; Evans et al, 1988; Bird and Evenden, 1994). Clay minerals generally have a low affinity for cobalt (Jenne and Wahlberg, 1965; McClaren et al, 1986). Aston and Duursma (1973) showed that no positive correlation existed between the clay mineral content of the sediment and the amount of ^{60}Co sorbed. In contrast to this, studies by Kharkar et al (1968) concluded that illite can sorb significant amounts of cobalt from solution.

Adsorption of cobalt on to manganese oxides is rapid (McKenzie, 1970; Murray, 1975b). Although Murray (1975b) observed equilibration within 1 - 3 hours, McKenzie (1970) observed a slower period of sorption following the initial rapid uptake which continued for the duration of the experiment (40 days). Studies of cobalt sorption on to other mineralogical phases have shown similar sorption kinetics. McClaren et al (1986) found that humic acid, soil oxides and montmorillonite took up the bulk of cobalt from solution within 1 - 2 hours. Sorption on to soil oxides and montmorillonite continued to take place for several further hours. Grutter et al (1994)

found that sorption on to clay minerals was still incomplete after 56 days. Uptake of cobalt on to marine sediments also displays these two-step kinetics, with an initially rapid period of sorption followed by a slower uptake that continues for the duration of the experiment, implying that equilibrium is not reached (Abdel Gawad et al, 1977; Li et al, 1984; Nyffeler et al, 1984; Lima and Mazzilli, 1994). Nyffeler et al (1984) found that sorption of cobalt continued even after 108 days.

Competing cations seem to have little effect on Co sorption to manganese oxides (Murray, 1973), indicating processes in addition to ion exchange are taking place. Tewari et al (1972) found the presence of Ba^{2+} and Mg^{2+} made no significant difference to cobalt sorption in the pH range 6 - 8 and the competitive effects of Ca^{2+}, Mg^{2+} and Na^{+} were only noticed at very low concentrations of cobalt (Murray, 1975b). Gutierrez and Fuentes (1991) studied the competitive effects of simultaneous sorption of cobalt, strontium and caesium on to soils and concluded that cobalt and caesium do not compete for sites as much as cobalt and strontium.

Complexing of cobalt in groundwaters can promote mobility in the aquatic environment. Comparison of ^{60}Co distribution coefficients measured with and without the presence of a complexing agent indicated that sorption was greatly inhibited when EDTA was present (Means et al, 1978b). At pH 6.7, without the complexing agent, the distribution coefficient was $7.0x10^{4}$ mlg^{-1} and at pH 12.0 it was $1.2x10^{3}$ mlg^{-1}. In the presence of 10^{-5}M EDTA, however, sorption was significantly reduced. At pH 6.7, the Kd had been reduced to 2.9 mlg^{-1} and at pH 12.0 the Kd was reduced to only 0.8 mlg^{-1}. Olsen et al (1986) also attributed the mobility of ^{60}Co in a contaminated trench to low molecular weight anionic complexing (such as that with EDTA). This mobility in the presence of potential complexing agents is particularly important when

considering the methods and chemicals used in decontamination and waste disposal treatments.

Desorption studies have been carried out using a number of extractants. The most direct test of sorption reversibility is to use the same aqueous phase in both the adsorption and desorption studies. Abdel Gawad et al (1977) used canal water to study cobalt release into the water column and found that small, but increasing amounts of cobalt were released with increasing desorption times (5.5% extracted after 1 hour, 6.6% after 1 day and 14.5% after 6 days). Although studies by Nyffeler et al (1984) also observed cobalt being released back into the water column (lower and decreasing desorption Kd values were obtained compared to the adsorption values) it was proposed that this phenomenon could be due to bacterial activity changing the redox and pH conditions in the system, which stresses the importance of these parameters, in addition to the nature of the solid and the solution phases, on cobalt sorption.

Extracting solutions of increasing ionic strength have also been used. Abdel Gawad et al (1977) extracted cobalt from canal sediments using 0.1M $CaCl_2$. Although increasing amounts of cobalt were released with increasing desorption times (5.2% extracted after 1 hour, 8.3% after 1 day and 18.2% after 6 days) the quantities of cobalt released into solution were very similar to the quantities released when canal water (of considerably lower ionic strength) was used as the extractant. McClaren et al (1986) however found that cobalt was easily desorbed from humic material using 0.01M $CaCl_2$. Fukui (1990) concluded that ammonium acetate, which is commonly used to identify the extractable fraction of radionuclide in a sediment, extracted more strontium and caesium than cobalt, which indicates slightly different sorption mechanisms. Ammonium oxalate however, desorbed cobalt more easily. This was

ascribed to the reducing properties of this extractant, which will decompose any oxides present in the sediment, and therefore release any cobalt sorbed. Higher desorption yields were also observed on addition of EDTA due to formation of soluble cobalt complexes.

Another way of studying desorption potential is to study the isotopic exchangeability. Abdel Gawad et al (1977) used 0.1M $CoCl_2$ and found that considerably more cobalt was desorbed than had previously been observed with other extractants, although the majority of cobalt still seemed to be held in non-exchangeable sites (17.3% exchanged after 1 hour, 29.3% after 1 day and 38.3% after 6 days). Although McClaren et al (1986) observed that a large proportion of sorbed cobalt remained isotopically exchangeable from humic acid (approximately 70%), cobalt sorbed by soil oxides was not easily desorbed back into solution and it rapidly became non-isotopically exchangeable. On comparison of different mineralogical phases, it was concluded that cobalt sorbed to montmorillonite was more easily desorbed than cobalt sorbed to soil oxides but less easily desorbed than the cobalt sorbed to humic acid. The apparent fixation of cobalt on to soil oxides has also been reported by other studies. Cerling and Turner (1982) reported only 70-80% of cobalt was extractable with 2% hydroxylamine hydrochloride in 0.3M ammonium citrate (pH7). Spalding and Cerling (1979) and Cerling and Spalding (1981) found that only hot HNO_3 was able to extract all the ^{60}Co associated with the oxide material. Desorption of ^{60}Co under oxidising conditions was very slow (in the order of several years). By comparison however, strong reducing conditions caused the dissolution of the oxide material, releasing most of the sorbed ^{60}Co back into the aqueous phase after 8 months. It was therefore concluded that once a sediment has been contaminated, cobalt will not be released until all the iron and manganese oxide material is destroyed (Cerling and Turner,

1982).

1.7.2 Strontium

Geochemistry

Due to its affinity for silicates, strontium is classed as a lithophile. It tends to be associated with calcium and barium and calcium carbonate formed in the sea always contains some strontium. It is widely distributed throughout minerals (average crustal rock abundance of approximately 300 ppm) and in the marine environment (average concentration of 400 ppb in freshwater), and is mainly found in the minerals strontianite and celestite ($SrCO_3$ and $SrSO_4$) (Rose et al, 1979).

Chemical properties

Strontium was discovered by Davy in 1808. It has atomic number 38 and is referred to as an "alkaline earth metal", situated below calcium and above barium in Group 2 of the periodic table.

Softer than calcium, it is a silvery coloured metal when first cut, rapidly turning a yellowish colour due to the formation of the oxide, and it therefore needs to be kept under kerosene to prevent oxidation. Although it is less reactive than sodium its chemical properties are similar, and if the metal is finely divided it will ignite spontaneously in air. When heated, strontium metal can combine with oxygen, nitrogen, sulphur and the halogens, and it can also combine with hydrogen. A highly electropositive element, it exists only in oxidation state +2, forming few complexes

in aqueous solution.

Radiostrontium accidentally released into the environment as a result of an accident in a nuclear energy plant is acknowledged to be a serious public health problem, as the chemical similarity of strontium to calcium means that it may be incorporated with calcium phosphate in bone (Sharpe, 1986; Cotton and Wilkinson, 1988).

Nuclear properties

Many of the unstable isotopes of strontium are both beta and gamma emitters. The shortest-lived isotope has a half-life of just under half a second whereas the longest lived of these radioisotopes, ^{90}Sr, is a beta emitter and fission product of uranium (fission yield 5.772%) or plutonium, with a half-life of over 28 years. ^{85}Sr is the radioisotope used in this work (fission yield 1.318%). It has a half-life of 64.9 days and it emits gamma rays of principal energy 514 keV.

Behaviour in the environment

In natural waters, strontium occurs as an uncomplexed divalent cation and may therefore exchange with other ions on clays or other minerals that have a significant cation exchange capacity (Tamura, 1965; Shiao et al, 1979; Erten et al, 1988). As a result of this, a correlation between the cation exchange capacity of the sorbing material and strontium sorption has been observed as well as a dependence upon the ionic strength of the aqueous solution (which is a source of competing cations) and pH (Wiklander, 1964; Torstenfelt et al, 1982).

Strontium sorption on to clay-sized particles has been observed to reach an equilibrium after an adsorption time in the order of several days. Garder and Skulberg (1964) determined that equilibration had been reached after 1 day when approximately 7% sorption had been reached. The low percentage of sorption was ascribed to the low cation exchange capacity of the material used (mainly quartz and feldspar with a small amount of illite and chlorite). This rapid equilibration time has also been observed by Torstenfelt et al (1982). Erten et al (1988), however, found an equilibrium was reached only after adsorption had continued for 7-11 days. Similar trends but different kinetics have been obtained for strontium sorption on to sediments and soils. Keren and O'Connor (1983) observed an equilibrium being established within less than an hour, whereas Nyffeler et al (1984) observed a longer equilibration time of several days. Benes and Poliak (1990) however observed two step kinetics. A rapid uptake of strontium occurred for the first 100 minutes, followed by a small, slow increase. The initial, rapid uptake was attributed to isotope exchange with easily accessible exchangeable strontium. The slower increase in sorption was interpreted as either isotope exchange with less accessible strontium in the sediment or a change in the sorption properties of the sediment.

Due to the high exchange capacity of manganese oxides, discussed previously in Section 1.5.1, these have also been studied in relation to strontium sorption. Singh and Tandon (1977) concluded that sorption of strontium on to hydrous manganese oxides was low, with an equilibrium being established within 15 minutes. When a competing cation such as Na^+ was added to the system in concentrations comparable to ocean water, then strontium sorption on to the oxide was reduced to a negligible amount. Other competing cations such as K^+, Mg^{2+} and Ca^{2+} also had this effect and so they concluded that hydrous manganese oxides, under realistic environmental conditions,

were poor scavengers of strontium. Cerling and Turner (1982) also observed relatively low sorption of strontium on to iron and manganese oxide coatings which had formed on stream gravel. Distribution coefficients were approximately 30-60 mlg^{-1}. Although uptake of strontium was rapid, it took up to a week before equilibrium was reached in the system. Strontium was held primarily as an exchangeable cation and desorption was rapid, but in hydrous manganese oxides which had been freshly formed, some (approximately 20%) non-exchangeable strontium was observed. Desorption of this non-exchangeable strontium was much slower and even after 8 months only about one half had been lost. Adsorption of strontium on to the hydrous oxides of aluminium has also been studied (Kinniburgh et al, 1975). It was concluded that Sr^{2+} was adsorbed through coordination to hydroxy ions, with approximately one proton released for each Sr^{2+} sorbed.

As the main mechanism of strontium sorption is ion exchange, a dependence on the nature and concentration of the competing cations should be expected. A comparison of competing cations by Abdel Gawad et al (1977) indicates that competition is greatest, and strontium sorption is reduced most, when Ca^{2+} cations are present in the solution, although Mg^{2+} cations were also observed to cause a decrease in sorption. The effect of competing cations increased with the concentrations of cations in the solution. The presence of Na^{+} cations in solution had no observable effect on strontium sorption. The apparent inability of Na^{+} to compete with strontium for sites was believed to be due to its single charge, which inhibited its competing for sites as effectively as the doubly charged Ca^{2+} and Mg^{2+}. The difference in competing ability between Mg^{2+} and Ca^{2+} was believed to be due to the difference in solvation between the two ions.

Although strontium forms few complexes in solution, high concentrations of carbonate in groundwater can cause strontium to precipitate. Torstenfelt et al (1982) observed a marked increase in strontium sorption above pH 10, which was believed to be due to the formation of strontium carbonate complexes. Due to the relatively high carbonate concentrations in the groundwater, significant amounts of strontium in solution would exist as $SrHCO_3^+$ and $SrCO_3$, and the strontium carbonate would precipitate at high pH. In an aqueous phase containing no carbonate, the marked increase in distribution coefficient was not observed, eliminating the unlikely possibility that hydrolysis was occurring. Olsen et al (1986) also noticed similar effects in highly alkaline environments.

Desorption of strontium has been found to be rapid and easy, again implying that strontium is held on easily accessible, readily exchangeable sites (Benes and Poliak, 1990; Fukui, 1990). The length of time needed to produce 100% desorption has been found to depend upon the extracting agent (Schulz and Riedel, 1960). Fukui (1990), for example, found that the ammonium ion could more readily desorb strontium from sediments than Na^+ cations, but ammonium acetate was also found to be a less efficient extractant than Ca^{2+} or Sr^{2+} (Schulz and Riedel, 1960). Abdel Gawad et al (1977) concluded that ^{89}Sr could be easily desorbed by any of the leaching agents used. When 0.1M $CaCl_2$ was used 63.9% of strontium was extracted after 1 hour, 96.5% after 1 day and 100% after 6 days. Virtually all of the sorbed strontium remained isotopically exchangeable. When 0.1M $SrCl_2$ was added, 99.3% of strontium was exchanged after 1 hour, 95.4% after 1 day and 100% after 6 days. Desorption was lower in canal water, due to the lower ionic strength, with only 49.4% of strontium leached after 1 hour, 63.2% after 1 day and 60.0% after 6 days. Slightly more complicated desorption behaviour was observed by Erten et al (1988). Initially

desorption was rapid but this was followed by an apparent readsorption of strontium until an equilibrium was established.

Although the majority of studies have reported that strontium is easily and rapidly exchanged, a slow fixation of strontium in non-exchangeable sites has also been observed with increasing adsorption times (Martin et al, 1957; Libby, 1958). It is possible that this fixation effect has been overlooked in the majority of studies, because of the long adsorption times which are needed to produce this phenomenon. Adsorption times of several years are apparently needed in order to produce a small, but nonetheless noticeable, fixation. Schulz and Riedel (1960) in explaining the non-exchangeable strontium, suggested that a small quantity of ^{90}Sr which had sorbed to the soil had diffused into insoluble strontium or calcium phosphates, or other insoluble phases. Wiklander (1964) found approximately 10-12% of the sorbed strontium remained non-extractable by ammonium acetate after an adsorption time of 3 years and this was ascribed again to isomorphic substitution of strontium into calcium containing minerals.

1.7.3 Ruthenium

Geochemistry

Due to its affinity for metallic iron, ruthenium is a siderophile in Goldschmidt's classification of the elements. It occurs in the environment together with the platinum metals, either as the metal, or in the sulphide ores of copper and nickel. Commonly associated with copper, silver and gold, ruthenium and all of the platinum metals are rare, with typical abundances in the Earth's crust of approximately 10^{-7}%. They are

found mainly in South Africa, the USSR and Canada (Rose et al, 1979).

Chemical properties

In 1827, Berzelius and Osann examined the residue which remained after dissolving crude platinum in aqua regia. Osann thought he saw three new metals, one of which he named ruthenium. It was not until 1844, however, that Klaus (who is generally recognised as the discoverer) showed that Osann's ruthenium oxide was very impure, and actually managed to separate 6g of ruthenium from the portion of crude platinum which was insoluble in aqua regia.

Industrially, the platinum metals can be separated using methods based on their different oxidation state stabilities following the electrolytic refinement of copper or nickel ores although, as a group, the platinum metals are thought to be relatively noble.

Ruthenium is a grey-white coloured metal, brittle but fairly hard, and it does not tarnish at room temperature. Oxidation states between 2 - 8 have been observed although the oxidation states of 3,4 and 6 are generally the most stable. Simple cations of ruthenium are almost unknown and its chemistry is almost entirely dominated by that of its complexes (aqua ions of ruthenium in oxidation states 2 and 3 are known but often only as complicated complexes). Ruthenium is not attacked by hot or cold acids or aqua regia but when potassium chlorate is added to the solution, it oxidises explosively. It is also attacked by halogens and hydroxides.

When heated with oxygen, ruthenium forms the volatile and toxic yellow oxide, RuO_4,

which is a very powerful oxidant. The action of nitrous acid on $[Ru(NH_3)_6]^{2+}$ can produce numerous ruthenium nitrosyl complexes, for example $[Ru(NH_3)_5NO]^{3+}$. These complexes are stable and many are extremely soluble in organic solvents. This solubility often causes difficulties in the recovery of uranium and plutonium from irradiated fuel as it makes the removal of the ruthenium nitrosyl complexes a difficult operation. Other complexes of ruthenium, such as bipyridyl complexes, are of photochemical interest. $[Ru(bipy)_3]^{2+}$ is used extensively as a photosensitiser (Sharpe, 1986; Cotton and Wilkinson, 1988).

Nuclear properties

Many of the unstable isotopes of ruthenium are both beta and gamma emitters. Those produced in fission are all relatively short-lived, with ^{106}Ru being the longest-lived with a half-life of 368 days. The radioisotope used in this work is ^{103}Ru with a half-life of 39 days and a principal gamma energy of 497 keV.

Behaviour in the environment

Since the chemistry of ruthenium is so complex, mechanisms of ruthenium sorption can include most types of reaction, including isotopic exchange, coprecipitation, dissolution reactions or the formation of compounds (Jones, 1960; Patel et al, 1978; Duursma and Gross, 1971), depending upon which oxidation state or complex of ruthenium is present. This leads to inconsistent distribution coefficients, with those reported for ruthenium varying by a couple orders of magnitude, for example, 10^2 (Bachhuber et al, 1986) to 10^4 (Aston and Duursma, 1973). It is generally thought that, under acidic conditions, the dominant oxidation states will be +3 or +4

(Essington et al, 1963). In general, cationic forms of ruthenium are thought to become fixed, whilst anionic forms will remain mobile (Schulz, 1965; Andersson and Roed, 1994). It is possible, however, that anionic forms of ruthenium, such as those present in nitrosyl complexes, can form insoluble complexes with the surface layer of ferric hydroxide on sediment, sand and silt particles (Jones, 1960).

Ruthenium is observed to have an affinity for organic matter (Pillai et al, 1975; Santschi et al, 1988b; Polar and Bayulgen, 1991; Robbins et al, 1992). Andersson and Roed (1994) noticed that ruthenium had migrated much deeper into a Chernobyl soil than expected (only 44% remained in the top 8mm layer compared to 72% of caesium) and this was thought to be due to the generally weaker ruthenium-organic bonds compared to the strong caesium-clay bonds. Further analyses on the soil showed that ruthenium was present only in the layers of soil where organic content was high and selective extraction revealed approximately 67% of the ruthenium was contained within the organic fraction.

A lower association between ruthenium and clay particles has been observed. Garder and Skulberg (1964) reported the continuing sorption of ruthenium on to clay particles in distilled water even after 9 days. This is consistent with the results of Aston and Duursma (1973) who reported that sorption of ruthenium on to marine sediments occurred at a slower rate than that of cobalt and caesium, with an equilibrium being established only after approximately 200 hours. Garder and Skulberg (1964) also noticed a dependence upon competing cations when sorption was carried out in river water. Sorption was greatly reduced - from 34% to just 7%. Ruthenium ions have been found to be more easily desorbed from clays than caesium (Livens and Baxter, 1988; Polar and Bayulgen, 1991), which is probably due to the size of the ion and

also the hydration energy. This also suggests however that sorption on to clays occurs by ion exchange.

Nishita et al (1956) found greater quantities of water-soluble ruthenium were released from soils than either strontium or caesium, although Jones (1960) observed that ^{106}Ru was not easily desorbed when washed with seawater at pH 2 - 6. Pillai et al (1975) found that ruthenium could be easily complexed with EDTA and sodium hydroxide was found to release greater amounts of ruthenium than neutral ammonium acetate (Nishita et al, 1956).

1.7.4 Caesium

Geochemistry

Caesium is found mainly in relatively small amounts in various silicate minerals (e.g. lepidolite and pollucite). The most important source is in Manitoba. It has an average abundance in crustal rocks of approximately 3 ppm (Rose et al, 1979).

Chemical properties

Caesium was discovered spectroscopically in mineral water from Durkheim by Bunsen and Kirchhoff in 1860. It has an atomic number of 55, and is referred to as an "alkali metal", found in Group 1 of the periodic table, situated below rubidium and above francium.

The most electropositive and alkaline element, it is a soft, yellowy coloured metal

which must be handled in an inert atmosphere. On contact with water, caesium reacts violently, and the hydrogen which is liberated ignites. CsOH is the strongest base known and even reacts with glass.

With oxygen, caesium forms the superoxide CsO_2, although with a limited amount of air Cs_2O can be obtained. At low temperatures partial oxidation is possible, resulting in the formation of suboxides such as Cs_7O, which involve metal-metal bonding.

The caesium cation (oxidation state +1) is hydrated in aqueous solutions, although it is difficult to estimate the number of water molecules surrounding the ion as the exchange of water between the hydrated ion and the solvent is very fast. Although it rarely happens in aqueous solution, caesium is capable of forming stable complexes with, for example, EDTA and crown ethers.

The fact that radiocaesium does not associate itself with any particular organ of the body, but is assimilated within body tissues, similar to potassium, means that releases of radiocaesium into the environment lead to concerns for public health (Sharpe, 1986; Cotton and Wilkinson, 1988).

Nuclear properties

There are many unstable isotopes of caesium, most of which are beta and gamma emitters. Half lives range from less than a quarter of a second to over two million years. ^{137}Cs is the most widespread radioisotope and is of greatest concern due to its longer half-life (30 years). The isotope used in this work is ^{134}Cs with a half-life of 2.06 years and gamma rays of principal energies 605 and 796 keV.

Early studies into caesium sorption identified an affinity between caesium and clay minerals. Nishita et al (1956) found that relatively large amounts of caesium were held in fixed positions in kaolinite. In contrast, however, Schulz et al (1960) observed virtually no fixation of caesium in kaolinite or montmorillonite, but a high concentration of non-exchangeable, or fixed, caesium in vermiculite. It was also found that the total amount of caesium sorbed from solution exceeded the cation exchange capacity in the majority of soils and minerals studied, implying that sorption mechanisms in addition to ion exchange were taking place. Desorption studies showed that the amount of caesium which could be easily exchanged with Cs^+ or Ca^{2+} was generally the same as the cation exchange capacity of the soil. They concluded that caesium was somehow precipitated on the surface of micaceous minerals, and during the course of this precipitation the mineral lattice was altered so that caesium was incorporated into the crystal structure, thereby keeping it in a fixed position, unable to be exchanged for H^+, Na^+, Ca^{2+}, Mg^{2+} and Ba^{2+} because these ions could not fit into the lattice. Ions such as K^+, NH_4^+ and Cs^+ could release sorbed radiocaesium to a certain extent because they were able to substitute for it in the lattice.

In addition to this observed fixation, certain clays also seemed to sorb K^+ and Cs^+ ions in preference to other cations present in solution in a manner which was unrelated to their cation exchange capacity (Wiklander, 1950; Marshall and Garcia, 1959). Illite and vermiculite sorbed caesium more selectively than montmorillonite and kaolinite, and selectivity was observed to increase when caesium concentration decreased (Jacobs and Tamura, 1960). Bolt et al (1963) proposed that three different sorption sites on clay minerals existed, regular surface exchange sites, edge interlayer sites

(frayed edge sites) and interlayer sites in the interior of the clay. Each of these sites is increasingly more selective for caesium sorption. Any differences in selectivity which existed between the different clay minerals were related to both the density of layer charge, and the area of frayed edge sites (Sawhney, 1970). For example, selectivity differences between vermiculite and montmorillonite, and illite and montmorillonite, are related to the layer charge density, whilst the difference in selectivity between illite and vermiculite is related to the area of frayed edge sites (even though illite has a lower cation exchange capacity, it has a higher proportion of frayed edge sites and therefore a higher selectivity for caesium). The greater the layer charge density, the more easily interlayer collapse occurs (Sawhney, 1969) and therefore the greater the selectivity for the cations that produce interlayer collapse. Any cations with a low hydration energy, such as K^+, NH_4^+, Rb^+ and Cs^+, can produce interlayer collapse.

Due to their low hydration energy, these cations can lose their water of hydration in the interlayer spaces in the frayed edge sites. This dehydration allows a closer approach to the tetrahedral silicate layers and the formation of polar bonds with the structural oxygen atoms. The unhydrated ions cause dehydration due to the interlayer solution becoming more dilute, causing water to diffuse out across the concentration gradient. The interlayer then collapses, causing the cation to become fixed. As Cs^+ ions have a smaller hydration energy than K^+ ions, they collapse the interlayer more strongly and are therefore more firmly fixed. Any cations with a large hydration energy, such as Ca^{2+}, Mg^{2+} and Sr^{2+}, produce expanded interlayers and therefore do not become fixed (Sawhney, 1972). More recently, it has been found that, in addition to the factors described above, a minimum concentration of 0.60 to 0.75mM of caesium is required in the vicinity of the frayed edge sites before fixation of this

cation can occur in the interlayers (Hird et al, 1996). As the concentration of frayed edge sites is very low, the majority of exchange sites on illite are actually regular surface sites that are not selective. Therefore at greater concentrations of caesium, the selectivity of illite decreases due to sorption on these sites. Effective extracting agents of caesium from these sites are those cations which are similar in size and hydration energy to caesium, such as K^+ and NH_4^+. Cations such as Ca^{2+} and Mg^{2+} which are not selectively sorbed by these sites are not suitable leaching agents for caesium (Sawhney, 1972; Evans et al, 1983; Pardue et al, 1989; Fukui, 1990).

The link between caesium and clay minerals, particularly micaceous clays, is therefore well established (Francis and Brinkley, 1976; Patel et al, 1978; Olsen et al, 1986; Cremers et al, 1988; Erten et al, 1988; Benes et al, 1989; Davies and Shaw, 1993) and as well as a qualitative correlation between caesium sorption and the cation exchange capacity of the soil (Torstenfelt et al, 1982), a quantitative correlation has also been observed between the amount of caesium sorbed and the percentage of illite clay present (Aston and Duursma, 1973). Consistent with the identifying features of ion exchange reactions it has been shown that the presence of competing cations suppresses caesium sorption (Garder and Skulberg, 1964; Aston and Duursma, 1973; Singh and Tandon, 1977; Torstenfelt et al, 1982; Benes et al, 1989). Sorption of caesium on to other geological media present in soils and sediments has been shown to be low. Hydrous manganese oxides, and also iron oxides, have been shown to be poor scavengers of caesium (Singh and Tandon, 1977; Cerling and Turner, 1982; Evans et al, 1983) and caesium has little affinity for organic matter (Nishita and Essington, 1967; Schell et al, 1980; Evans et al, 1983; Sholkovitz et al, 1983; Davies and Shaw, 1993).

A number of studies have reported an initial rapid period of caesium uptake (Garder and Skulberg, 1964; Aston and Duursma, 1973; Singh and Tandon, 1977; Torstenfelt et al, 1982; Li et al, 1984; Nyffeler et al, 1984; Erten et al, 1988; Comans et al, 1991) after which equilibrium was established. The times required for equilibration ranged from less than 1 hour to several days. Torstenfelt et al (1982) and Comans et al (1991) however, observed a slower period of caesium uptake which continued for the duration of the experiment. After 2 weeks, the slow sorption was still continuing and appeared to be slightly faster with Ca-saturated illite than with K-saturated illite (Comans et al, 1991). The fast period of sorption was ascribed to sorption on to accessible surface sites and the slower period of uptake was described as the diffusion controlled process into interlayer sites in the interior of the clay. Sorption was believed to be faster with Ca-illite as it would be expected that the layers would be expanded, whereas K-illite would probably have collapsed interlayers.

Very little caesium can be leached due to its fixation in clays and therefore only partial desorption is observed, dependent upon the initial adsorption time (Evans et al, 1983; Erten et al, 1988; Comans et al, 1991). Increasing adsorption times generally lead to a greater fixation of caesium. For example, Evans et al (1983) could only extract 20% of the sorbed caesium after an adsorption time of 180 days but this was still twice the amount of caesium extractable from a sediment which had been in contact with caesium for more than 15 years. It was also found that more than half of the caesium can migrate into sites not exchangeable with ammonium within several days. Hence caesium ions are less easily desorbed than cobalt and strontium ions (Abdel Gawad et al, 1977).

As mentioned previously, desorption yields are also dependent upon the extracting

agent. Nishita et al (1956) found that 1M ammonium acetate desorbed caesium more effectively than 0.04M nitric acid and this was ascribed to its higher ionic strength. Patel et al (1978) also found that desorption yields were dependent upon ionic strength of the extracting agent. Desorption with 1M ammonium acetate (pH 7.0) yielded 13-15%, 1M ammonium acetate with acetic acid (pH 5.4) leached higher yields of 22-26% and 5% EDTA (pH 7.0) desorbed 15-24%. Fahad et al (1989) and Davies and Shaw (1993) obtained similar results, implying that only very small amounts of caesium are labile. Fukui (1990) concluded that desorption into both distilled and lake water was low, and very little desorption occurred with 1M HCl. Differences in desorption yield were observed at higher molarities (6M HCl), probably due to destruction of the mineral lattice and diffusion of caesium out of its fixed positions. Very little was desorbed by EDTA and this was indicative of low complex formation. Comans et al (1991) observed a rapid desorption into aqueous solution, followed by a slower phase where caesium was slowly readsorbed by the solid. This readsorption did not reach equilibration within the time scale of the experiment. Approximately 70% of the caesium was isotopically exchangeable within one day.

Despite this apparently irreversible fixation, concern has grown over the apparent remobilization of caesium from sediments into the water column of freshwater lakes. This phenomenon appears to be on an annual cycle coincident with summer thermal stratification and hypolimnetic anoxia (Alberts et al, 1979). Evans et al (1983) concluded that it was due to the enhanced concentrations of the NH_4^+ ions present in the water column at this time. The linear relationship found between Kd values and ammonium concentrations prompted Comans et al (1989) and Das (1992) to conclude that the decrease in Kd of caesium with sediment depth was also due to ion exchange with pore water ammonium and therefore it was important not to consider that

radiocaesium, once sorbed, would be indefinitely immobilised in freshwater sediments.

Microbial activity was also seen to influence the sorption of caesium on to geological media. Distribution coefficients suggested competition between microbes and caesium ions for sorption sites. As microorganisms are larger than caesium ions, one microbe could cover many sorption sites resulting in decreased caesium sorption (West et al, 1991).

CHAPTER 2 - COLLECTION AND CHARACTERISATION OF SAMPLES

CHAPTER 2 - COLLECTION AND CHARACTERISATION OF FIELD SAMPLES

2.1 Introduction

This section describes in detail the methods used to characterise the sediment and water samples used in the sorption experiments. Details of the two field sites are included, as well as the sampling techniques which were used.

2.2 Field Sites

Sediment and water were obtained from two different freshwater environments; Botany Pond in Dorset, and Esthwaite Water in Cumbria. The two sites were chosen because of their easy accessibility and because they both have different environmental settings and biogeochemistries. This means that they will have different sediment and water chemistries, with respect to the mineral and major ion content. These different sediment and water chemistries allow us to examine more closely and compare the effects of the various mineral phases and major ions on sorption processes.

Site 1 : BOTANY POND

Botany Pond is a small pond (depth 0.5m; area $20m^2$), run by the Institute of Freshwater Ecology, located at the River Laboratory just outside Wareham in Dorset (UK National Grid Reference: SY870867). Sediment and water are collected from the pond on a regular basis and these samples are then used by various industries to test the environmental effects of various chemicals used in agriculture. Figure 2.1 shows

Figure 2.1 Location of Botany Pond in Dorset

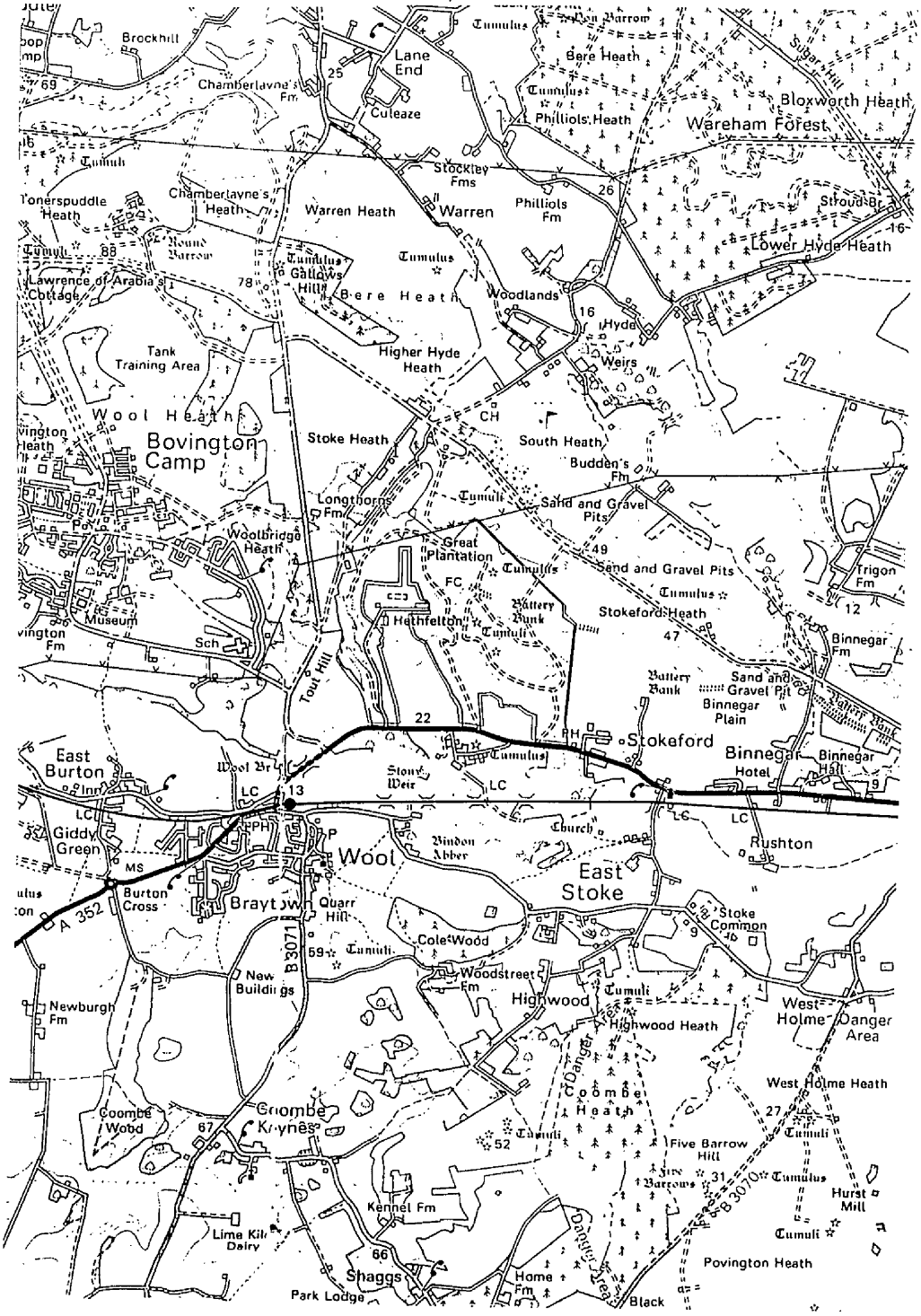

the location of Botany Pond in Dorset.

Site 2 : ESTHWAITE WATER

Esthwaite Water is a small, relatively shallow lake (physical parameters are given in Table 2.1) in the Lake District (UK National Grid Reference: SD360960), lying entirely on the Bannisdale Slates. The area which surrounds the lake is fertile and lends itself well to agricultural uses, with the rocks and soils readily giving up their salts to Esthwaite Water, ensuring that the lake remains nutrient rich. Figure 2.2 shows the location of Esthwaite Water in Cumbria.

Table 2.1 Physical parameters of Esthwaite Water

PARAMETER	MEASURED VALUE
Surface area	1.0 km^2
Mean depth	6.4 m
Maximum depth	15.5 m
Water volume	$6.4x10^6$ m^3
Typical residence time	approximately 13 weeks

Esthwaite Water has received a great deal of attention from biologists, hydrologists and chemists for over 50 years (eg. Mortimer, 1941, 1942; Heaney, 1976; Morris et al, 1994). These studies have provided much information about the lake's geochemical and biological behaviour, as well as an insight into the general geochemical behaviour of the elements. The lake has a high biological productivity - it is one of the most productive in the Lake District - and it exhibits a well-documented seasonal cycle of phytoplankton production (Heaney, 1976). During thermal stratification in the summer, the deep basinal waters of the lake become anoxic. This is important because

Figure 2.2 Location of Esthwaite Water in Cumbria

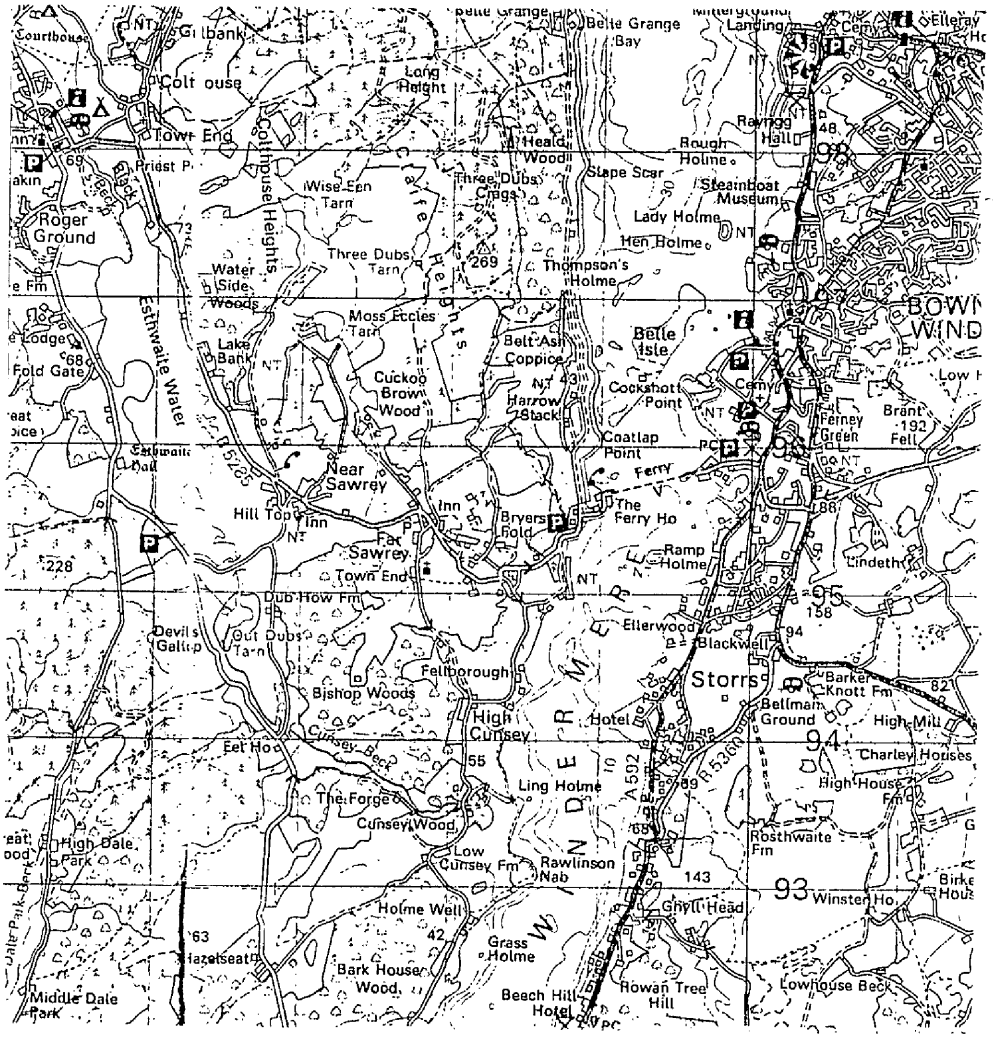

it causes the redox conditions in the lake to change, and hence, the distribution of some particulate and dissolved phases (eg. iron (III) oxides) also changes at this time. This in turn can lead to the adsorption and release of other elements (Mortimer, 1941, 1942; Sholkovitz and Copland, 1982).

Figure 2.3 shows a bathymetric map of Esthwaite Water from an echo-sounding survey by Mortimer in 1941.

2.3 Sample Collection

Samples were collected from both field sites during November 1993. Throughout the collection and pre-treatment of samples, both the wet sediment and lake water were stored at 4°C. Different sampling methods were used at each site because of their different environmental settings.

Site 1 : BOTANY POND

Pond water was collected and then filtered, using Whatman GF/C papers, into pre-rinsed plastic storage containers. Wet sediment was collected using a drag net procedure; each drag was approximately 1 metre in length and 25 cm in width. The wet sediment was sieved through a stainless steel 2 mm sieve, and the >2 mm fraction discarded. The excess water was taken off the sediment by centrifugation and decantation.

Figure 2.3 Bathymetric map of Esthwaite Water (Mortimer, 1941)

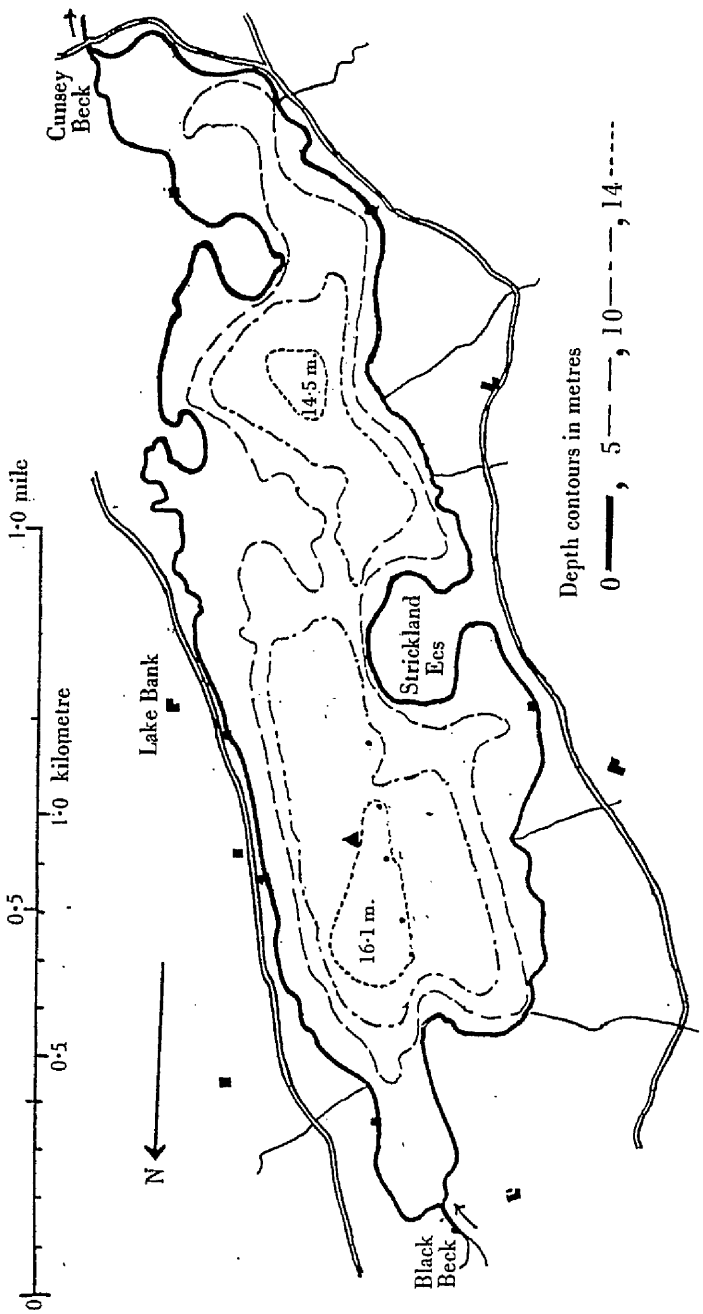

Lake water was collected from a depth of 7 metres, and then filtered, using Whatman GF/C papers, into pre-rinsed plastic storage containers. Wet sediment was collected from a depth of 14 metres, using a Jenkin corer. This provided the most useful means of sampling the surface mud whilst causing the least possible disturbance. A basic model of the Jenkin corer is shown in Figure 2.4 (Mortimer, 1942).

The sample of sediment is taken in a perspex tube (a) which is mounted in a framework, constructed in such a manner so that the tube remains vertical throughout the whole procedure. When the sampling tube is in position, and completely open, the apparatus is lowered carefully to the mud surface. The framework legs are weighted so that once the corer reaches the surface, its momentum carries the sampling tube to about one-quarter of its length into the soft surface mud. The cable holding the corer then goes slack and the weight (b) falls and releases the trip-catch (c). The tension of the springs (d) then pulls the arms carrying the lids anti-clockwise, thus closing the tube. These springs are powerful enough to cause the bottom lid to slice through the mud and close the bottom of the tube. The corer can then be pulled up carefully and the perspex sampling tube removed (Mortimer, 1942).

The top 15 cm of sediment was sliced from each core and sieved through a stainless steel 2mm sieve. The >2 mm fraction was discarded.

2.4 Sample Treatment

As the sediments and water from the two lakes would be combined with each other

Figure 2.4 Diagram of Jenkin corer (A) Details of lid (B) Open position (C) Closed position (Mortimer, 1942)

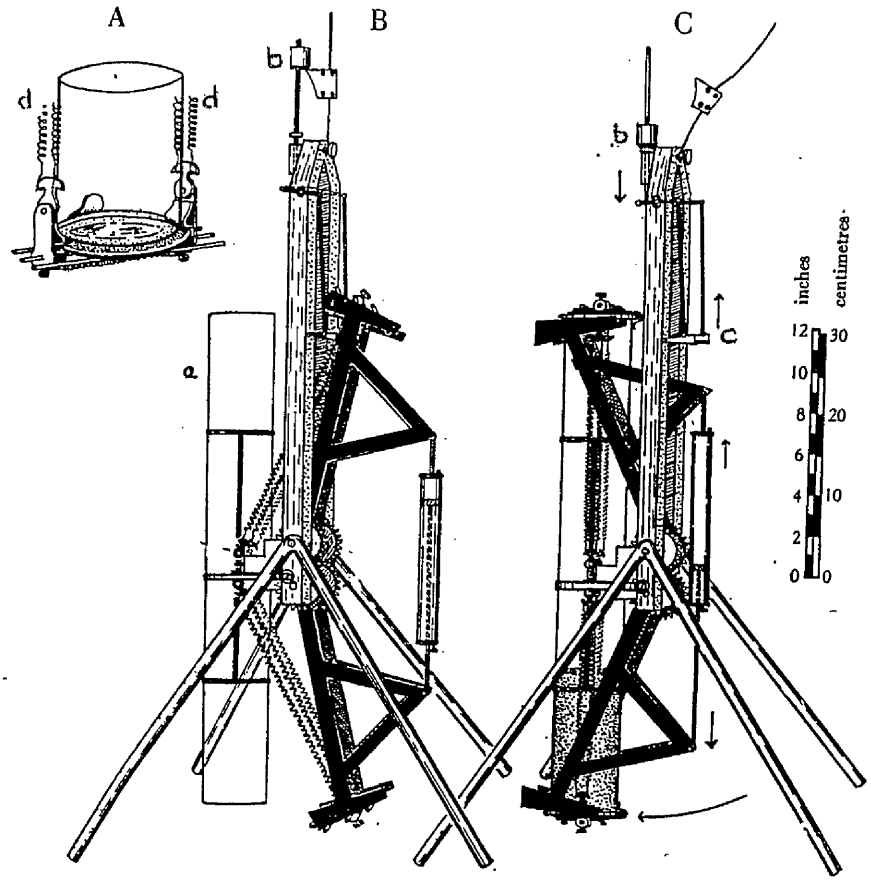

during the sorption experiments, it was necessary to ensure that they were in equilibrium with each other (Torstenfelt et al, 1982; Erten et al, 1988). Carrying out a pre-equilibration would limit the possibility of any chemical changes occurring over time between the two phases, thereby keeping experimental conditions constant, as any changes which occur would almost certainly affect the sorption behaviour of the radionuclides.

2.4.1 Sediment pre-equilibration

Both sediments were split equally into two samples, one half to be equilibrated with Botany Pond water and the other to be equilibrated with Esthwaite water. Equilibration was achieved by shaking the wet sediment continuously with fresh equilibration water for increasing time periods, varying from 30 minutes to 24 hours. After each time period, the equilibration water was analysed for sodium content by atomic absorption spectrometry. The sediments were considered to be equilibrated with the water when the sodium content remained constant. Figure 2.5 illustrates the change in sodium content over time for two of the systems. As can be seen, there was no change in Na^+ concentration after a cumulative pre-equilibration time of 1 hour.

2.4.2 Further treatment

Once equilibrated, the sediment was dried to a constant weight at 40-50°C, ground finely with an agate pestle and mortar until the sediment was well homogenised and stored, dry, in a plastic bag.

Figure 2.5 Equilibration graph

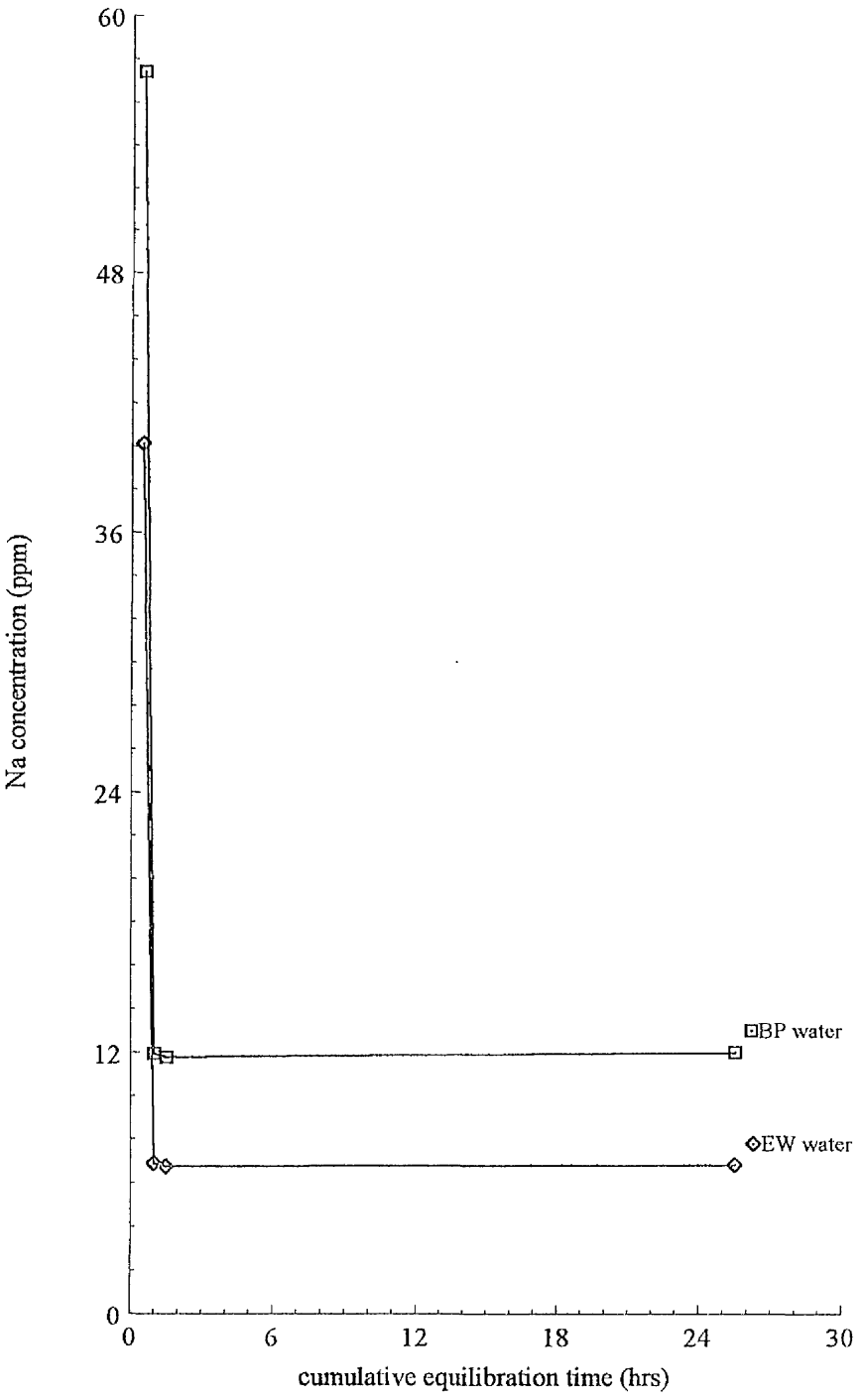

2.5 Methods Used for Sample Analysis

A trace and major cation analysis was performed on both lake waters. The sediment was analysed only for those components which are widely recognised to play an important part in sorption. A full elemental analysis of the sediment was not performed as this would not have helped in the interpretation of the sorption experiments or in our understanding of the processes which were occurring.

Freshwater Analysis

2.5.1 Determination of major cation concentrations

Three replicate samples of undiluted Botany Pond and Esthwaite water were analysed for Na^+, K^+, Ca^{2+} and Mg^{2+} concentrations using ICP - Atomic Emission.

2.5.2 Determination of trace cations

Trace cation content was determined by diluting samples of both lake waters 10 fold and passing these through an ICP - Mass Spectrometer (Fisons ICPMS - PQ2) in scan mode. The scan was analysed, and those elements which were detected at levels higher than background were analysed quantitatively using the ICP - Mass Spectrometer in peak jumping mode, using matrix-matched calibration standards and correcting for variations in instrument response.

2.5.3 Determination of total dissolved solids

TDS in both waters was determined using the procedure described in Allen (1989). 100 ml of lake water was added to an accurately weighed glass beaker and then evaporated to constant weight under a heat lamp. The difference between the mass of the empty glass beaker and the final mass recorded gave the total dissolved solids content.

Sediment Analysis

2.5.4 Determination of carbonate content

This method relies on dissolution with standard hydrochloric acid and back titration of unused acid with sodium hydroxide.

2 g of dried, sieved sediment were weighed into a 250 ml beaker and 40 ml of standard 0.5M HCl added. This was mixed well and then left to stand for two hours at room temperature. The excess acid which remained in the beaker was then titrated with 0.5M NaOH, using phenolphthalein as the indicator. Three replicates of each sediment were used, together with titration blanks of 40 ml of acid.

2.5.5 Determination of organic carbon

Samples of finely ground sediment were analysed for C, H, N content using a Carlo-Erba 1108 Analyser. Organic carbon content was found by subtracting from the analysis the mass of carbon present in the sediment in the form of carbonate.

2.5.6 Determination of Fe/Mn oxide content

The method used to strip the reducible Fe/Mn oxides from the sediment was based on that of Tessier et al (1979). 0.04M hydroxylamine hydrochloride in 25% v/v acetic acid (20 ml) was added to one gram of dried sediment. The samples were then heated in a constant temperature water bath (75°C/8 hours) and shaken well once every hour. After this time, the samples were centrifuged (7000 rpm/30 mins) and the supernatant containing the leached Fe/Mn was decanted. The supernatant samples were diluted 100-fold and analysed by ICP - Atomic Emission Spectrometry for Fe and Mn concentrations. Five replicates of each sediment were used.

2.5.7 Determination of Clay Mineralogy

Size Fractionation

A size separation was performed on each sediment, in order to obtain the <2, 2-8 and >8 μm fractions. The sediment was left overnight in deionised water, shaking end over end, in order to disaggregate any large lumps. The sediment was then equally distributed between a number of settling tubes. These tubes were filled with deionised water to a depth of 30 cm, and shaken well. The settling tubes were then placed in a water bath at constant temperature (21°C), covered with cling film to avoid contamination and left for 1 hour and 25 minutes. After this time, the deionised water was siphoned off (this contains the <8 μm fraction of the sediment), the sediment was resuspended in 30 cm of deionised water and the above procedure was repeated until the siphoned water being taken off was clear (ie. all the <8 μm particles had been separated). The sediment remaining in the bottom of the settling tubes contained the

>8 μm fraction. This was left to air dry.

The siphoned deionised water which contains the <8 μm fraction was centrifuged (1000 rpm/4mins 21 secs) and the supernatant decanted (this contains the <2 μm fraction). The 2-8 μm fraction which remained at the bottom was allowed to air dry. The supernatant solution (containing the <2 μm fraction) was centrifuged (3660 rpm/ 45 mins) until the sediment was spun out. The supernatant liquid was discarded and the <2 μm sediment fraction was left to air dry.

XRD Analysis

The best XRD analyses are obtained on the <2 μm fractions, as these are the clay size fractions and therefore should be less noisy. Analyses were carried out on a Philips PW 1730 X-ray generator running a Philips PW 1050 diffractometer. This was fitted with a curved, graphite - crystal secondary monochromator and a proportional detector. The X-ray generator was run at 40 kV, with a current of 20 mA, using a copper anode. This produced radiation with a 1.5406Å wavelength. The diffractometer was set up to run from 2θ = 3-40° with a step size of 0.02°.

Approximately 200 mg of <2 μm material was mixed with approximately 4 ml of deionised water. Any lumps in the mixture were dispersed by using a rotamixer or ultrasonic bath. Using a plastic pipette, an XRD slide was completely covered in the suspension and allowed to air dry for several days. During this time the slides were covered to avoid contamination. Once dry, the left hand side of the slide was wiped clean until a thin strip of sediment approximately 1 cm wide remained. The slide was then placed into the diffractometer and the computer programme set up.

The spectrum for Botany Pond was quite noisy, so it is possible that the peak at 14.03° was background and not a chlorite signal. This would mean that the peak observed at 7.154° was due to kaolinite and not chlorite. To distinguish between the chlorite/kaolinite peak at 7.154°, an additional slide was made, as described previously, and then heated to 550°C in a furnace for approximately 16 hours. If kaolinite was present, it will decompose and the changes in the XRD trace will be diagnostic. As will be shown later (see Figures 2.6 and 2.7), the kaolinite trace does disappear on heating.

2.5.8 Determination of cation exchange capacity (CEC)

The cation exchange capacity can be defined as the sum of the exchangeable cations that a mineral can adsorb at a specific pH, which can arise from isomorphous substitution within the mineral structure, broken bonds at mineral edges and external surfaces as well as the dissociation of accessible hydroxyl groups. There are four basic techniques which can be employed in the calculation of the cation exchange capacity.

1. summation method - involving the measurement of the displaced, exchangeable cations.
2. direct displacement of a saturating index cation.
3. displacement of a saturating index cation after washing free from the saturating salt.
4. radiotracer measurement of the index cations.

The best technique to use to determine the CEC depends on the type of mineral/soil which is to be analysed. Most CEC calculations are based on saturation with ammonium as the index cation. Low results can be obtained using this method with,

for example, 1:1 clays such as kaolinite in which ammonium cannot completely replace aluminium and hydrogen, and with 2:1 minerals where ammonium may become fixed and cannot be exchanged. Ammonium as the saturating cation should also be avoided when calculating CEC for sediments containing a high concentration of carbonate, as the ammonium cation can attack and dissolve carbonate material. It was therefore decided to use sodium saturation to determine CEC in this work.

100 mg of sediment was weighed into a 50 ml Oak Ridge centrifuge tube. 10 ml of 1M NaOAc, pH 8.2 was added, shaken and then left overnight. This was then centrifuged, and the supernatant decanted. A further 10 ml of NaOAc was added and the saturation process repeated another four times. The sediment was then shaken with 10 ml ammonium acetate, centrifuged and the supernatant decanted into a 100 ml flask. This was repeated another six times and the solution diluted to 100 ml. The concentration of Na^+ ions was determined by ICP - Atomic Emission Spectrometry. Three replicates were used from each sediment.

$$CEC = \frac{Na^+ \text{ displaced (mol)}}{\text{mass of sediment used (g)}} \times 1000 \quad (\text{UNITS } mol_c kg^{-1})$$

2.6 Results and Discussion

The results of the major and trace element analysis on the lake waters are shown in Table 2.2. In addition to the major cations, the scan on the ICP - Mass Spectrometer detected the presence of iron and strontium in both waters, and uranium in Botany Pond water. Botany Pond water contains a high concentration of calcium ions and also a significant concentration of sodium ions. The concentrations of magnesium and

potassium in this water are fairly low in comparison. In contrast, Esthwaite water has a much lower ionic strength, with lower concentrations of both calcium and sodium ions, although again these are still the dominating cations.

On evaporation, the cations present in both lake waters will be present not only as oxides, but also as silicates, sulphates, phosphates, chlorides and nitrates, which explains the large difference in mass between the total cation concentration and the total dissolved solids content.

Table 2.2 Results of lake water analysis

	CONCENTRATION (mgl^{-1})	
CATION	BOTANY POND	ESTHWAITE WATER
Ca(±1SD)	59.9±0.9	11.9±0.4
Mg(±1SD)	2.6±0.02	1.6±0.02
Na(±1SD)	15.4±2	7.1±0.5
K(±1SD)	2.1±0.3	0.74±0.1
Fe	0.69	0.18
Sr	0.21	0.04
U	$1.2x10^{-4}$	$<5x10^{-5}$
pH	7.0	5.5
TDS	278	70

Results of the sediment analyses are shown in Table 2.3. Botany Pond is a carbonate rich sediment, containing a significant quantity of reducible iron and manganese and also organic carbon. By comparison, Esthwaite Water sediment contains undetectable carbonate but has higher concentrations of organic carbon and reducible iron and manganese. The cation exchange capacity was observed to be higher in Esthwaite

Water sediment than in Botany Pond sediment.

Table 2.3 Results of sediment analysis

CONSTITUENT	CONCENTRATION (mgg^{-1})	
	BOTANY POND	ESTHWAITE WATER
carbonate	229±10	<1.3
reducible Fe	6.0±0.2	16.4±0.6
reducible Mn	0.44±0.02	0.70±0.03
organic carbon	79.0±0.7	118±3
CEC ($mol_c kg^{-1}$)	0.50±0.01	0.60±0.01

Figures 2.6-2.8 show the XRD traces for the two sediments. Quantitative analysis of the clay mineralogy content was not attempted as this can be unreliable. The possibility of over-coating of clays with hydrous iron oxide phases and particularly carbonates, together with the presence of poorly crystalline and mixed-layer clay minerals only leads to semi-quantitative results at best, and therefore inclusion of such data can actually be misleading.

As well as containing quartz, Botany Pond sediment was seen to contain quantities of muscovite and kaolinite. Analysis of Esthwaite Water sediment revealed the presence of quartz, muscovite and chlorite.

Figure 2.6 XRD analysis of Botany Pond sediment

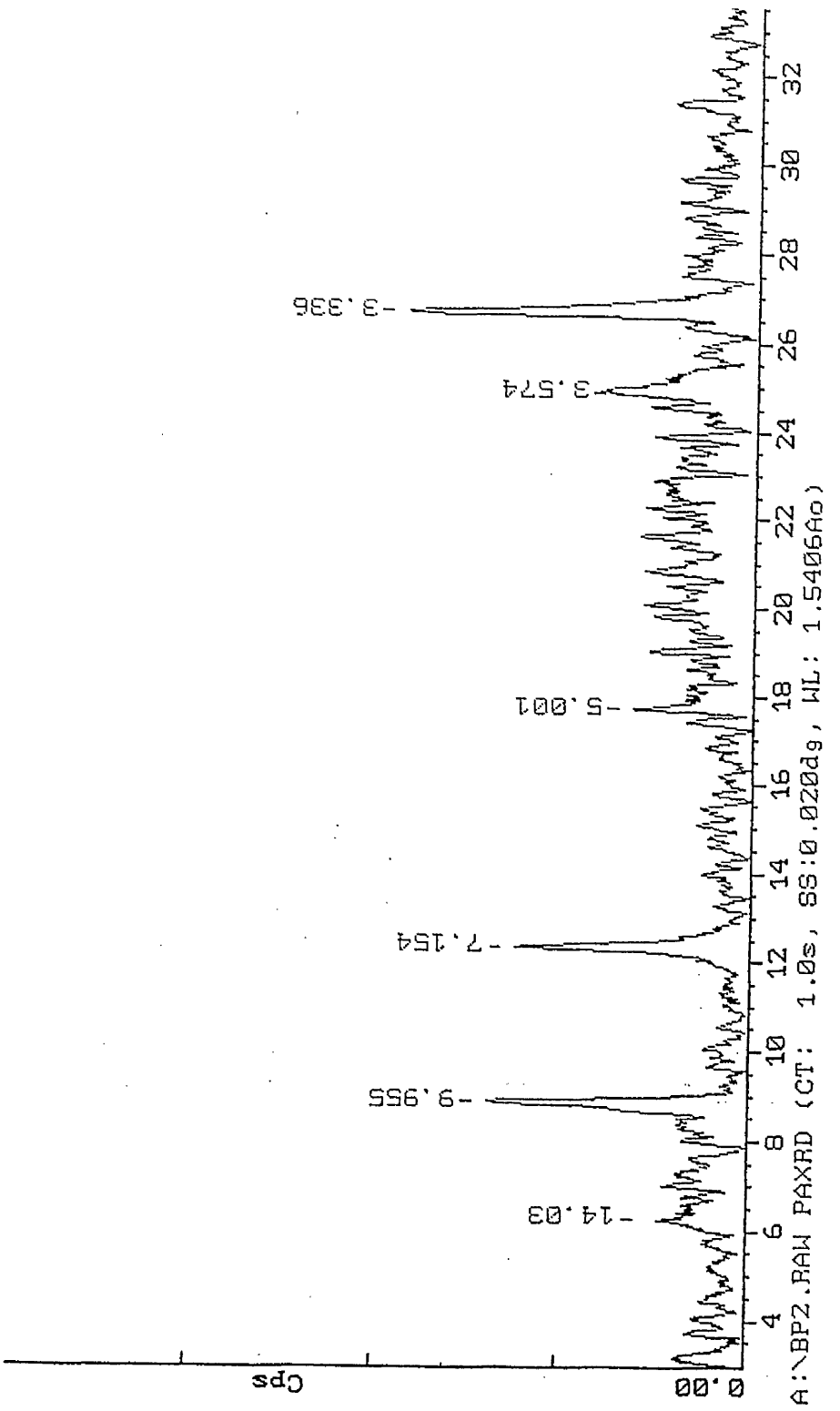

Figure 2.7 XRD analysis of Botany Pond sediment after heating to 550°C

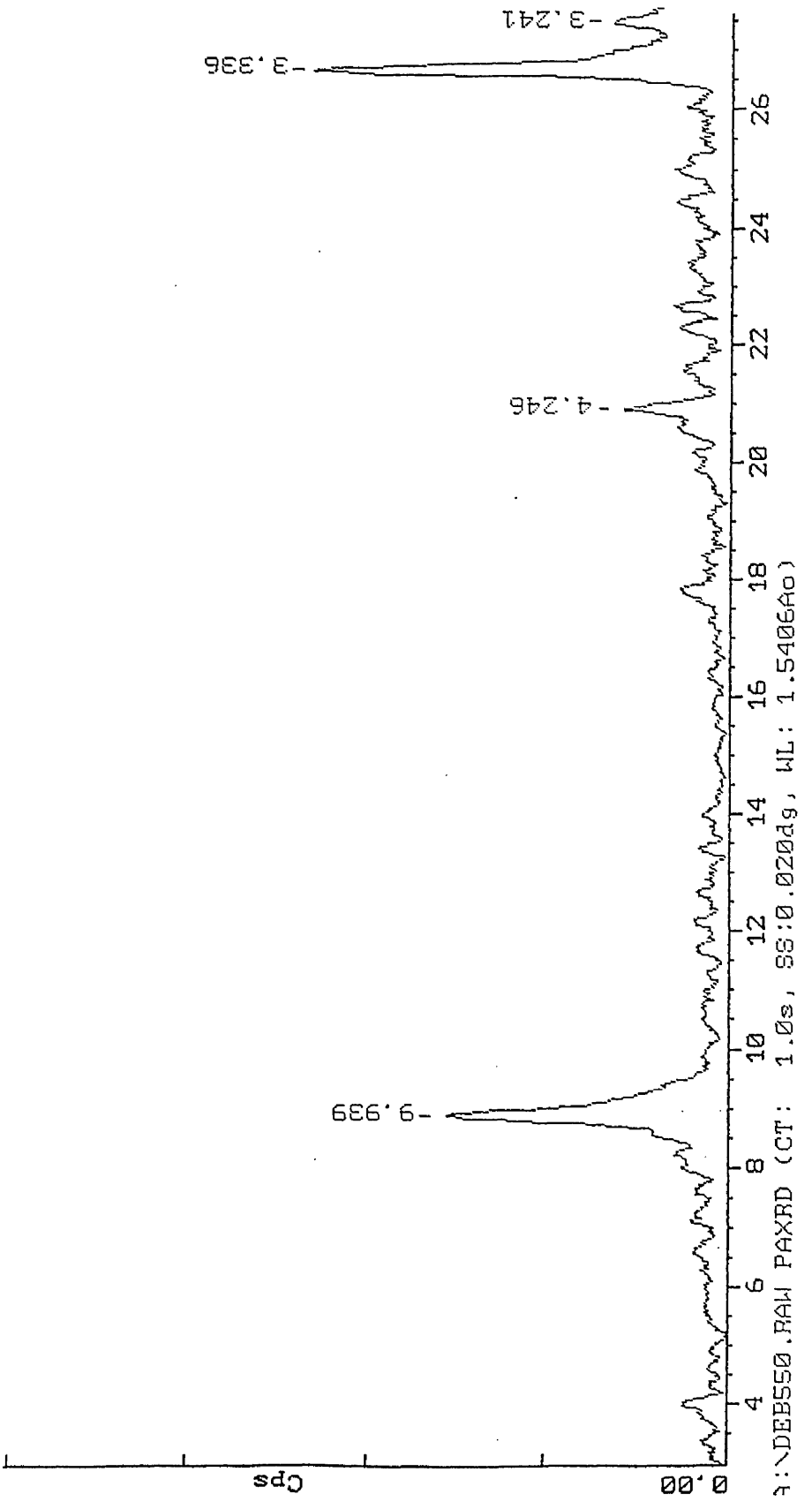

Figure 2.8 XRD analysis of Esthwaite Water sediment

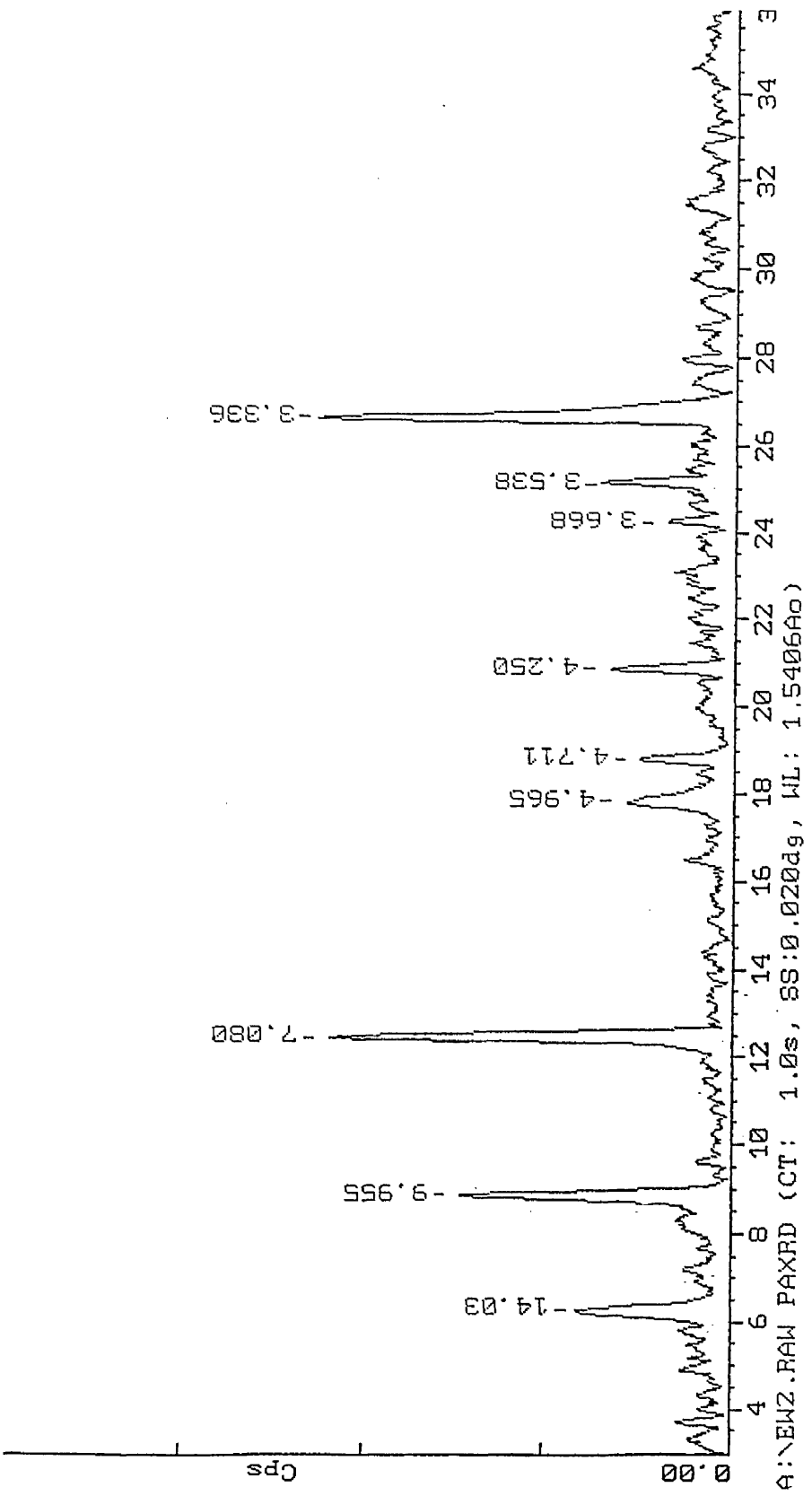

CHAPTER 3 - ADSORPTION STUDIES

CHAPTER 3 - ADSORPTION STUDIES

3.1 Introduction

There are several methods which can be used to measure the solid-solution partitioning of a radionuclide following sorption. Duursma and Bosch (1970) compared results from sorption experiments using three different techniques.

The *suspension technique* (shown in Figure 3.1) was very similar in procedure to the commonly used batch method. A known amount of sediment and water was spiked with radioisotope and then sampled periodically to determine the spike content remaining in solution. Phase separation was achieved by filtration through two Millipore filters (0.45μm), the lower one serving as a blank. The *thin layer technique* (shown in Figure 3.2) used 10 mg of sediment spread evenly over the surface of a set of filters which were then placed carefully in a dish containing filtered water and a known amount of spike. After the sorption time had elapsed, 1ml of solution, one filter with sediment and one blank filter were removed from the dish. Spike content in each was then determined and the distribution coefficient calculated. The *sedimentation method* (shown in Figure 3.3) used a 250 ml cylinder which contained filtered water and a known amount of spike. After thoroughly mixing, a known quantity of sediment was added to the top of the water column and allowed to settle. Samples of water were taken from the top of the cylinder over a period of days and the spike content determined.

Generally, the suspension and thin layer techniques gave comparable results although the thin layer technique took slightly longer to reach equilibrium. The sedimentation

Figure 3.1 Diagram to illustrate the suspension technique (Duursma and Bosch, 1970)

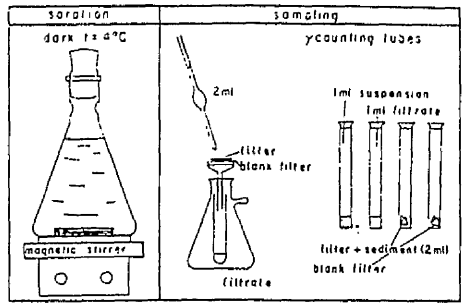

Figure 3.2 Diagram to illustrate the thin layer technique (Duursma and Bosch, 1970)

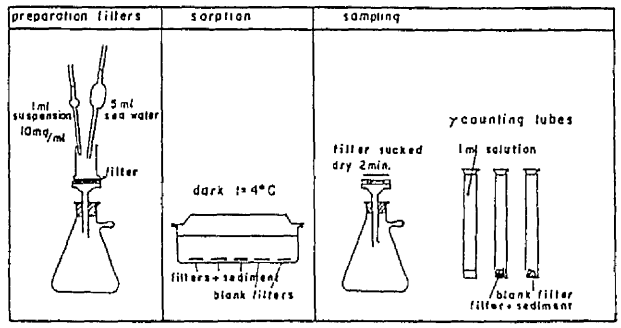

Figure 3.3 Diagram to illustrate the sedimentation technique (Duursma and Bosch, 1970)

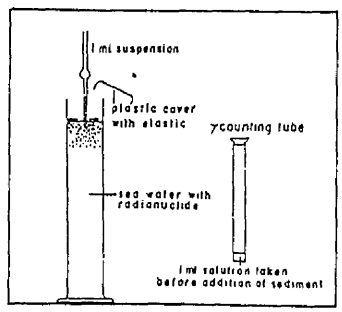

method was found to be the easiest method, and especially applicable in the study of scavenging processes.

Other methods which have been used include through-diffusion and high pressure convection (Berry et al, 1988). These methods studied more closely the rate at which the spike diffused through a sample (shown in Figures 3.4 and 3.5). It is also possible to measure distribution coefficients in-situ, by measuring the concentrations of naturally occuring radionuclides in a rock and pore water from an appropriate source (Santschi et al, 1988a). The problems with this method and the applicability of in-situ Kd values are discussed by McKinley and Alexander (1992). All of these methods attempt to resemble the situation in the field more closely, thereby eliminating many of the variable parameters which can be encountered when using the simpler batch method.

Despite the development of these other, sometimes more realistic experimental procedures, the batch method continues to be the most popular technique used to measure the solid-solution partitioning of a radionuclide (Torstenfelt et al, 1982; West et al, 1991; Davies and Shaw, 1993; Meier et al, 1994). The main advantages of the batch process are that it is relatively easy to carry out and obtain results within a reasonably short time frame, without needing great amounts of solid, solution and radionuclide and it is also quite easy to change the conditions under which sorption is taking place (e.g. pH, temperature), whereas the other methods often require longer equilibration times and more elaborate equipment. It is also possible to adapt the batch experiment to study both adsorption and desorption behaviour, which is not possible for some of the other methods. However, the batch method also has some well documented problems associated with it (Benes et al, 1994). It is often considered to

Figure 3.4 Diagram to illustrate the through diffusion technique (Berry et al, 1988)

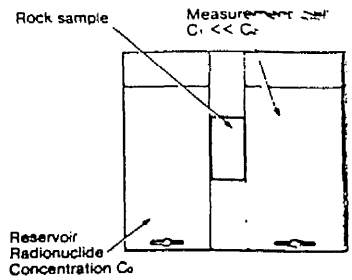

Figure 3.5 Diagram to illustrate the high pressure convection technique (Berry et al, 1988)

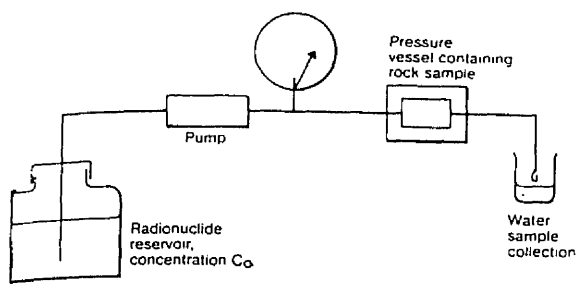

be unrealistic, not accurately reflecting the environmental conditions which are found in natural systems. The volume : mass ratios used in the batch process, due to practical considerations (e.g. obtaining complete phase separation), are much larger than those found in natural systems (V/M ratio in geological environments <<1 ml/g, whereas ratios used in the batch process are frequently a couple of orders of magnitude larger). Sorption has been found to be dependent on this volume : mass ratio, an increase in distribution coefficient being observed with an increase in the ratio (Garder and Skulberg, 1964; Benes and Poliak, 1990; Meier et al, 1994; Hsu and Chang, 1995), although Torstenfelt et al (1982), noticed very little effect on sorption for short term experiments.

Also important, particularly with radiocaesium, is the quantity of radionuclide added to the experiment. Very often the concentration of radionuclide used in the batch process greatly exceeds the concentrations found in nature and this can affect sorption behaviour. At low concentrations ($<10^{-8}$ M) the distribution coefficient is independent of the concentration of radionuclide. However, at higher concentrations, sorption is non-linear, i.e. uptake is not proportional to the concentration. Non-linear behaviour means that a Kd value is only valid for one particular radionuclide concentration. A decrease in Kd has been observed with an increase in initial Cs concentration (Benes et al, 1989; Meier et al, 1994; Staunton, 1994) due to the existence of distinct exchange sites of increasing Cs selectivity (refer to Section 1.7.4).

Other problems with the batch technique include incomplete phase separation, loss of radionuclide to the vessel walls, abrasion of the particles by collision with the vessel walls during shaking/stirring, and also the effect of the pretreatment of the particles (eg. sieving, drying and grinding). Using particles where there has been no prior

treatment can cause difficulties in experimental reproducibility, as the solid particles are often taken from inhomogeneous bulk samples which will exhibit different sorptive properties. Pretreatment ensures that the solid particles are representative of the bulk sample.

The importance of these experimental conditions mean that data from different batch experiments cannot be compared unless conditions were identical. Providing a thorough, detailed report of the conditions in which the batch experiment was carried out helps to allow comparison of results between different laboratories. By understanding the experimental limitations of the batch method however, and by exercising a suitable amount of caution when interpreting the results (as with any experimental data), it is possible to obtain good, reproducible and, most importantly, useful data which reflect the sorptive behaviour of radionuclides.

3.2 Application of the batch technique

In order to compare the effect of different sediment and water chemistries on sorption, work was carried out using both sediment and water from the same lake and also using a mixture of sediment and water from the two different lakes. Hence, there were four different freshwater systems in total;

Botany Pond sediment - Botany Pond water	(BPBP)
Botany Pond sediment - Esthwaite water	(BPEW)
Esthwaite sediment - Botany Pond water	(EWBP)
Esthwaite sediment - Esthwaite water	(EWEW)

The sorption experiments were carried out in 50 ml polypropylene Oak Ridge centrifuge tubes, using 5 identical replicates, enabling a mean value of the distribution ratio and a standard deviation to be found.

Finely ground sediment particles (300 mg) and lake water (30 ml) were allowed to hydrate for 24 hours, before a spike containing ^{57}Co (1.122 kBq), ^{85}Sr (0.984 kBq), ^{103}Ru (1.111 kBq) and ^{134}Cs (8.102 kBq) was added. The radionuclides were obtained from Amersham UK (^{85}Sr and ^{134}Cs) and CEA DAMRI (^{57}Co and ^{103}Ru). The total volume of spike added to each experiment did not exceed 0.5 ml. All of the radioisotopes were diluted before use so that the amount of carrier used in each experiment was less than 0.5 μg of each element. The samples were shaken well and kept in the dark for a specified contact time at room temperature. The adsorption contact times were chosen so that both short term and long term processes could be studied. These times ranged from 30 minutes to over two months. During this time, the samples were kept aerated to keep microbial activity to a minimum, and they were shaken daily. A control experiment was set up so that pH could be monitored throughout the experiment (pH values for the four freshwater systems are shown in Table 3.1). It was found to remain constant (within 0.2 units). This was as expected, due to the pre-equilibration of the sediment and water.

Table 3.1 Experimental pH values for the four systems

SYSTEM	pH
BPBP	7.2
BPEW	7.2
EWBP	6.6
EWEW	5.9

After the contact time had elapsed, the samples were centrifuged (12,000g/45mins) and the lake water decanted. The supernatant was counted on a gamma photon detector and the resulting spectrum analysed to determine radioisotope content.

A set of blanks were also set up, containing just spike and water, to determine any spike loss via precipitation and sorption to tube walls. These were counted periodically on a germanium-lithium gamma detector and the resulting spectra analysed for spike content. Losses of each isotope were found to be less than 2% and were therefore treated as negligible. The used centrifuge tubes were also counted in order to measure losses to the tube walls. No activity was detected.

Adsorption results are presented in Section 3.7.1.

3.3 Phase Separation

It is important to obtain a complete phase separation following sorption, as even a tiny amount of the spiked solid remaining in solution will lead to an imprecise and misleading measurement of the distribution of the radionuclide, particularly if only small amounts of activity are being dealt with or if the radionuclide has a high Kd. In order to achieve complete separation both centrifugation and filtration can be used. Problems can be encountered during filtration however, as the size of the particles which are separated is dependent only on the pore size of the filter membrane and losses of activity are possible, due to sorption onto papers and filtration equipment, although these have been reported to be low for the isotopes used in this work (Garder and Skulberg, 1964; Bunzl and Schimmack, 1991). To determine the best method of phase separation, simultaneous adsorption experiments were carried out under identical

conditions. Using the adsorption procedure described in Section 3.2, five replicate samples for each freshwater system were spiked with ^{57}Co (0.714 kBq), ^{85}Sr (1.16 kBq), ^{103}Ru (0.480 kBq) and ^{134}Cs (9.79 kBq) and then left for an adsorption time of 8 hours. One set of replicate samples was then separated by centrifugation only (12,000g/45mins), and the other set of replicate samples was separated by centrifugation (12,000g/45mins) followed by microfiltration using Whatman GF/A paper prefilters and Whatman cellulose nitrate 0.45 μm membrane circles. Following phase separation, the aqueous solutions were analysed on a gamma photon detector. The results of this study are discussed in Section 3.7.2.

3.4 Reproducibility

To ensure that the sediment and water used in each experiment was homogeneous and representative of the bulk sample, 5 identical replicate samples were used for each time point (as explained in Section 3.2). An indication of the reproducibility of the experiment is given by the standard deviation of the results.

In addition to this, using the adsorption method described previously in Section 3.2, a spike of ^{134}Cs was added to Botany Pond sediment and water, and sorption measured at several different time points to ensure that the results could be reproduced. The results of this study are discussed in Section 3.7.3.

3.5 Sterilisation

During the adsorption experiment, spiked samples were stored in the dark and kept aerated in order to minimise microbial activity. However, as these samples contained

real lake sediment and water, there will always be some biological activity present. Several strange observations were made at longer sorption times, particularly with the Esthwaite Water sediment. It was thought that these could be ascribed to biological activity. Biological activity within the sample could have several effects. The radionuclides could be taken up by the microorganisms, then released into solution again when they die. It is also possible that the microorganisms could actually compete with the radionuclides for sorbing sites. Biological activity could also change the conditions, such as pH and Eh, within the system, thereby affecting the sorption behaviour of redox sensitive elements such as cobalt and ruthenium.

There are several methods which can be used for sterilisation. These include the addition of compounds such as sodium azide (an aerobe growth inhibitor) although this would change the composition and the ionic strength of the solution and possibly alter the distribution ratio. Irradiation of the samples could possibly cause radiolysis, generating reactive species, and autoclaving could possibly change clay structure and alter the sorptive properties of the sediment. West et al (1991), however found little difference in the Rd values of ^{137}Cs following sorption on to unaltered rock and rock which had been autoclaved. Interestingly, rock which had been dry sterilised in a warm air oven was seen to have a higher capacity for sorption, and this was ascribed to changes in the montmorillonite layer structure. It was eventually decided that the samples used in this study should be autoclaved.

Finely ground Esthwaite Water sediment particles (300 mg) and Esthwaite lake water (30 ml) were allowed to hydrate for 24 hours, before a spike containing ^{57}Co (0.732 kBq) and ^{134}Cs (9.617 kBq) was added. Five identical replicates were used for each time point. The samples were shaken well in a sealed tube and then left in a pressure

cooker for 15 minutes at approximately 120°C and elevated pressure. Sterilisation was shown to be complete when the autoclave tape went black.

The sterilised samples were kept sealed, shaken daily and stored in the dark at room temperature, until the contact time had elapsed. Contact times ranged between 6-10 weeks. After this time, the samples were centrifuged (12,000g/45 mins) and the supernatants decanted. The solutions were counted on a gamma photon detector, and the resulting spectra analysed for spike content. The results of this study are discussed in Section 3.7.4.

3.6 Sample analysis and counting

3.6.1 Sample preparation

The supernatant samples collected from the experimental procedures described in Sections 3.2-3.5 were decanted carefully into sterile 60 ml polystyrene specimen containers. As the spike activity in solution was often low, particularly for ^{134}Cs, all of the supernatant solution was used in sample analysis (i.e. 30 ml). This also ensured that counting geometry remained constant throughout the work. It was not found to be necessary to acidify the samples prior to analysis. After decanting, the solutions were checked to make sure that no sediment had entered the counting pot as this would have a significant effect on the spike activity measured.

3.6.2 Equipment used in sample analysis

Gamma spectrometry was used to detect ^{57}Co (122 keV), ^{85}Sr (514 keV), ^{103}Ru (497

keV) and ^{134}Cs (796 keV). The counting equipment consisted of two high purity germanium semi-conductor gamma photon detectors and one lithium drifted germanium gamma photon detector, each surrouded by 2-4 inches of lead shielding. The detectors were energy calibrated periodically using a sealed ^{152}Eu source.

3.6.3 Sample analysis

Sample analysis was performed as quickly as possible after decantation to avoid increasing counting errors due to radioactive decay. A counting time of 10,000 seconds was used for each sample. A matrix-matched standard of the isotopes of identical counting geometry was also counted at regular intervals in order to determine the spectrometer efficiency.

3.6.4 Data analysis

The resulting spectra were analysed and the peak areas (cps) calculated using an in-house interactive gamma ray analysis programme. The activity of spike present in the sample was then calculated by taking the counting efficiency of the spectrometer into account. Due to the short half-lives of the radioisotopes used, the activities of the radioisotopes were also decay corrected back to the date of spiking and then the distribution ratios and the percentage of spike sorbed on to the sediment were calculated.

3.7 Results and Discussion

3.7.1 Change in sorption over time

It is important to note that in all of these graphs, the x-axis is (contact time)$^{1/2}$. This was necessary in order to accomodate the wide range of contact times.

(1) ^{57}Co

Sorption of ^{57}Co on to Botany Pond sediment (shown in Figure 3.6) is seen to increase with time, with approximately 60% being sorbed after just 30 minutes. Sorption then continues at a slower rate - indicated by a gradual change in Rd - for the duration of the experiment. This is consistent with observations from other studies (Abdel Gawad et al, 1977; Li et al, 1984; Nyffeler et al, 1984; Lima et al, 1994). The distribution ratio continues to increase which suggests that sorption of ^{57}Co on to Botany Pond sediment is still continuing after 1700 hours. Grutter et al (1994) found that sorption was incomplete after 56 days and Nyffeler et al (1984) found that sorption still continued after 108 days. The slow increase which is observed could be due to the oxidation and incorporation of cobalt into manganese oxides present in the sediment, as previously mentioned in Section 1.7.1.

As the presence of competing cations has no observed effect on the sorption of cobalt (Tewari et al, 1972; Murray, 1973) it would be expected that the only differences in sorption observed on comparison of the two sediments would be due to differences in sediment composition, particularly in the manganese content. As Esthwaite Water sediment has a greater concentration of manganese it would be expected that sorption

Figure 3.6 ^{57}Co sorption in BPBP system

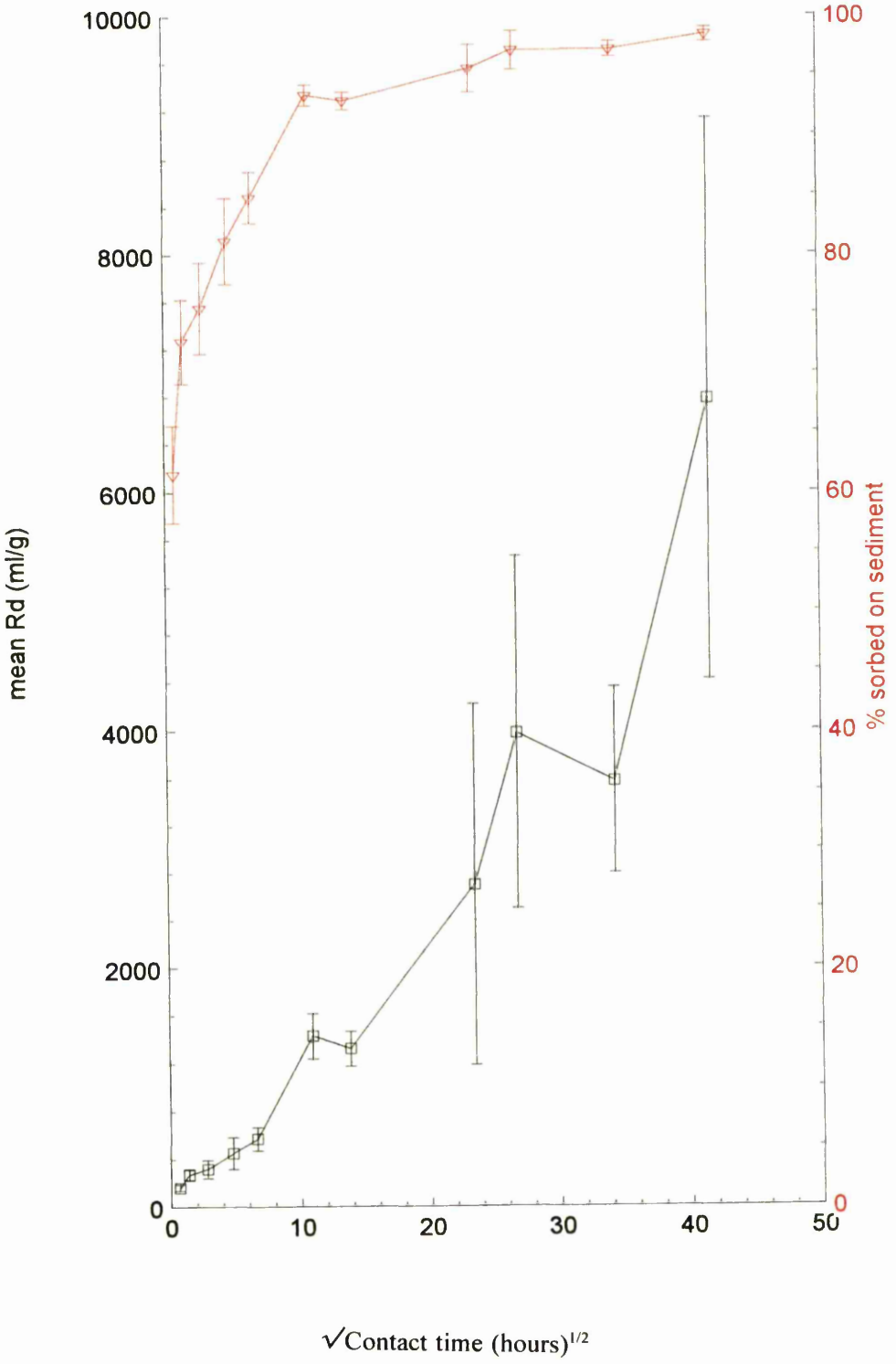

Figure 3.7 ^{57}Co sorption in EWEW system

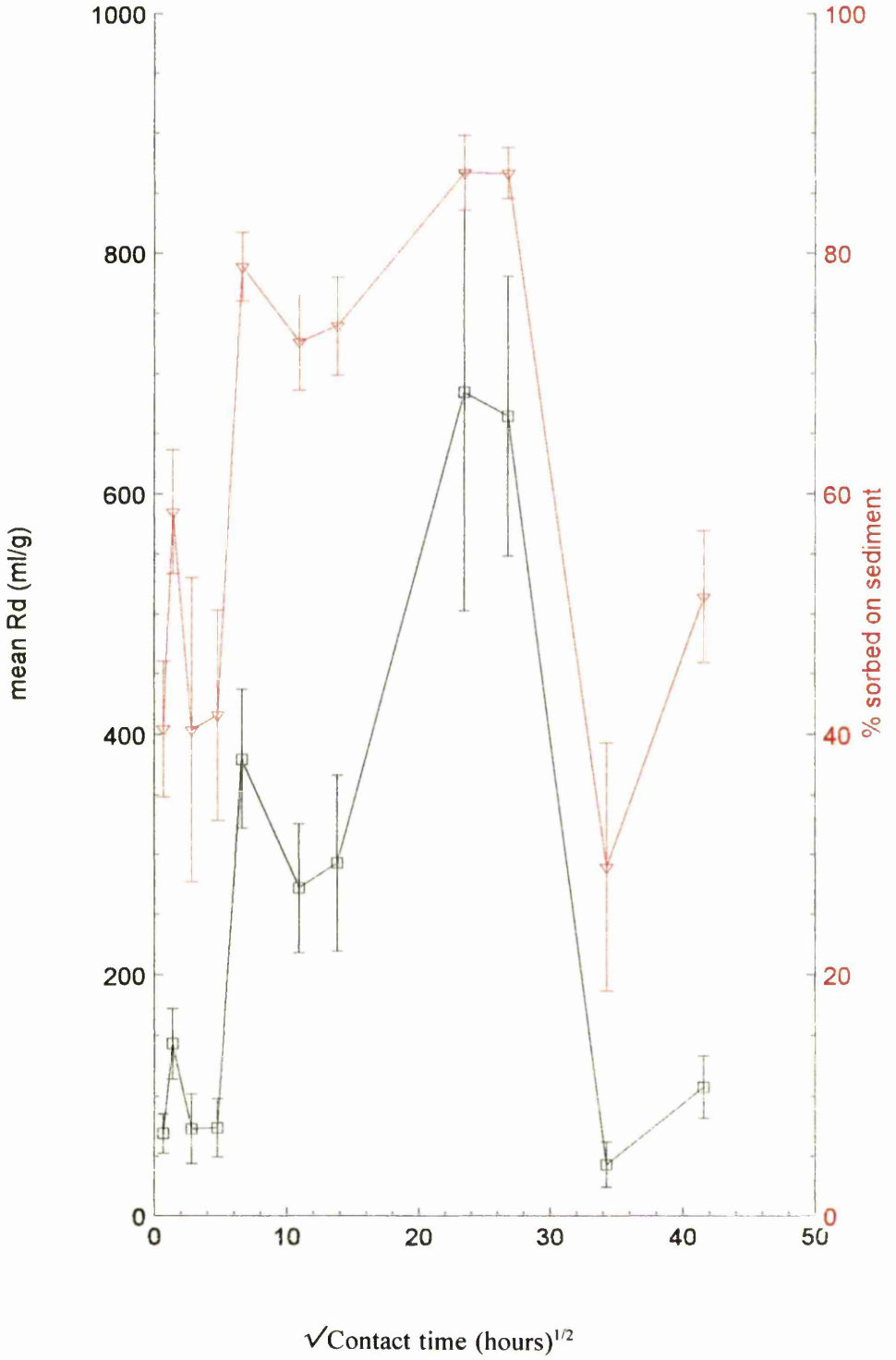

Figure 3.8 ^{57}Co sorption in BPEW system

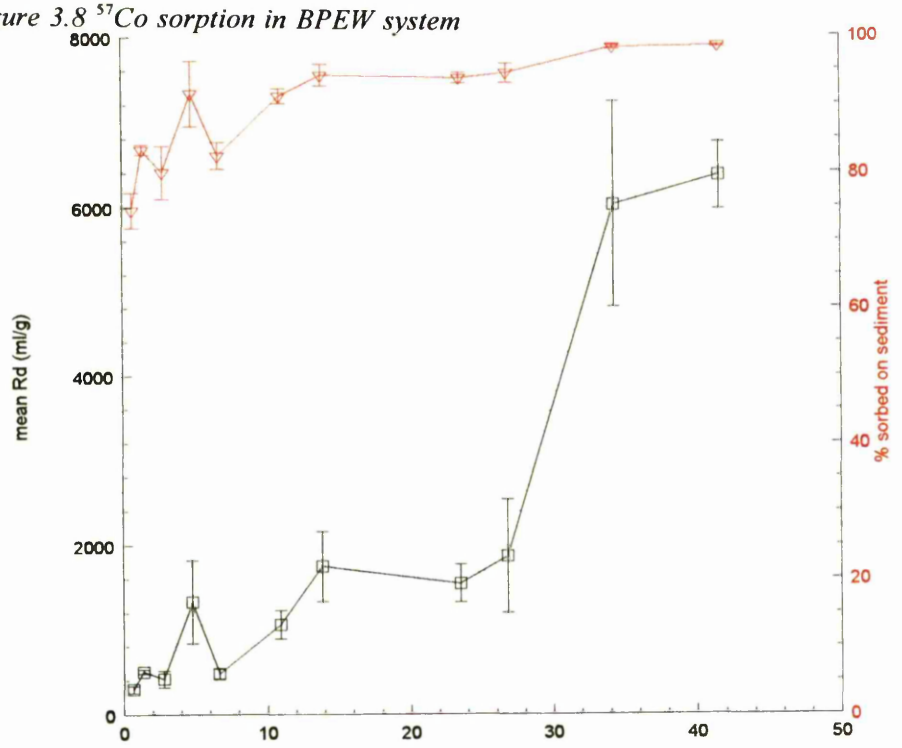

√Contact time (hours)$^{1/2}$

Figure 3.9 ^{57}Co sorption in EWBP system

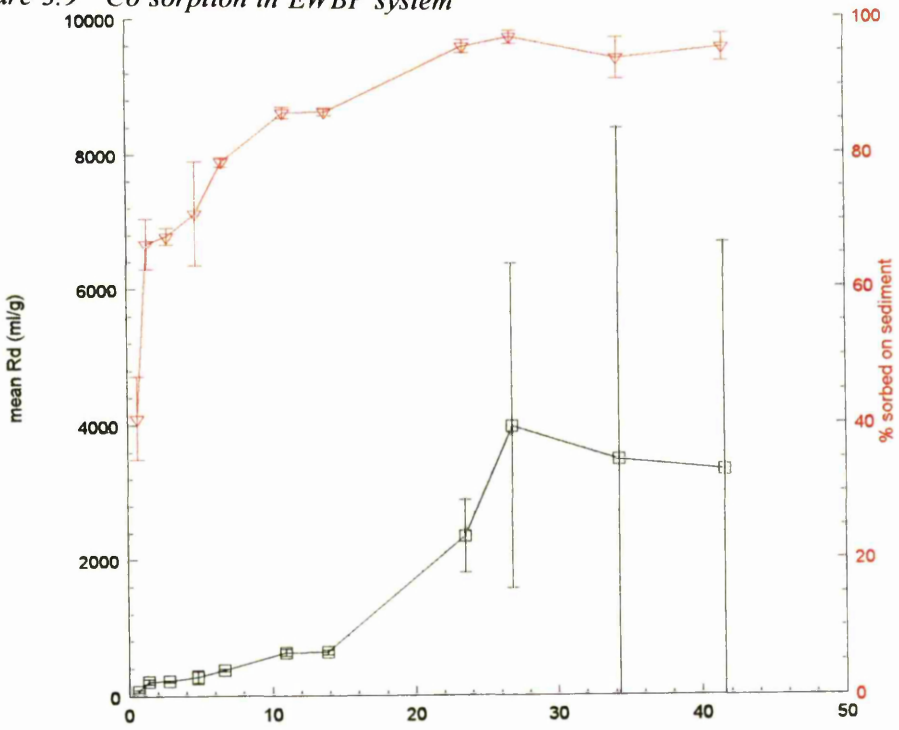

√Contact time (hours)$^{1/2}$

of cobalt would be greater on this sediment since Nyffeler et al (1984) observed higher distribution coefficients for a sediment which was enriched in manganese oxides. However, this was not observed. This could be due to a large excess of sorption sites in both systems, resulting from high concentrations of Mn oxide and a comparatively low concentration of cobalt in solution.

Sorption of ^{57}Co on to Esthwaite Water sediment (shown in Figure 3.7) is a little noisier although certain trends can still be observed. ^{57}Co sorption occurs to a lesser extent, compared with Botany Pond sediment, with only approximately 40% of Co being sorbed after 30 minutes. Generally, Co is seen to sorb slowly on to the sediment until approximately 85% sorption is reached. After 1000 hours, a significant decrease in sorption occurs with only approximately 40% of ^{57}Co now sorbed to the sediment.

The noisiness of the data compared to the data from Botany Pond implies that there are certain processes occurring which are interfering with cobalt sorption. As the stability of manganese oxides is known to be dependent upon both pH and Eh, it could be that these parameters are not remaining constant within this system during the time scale of the experiment. Manganese oxide solubility is greatest at low pH and/or low Eh (Crerar et al, 1972), but as pH was monitored throughout the experiment and anaerobic conditions were avoided by keeping the samples well oxygenated, it seems unlikely that manganese oxide dissolution was the cause of the unusual sorption behaviour at longer adsorption times.

The effect of solution chemistry upon cobalt sorption was studied by using Botany Pond sediment with Esthwaite water, and Esthwaite Water sediment with Botany Pond water (shown in Figures 3.8 and 3.9 respectively). Esthwaite water has fewer potential

competing cations, and so a slight increase in sorption was observed when this water was used with Botany Pond sediment (especially at the earlier time points). Sorption on to Esthwaite Water sediment using Botany Pond water was considerably less noisy at earlier time points than when Esthwaite water was used. At later time points however, the error bars are >100%. This is due to the existence of a "flyer" within the data set. Without including the "flyer" in the mean Rd value gives a mean Rd (±1SD) of 1290 (±190) mlg^{-1} after an adsorption time of approximately 1000 hours and a mean Rd value (±1SD) of 1820 (±300) mlg^{-1} after an adsorption time of approximately 1700 hours. This suggests that a decrease in sorption is still being observed (as with the EWEW system), although it is less pronounced. In general sorption was greater on to Esthwaite Water sediment when using Botany Pond water, but the amount of Co sorbed was still less than the amount of sorption which took place on Botany Pond sediment.

(2) ^{85}Sr

Figure 3.10 illustrates the change in sorption over time of ^{85}Sr on to Botany Pond sediment. Within 30 minutes, approximately 55% sorption has occurred. This rapid initial uptake of strontium has also been observed by Torstenfelt et al (1982) and Keren and O'Connor (1983). Whereas an equilibrium was then observed in those studies, sorption on to Botany Pond sediment is seen to increase with time to approximately 70% sorption. Benes and Poliak (1990) also observed a slower period of sorption following an initial rapid uptake of approximately 100 minutes. They concluded that the rapid sorption arose from ion exchange with easily exchangeable strontium. The slower increase was described as either isotope exchange with less accessible strontium in the sediment or to a slow change in the sorption properties of

the sediment. Sorption on to Botany Pond sediment then decreased gradually at 500 hours until it remained reasonably constant at approximately 60%. As with ^{57}Co, several of the mean Rd values have variation coefficients which are >100%. In each case, this is due to a single exceptionally high Rd value within the five replicate samples. Without taking this Rd value into account, the following mean Rd values are obtained: after an adsorption time of 8 hours, the mean Rd (±1SD) is 81 (±14) mlg^{-1}, after approximately 24 hours, 97 (±3) mlg^{-1}, and after an adsorption time of approximately 1000 hours a mean Rd (±1SD) of 103 (±4) mlg^{-1} is calculated.

Strontium sorption is known to be dependent upon both the cation exchange capacity of the sediment and the ionic strength of the solution (Torstenfelt et al, 1982). As Esthwaite Water sediment has a higher cation exchange capacity than Botany Pond sediment and Esthwaite water has a lower ionic strength than Botany Pond water, it would be expected that strontium sorption would be much greater in this system. Initially, this is observed. Sorption on to Esthwaite Water sediment (shown in Figure 3.11) shows an initial rapid uptake, with approximately 60% sorption occurring within 30 minutes. Sorption then increases slowly to 80% until 100 hours is reached, at which time sorption decreases rapidly until 1000 hours where it then remains constant at approximately 40%. The more significant decrease which is observed at approximately 1000 hours is again similar to that seen in this system during cobalt sorption, providing further evidence that a change might have occurred in the system at this time.

Results from mixing the sediments and water show the dependence of strontium sorption on the competing cations in solution. When Botany Pond sediment was mixed with Esthwaite water (shown in Figure 3.12), a higher percentage of strontium was

Figure 3.10 ^{85}Sr sorption in BPBP system

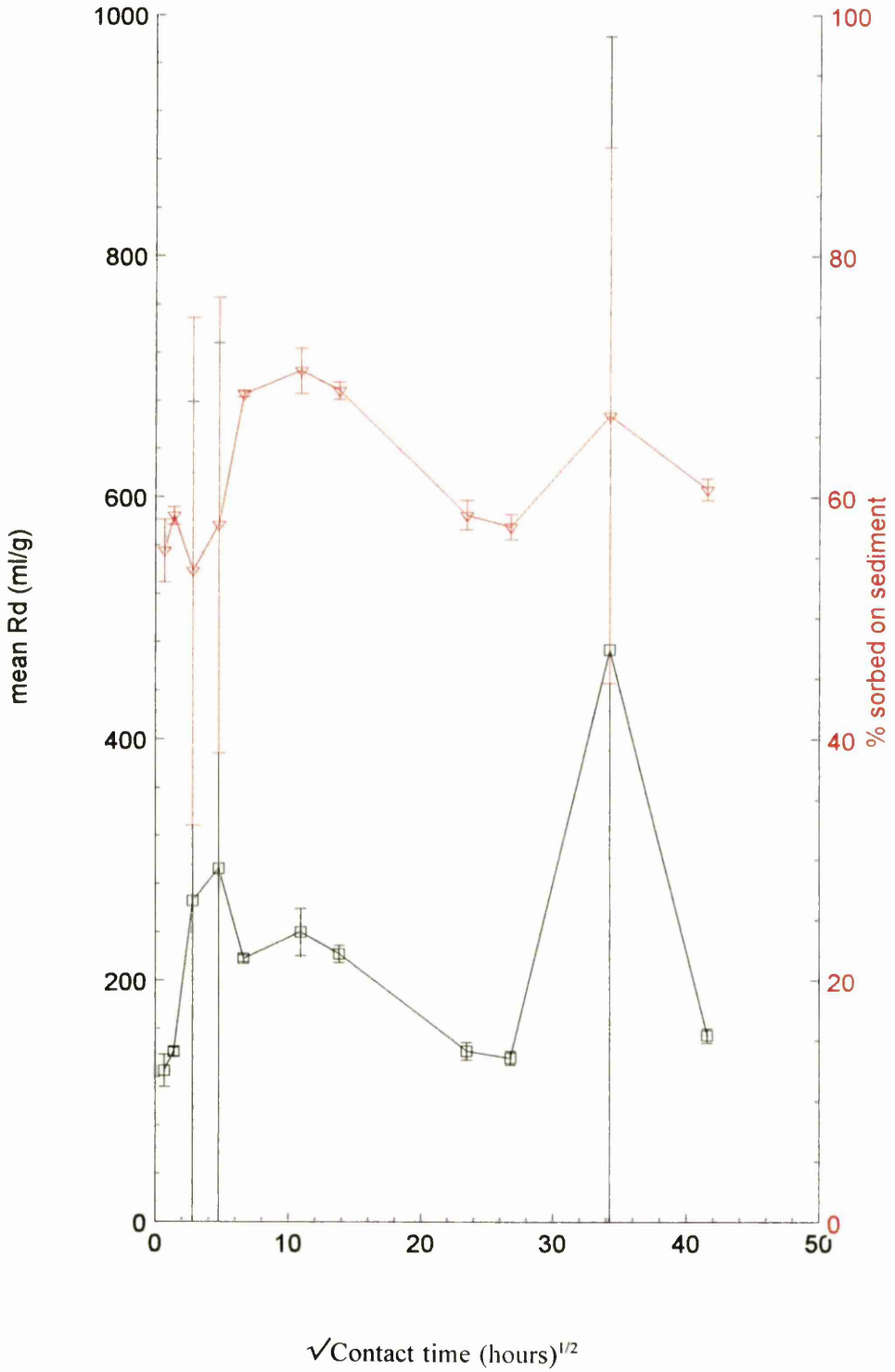

Figure 3.11 ^{85}Sr sorption in EWEW system

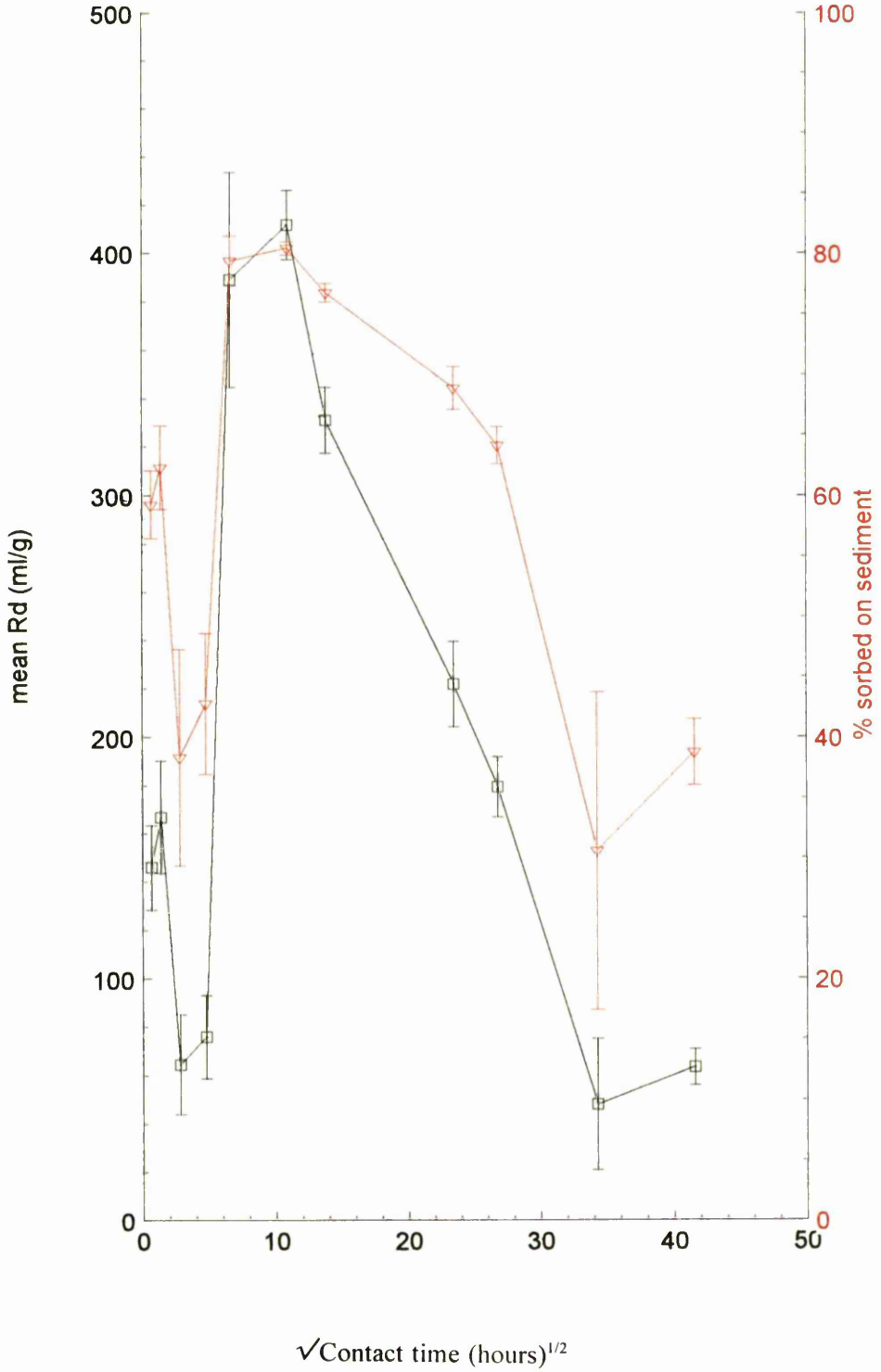

Figure 3.12 ^{85}Sr sorption in BPEW system

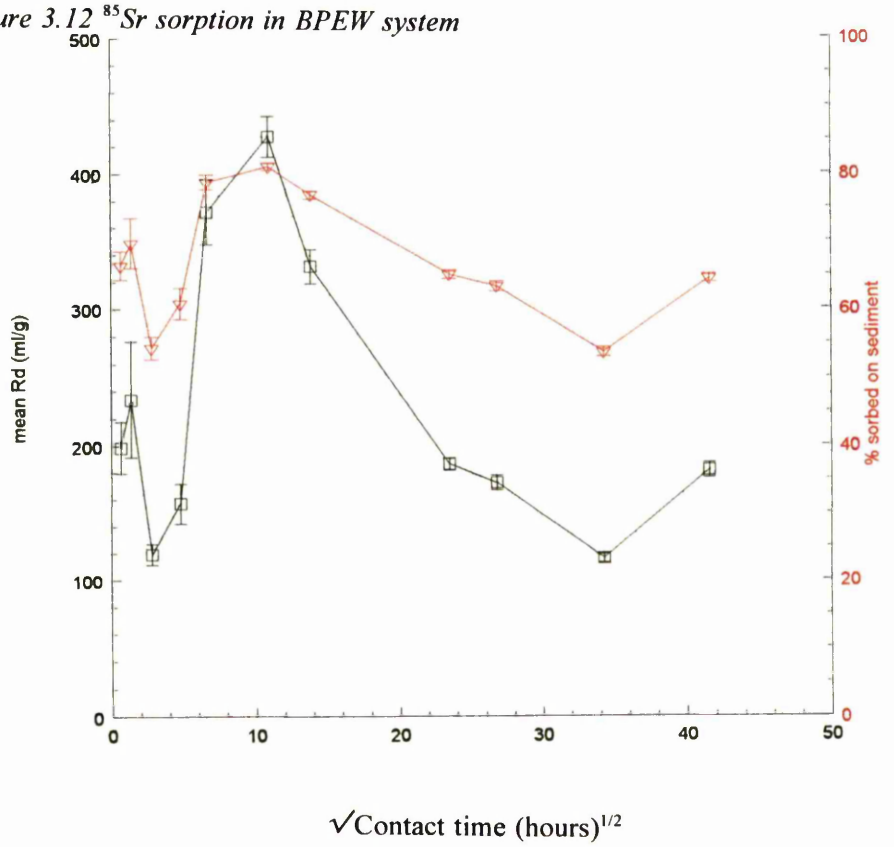

Figure 3.13 ^{85}Sr sorption in EWBP system

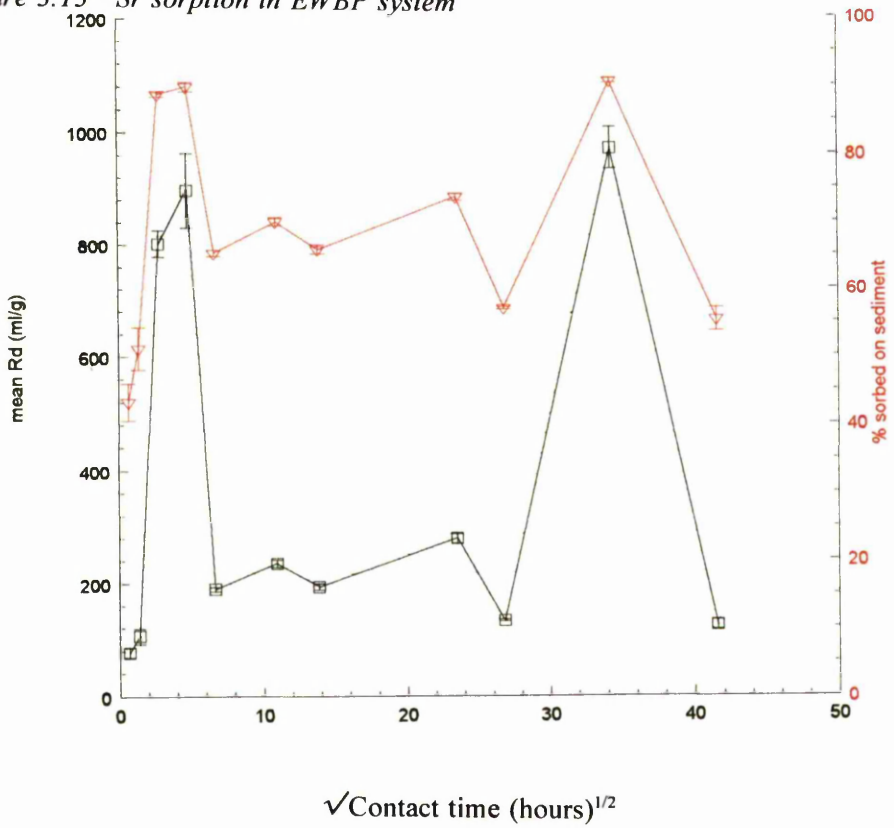

sorbed than when Botany Pond water had been used. This is possibly due to the lower concentration of competing cations in Esthwaite water compared to Botany Pond water. Rather strange behaviour was observed in the Esthwaite Water sediment - Botany Pond water system (shown in Figure 3.13). Although an initial lower percentage of strontium was sorbed after 30 minutes than when Esthwaite water had been used (again expected, due to the importance of co-ions in solution), rather erratic behaviour was observed after this time, making it difficult to draw any definite conclusions.

(3) ^{103}Ru

The complex chemistry of ruthenium makes it difficult to comment on its behaviour in the aquatic environment unless its speciation in solution is known. Sorption on to Botany Pond sediment (shown in Figure 3.14) occurs rapidly, over 90% sorption within 24 hours. Although Aston and Duursma (1973) observed an equilibrium after 200 hours for 95-100% sorption, it can be seen from the data that sorption on to Botany Pond sediment, although between 95-100%, continues to increase for the duration of the experiment. This is in agreement with Garder and Skulberg (1964) who reported that ruthenium sorption on to clay particles had not reached an equilibrium even after 9 days. The continual increase in distribution ratio implies that sorption is still incomplete after 1700 hours.

Having an observed dependence upon the concentration of competing cations in solution (Garder and Skulberg, 1964) and an affinity for organic matter (Pillai et al, 1975; Santschi et al, 1988b; Polar and Bayulgen, 1991; Robbins et al, 1992), it would be expected that sorption on to Esthwaite Water sediment (shown in Figure 3.15)

Figure 3.14 ^{103}Ru sorption in BPBP system

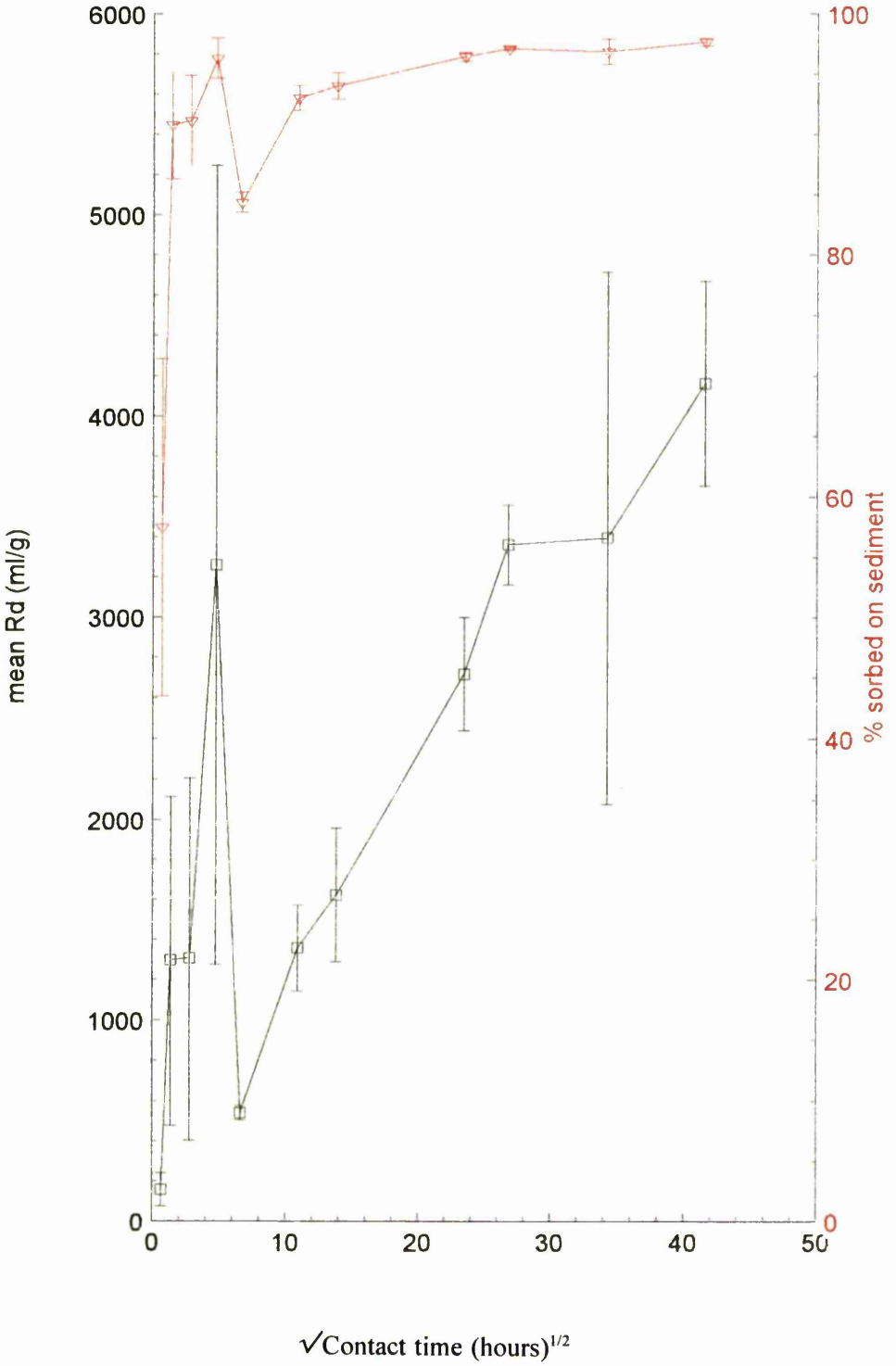

Figure 3.15 ^{103}Ru sorption in EWEW system

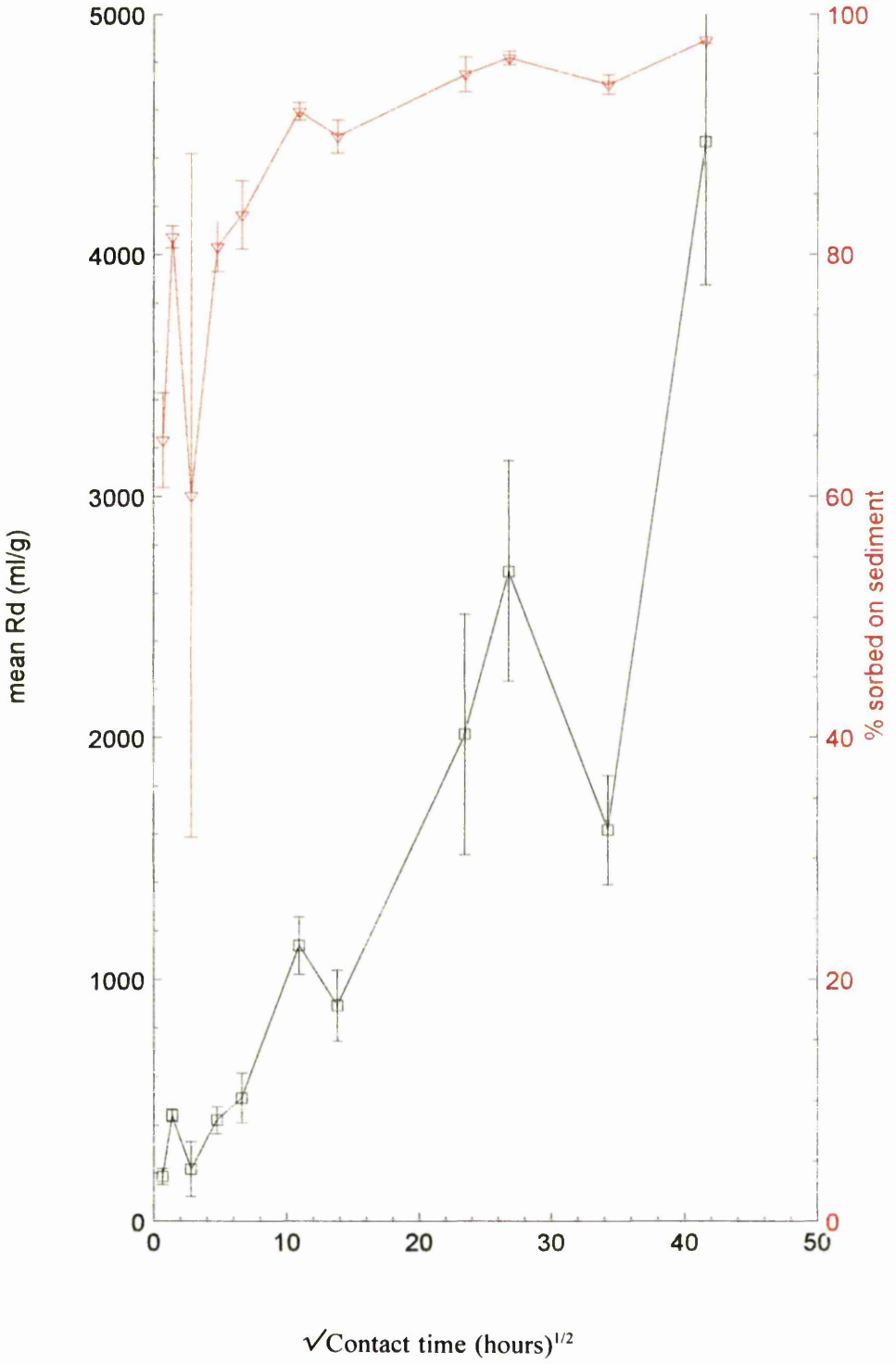

Figure 3.16 ^{103}*Ru sorption in BPEW system*

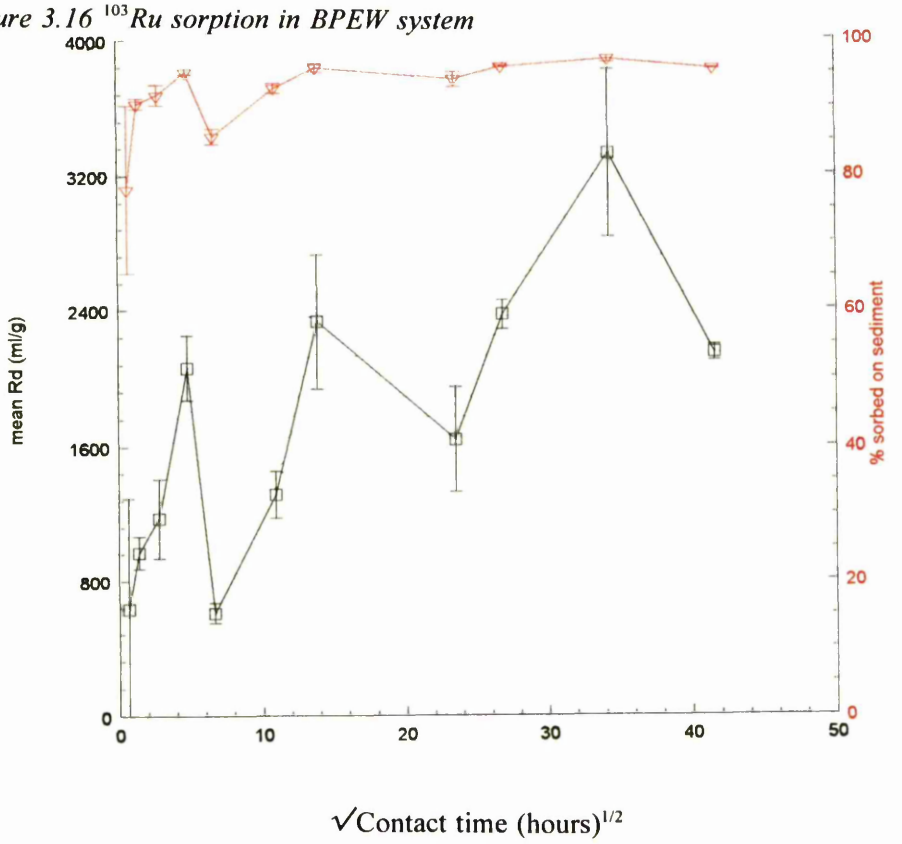

Figure 3.17 ^{103}*Ru sorption in EWBP system*

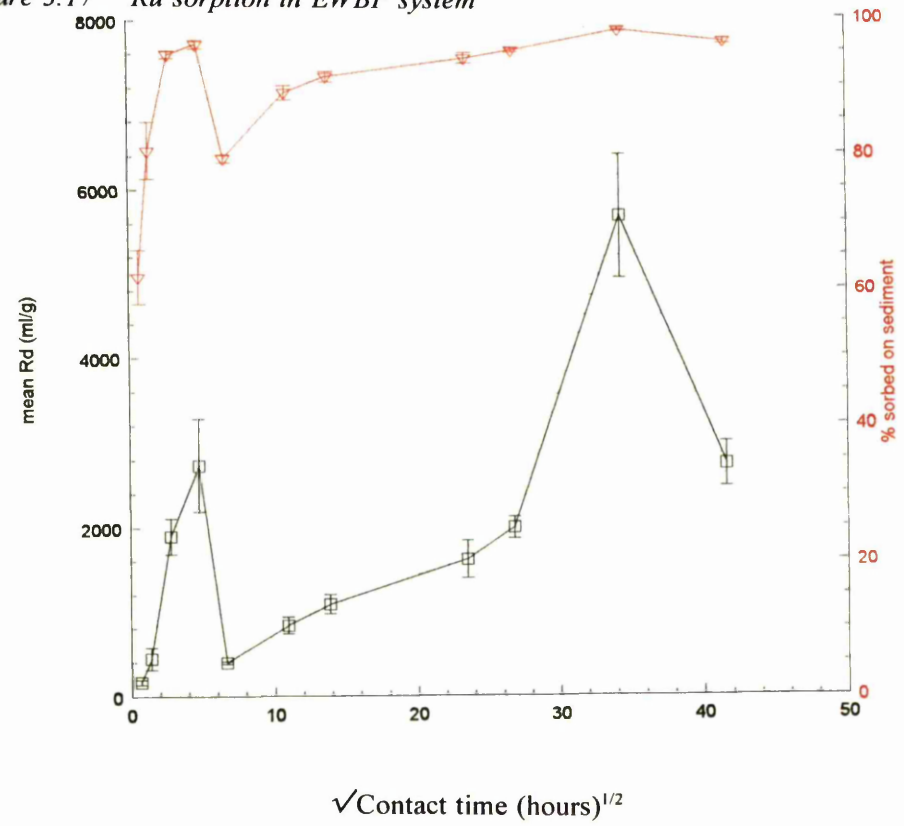

would occur to a greater extent. Although the initial amount of Ru sorbed in this system is greater, sorption occurs at a much slower rate. Approximately 90% sorption occurs in this system only after a contact time of 500 hours has been reached (compared to 24 hours in the Botany Pond system). Sorption is also seen to continue for the duration of the experiment for this system.

Sorption after 30 minutes on to Botany Pond sediment is increased by approximately 20% when Esthwaite water has been used (shown in Figure 3.16), which indicates a dependence of ruthenium sorption upon ionic strength. However, the data indicate that slightly more ruthenium might be sorbed after longer adsorption times in the BPBP system. There are no significant differences between sorption of ^{103}Ru in the EWBP system (shown in Figure 3.17) and the EWEW system.

(4) ^{134}Cs

Consistent with studies by Torstenfelt et al (1982) and Comans et al (1991), a rapid uptake of caesium is observed, almost instantaneously, with over 90% of caesium being sorbed on to Botany Pond sediment (shown in Figure 3.18) after just 30 minutes. A slower period of uptake then continued for the duration of the experiment. Even though the percentage of caesium sorbed was so high it appeared almost constant, it was apparent from the significant increase in Rd that sorption was still incomplete after 1700 hours. The slower period of uptake could therefore be due to the Cs^+ ions diffusing into interlayer sites in the interior of the clay.

Although sorption on to Esthwaite Water sediment (shown in Figure 3.19) also occurred almost instantaneously, it occurred to a lesser extent - only approximately

Figure 3.18 ^{134}Cs sorption in BPBP system

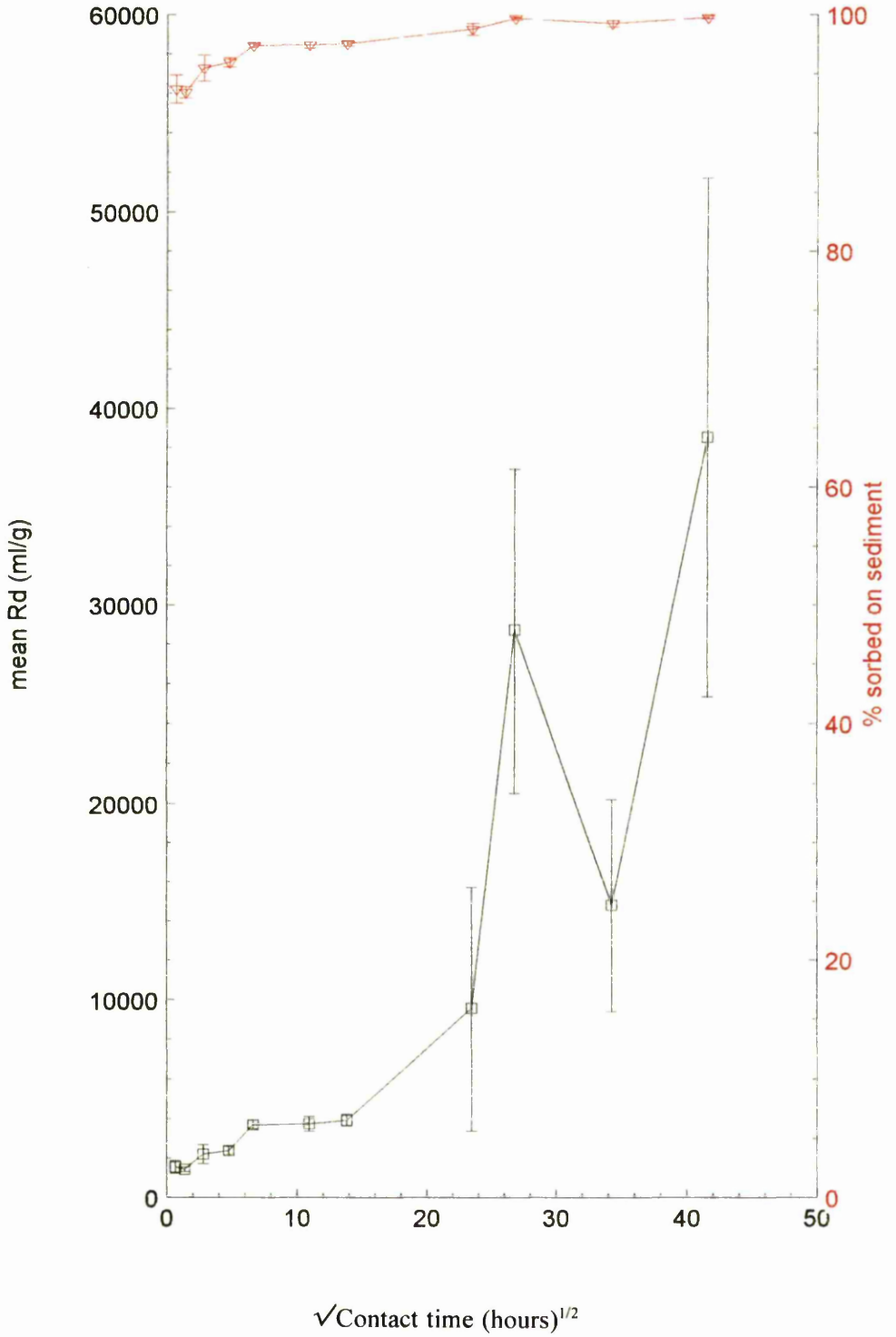

Figure 3.19 ^{134}Cs sorption in EWEW system

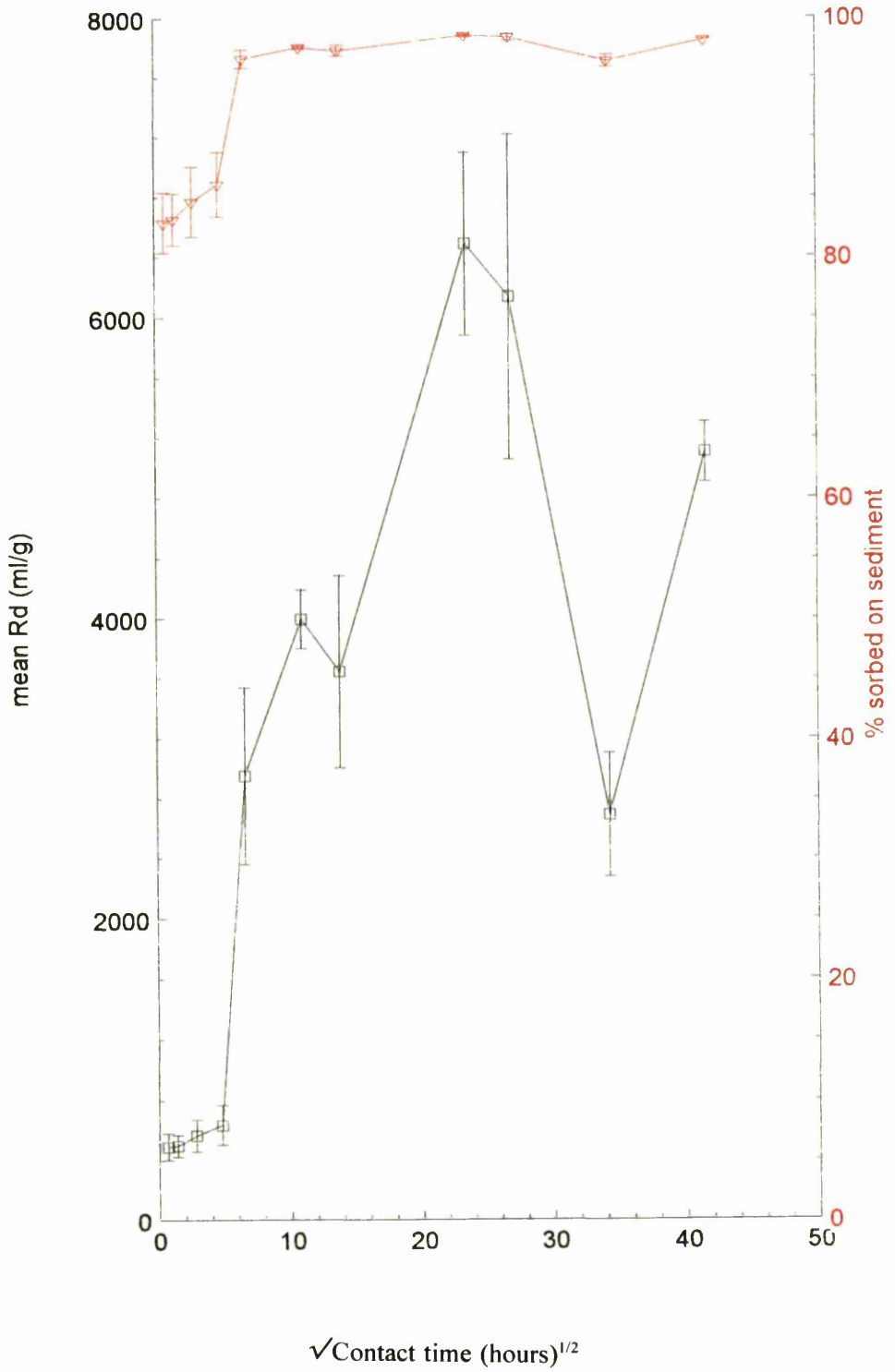

Figure 3.20 ^{134}Cs *sorption in BPEW system*

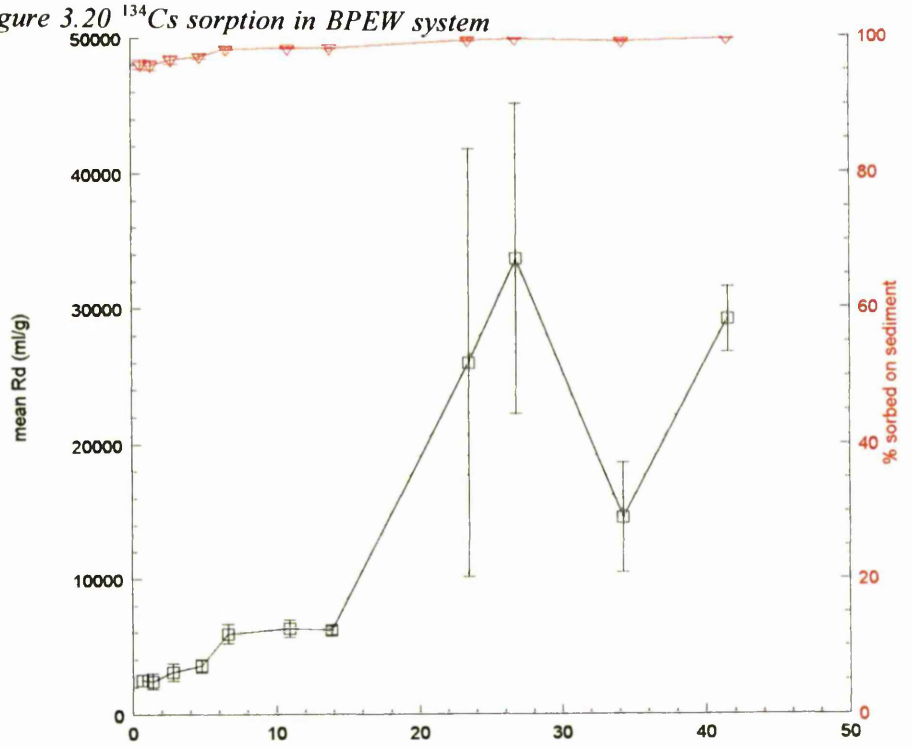

Figure 3.21 ^{134}Cs *sorption in EWBP system*

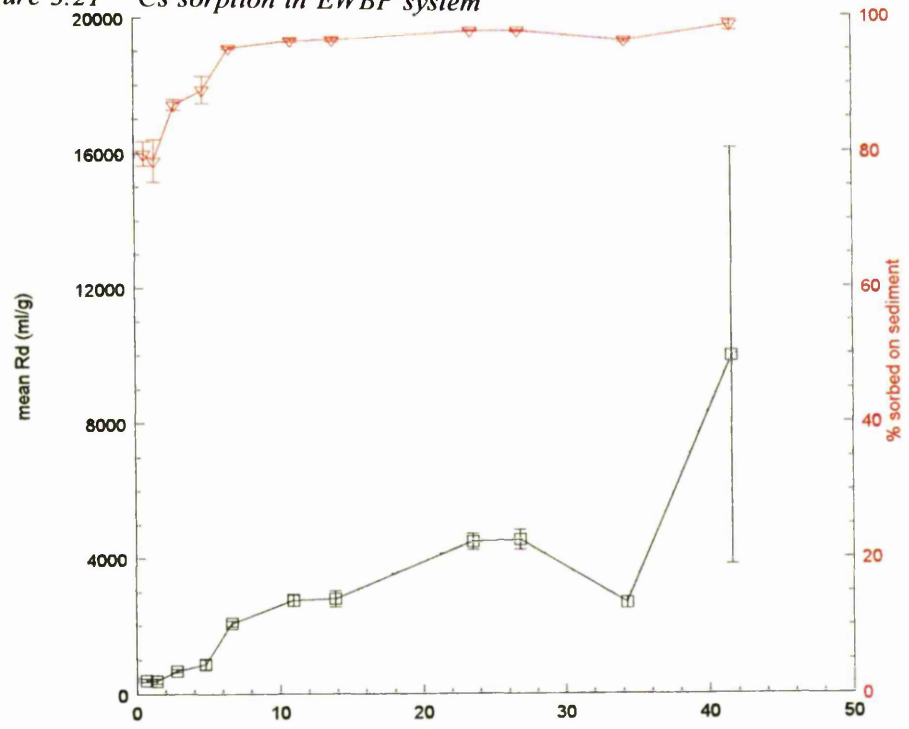

82% sorption after 30 minutes. Sorption on to this sediment is less which is probably a reflection of the different clay mineralogy. A decrease in sorption occurs after 700 hours - which is again similar to the decrease observed with cobalt and strontium sorption in this system.

The percentage of caesium sorbed initially after a contact time of just 30 minutes is greater on Botany Pond sediment when Esthwaite water is used (shown in Figure 3.20) rather than Botany Pond water. This shows the importance of competing cations on caesium sorption. After 700 hours however, a decrease in sorption was observed. The effect of competing cations on caesium sorption was illustrated again on comparison of the EWBP (shown in Figure 3.21) and EWEW systems. After 30 minutes, only approximately 80% caesium was sorbed in the EWBP system compared to approximately 82% sorption measured in the EWEW system.

Comparison of elements

Different behaviour was displayed by each radionuclide, reflective of different sorption mechanisms and sorption on to different mineralogical components in the sediment. Sorption was greatest for ^{134}Cs - distribution ratios for this radionuclide reached 10^4 mlg^{-1} for sorption on to Botany Pond sediment. Although an equilibrium appeared to have been established for sorption of this isotope on to Esthwaite Water sediment, sorption on to Botany Pond sediment continued for the duration of the experiment. A dependence upon the ionic strength of the solution was observed for this radionuclide. For all four freshwater systems, ^{134}Cs sorption appeared to occur in two stages, an initial rapid period of sorption, followed by a much slower uptake of varying duration. This is similar to the behaviour of ^{57}Co. Although sorption of this

isotope was less than that for ^{134}Cs, uptake was still high (Rd reaching approximately 8000 $ml g^{-1}$ for sorption to Botany Pond sediment). Again sorption of this radionuclide on to Botany Pond sediment continued for the duration of the experiment and appeared to occur in two stages - an initial rapid period of sorption followed by a slower uptake. Sorption of ^{85}Sr was much lower than both ^{57}Co and ^{134}Cs with distribution ratios for Esthwaite Water sediment only reaching approximately 400 ml g^{-1}. Unlike ^{57}Co and ^{134}Cs, sorption of ^{85}Sr was greatest for Esthwaite Water sediment (the sediment with the highest cation exchange capacity), suggesting that ^{57}Co and ^{134}Cs sorption proceeds by sorption mechanisms in addition to ion exchange or on to exchange sites which are unavailable to ^{85}Sr. A strong dependence upon the ionic strength of the solution was observed for ^{85}Sr sorption. Sorption of ^{103}Ru was high, but occurred to a slightly lesser extent than ^{57}Co sorption (apart from ^{103}Ru sorption on Esthwaite Water sediment which was higher). Unlike ^{57}Co and ^{134}Cs sorption, ^{103}Ru sorption continued for the duration of the experiment in all four systems, suggesting that reactions in addition to ion exchange were occurring and also that sorption of this radionuclide occurred by different mechanisms to ^{57}Co and ^{134}Cs.

3.7.2 Phase separation

The results of the phase separation experiment are contained in Tables 3.2-3.5. The distribution ratios for ^{57}Co, ^{85}Sr and ^{103}Ru show excellent agreement regardless of whether the method of phase separation employed was centrifugation or centrifugation followed by filtration. This indicates that filtration is unecessary for these isotopes providing that the length and speed of centrifugation is adequate.

Table 3.2 Mean Rd values following different phase separation procedures for ^{57}Co.

	MEAN Rd (mlg^{-1})±1SD	
SYSTEM	CENTRIFUGATION	CENTRIFUGATION AND FILTRATION
BPBP	389±130	641±130
BPEW	427±70	454±150
EWBP	251±9	266±19
EWEW	55±14	60±7

Table 3.3 Mean Rd values following different phase separation procedures for ^{85}Sr.

	MEAN Rd (mlg^{-1})±1SD	
SYSTEM	CENTRIFUGATION	CENTRIFUGATION AND FILTRATION
BPBP	97±25	124±7
BPEW	95±3	108±7
EWBP	72±4	76±3
EWEW	41±7	45±5

Table 3.4 Mean Rd values following different phase separation procedures for ^{103}Ru.

	MEAN Rd (mlg^{-1})±1SD	
SYSTEM	CENTRIFUGATION	CENTRIFUGATION AND FILTRATION
BPEW	1440±210	1850±250
EWBP	954±64	1030±74
EWEW	124±14	140±16

The distribution ratios for ^{134}Cs however are approximately double when centrifugation and filtration have been used to separate the phases, indicating that a greater proportion of spike is being detected in solution following just centrifugation. There

are two possible explanations for this. It is possible that a small amount of spiked solid is escaping into the solution during decantation, thereby giving the solution a higher activity and a lower Rd for the centrifugation only means of separation. It is also possible however that ^{134}Cs is sorbing to the filtration equipment and/or filter papers thereby giving a lower activity in solution and a higher Rd for those samples which had been filtered.

Table 3.5 Mean Rd values following different phase separation procedures for ^{134}Cs.

	MEAN Rd ($ml g^{-1}$)±1SD	
SYSTEM	CENTRIFUGATION	CENTRIFUGATION AND FILTRATION
BPBP	2300±520	5980±830
BPEW	3360±580	7900±1600
EWBP	1010±76	2250±320
EWEW	590±46	1860±1100

Further analysis detected the presence of ^{134}Cs on the filter paper which could mean that a small amount of very fine colloidal material is being caught on the filter. Inspection of the filter paper however, revealed no visible deposits and it could also be argued that if very small particles were being caught on the filter paper, then ^{57}Co, ^{85}Sr and ^{103}Ru would also be detected, which would also lead to differences in the distribution ratios of these radionuclides. As no solid could be seen in solution following decantation, and ^{134}Cs alone was detected on the filter papers, it seems likely that sorption is taking place during filtration. This emphasises the caution that must be taken during phase separation, and questions the reliability of results obtained for certain isotopes when filtration has been used.

3.7.3 Reproducibility

The variation coefficients of the data shown in Figures 3.6-3.21 suggest that the success with which the distribution ratio is reproduced within a small group of replicate samples depends upon the radionuclide being studied. Generally, reproducibility is best for ^{85}Sr data - the majority of time points have a standard deviation of <10%. Most ^{103}Ru standard deviations are <17% and ^{134}Cs standard deviations are generally <20%. Sorption data for ^{57}Co have the worst agreement -the majority of time points only had a standard deviation of <25%. The reasonably good errors obtained for ^{85}Sr suggest that the sediment and water is well homogenised and that the large spread of variation coefficients between the four radionuclides is more an indication of the complexity of the reaction by which the radionuclide is being sorbed. It could also indicate radionuclide sensitivity to certain conditions within the system (eg. Eh and pH) which might be changing in some replicates. The general spread of data does stress the importance of using replicate samples and also using a sufficient number of samples for trends to be observed.

It will be observed that several mean Rd values in Figures 3.6-3.21 actually have variation coefficients >100%. This is invariably due to the presence of a "flyer" within the five replicates (ie. four Rd values in close agreement and one value which was exceptionally high or low). Although it could be statistically justifiable to remove this "flyer" from the data set and base the mean Rd value on the remaining four values instead, it was decided to keep the "flyer" in the data as it is an observable, experimental phenomenon. It is unlikely that the "flyer" values are due to inhomogeneous sediment and water samples as this phenomenon has also been observed using a single mineralogical phase and artificial groundwater (L.Moyes -

pers.comm.). When these values have occurred during this work, the mean Rd value has also been calculated without the "flyer" value and this has been reported in the appropriate discussion section. It was due to the sensitive nature of the Rd value that it was felt necessary to include the percentage of radionuclide sorbed on Figures 3.6-3.21. As discussed in Section 1.6.1, this is a less sensitive means of describing sorption, yet it does provide useful and additional information to the Rd value when there is a "flyer" in the data set.

Table 3.6 contains the mean Rd values from the experiments in which Cs sorption was repeated for several adsorption times.

Table 3.6 Reproducibility of ^{134}Cs data.

	MEAN Rd (mlg^{-1})±1SD	
SORPTION TIME (hrs)	ORIGINAL EXPT.	REPEAT EXPT.
8	2190±480	1950±98
120	3750±370	3460±2300
192	3910±300	4760±100

Excellent agreement is obtained between the distribution ratios for the shorter adsorption time. Although good agreement is also obtained for a sorption time of 120 hours, there is a large standard deviation on the repeat experiment due to one higher Rd value in the data set. Reasonable agreement is reached between the Rd values after an adsorption time of 192 hours. This suggests that the sorption experiments can be repeated under identical experimental conditions and comparable results obtained.

3.7.4 Sterilisation

Figures 3.22 and 3.23 show the distribution ratios for ^{57}Co and ^{134}Cs sorption after the samples have been autoclaved. Instead of a significant decrease in sorption after approximately 1000 hours as seen previously with Esthwaite Water sediment, sorption of both isotopes seems to remain constant. This seems to suggest that despite keeping samples in the dark and aerating regularly to keep microbial activity to a minimum, biological activity could be responsible for the irregular behaviour that is observed in this sediment at longer time points. It is unlikely that it is due to experimental design as this behaviour was not observed with Botany Pond sediment.

Decreased sorption of caesium has been observed by West et al (1991) in the presence of microbial activity. It was suggested that microbes competed with Cs^+ ions for sorption sites. As these microbes are much larger than a Cs^+ ion, one microorganism would cover more than one site, thereby limiting the amount of caesium sorption which can take place.

It is possible however that by sterilising the samples, conditions in the system were changed in some way. Clay structure could have been altered, thereby increasing the sorption capacity. As the majority of ^{57}Co and ^{134}Cs are thought to sorb to different geologic media, this would mean all sorptive components of the sediment would have to have been altered. It is also unlikely because if the sorptive capacity of the sediment had increased, then the distribution ratio and the percentage of isotope sorbed following sterilisation would have increased greatly from the Rd and percentage sorbed for the samples which had not been sterilised. This was not observed. Sorption following sterilisation seems to remain at approximately the same

Figure 3.22 ^{57}Co sorption in sterilised EWEW system

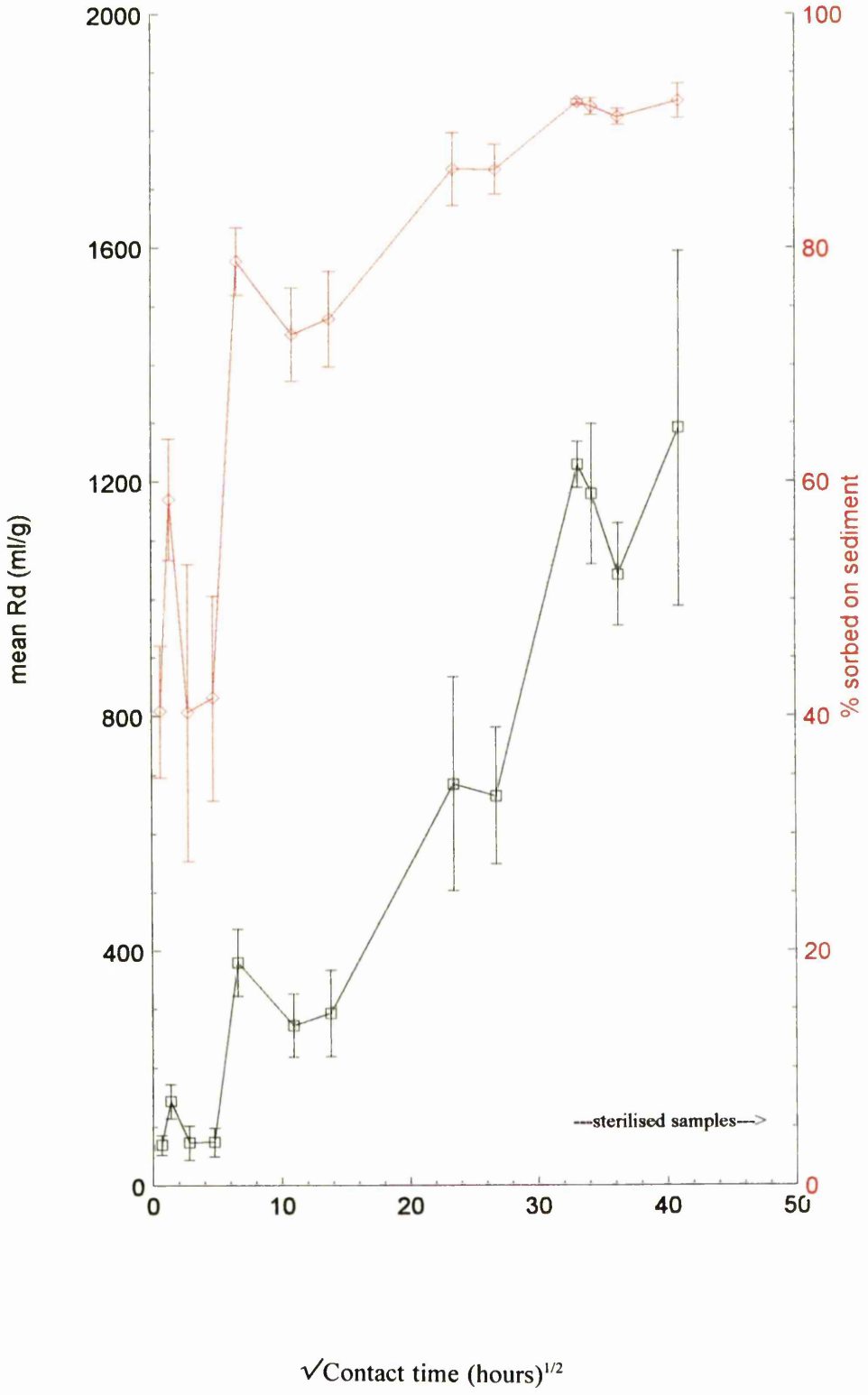

Figure 3.23 ^{134}Cs sorption in sterilised EWEW system

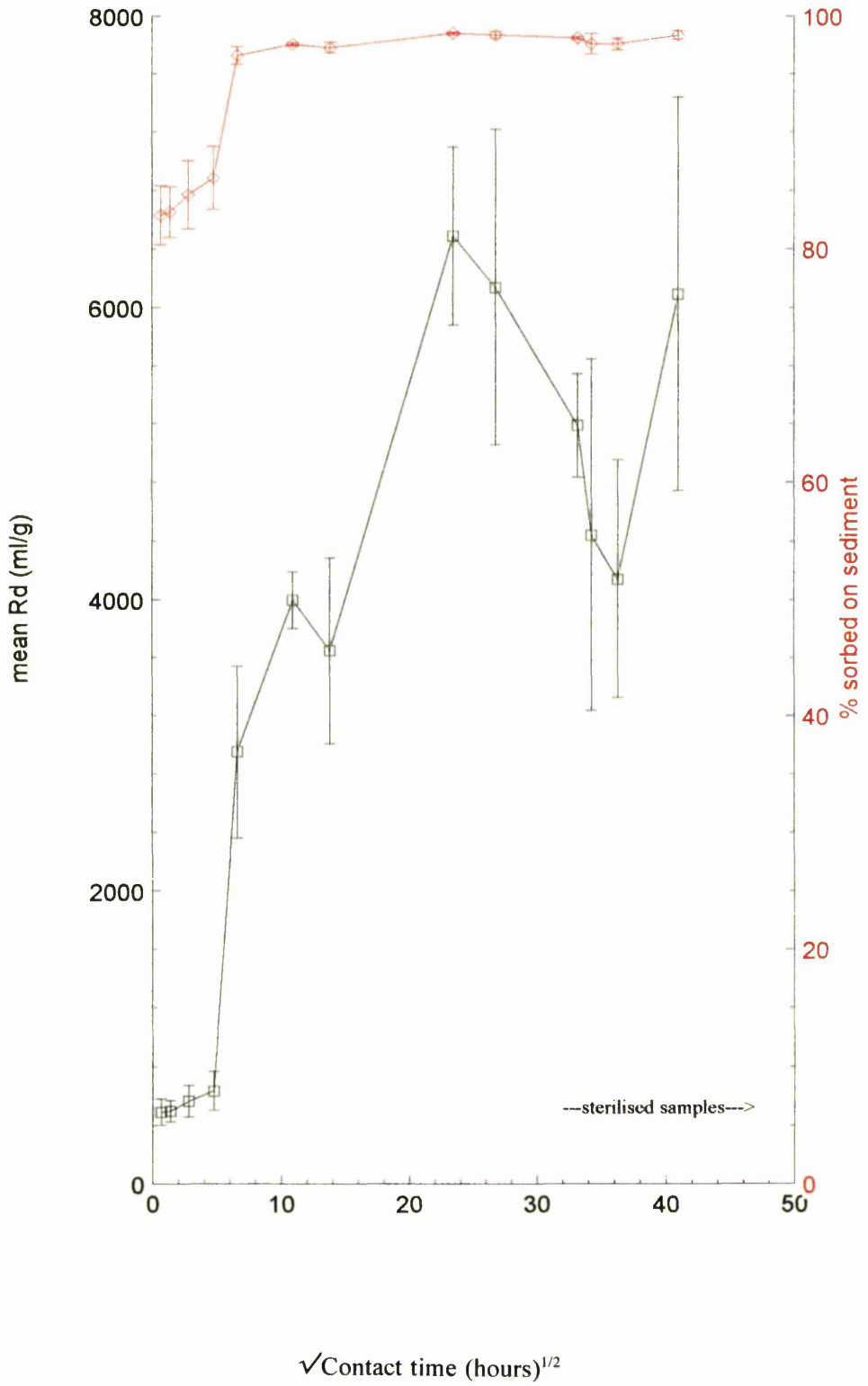

level as was observed in the original samples before sorption was seen to fall.

Unexplainable and irregular changes in sorption for strontium and caesium at contact times on the scale of months have also been observed by Torstenfelt et al (1982). Significantly reduced or enhanced values of distribution coefficient were obtained and it was suggested that this was reflecting the gradual formation of weathering products in the experimental system, thereby changing the sorptive properties. It was also suggested that colloidal particles could form after long periods of sorption.

3.8 Summary

1. Sorption occurred in the order, $^{134}Cs > ^{57}Co > ^{103}Ru > ^{85}Sr$.

2. A strong dependence upon the ionic strength of the solution was revealed for ^{85}Sr and ^{134}Cs sorption.

3. Sorption on to Botany Pond sediment continued for the duration of the experiment for all of the radionuclides apart from ^{85}Sr.

4. Sorption on to Esthwaite Water sediment appeared to have finished for all of the radionuclides apart from ^{103}Ru. Sorption of this radionuclide on to Esthwaite Water sediment continued for the duration of the experiment.

5. Care needs to be take in the phase separation procedure when using ^{134}Cs as it is possible that this radionuclide sorbs to filtration equipment.

6. Reproducibility of the experimental data was generally good, although the existence of "flyers" in the data set sometimes gave rise to variation coefficients >100%.

7. Sterilisation of samples which were to be left for longer adsorption times appeared to eliminate the unusual behaviour which was exhibited by certain radionuclides with Esthwaite Water sediment suggesting that biological activity could be responsible.

CHAPTER 4 - DESORPTION STUDIES

CHAPTER 4 - DESORPTION STUDIES

4.1 Introduction

Once sorbed to the sediment, the radionuclide can be considered as "fixed" and effectively removed from solution, but the extent of this immobilisation - ie. the ability of the sediment to retain the radionuclide indefinitely - will be influenced not only by the mineralogical composition of the sediment but also by any changes which might occur in environmental conditions, such as variations in redox conditions and solution composition. Studying the desorption behaviour of a particular sediment/radionuclide system will enable the ease by which a radionuclide is released back into the environment to be determined.

There are several experimental methods which can be used to study desorption behaviour. The batch technique (described previously in Section 3.1 to measure adsorption) can be easily adapted to study desorption by measuring the quantity of radionuclide released when a suitable extracting agent is added to the spiked sediment. Although the batch technique is widely used to study desorption (Erten et al, 1988; Fukui, 1990; Hsu and Chang, 1995) there are a number of disadvantages associated with this method. Not only are desorption yields dependent upon V/M ratios (as discussed in Section 3.1), but they are also dependent upon the concentration and identity of the extracting cation, desorption time and the levels of radionuclide accumulated in the solution phase (high concentrations of radionuclide in solution can be generated which can, in turn, become rate-limiting for radionuclide desorption from the sediment). Despite this, the batch technique remains the most popular method in studying desorption (the advantages of this method have been discussed in Section

3.1).

The infinite bath technique used by Madruga (1993) and Wauters (1994) was developed to eliminate the problems which can occur in the batch method. Experimental design means that there is an "infinite" dilution of radionuclide in the solution phase, thereby eliminating the problem of high concentrations of radionuclide building up in solution during desorption. More realistic conditions can be maintained using this method, in terms of the ionic strength and composition of the solution phase. There is no dependence upon V/M ratio and a lower dependence upon the concentration and identity of the competing cation. A schematic representation of the infinite bath technique is shown in Figure 4.1. Loosely based on the batch method, an absorbent has been added to the sediment/extractant system that has sorptive properties far greater than the sediment which is being studied. This results in the desorbed radionuclide becoming trapped in the absorbent, thereby eliminating the problem of high levels of radionuclide accumulating in solution. It does however become increasingly difficult to maintain conditions in the system. Madruga (1993) reported significantly higher desorption yields using this method than with the more widely used batch technique.

Other desorption techniques include the leaching column method used by Fahad et al (1989). This involved packing a Perspex column with soil and spiking the surface. Following sorption, the columns were leached with various extractants. Nuclide sorption was studied by monitoring the distribution of spike down the column during the experiment, and also measuring the spike content of the effluent samples which had passed through the column. Nyffeler et al (1984) adapted the thin layer technique (previously described in Section 3.1 to study adsorption) to study desorption

Figure 4.1 Schematic representation of the infinite bath technique (Wauters, 1994)

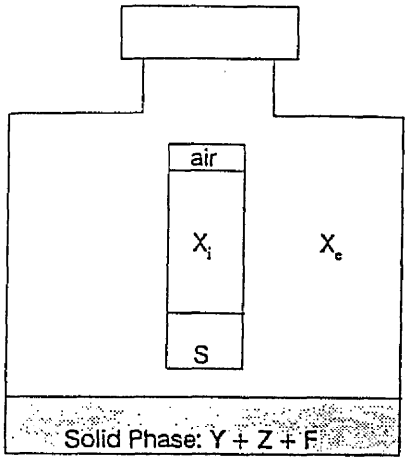

X_e = outer solution
X_i = inner solution
S = accumulator adsorbent
Y = instantaneous equilibrium sites
Z = slow sorption sites
F = irreversible sites

behaviour.

In addition to choosing the most appropriate desorption technique, it is also necessary to consider the extractant which should be used. Different extractants will give different desorption yields but ultimately the choice of extractant should depend upon which radionuclide is being studied.

If the radionuclide desorption potential under the aqueous phase conditions found at the sampling site is being investigated then it is most appropriate to use a fresh solution of that which was used in the adsorption study, e.g. fresh lake water (Abdel Gawad et al, 1977; Nyffeler et al, 1984; Erten et al, 1988; Fukui, 1990). Although this is the most realistic in terms of solution composition, this extractant usually provides the lowest desorption yields due to the relatively low ionic strength, and therefore the lowest concentration of exchangeable cations. Solutions containing monovalent cations, such as Na^+ and NH_4^+, can also be used as extracting agents (Evans et al, 1983; Fukui, 1990) or solutions containing bivalent cations, such as Ca^{2+} and Mg^{2+} (Abdel Gawad et al, 1977). Solutions such as these contain high concentrations of cations and therefore have a much greater ionic strength than would be found in the field, but they are useful in finding the total exchangeable fraction of radionuclide. The use of NH_4^+ is particularly widespread in finding the exchangeable fraction of radiocaesium, as monovalent ions with a low hydration energy and an ionic radius similar to Cs^+ are known to compete with Cs^+ for the more selective ion exchange sites (Sawhney, 1972). As NH_4^+ is released in anoxic pore waters during lake stratification, there is the possibility that this cation will release sediment-bound radiocaesium back to the water column, as has been observed (Evans et al, 1983; Comans et al, 1989).

Other leaching agents which can be used include solutions of isotopic carrier (Abdel Gawad et al, 1977; Hsu and Chang, 1995) and extractants which might form complexes with the radionuclide, such as Na_2EDTA. This would measure the possible formation of chelate compounds which is particularly important with heavy metals (Patel et al, 1978; Fukui, 1990).

This chapter describes the experimental procedures used in this project to investigate the desorption behaviour of the four radionuclides and the results which were obtained.

4.2 Desorption into fresh lake water

In order to determine the concentration of radionuclide which would be released back into the freshwater environment following adsorption, desorptions into lake water were carried out.

After the adsorption procedure described in Section 3.2 was completed, a sample of fresh lake water (30 ml) was added to the spiked sediment. The tubes were shaken well and then stored in the dark at room temperature for a specified desorption time. Desorption times were 4 days for those samples which had longer adsorption times (i.e. those of 4 days or over), and desorption times were equal to adsorption times for those samples which had adsorption times of less than 4 days.

After the desorption time had elapsed, the tubes were centrifuged (12,000g/45mins) and the lake water was decanted. The supernatant was counted on a gamma photon detector and the resulting spectrum analysed for spike content.

4.3 Desorption into fresh lake water of sterilised samples

As it is possible that the structure of the sediment was altered in some way during the sterilisation procedure described in Section 3.5, desorption of the radionuclides from these sterilised samples was also studied to allow more definite conclusions on the effect of sterilisation to be drawn.

Following the sterilisation procedure described in Section 3.5, a sample of fresh lake water (30 ml) was added to the spiked sediment. The tubes were shaken well and then stored in the dark at room temperature for four days. After the desorption time had elapsed, the tubes were centrifuged (12,000g/45mins) and the lake water decanted. The supernatant was counted on a gamma photon detector and the resulting spectrum analysed for spike content.

4.4 Ammonium acetate extractions

As mentioned previously in Section 4.1, the use of the ammonium ion is particularly widespread when trying to find the total exchangeable fraction of radionuclide on the sediment, especially when caesium is the radionuclide being studied.

Using the adsorption procedure outlined in Section 3.2, a spike of ^{57}Co (1.122 kBq), ^{85}Sr (0.984 kBq), ^{103}Ru (1.111 kBq) and ^{134}Cs (8.103 kBq) was added and the samples were left for contact times ranging from 1 day to over 2 months. Samples from each freshwater system were used with three replicates for each time point. 1M ammonium acetate, adjusted to pH 6.9 with acetic acid, (30 ml) was then added to the spiked sediment and the samples were shaken well and stored in the dark, at room

temperature, for 18 hours. After this time, the samples were centrifuged (12,000g/45mins), the supernatant was decanted and then analysed for spike content on a gamma photon detector.

As a considerable quantity of spike is usually extracted, the system soon reaches an equilibrium, so it is not usually adequate to perform just one ammonium acetate extraction. The procedure was therefore repeated on each sample twice more, so that three consecutive extractions had been performed, i.e. total extraction time is 54 hours. This extraction time was found to be sufficient to desorb all ^{85}Sr from both sediments. As strontium is known to sorb on regular exchange sites by simple ion-exchange reactions, a total extraction time of 54 hours was therefore expected to be sufficient to desorb the extractable fraction of ^{57}Co, ^{103}Ru and ^{134}Cs sorbed on the sediment. The total extracted activity was calculated by summing together the spike activity which each solution contained.

4.5 Successive desorptions into fresh lake water

The concentrations of radionuclide extracted after performing the procedure described in Section 4.2 were very small so it seemed unlikely that high desorption yields in solution were becoming a limiting factor, but nevertheless successive desorptions were also carried out using this extractant, to ascertain if desorption into fresh lake water would carry on indefinitely until yields similar to those found using ammonium acetate as the extracting agent were obtained (see Section 4.4).

Using the adsorption procedure in Section 3.2 and three replicates for each time point, Botany Pond sediment was spiked with ^{57}Co (1.000 kBq), ^{85}Sr (0.963 kBq) and ^{134}Cs

(9.509 kBq) and equilibrated for adsorption times of 30 minutes and 11 days. After adsorption, fresh lake water (30 ml) was added to the spiked sediment. The samples were shaken well and stored in the dark for a short desorption time (0.5 hours).

After this time, the samples were centrifuged (12,000g/45mins) and the lake water decanted. Fresh lake water (30 ml) was again added to the spiked sediment, shaken well and stored in the dark for a specified desorption time, after which the samples were centrifuged (12,000g/45mins) and the supernatant decanted as before. This procedure was repeated with desorption times increasing up to several weeks until no more spike could be detected in the supernatant. In total, at least six changes of desorbing solution were needed. The supernatants were counted on a gamma photon detector and the resulting spectra analysed for spike content.

4.6 Method used for sequential leach

Sequential extraction experiments were carried out to investigate the association of ^{57}Co, ^{85}Sr and ^{134}Cs with the different mineral fractions in both sediments following adsorption times of increasing duration. A sequential extraction uses a series of reagents of increasing leaching ability to remove one particular mineral component. Sequential extraction procedures are rather arbitrary due to the presence of poorly defined mineral fractions and the unsuitability of certain procedures for different sediments. Results from these sequential extraction procedures must therefore be interpreted with caution, and this is emphasised in Section 4.7.5. Although precise conclusions cannot be drawn, these procedures are still useful as a comparative exercise for the three radionuclides used in this experiment.

Using the adsorption procedure described in Section 3.2, one gram of sediment (3 replicates were used for each time point) was spiked with ^{57}Co (1.156 kBq), ^{85}Sr (1.070 kBq) and ^{134}Cs (10.162 kBq) and left for adsorption contact times of 7 days, 34 days and 62 days, before the leaching procedure of Tessier et al (1979) was carried out.

8 ml of 1M magnesium chloride (pH 7.0) was added to the spiked sediment and gently agitated for one hour at room temperature to determine the exchangeable fraction of radionuclide and the extract was separated (see below). This was followed by 8 ml of 1M sodium acetate (pH 5.0) in order to determine the fraction of radionuclide bound to carbonates. Continuous agitation was maintained for 5 hours at room temperature. The third extraction used 20 ml 0.04M hydroxylamine hydrochloride in 25% acetic acid (v/v) which was then heated to 96°C for 6 hours in order to reduce the iron and manganese oxides present in the sediment. Finally, the organic matter in the sediment was oxidised using 3 ml of 0.02M nitric acid and 5 ml 30% hydrogen peroxide (pH 2.0) heated to 85°C for 2 hours with occasional agitation. A further 3 ml of 30% hydrogen peroxide was added after this time, before the samples were heated again to 85°C for a further 3 hours. The samples were then left to cool before 5 ml of 3.2M ammonium acetate in 20% nitric acid (v/v) was added to prevent readsorption of released radionuclides to the oxidised sediment. The samples were diluted to 20 ml with deionised water and shaken continuously for 30 minutes.

Between each leaching step, separation was carried out by centrifugation (12,000g/30 mins) and decantation. Before carrying out the next leach, the residue was washed with 8 ml of deionised water to avoid carry over of solution. The samples were

centrifuged (12,000g/30 mins) and the wash discarded. The leachates were diluted to 30 ml (standard counting geometry) and analysed on a gamma photon detector for spike content.

The percentage of radionuclide extracted by each separate leach has been calculated and is presented in Section 4.7.5. The percentage of spike remaining on the sediment after all the extractions had been performed has been labelled the residual fraction.

4.7 Results and Discussion

4.7.1 Desorption into fresh lake water

Again the x-axis used on these graphs is (adsorption time)$^{1/2}$ due to the wide range of x values.

(1) ^{57}Co

Desorption from Botany Pond sediment is shown in Figure 4.2. For both lake waters, there is a gradual decrease in the percentage of ^{57}Co desorbed as the length of the adsorption contact time was increased. Botany Pond water desorbs more ^{57}Co than Esthwaite water, perhaps due to its higher ionic strength. After an adsorption time of 30 minutes, it was possible to desorb 6% with Botany Pond water, compared to just over 3% with Esthwaite water. This decreased to approximately 1% with both waters at an adsorption time of over 1700 hours, implying some kind of fixation process is taking place, as observed by McKenzie (1967). Figure 4.3 shows the percentage of ^{57}Co desorbed from Esthwaite Water sediment. The percentage of ^{57}Co desorbed from

Figure 4.2 Desorption of ^{57}Co from Botany Pond sediment

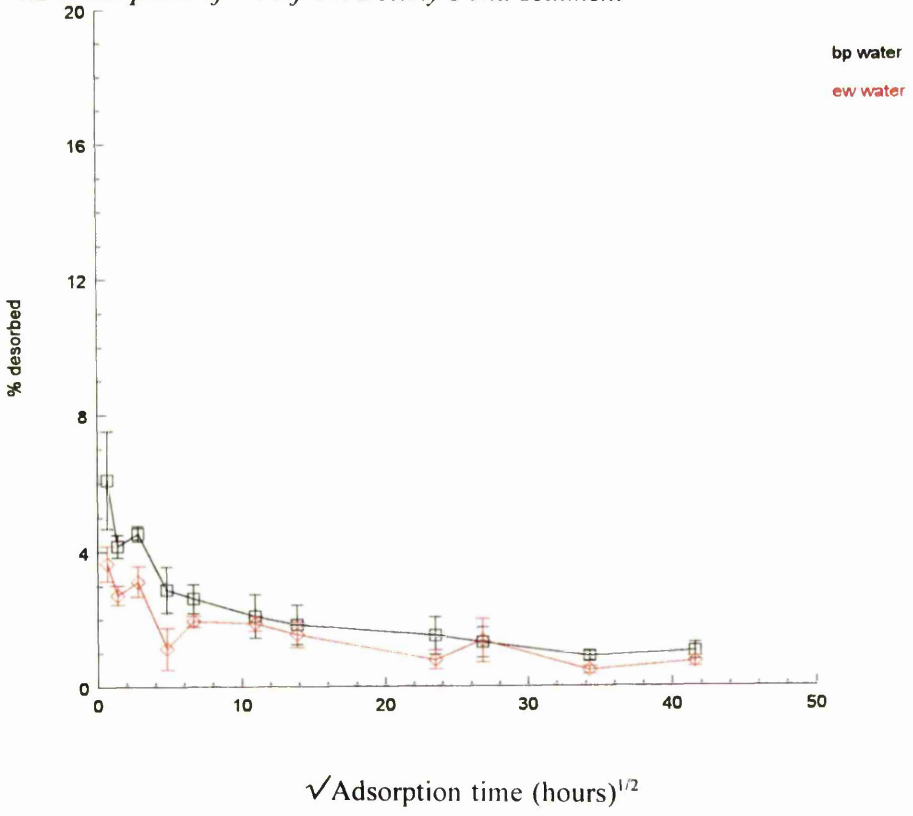

Figure 4.3 Desorption of ^{57}Co from Esthwaite Water sediment

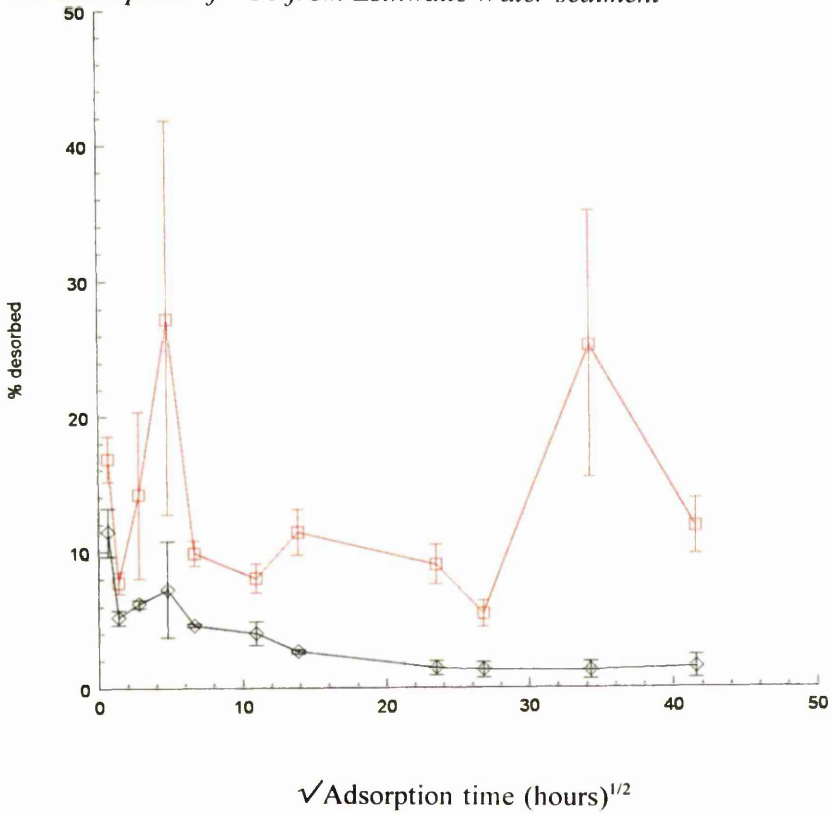

this sediment is greater than that desorbed from Botany Pond sediment which is unexpected as Esthwaite Water sediment contains higher concentrations of Mn and it might be expected that ^{57}Co would be harder to desorb from this sediment, as found by Cerling and Turner (1982) and McClaren et al (1986). Esthwaite water appears to desorb more ^{57}Co from this sediment than Botany Pond water, although the data for this water are quite noisy, making it difficult to distinguish any trends. The rise in desorption yields at longer adsorption times perhaps reflects the unexpected changes observed during adsorption at these times (possibly due to microbial activity changing the conditions within the sample). Desorption into Botany Pond water decreases as the length of adsorption increases, as before. After an adsorption time of only 30 minutes, approximately 10% could be desorbed, but at longer adsorption times just over 1% could be extracted. The small desorption yields obtained by using lake water as the extracting agent are consistent with those obtained with canal water by Abdel Gawad et al (1977).

(2) *^{85}Sr*

Higher desorption yields are obtained for ^{85}Sr. This is expected as it is known to exist on easily accessible sites and to exchange readily with other cations (Keren and O'Connor, 1983; Benes and Poliak, 1990; Fukui, 1990). Figure 4.4 shows the desorption of ^{85}Sr from Botany Pond sediment with increasing adsorption contact times. For both waters, an increase in the percentage of ^{85}Sr desorbed is observed as the adsorption contact time is increased. The increased desorption yields at longer adsorption times corresponds to the decrease in adsorption which was previously observed. The percentage of ^{85}Sr desorbed is greater with Botany Pond water than with Esthwaite water, probably due to the higher ionic strength of Botany Pond water,

Figure 4.4 Desorption of ^{85}Sr from Botany Pond sediment

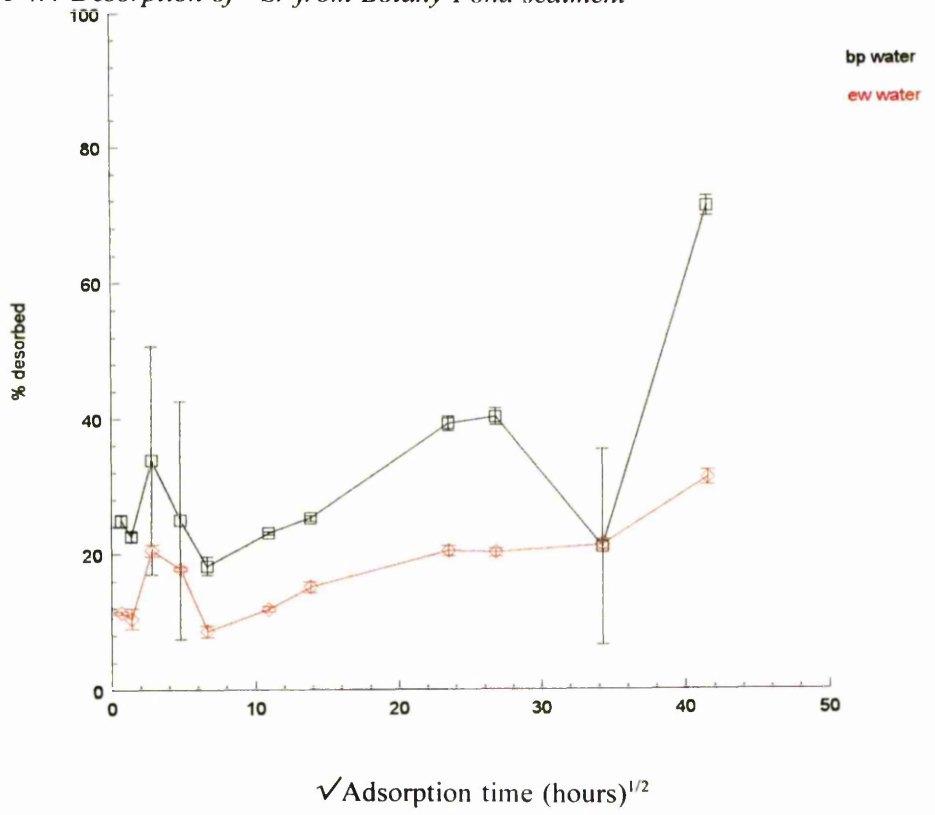

Figure 4.5 Desorption of ^{85}Sr from Esthwaite Water sediment

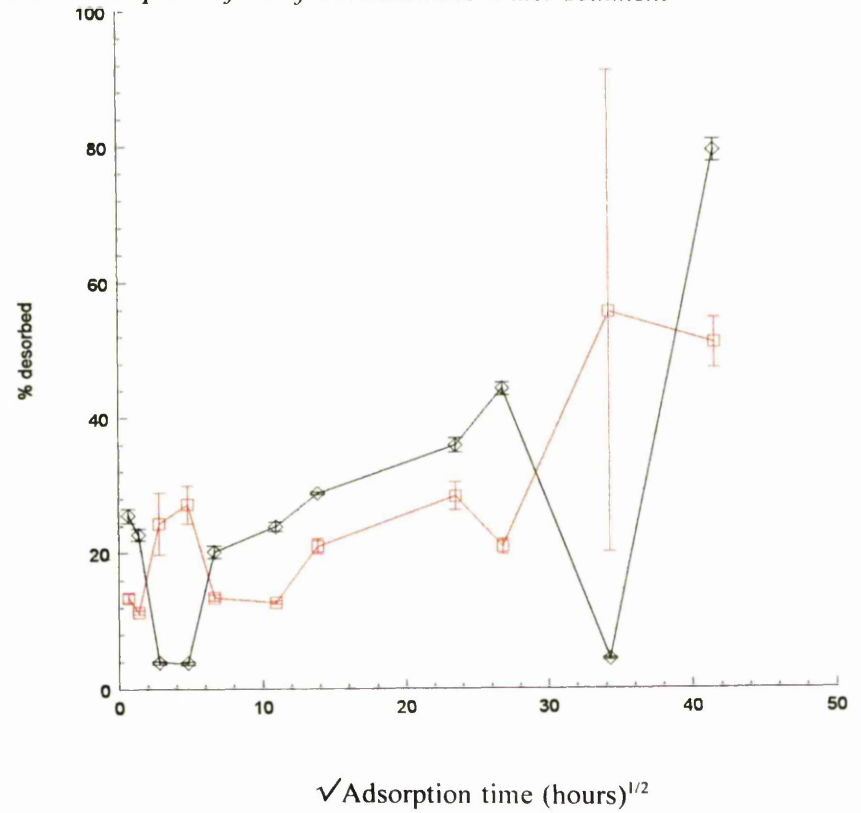

and particularly its higher concentrations of magnesium and calcium cations, which are known to be particularly effective at displacing strontium (Abdel Gawad et al, 1977). After an adsorption time of 30 minutes, approximately 11% of ^{85}Sr is extractable with Esthwaite water compared to 24% with Botany Pond water. When the adsorption time is increased to over 1700 hours, Esthwaite water is then able to extract approximately 30% of ^{85}Sr, and approximately 70% is extractable with Botany Pond water. Desorption of ^{85}Sr from Esthwaite sediment is shown in Figure 4.5. Again, an increase in ^{85}Sr desorption is observed when adsorption times are increased. The data for Botany Pond water are a little noisy but generally this water desorbs more ^{85}Sr than Esthwaite water, as before. After an adsorption time of 30 minutes, approximately 13% of ^{85}Sr is desorbed with Esthwaite water, rising to approximately 50% when the adsorption time is increased to over 1700 hours. Desorption into Botany Pond water, after an adsorption time of 30 minutes, is approximately 25% but this increases to approximately 80% when the adsorption time is increased to over 1700 hours. Similar desorption yields were obtained by Abdel Gawad et al (1977) when using canal water.

(3) ^{103}Ru

Although only small desorption yields of ^{103}Ru are obtained, more ^{103}Ru is desorbed than caesium. Nishita et al (1956) found greater quantities of ruthenium than strontium were released from soils, but that was not observed here. Desorption of ^{103}Ru from Botany Pond sediment is shown in Figure 4.6. The percentage of Ru extractable from this sediment decreases rapidly when the adsorption time is increased from 30 minutes to 1 day, after which desorption increases slowly with increasing adsorption times. Desorption is approximately the same with both waters, with Esthwaite water possibly

Figure 4.6 Desorption of ^{103}Ru from Botany Pond sediment

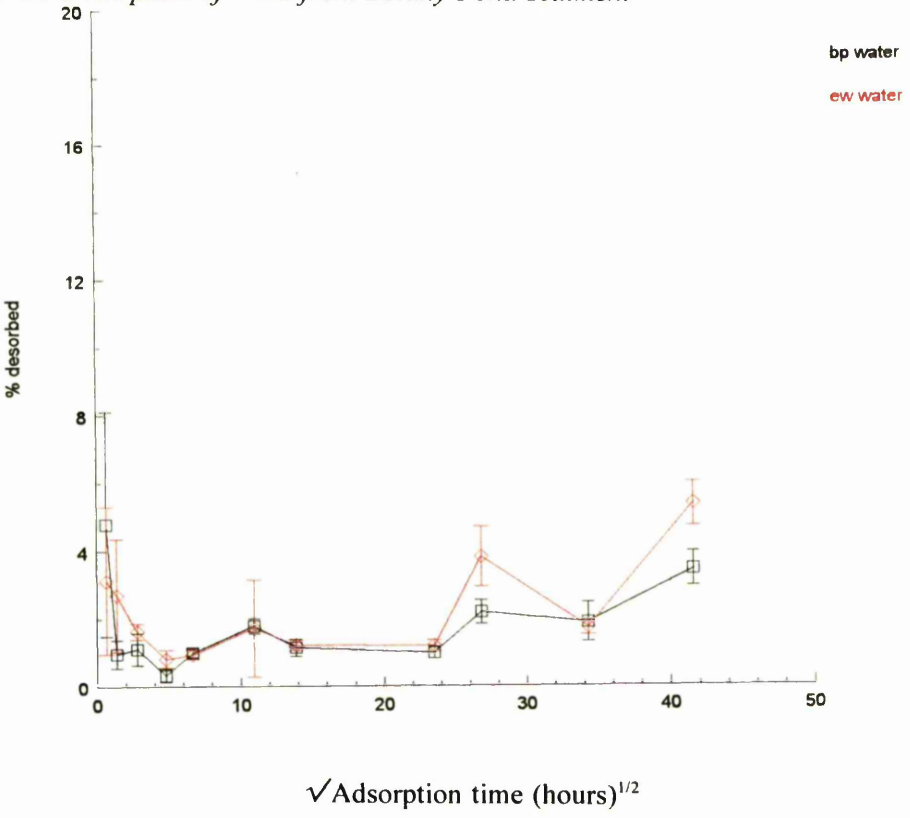

Figure 4.7 Desorption of ^{103}Ru from Esthwaite Water sediment

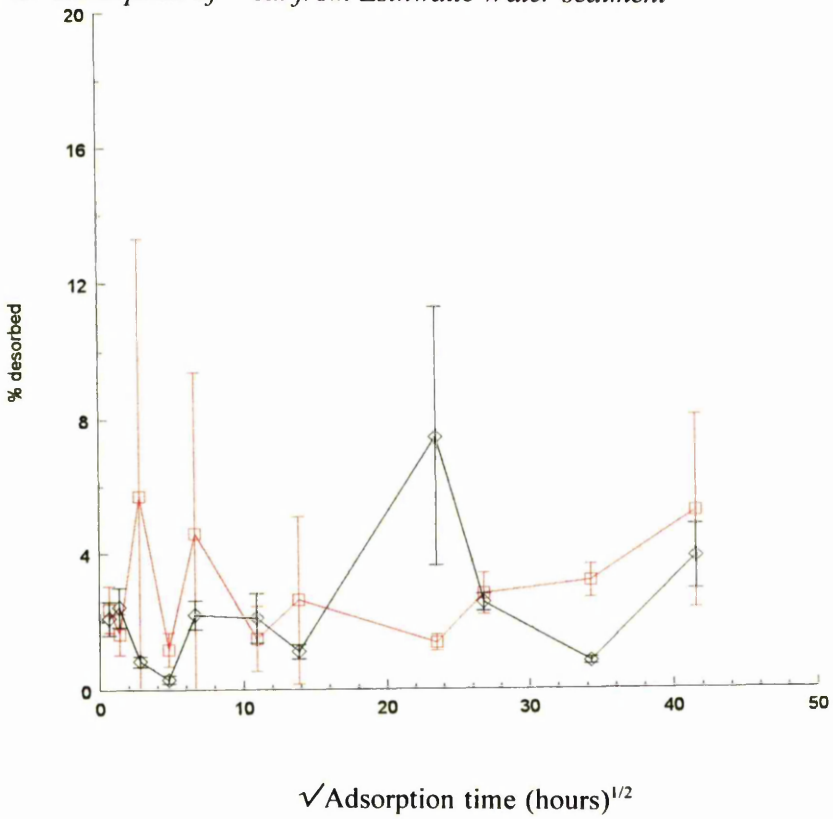

desorbing slightly more ^{103}Ru. After an adsorption time of over 1700 hours, Botany Pond water desorbs approximately 3% of ^{103}Ru and approximately 5% is desorbed with Esthwaite water. There appears to be no relationship with the ionic strength of the extracting solution, which implies that desorption mechanisms other than simple ion-exchange are important. Figure 4.7 shows the amount of ^{103}Ru desorbed from Esthwaite Water sediment. Desorption remains approximately constant, with a possible increase in the percentage desorbed when the length of adsorption time is increased. Desorption of ^{103}Ru is slightly greater from this sediment than from Botany Pond sediment.

(4) *^{134}Cs*

Caesium is much less easily desorbed than cobalt, strontium and ruthenium which is consistent with the results of Abdel Gawad et al (1977). Figure 4.8 shows the amount of ^{134}Cs desorbed from Botany Pond sediment. There is a gradual decrease in the percentage of ^{134}Cs which can be desorbed as the adsorption time increases, indicating a gradual fixation of Cs in the sediment, similar to that observed by other workers (Evans et al, 1983; Erten et al, 1988; Comans et al, 1991). More ^{134}Cs is desorbed with Botany Pond water than with Esthwaite water which is probably due to the higher ionic strength of Botany Pond water (particularly the higher concentrations of potassium). Desorption of ^{134}Cs from Esthwaite Water sediment is shown in Figure 4.9. Desorption of ^{134}Cs is greater from this sediment than Botany Pond sediment, perhaps reflecting the different clay mineralogy. Again, a gradual decrease in ^{134}Cs desorption is observed as the adsorption time is increased and, similarly, more ^{134}Cs is desorbed with Botany Pond water than Esthwaite water. Less than 1% of ^{134}Cs is desorbed from both sediments with either water when the adsorption time exceeds

Figure 4.8 Desorption of ^{134}Cs from Botany Pond sediment

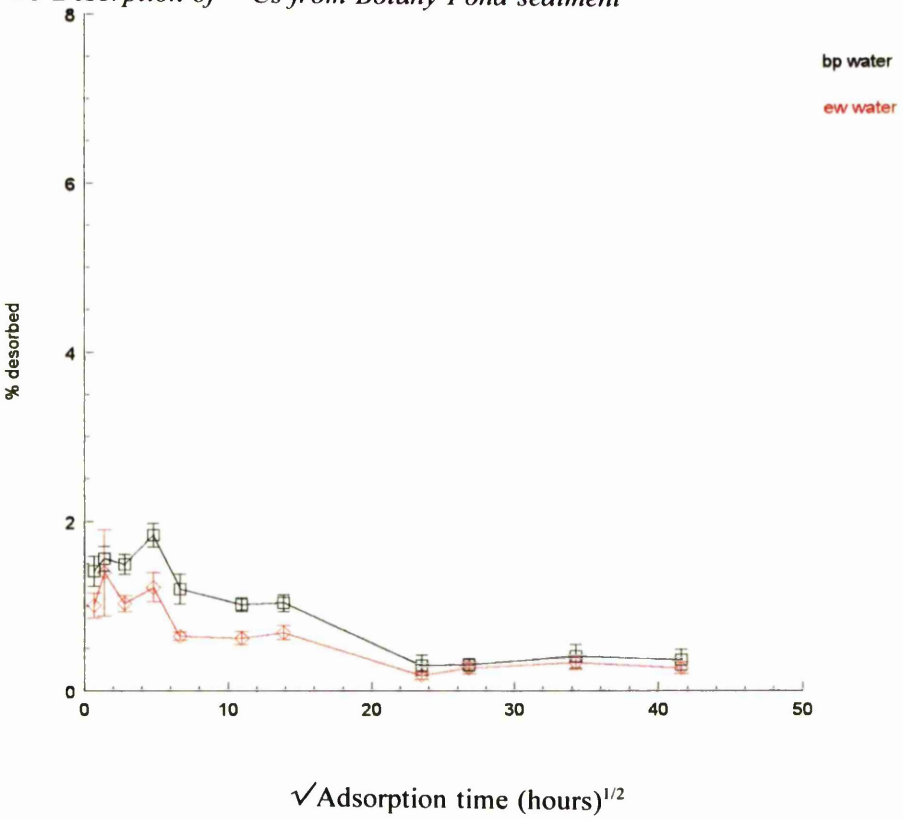

Figure 4.9 Desorption of ^{134}Cs from Esthwaite Water sediment

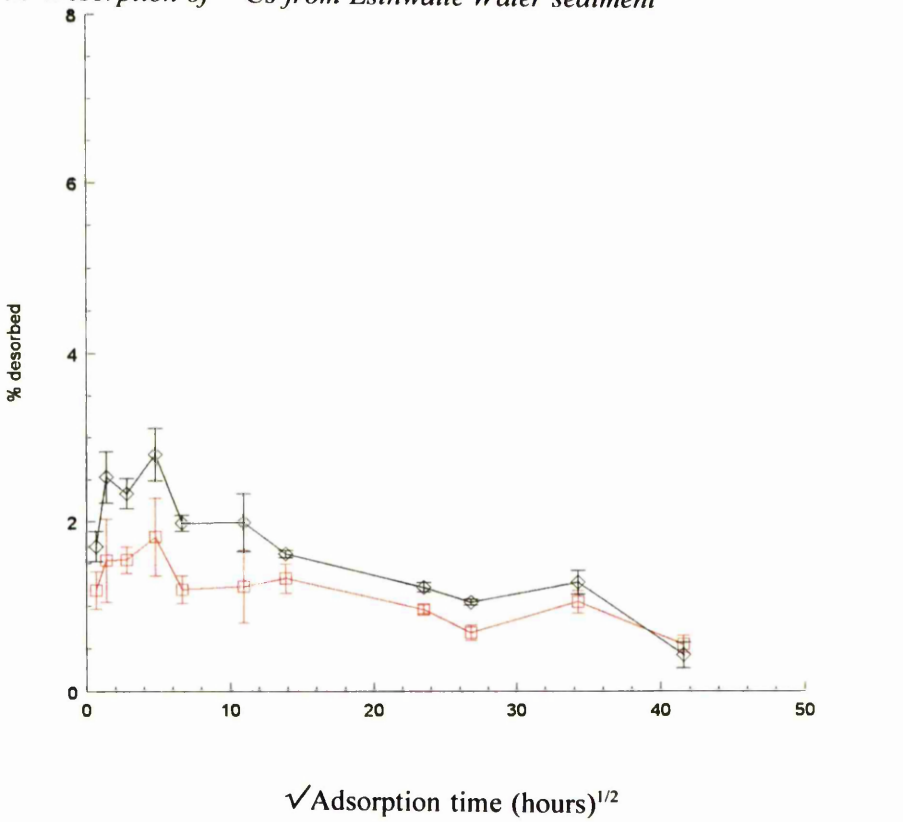

1700 hours.

Comparison of elements

Desorption yields of ^{57}Co decreased as adsorption time increased, suggesting that some kind of fixation process is taking place on both sediments. Desorption yields were small, only approximately 1% when the adsorption time was over 1700 hours. Slightly lower yields of ^{57}Co were desorbed from Botany Pond sediment. Desorption from Esthwaite Water sediment using Esthwaite water gave significantly higher desorption yields, possibly due to biological activity. Desorption of ^{134}Cs showed similar behaviour although desorption yields were smaller. A dependence upon the ionic strength of the desorbing solution was displayed, which suggests that ion-exchange reactions are occurring although the very low desorption yields and the observed fixation within the sediment imply that only a very small amount of caesium remains on easily accessible sites. Desorption of ^{134}Cs was greater from Esthwaite Water sediment, as with ^{57}Co.

Although desorption yields of ^{103}Ru were also small (but slightly higher than ^{57}Co and ^{134}Cs yields) and desorption was again greater from Esthwaite Water sediment, the general desorption behaviour displayed by this radionuclide was very different to the other isotopes used. An initial rapid decrease in desorption yields (when the adsorption time was increased from 0.5 hours to approximately 1 day) was then followed by a slow increase in desorption when the adsorption time was increased to over 1700 hours. No dependence upon the ionic strength of the desorbing solution was observed suggesting that reactions other than ion-exchange are taking place. This behaviour is in contrast to ^{85}Sr which gave much higher desorption yields and displayed a strong

dependence upon the ionic strength of the desorbing solution.

4.7.2 Desorption of sterilised samples into fresh lake water

(1) ^{57}Co

Table 4.1 compares the percentage of ^{57}Co which was desorbed from Esthwaite Water sediment using Esthwaite water, using samples which were non-sterilised and samples which had been sterilised prior to adsorption.

Table 4.1 Comparison of desorption yields for ^{57}Co for sterilised and non-sterilised samples.

ADSORPTION TIME (hrs)	MEAN % DESORBED±1SD	
	NON-STERILISED	STERILISED
720	5.44±1.0	
1104		2.68±0.3
1176	25.2±9.8	3.47±0.4
1320		3.67±2
1680		3.44±0.5
1728	11.8±2.0	

The samples which had been autoclaved give much lower desorption yields than the non-sterilised samples. This could be due to microbes affecting the the pH and redox conditions in the non-sterilised samples, causing a much higher release of ^{57}Co into the lake water following desorption. Alternatively, it could be due to alteration of the phases upon which the Co is sorbed, thereby trapping the ^{57}Co and making it harder to release. The desorption yields of the sterilised EWEW samples are similar to the

desorption yields measured in the EWBP system (see Section 4.7.1). Although the yields cannot be expected to be identical due to the different ionic compositions of Botany Pond and Esthwaite water, the similarity suggests that the sediment has not been altered significantly during the sterilisation procedure. Nyffeler et al (1984) proposed that high desorption yields of cobalt were also due to a change in conditions within the system caused by biological activity.

(2) *^{134}Cs*

Table 4.2 compares the desorption yields for ^{134}Cs following the addition of fresh lake water to spiked sediment samples, some of which had been sterilised. Desorption yields appear to be similar regardless of treatment which implies that any microbes which were present in the samples had no effect on the desorption of yields of ^{134}Cs, and that the sterilisation procedure had little effect on the sediment structure.

Table 4.2 Comparison of desorption yields of ^{134}Cs for sterilised and non-sterilised samples.

ADSORPTION TIME (hrs)	MEAN % DESORBED±1SD	
	NON-STERILISED	STERILISED
720	0.687±0.09	
1104		0.929±0.3
1176	1.04±0.1	1.24±0.2
1320		1.30±0.3
1680		1.09±0.2
1728	0.549±0.1	

4.7.3 Ammonium acetate extractions

Ammonium acetate is a much more efficient extracting agent than lake water, which is reflective of the higher ionic strength of the solution as well as the identity of the extracting species. The ease by which the radionuclides are extracted by ammonium acetate varies in the order $^{85}Sr > ^{134}Cs > ^{57}Co > ^{103}Ru$, which is in agreement with studies by Fukui (1990).

Table 4.3 shows the percentage of ^{57}Co remaining sorbed to the sediment following leaching by ammonium acetate. Generally, as the adsorption time increases, there is an increase in the amount of ^{57}Co remaining sorbed following the extraction, implying that it is becoming harder to extract from the sediment. After an adsorption time of 1176 hours, the percentage remaining on the sediment in the EWEW system falls significantly. This corresponds to the unusual behaviour observed during adsorption and is suggested to be due to microbial activity. Although significantly higher yields of ^{57}Co are extracted with ammonium acetate than lake water, consistent trends are observed.

Table 4.3 ^{57}Co ammonium acetate extraction data.

	% REMAINING ON SEDIMENT±1SD			
ADSORPTION TIME (hrs)	BPBP	BPEW	EWBP	EWEW
23	65.8±0.82	81.5±6.6	42.4±1.2	4.96±6.2
192	81.6±3.6	79.5±1.4	80.5±0.18	53.2±1.8
1176	83.4±1.9	84.2±0.44	82.7±0.67	23.9±9.4

The ammonium acetate extraction data for ^{85}Sr are shown in Table 4.4. Much higher

yields of ^{85}Sr are extracted with ammonium acetate than lake water. After an adsorption time of 23 hours, there is no ^{85}Sr left on the sediment following extraction with ammonium acetate, except in the EWBP system. When the adsorption time had been increased to 192 hours however, a small quantity of ^{85}Sr remained sorbed on the sediment in each system. Although this could imply a small degree of fixation was starting to occur, as has been observed in other studies (Martin et al, 1957; Libby, 1958) when the adsorption time was increased further and the extraction procedure was repeated again all of the ^{85}Sr was extracted from the sediment, except in the EWBP and possibly the BPBP system. These high desorption yields at long adsorption times are consistent with those obtained with lake water and, as previously mentioned, can possibly be ascribed to biological activity causing changes within the systems during adsorption. This makes it difficult to draw any definite conclusions. Nevertheless, it is apparent that the majority of ^{85}Sr sorbed on both sediments remains on readily exchangeable sites and is easily extracted with ammonium acetate.

Table 4.4 ^{85}Sr ammonium acetate extraction data.

	% REMAINING ON SEDIMENT±1SD			
ADSORPTION TIME (hrs)	BPBP	BPEW	EWBP	EWEW
23	0±0.85	0.11±1.3	63.2±0.15	0.66±2.8
192	11.7±0.7	9.36±0.54	14.7±0.30	12.7±0.77
1176	10.1±9.3	0±0.28	40.1±0.37	0±0.37

The ammonium acetate extraction data for ^{103}Ru are shown in Table 4.5. As the adsorption time increases the percentage of ^{103}Ru remaining on the sediment in each system decreases. Slightly higher yields are obtained than those measured when using lake water, although similar trends are observed. As ruthenium is known to have a

complex chemistry, this behaviour could be explained by a change in pH and Eh within the system which could affect the speciation, and therefore, behaviour of the ruthenium.

Table 4.5 ^{103}Ru ammonium acetate extraction data.

ADSORPTION TIME (hrs)	% REMAINING ON SEDIMENT±1SD			
	BPBP	BPEW	EWBP	EWEW
23	96.5±0.2	92.3±0.3	95.5±0.6	93.7±0.3
192	89.6±0.2	91.1±0.1	93.5±0.2	92.1±0.4
1176	79.8±0.9	80.8±0.3	86.7±0.3	78.3±1.0

Table 4.6 shows the percentage of ^{134}Cs remaining on the sediment following the ammonium acetate extraction procedure. Although higher desorption yields are obtained using ammonium acetate than lake water, similar trends are observed, with caesium becoming harder to extract as the adsorption time increases.

Table 4.6 ^{134}Cs ammonium acetate extraction data.

ADSORPTION TIME (hrs)	% REMAINING ON SEDIMENT±1SD			
	BPBP	BPEW	EWBP	EWEW
23	52.1±1.3	60.4±0.3	33.0±0.4	33.9±0.5
192	81.7±0.2	86.5±0.03	51.6±0.2	54.5±0.4
1176	78.4±0.6	83.2±0.4	48.5±2.0	50.3±0.5

This implies a gradual fixation process is occurring within the sediment, consistent with the results of other studies such as Evans et al (1983). Botany Pond sediment appears to retain caesium more effectively than Esthwaite Water sediment (by

approximately 30%) which is consistent with the differences in their clay mineralogies. Contacting either sediment with Esthwaite water during adsorption causes slightly less efficient extraction of caesium. This could be because Esthwaite water contains fewer K^+ ions than Botany Pond water, which are known to compete effectively for the same sites as Cs^+ ions during adsorption. There is apparently a small decrease in the amount of caesium retained by the sediment after an adsorption time of 1176 hours.

Comparison of elements

Differences were observed between ammonium acetate and lake water desorptions. This is a reflection of both the increased ionic strength and also the identity of the extracting species (an indication of the effectiveness of the NH_4^+ ion to displace different isotopes). Highest extraction yields (in some cases 100%) were obtained for ^{85}Sr and these showed no dependence upon adsorption time. A fixation of ^{57}Co and ^{134}Cs within the sediment was observed, with similar extraction yields for both radionuclides. Unusual behaviour was seen for ^{57}Co extraction in the EWEW system, and Botany Pond sediment was more effective in retaining both radionuclides than Esthwaite Water sediment. Interestingly, contacting either sediment with Esthwaite water caused a slightly less efficient extraction of ^{134}Cs. The lowest extraction yields were obtained for ^{103}Ru, although extraction yields increased as the adsorption time also increased, as with lake water desorption.

4.7.4 Successive desorptions into fresh lake water

(1) ^{57}Co

Figure 4.10 shows the total percentage of ^{57}Co desorbed from Botany Pond sediment after an adsorption time of 0.5 hours and using continuous extraction with either Botany Pond or Esthwaite water. Esthwaite water appears to desorb less ^{57}Co and, after a total desorption time of approximately 170 hours, desorption appears to remain constant at approximately 3.5% removal of ^{57}Co, suggesting only a very small fraction of ^{57}Co is ion-exchangeable. This is much lower than the extraction yields obtained by ammonium acetate. Figure 4.11 shows the percentage of ^{57}Co desorbed after an adsorption time of 11 days. Again Esthwaite water has a slower desorption and desorbs less compared to Botany Pond water. There appears to be 2 stages to desorption, an initial rapid desorption of approximately 4%, but unlike previously, there is also a slower desorption which continues for the duration of the experiment. Again, this is lower than the extraction yields obtained by ammonium acetate but also higher than the results reported in Section 4.7.1, when only one desorption into lake water was carried out. Abdel Gawad et al (1977) also noticed small but increasing amounts of cobalt were released with increasing desorption times, as was observed here.

(2) ^{85}Sr

Figure 4.12 shows the total percentage of ^{85}Sr desorbed from Botany Pond sediment after an adsorption time of 0.5 hours and using continuous extraction with either Botany Pond or Esthwaite water. Botany Pond water extracts all of the ^{85}Sr within 700

Figure 4.10 Successive desorption of ^{57}Co following 0.5 hour adsorption time

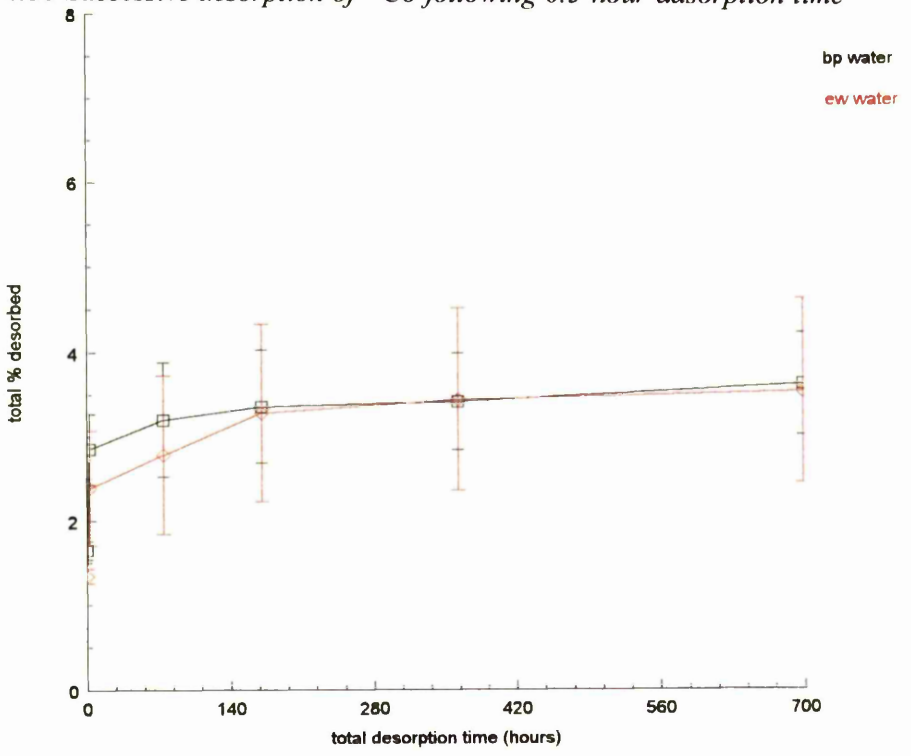

Figure 4.11 Successive desorption of ^{57}Co following 11 day adsorption time

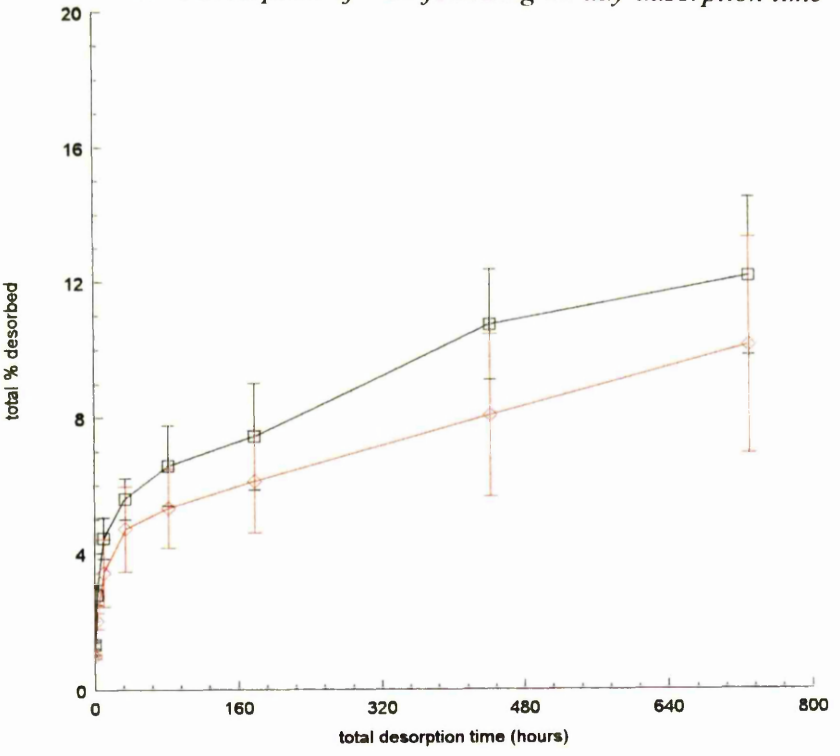

hours whereas Esthwaite water has extracted only 70% after this time. This implies that the ^{85}Sr held on this sediment is completely ion-exchangeable and the amount extracted during desorption is heavily dependent upon desorption time. Figure 4.13 shows the total percentage of ^{85}Sr desorbed after an adsorption time of 11 days. Again Esthwaite water desorption is not complete whereas 100% desorption has been achieved by Botany Pond water after just 90 hours.

(3) *^{134}Cs*

Figure 4.14 shows the total percentage of ^{134}Cs desorbed from Botany Pond sediment after an adsorption time of 0.5 hours following continuous extraction with Botany Pond and Esthwaite water. Botany Pond water extracts less ^{134}Cs than Esthwaite water until 700 hours, after which time desorption remains constant and both waters have extracted equal amounts (approximately 5%). This is a higher yield than the percentage desorbed when only one desorption was carried out (see Section 4.7.1), although considerably less than extracted by ammonium acetate. Figure 4.15 shows the total percentage of ^{134}Cs desorbed after an adsorption time of 11 days. Esthwaite water extracts less ^{134}Cs from the sediment than Botany Pond water. There are two stages of desorption observed, an initial rapid desorption, followed by a slower period of desorption which continues for the duration of the experiment. After this time, Botany Pond water has desorbed approximately 4% of ^{134}Cs, whereas Esthwaite water has desorbed approximately 3.5%. This indicates a fixation of ^{134}Cs is occurring within the sediment.

Figure 4.12 Successive desorption of ^{85}Sr following 0.5 hour adsorption time

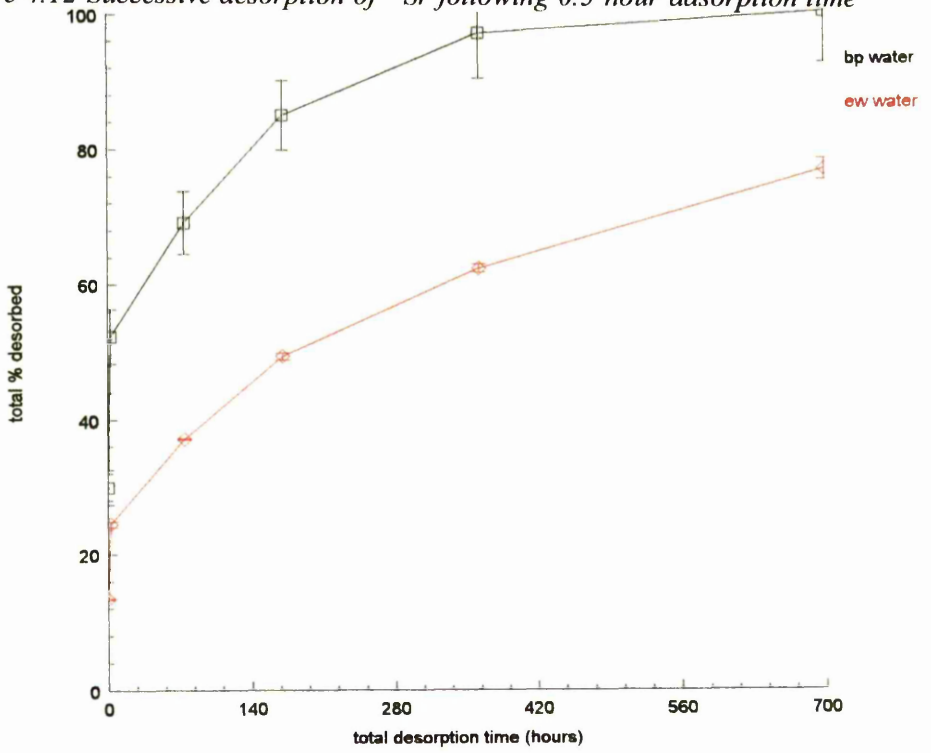

Figure 4.13 Successive desorption of ^{85}Sr following 11 day adsorption time

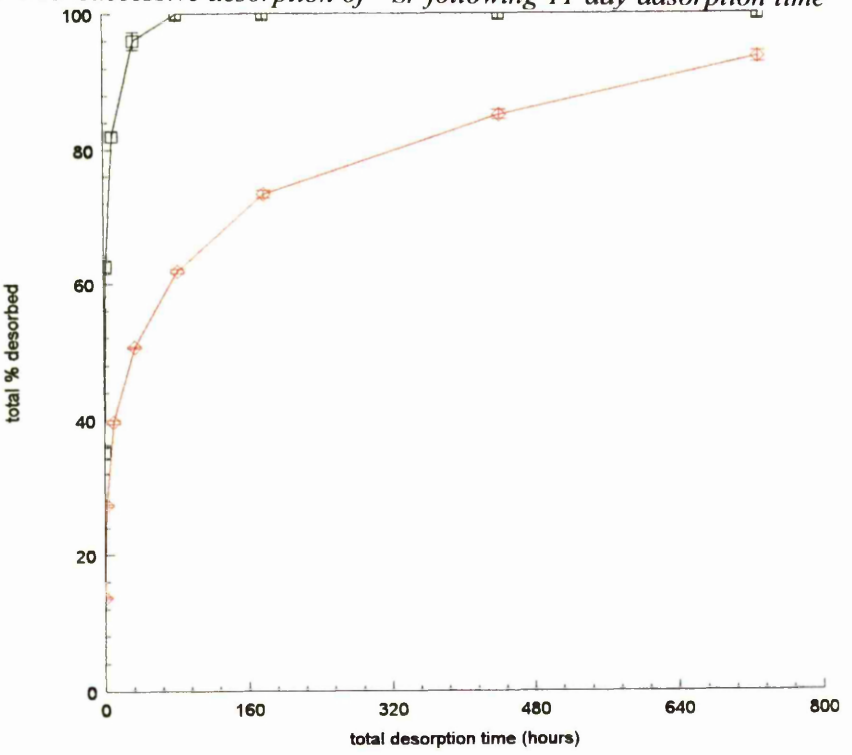

Figure 4.14 Successive desorption of ^{134}Cs following 0.5 hour adsorption time

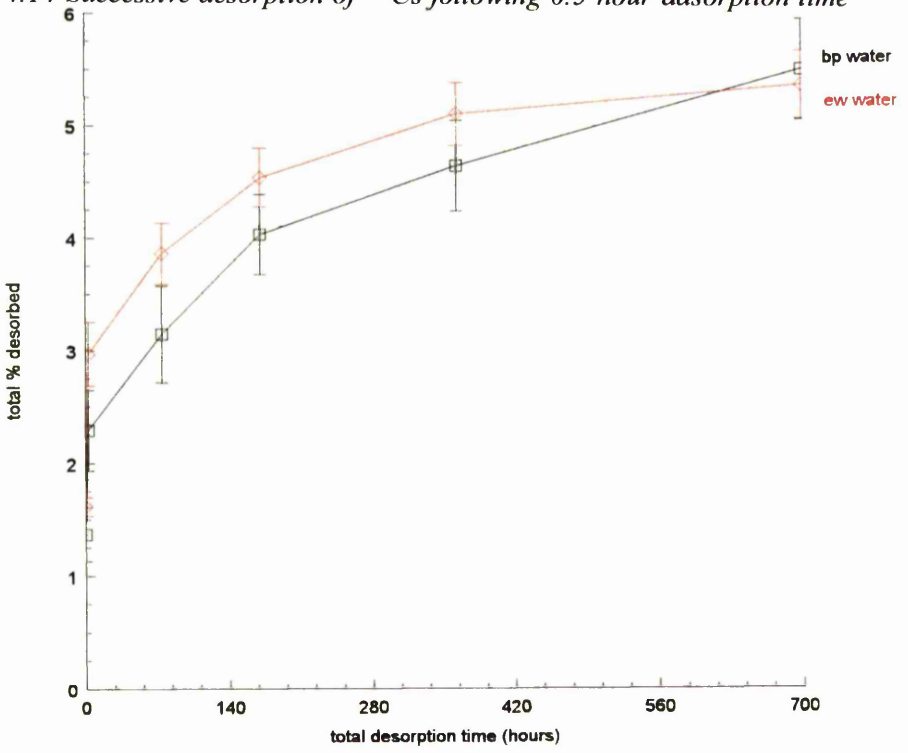

Figure 4.15 Successive desorption of ^{134}Cs following 11 day adsorption time

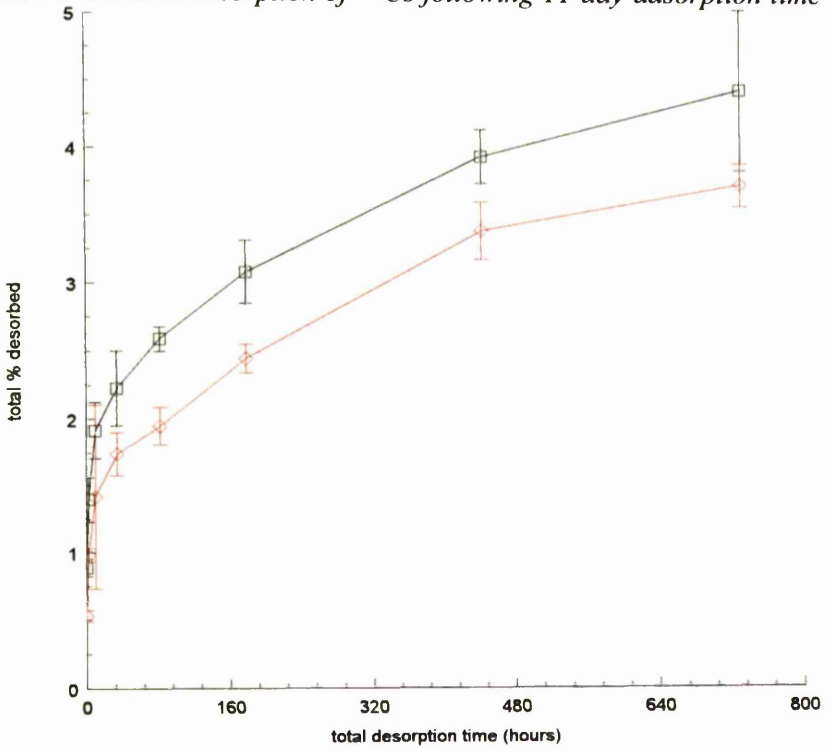

Eventually, 100% desorption was achieved for ^{85}Sr indicating that strontium remains on easily accessible sites and can be readily ion-exchanged. Total desorption yields of ^{57}Co and ^{134}Cs were much smaller and desorption appeared to occur in two stages - an initial rapid period of desorption, followed by a slower desorption which continued for the duration of the experiment.

4.7.5 Tessier extractions

(1) *^{57}Co*

Figures 4.16-4.18 show the results of the Tessier extraction procedure for ^{57}Co. After an adsorption time of 1 week, a high proportion of ^{57}Co is held in both the exchangeable fraction and the Fe/Mn oxide fraction of Esthwaite Water sediment, with the remainder being distributed between the other phases. Similarly, for Botany Pond sediment a high proportion of ^{57}Co is held in the Fe/Mn oxide fraction, but also in the carbonate fraction, with slightly less being held in the exchangeable pool. The high proportion of ^{57}Co observed in the Fe/Mn oxide fraction is unsurprising, given the well documented affinity that exists between cobalt and the manganese content of the sediment (see Section 1.7.1). Perhaps more surprising is the quantity of cobalt detected in the "carbonate" fraction of Esthwaite Water sediment, given that carbonate is undetectable in this sediment. This fraction should perhaps therefore be more accurately labelled the "acetate extractable" fraction of cobalt. It is possible that the true cause of the ^{57}Co release is the dissolution of a small amount of manganese oxide in response to the pH change.

Figure 4.16 Selective extraction of ^{57}Co following 168 hour adsorption time

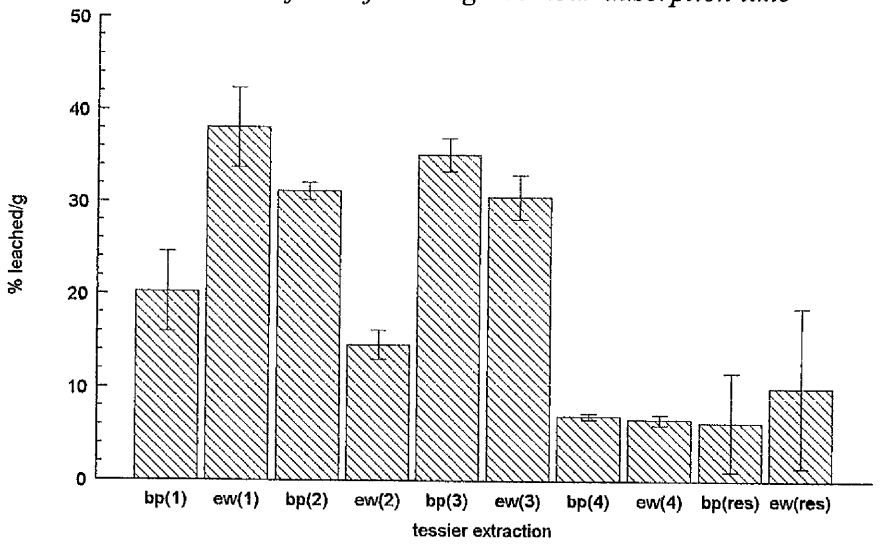

Figure 4.17 Selective extraction of ^{57}Co following 816 hour adsorption time

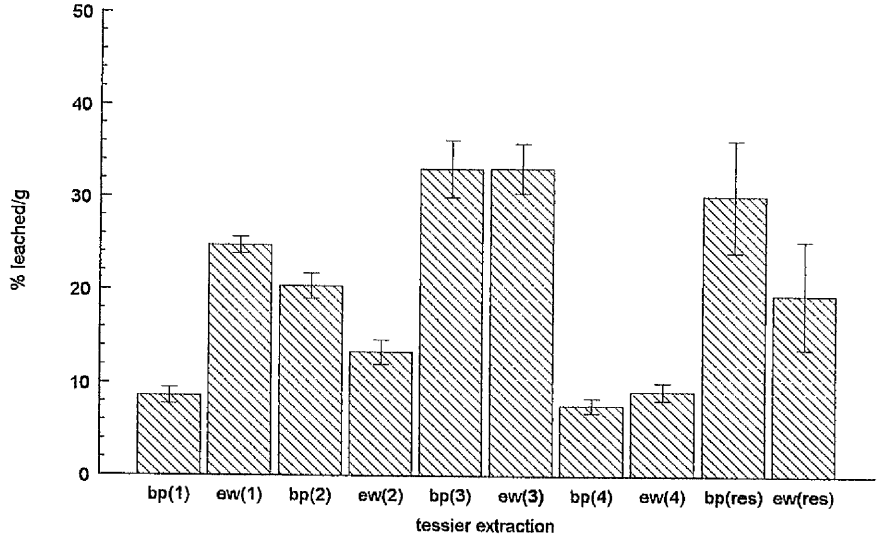

Figure 4.18 Selective extraction of ^{57}Co following 1488 hour adsorption time

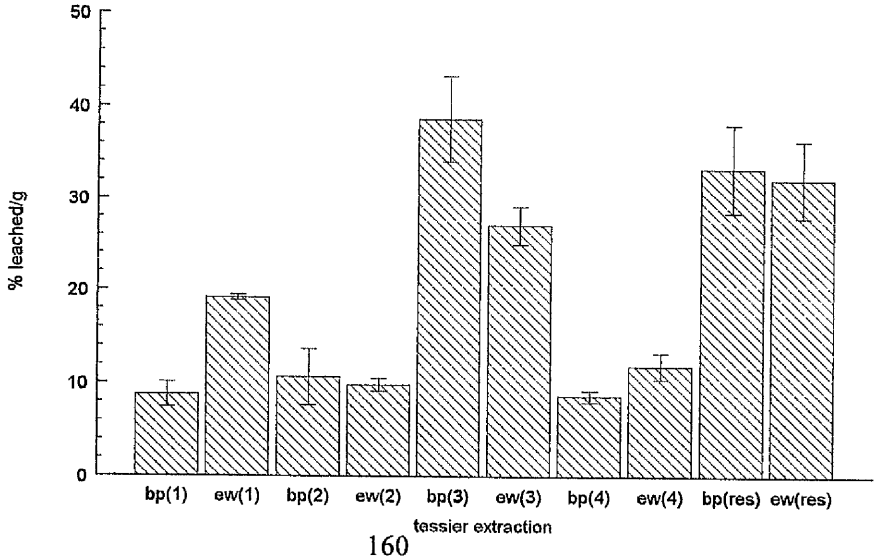

An increase in adsorption time to over 800 hours sees a significant decrease in ^{57}Co extracted from the exchangeable pool of both sediments, and also in the carbonate fraction of Botany Pond sediment. This is consistent with the desorption data shown in Sections 4.7.1 and 4.7.3 which also show a decrease in the availability of ^{57}Co as adsorption time increased. Whilst the other fractions seem to remain approximately constant, a large increase is seen in the residual fraction, implying that the majority of ^{57}Co in both sediments is now held within the Fe/Mn oxide fraction and the remaining residual pool. As the residual fraction is often referred to as the secondary aluminosilicate fraction, this shift of cobalt from the exchangeable pool to the residual fraction could mean that some cobalt is becoming irreversibly sorbed on to the clay minerals in the sediment, as was observed by Grutter et al (1994). It is also possible however, that cobalt bound in the residual fraction is actually fixed within the Fe/Mn oxide structures, as Cerling and Turner (1982) found that only 70-80% of cobalt sorbed on these oxides could be extracted by the hydroxylamine hydrochloride extraction procedure.

A further increase in adsorption time to approximately 1500 hours sees even more of a shift from the exchangeable pool and carbonate fraction of both sediments, to the Fe/Mn oxide and residual fractions. Interestingly, however, the exchangeable fraction of ^{57}Co in the EWEW system after this time, was not unusually high, as might be expected from the data in Sections 4.7.1 and 4.7.3.

(2) ^{85}Sr

Figures 4.19-4.21 show the results of the sequential leach procedure on ^{85}Sr. After an adsorption time of 1 week, the majority of ^{85}Sr is held in the exchangeable fraction

Figure 4.19 Selective extraction of ^{85}Sr following 168 hour adsorption time

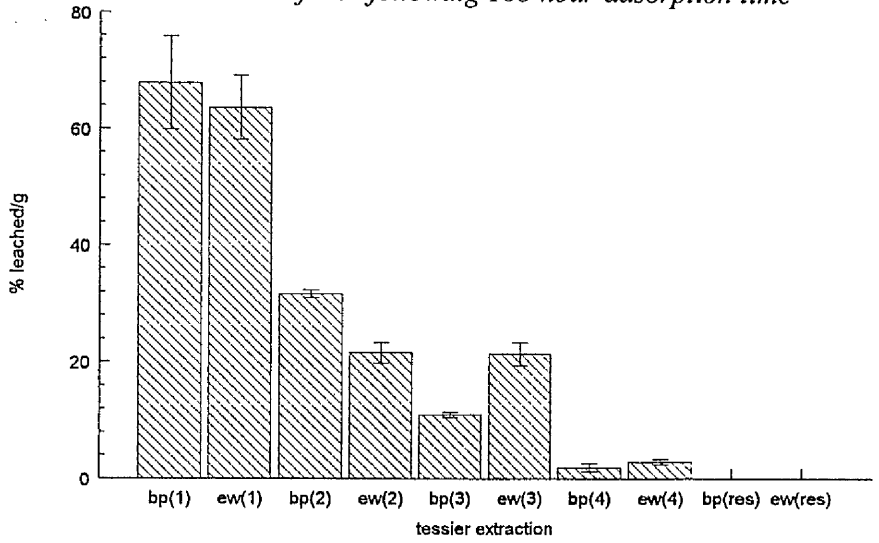

Figure 4.20 Selective extraction of ^{85}Sr following 816 hour adsorption time

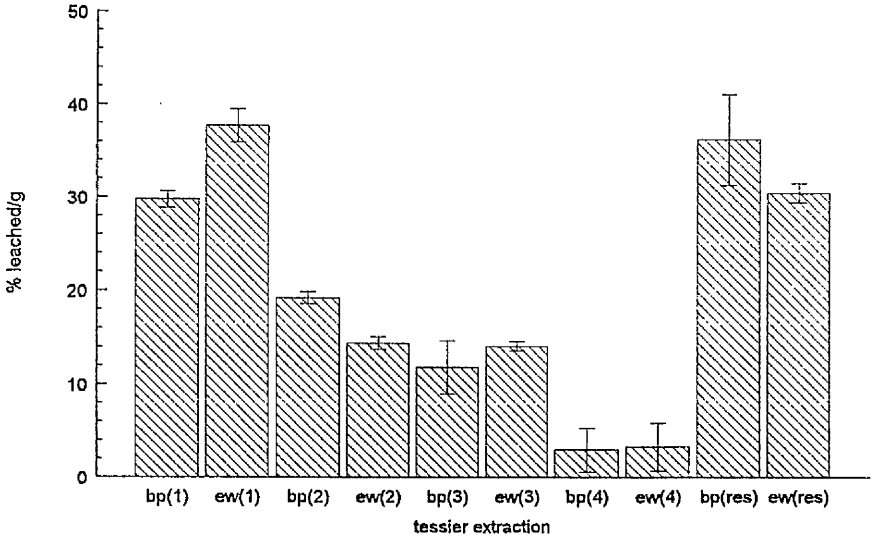

Figure 4.21 Selective extraction of ^{85}Sr following 1488 hour adsorption time

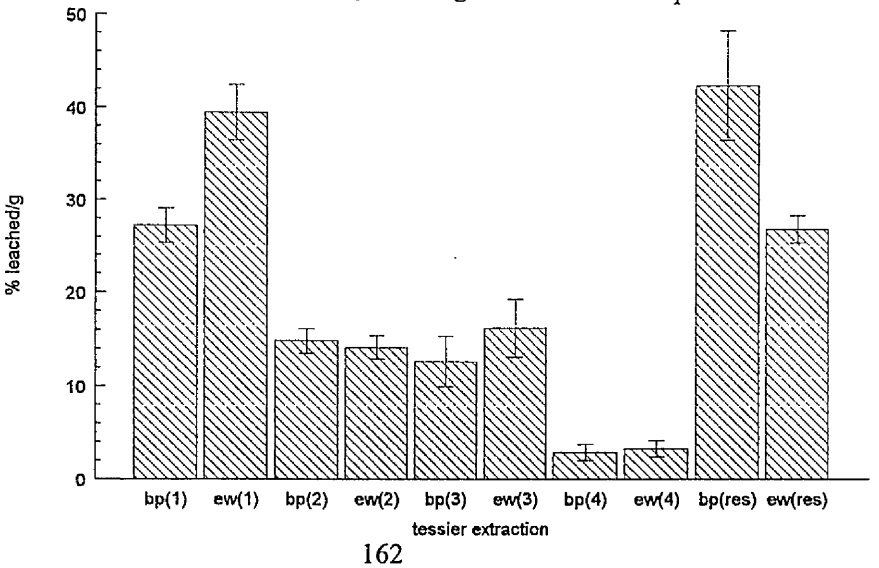

of both sediments, with the remainder being held in the carbonate and Fe/Mn oxide fractions. Only a very small quantity was held in the organic fraction and all the ^{85}Sr was exchangeable with none remaining in the residual fraction. As expected for a radionuclide which exhibits sorption by ion exchange, the majority of strontium is held in sites readily exchangeable by Mg^{2+} ions. This is consistent with the results in Section 4.7.3, which showed that all of the ^{85}Sr was easily extracted by ammonium acetate.

An increase in adsorption time to approximately 800 hours, leads to a large decrease in the amount of ^{85}Sr in the exchangeable and carbonate fraction of both sediments. This activity seems to be present in the residual fraction instead. This implies that strontium is becoming harder to desorb, possibly becoming slowly incorporated into insoluble phases such as calcium or magnesium containing minerals.

Very little further change occurs when the adsorption time is increased to over 1400 hours. This implies that adsorption and redistribution has finished after this time, with the majority of ^{85}Sr being held in the exchangeable and residual fractions of both sediments.

(3) ^{134}Cs

The Tessier extraction data for ^{134}Cs are shown in Figures 4.22-4.24. Even after an adsorption time of 1 week, ^{134}Cs is not easily desorbed (consistent with data shown in Sections 4.7.1 and 4.7.3), with the majority of ^{134}Cs already held in the residual fraction. Slightly more is in the residual fraction of Botany Pond sediment, whereas Esthwaite Water sediment also has a significant proportion held in the Fe/Mn oxide

Figure 4.22 Selective extraction of ^{134}Cs following 168 hour adsorption time

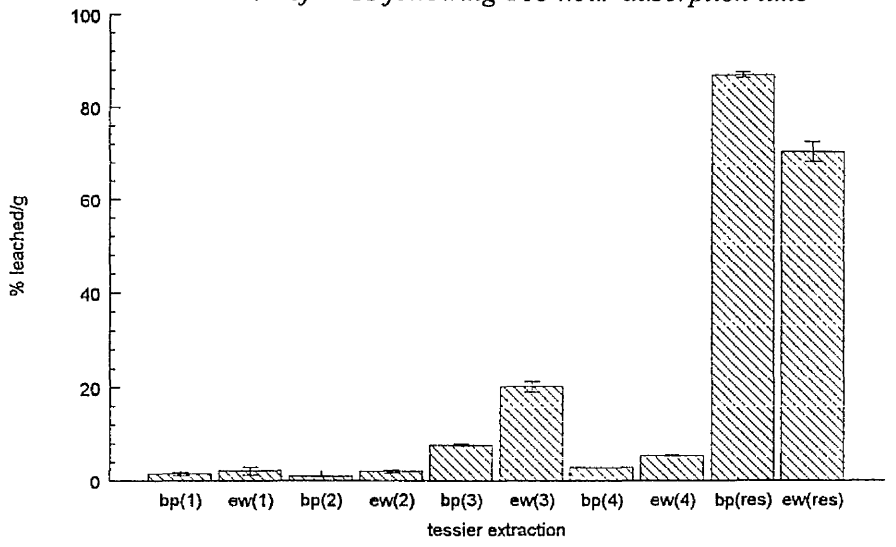

Figure 4.23 Selective extraction of ^{134}Cs following 816 hour adsorption time

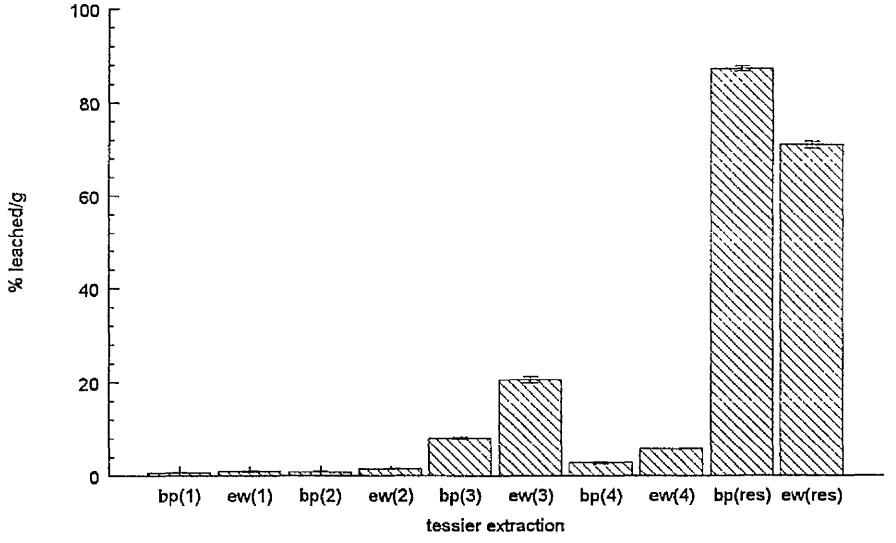

Figure 4.24 Selective extraction of ^{134}Cs following 1488 hour adsorption time

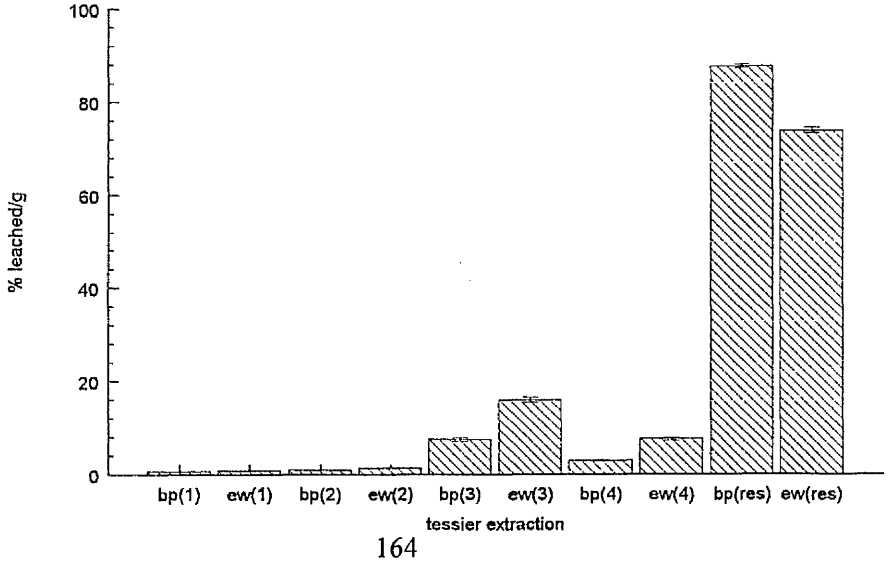

fraction. Very little caesium is held in readily exchangeable sites, although Mg^{2+} ions are known to be poor extractants of sorbed Cs^+ ions. This could imply that the Cs has already become fixed in interlayer sites in the clay from which it is not easily released. Since NH_4^+ (the most effective extractant of Cs) was not used during the extraction procedure however, it is not possible to draw more definite conclusions as to the "true" exchangeability of Cs. The caesium leached from the "Fe/Mn oxide" fraction may be an artefact arising from the reagents used in the reduction procedure. Evans et al (1983) found that the reducing reagents used in this procedure displaced 36-55% of sorbed caesium. However, a dithionite/citrate mixture, which is a stronger reducing agent, displaced only 13-14%, and the use of an even stronger reducing agent, $NaBH_4$, displaced only 3-6%. This suggests that, rather than being indicative of the amount of caesium sorbed on to the Fe/Mn oxide fraction of the sediment, the differences observed between the reducing agents arose due to other reactions. One possible explanation for the variation in extraction yields is the low pH of the hydroxylamine hydrochloride in acetic acid reaction mixture. At low pH fine and poorly crystalline clays dissolve readily, and this would release any sorbed radiocaesium into solution. The production of ammonium is also possible during hydroxylamine decomposition at high H^+ concentrations and ammonium ions are known to be effective at displacing caesium from FES. This fraction, rather than being an indication of the quantity of caesium sorbed by Fe/Mn oxides, could thus be an indication of the fraction of caesium held in the frayed edge sites of the clay structure.

When the adsorption time is increased to approximately 800 hours, the amount of ^{134}Cs held in the exchangeable and carbonate fractions decreases slightly, leading to a slight increase in the Fe/Mn oxide and residual fractions, a possible indication of the slow migration of Cs^+ cations into the interior of the clay. After an adsorption time

of over 1400 hours, the small decrease in ^{134}Cs content in the exchangeable and carbonate fractions continues, and is also seen in the Fe/Mn oxide fraction. This leads again to an increase of ^{134}Cs in the residual and also in the organic fraction.

Comparison of elements

The Tessier extraction procedure revealed that the majority of ^{57}Co was readily exchangeable and was desorbed during the first three extractions. As adsorption time was increased, less ^{57}Co was desorbed during the first two extractions, but a large increase was observed in the "unextractable" residual fraction. The content of ^{57}Co in the Fe/Mn oxide fraction seemed to remain constant throughout. A similar shift towards the residual fraction was observed for ^{85}Sr. After an adsorption time of approximately 170 hours, the majority of ^{85}Sr was readily exchangeable, but as adsorption time increased to over 800 hours the exchangeable fraction decreased. After this time, no further change occurred. The results of the sequential extraction procedure revealed very different behaviour for ^{134}Cs. After an adsorption time of just one week, very little ^{134}Cs was exchangeable with the reagents used, over 70% of ^{134}Cs was held in the residual fraction. As adsorption time was increased the percentage of ^{134}Cs held in the residual fraction also increased further.

4.8 Summary

1. Desorption yields of ^{57}Co, ^{103}Ru and ^{134}Cs into lake water were small, and for ^{57}Co and ^{134}Cs these yields decreased as the adsorption time was increased, suggesting that these two radionuclides were becoming fixed in the sediment. Although, desorption yields of ^{57}Co, ^{103}Ru and ^{134}Cs were significantly higher when ammonium acetate was

used as the extractant, a fixation process was still observed for ^{57}Co and ^{134}Cs.

2. Desorption of ^{85}Sr and ^{134}Cs depended on the ionic strength of the desorbing solution, implying ion-exchange is an important sorption mechanism for these two isotopes. Complete extraction of ^{85}Sr was possible when using ammonium acetate as the extractant, or if a sufficient number of desorptions into fresh lake water were carried out.

3. Desorption yields of ^{103}Ru increased as adsorption time was increased using either lake water or ammonium acetate as the extractant. This could be due to a change in the speciation of ruthenium.

4. Biological activity seemed to be responsible for the exceptionally high desorption yields of ^{57}Co which were measured using Esthwaite Water sediment and Esthwaite water. Lower but more realistic yields were measured on sterilised samples.

5. Desorption of ^{57}Co and ^{134}Cs into lake water seemed to occur in two stages. An initial rapid period of desorption was followed by a slower desorption which continued for the duration of the experiment.

6. The Tessier extraction procedure also revealed a fixation process taking place for ^{57}Co and ^{134}Cs, where a shift of these two radionuclides from the exchangeable fractions into the residual fraction was observed as the adsorption time was increased. The Fe/Mn oxide fraction also contained significant amounts of ^{57}Co, the percentage of ^{57}Co extracted from this fraction remained unchanged as the adsorption time was increased. Over 70% of ^{134}Cs was held in the residual fraction after an adsorption time of just one week. Radiostrontium was easily exchangeable, although the exchangeable pool decreased when the adsorption time was increased to over 800 hours. There was no further change observed for this radionuclide after this time.

CHAPTER 5 - THE KINETIC BOX MODEL

CHAPTER 5 - THE KINETIC BOX MODEL

5.1 Introduction

By developing a successful model to describe the sorption kinetics of radionuclides in freshwater systems, it is hoped that predictions regarding radionuclide behaviour in these systems can then be made and hypotheses tested. A kinetic model allows us to evaluate reaction parameters which are important in determining the mobility and rate of removal of radionuclides from the water column (Robbins et al, 1992; Smith and Comans, 1996).

A box-model has been adopted to describe the sorption kinetics of the four radionuclides used in this project, in each of the different freshwater environments. This chapter describes the box model and explains its application to the experimental data. The relative ability of the 1,2 and 3-box models to describe the solid-solution partitioning of the various radionuclides has been compared and rate constants for the reactions mechanisms have been calculated.

5.2 Analysis of sorption data using a linearization procedure

The total amount of tracer which is taken up by a sediment is the sum of a variety of different reactions or processes which are occurring within the system. This is illustrated by the data presented in Section 3.7.1, which implies that both short and long term sorption processes are occurring within the system, particularly with ^{57}Co, ^{103}Ru and ^{134}Cs. Jannasch et al (1988) developed a linearization method for the purpose of characterising these different reaction mechanisms. This provides further

information on the number of different processes taking place, as well as their timescales and hence illustrates their relative importance and also any relation to the chemistry of the radionuclide and freshwater system being studied.

In deriving the linearized equation, the assumptions are made that only one process at a time is controlling the rate of uptake of the tracer; that each of the different processes can be described as a first order reversible reaction; and also that each reaction is fast in relation to the next slower reaction. Each first order, reversible reaction can be written as follows (where i=1,2,3 ...n depending on the number of simultaneous reactions):

$$[Md] \underset{k_{-i}}{\overset{k_i}{\rightleftharpoons}} [Ms]$$

[Md] = concentration of tracer in solution at time, t (Bq l^{-1}).

$[Md]_e$ = concentration of tracer in solution at equilibrium (Bq l^{-1}).

[Mt] = total concentration of tracer available (Bq l^{-1}).

[Ms] = concentration of sorbed tracer (Bq kg^{-1}).

k_i = forward rate constant (hr^{-1}).

k_{-i} = backward rate constant (hr^{-1}).

Assuming the sum of the amount of sorbed tracer, Ms, and the amount of tracer in solution, Md, at time t, is equal to the total amount of tracer available, Mt, the linearized equation can be derived to give the final equation below:

$$\ln\left\{\frac{[Md] - [Md]_e}{[Mt] - [Md]_e}\right\} = (k_i + k_{-i}) \cdot t \quad \ldots (1)$$

A complete derivation of this equation is shown in Jannasch et al (1988). Linearization plots are obtained by plotting the l.h.s. of equation (1) versus time. Both the concentration of tracer in solution, [Md], and the total concentration of tracer available for uptake, [Mt], are known, but an estimation of the concentration of tracer in solution at equilibrium, $[Md]_e$, has to be made. Although using different $[Md]_e$ values in the equation will result in different gradients (and hence, k_i and k_{-i} values) and also a different intercept value (which is an indication of the extent of uptake of tracer by sorption processes occurring on even faster timescales), the total number of processes which are identified using this method will remain unchanged.

As might be expected, the interval of time over which sorption is measured will affect both the number and the timescale of the processes which are revealed by the linearization procedure (Jannasch et al, 1988; Comans and Hockley, 1992). It is possible that the initial, apparently instantaneous reaction which is often observed (see Figures 5.1-5.16) may be split into further reactions on the timescale of seconds and minutes if the experimental procedure allows accurate measurements to be made at such short sampling times. Similarly, measurements at longer times (after several months or more) could reveal slower processes which are occurring. Therefore, experimental measurements should be made on the timescale or range of timescales which is most relevant for the modelling work. As it was the intention of this project to study sorption in freshwater systems on longer timescales, of weeks to months, processes which are occurring on timescales of minutes or less are less relevant.

5.2.1 Application of the linearization procedure

Estimations of $[Md]_e$ values were made for each radionuclide - freshwater system

based on the last activity which was measured in solution. The $[Md]_e$ value which was used for each system during the linearization procedure is reported in the associated figure caption. An estimate of the number of different processes revealed by the procedure was determined by eye and the correlation coefficients were calculated.

The linearization plots for ^{57}Co are shown in Figures 5.1-5.4. Sorption of ^{57}Co in the BPBP system appears to consist of an initial, effectively instantaneous reaction and two further processes. Although this may also be true for ^{57}Co sorption in the BPEW system, the scatter in the data at $t \leq 200$ is large, so the correlation coefficient is low for the shorter timescale reaction and it is hard to draw more definite conclusions. It is apparent, however, that an apparently instantaneous reaction and at least one further process is occurring. This suggests that for either of these two systems a one component kinetic model is insufficient to describe ^{57}Co sorption data adequately. The last two data points for ^{57}Co sorption in the EWBP and EWEW systems have not been included in the linearization procedure. This is because of the uncertainty of the cause of the low sorption measurements in the EWEW system (possibly biological activity) and because of the large errors associated with these two data points in the EWBP system. The linearization procedure however has again revealed an apparently instantaneous reaction as well as at least one further process. Although the data for ^{57}Co sorption in the EWBP system suggests that there are two further reactions occurring, there are fewer data so it is more difficult to draw definite conclusions. If it is assumed instead that just one further reaction is taking place, the correlation coefficient is still good ($r^2 = 0.886$), which suggests that at least a two-box kinetic model is needed to describe these data adequately.

Figures 5.5-5.8 show the linearization procedure applied to ^{85}Sr adsorption data.

Figure 5.1 Linearization of ^{57}Co, BPBP sorption data; $[Md]_e$ = 500 Bq l^{-1}

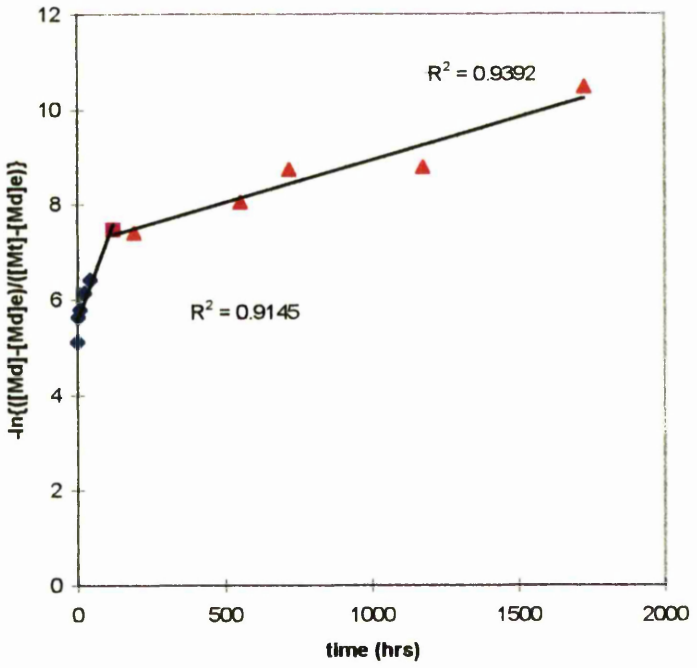

Figure 5.2 Linearization of ^{57}Co, BPEW sorption data; $[Md]_e$ = 500 Bq l^{-1}

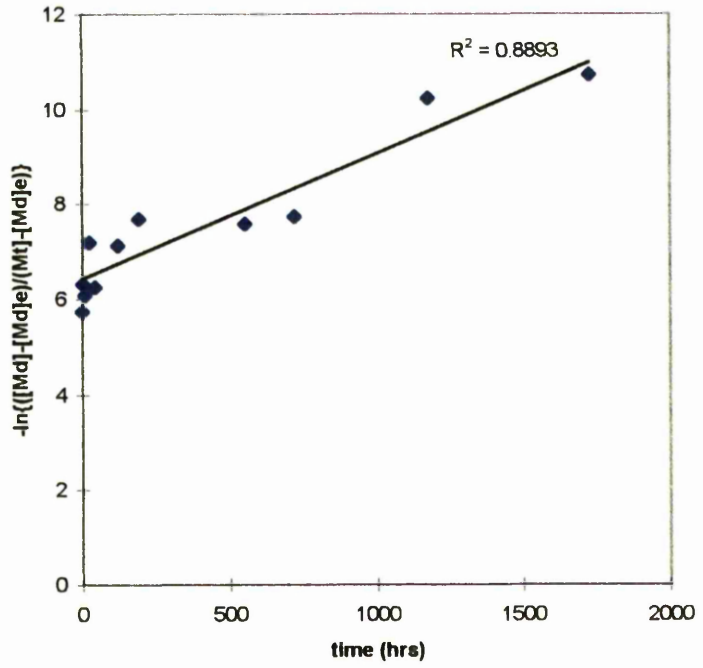

Figure 5.3 Linearization of ^{57}Co, EWEW sorption data; $[Md]_e$ = 4000 Bq l^{-1}

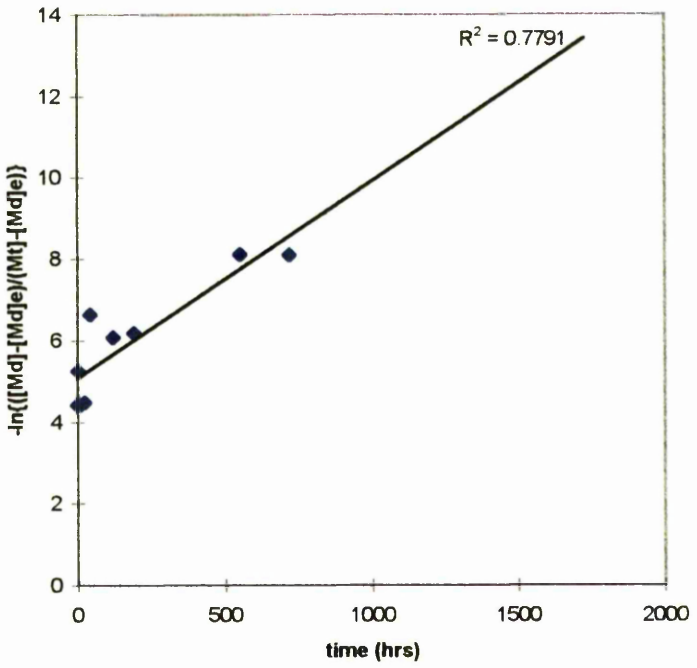

Figure 5.4 Linearization of ^{57}Co, EWBP sorption data; $[Md]_e$ = 500 Bq l^{-1}

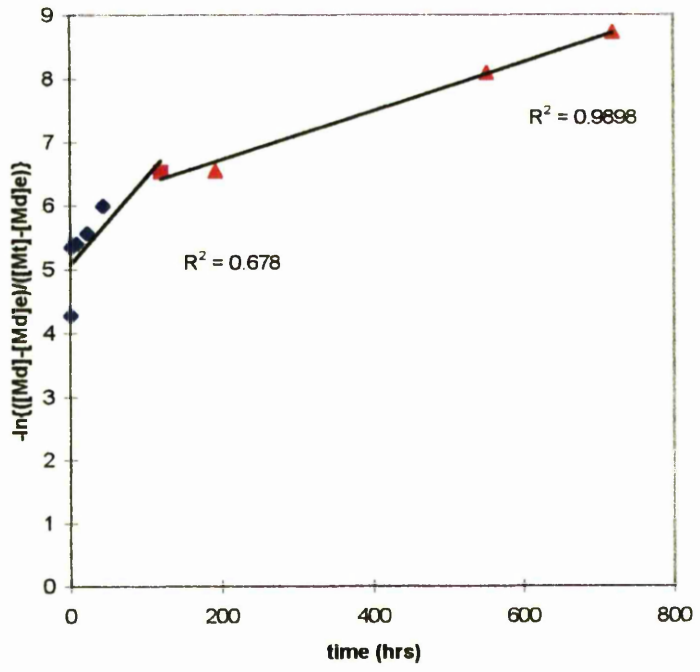

Figure 5.5 Linearization of ^{85}Sr, BPBP sorption data; $[Md]_e$ = 7500 Bq l^{-1}

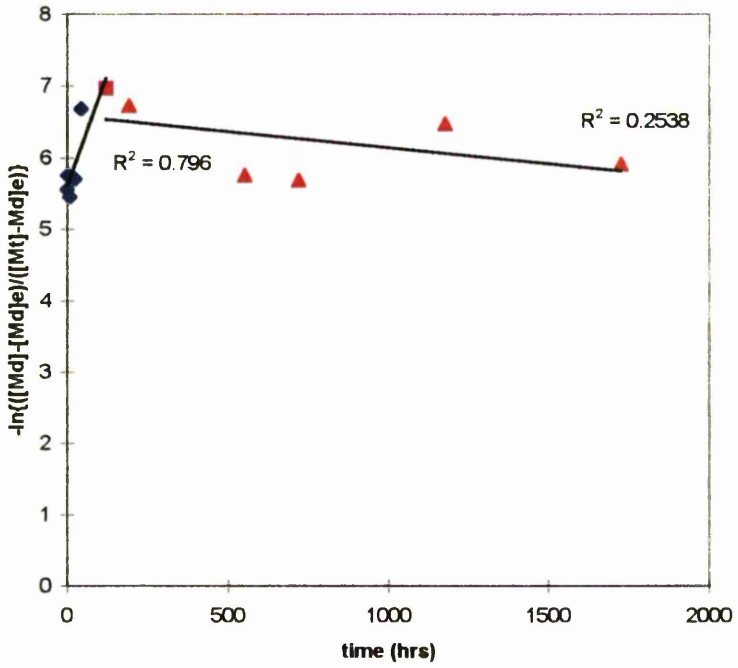

Figure 5.6 Linearization of ^{85}Sr, BPEW sorption data; $[Md]_e$ = 6000 Bq l^{-1}

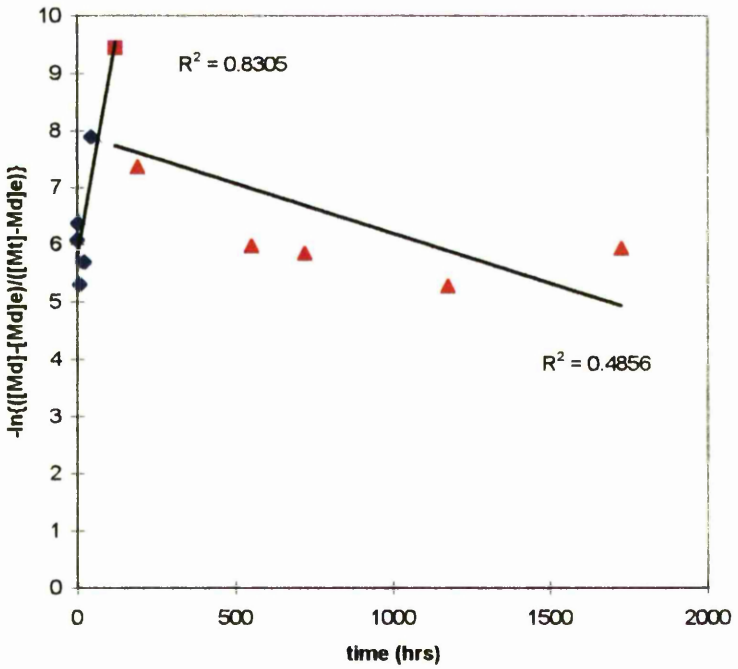

Figure 5.7 Linearization of ^{85}Sr, EWEW sorption data; $[Md]_e$ = 6000 Bq l^{-1}

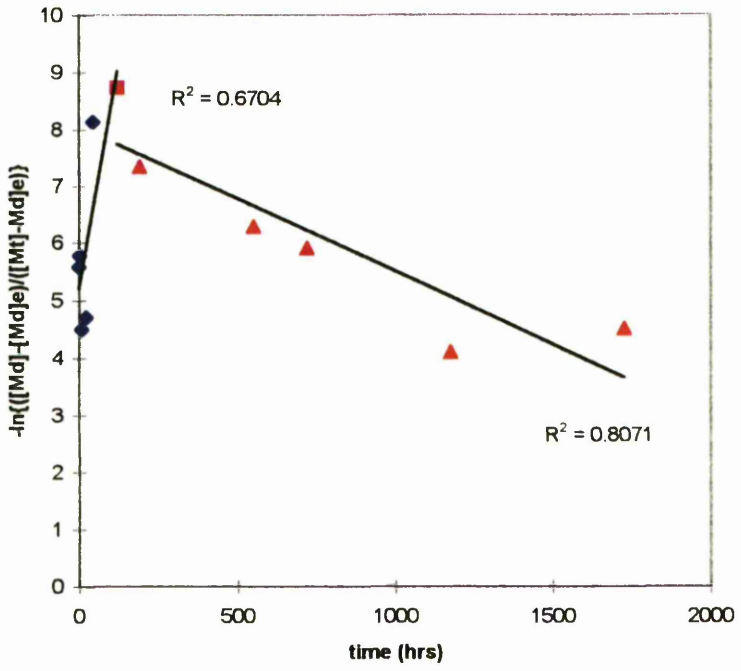

Figure 5.8 Linearization of ^{85}Sr, EWBP sorption data; $[Md]_e$ = 3000 Bq l^{-1}

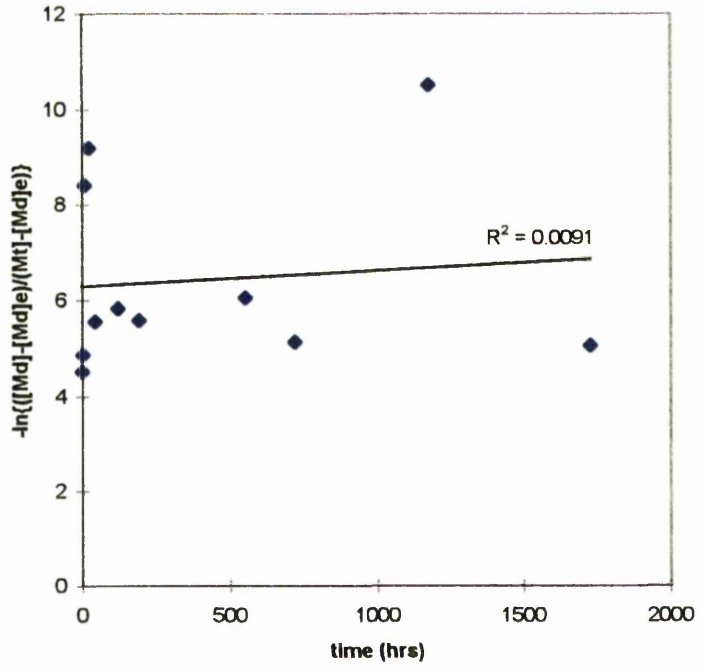

Although the data are noisy, it appears that sorption of ^{85}Sr on to Botany Pond sediment involves an apparently instantaneous reaction as well as a further reaction. The second trendline on both graphs (timescale 120-1728 hours) has a low correlation coefficient and a negative gradient, and this could suggest that, rather than another reaction taking place, an equilibrium has actually been reached after this time. Since the data are so noisy, it is difficult to draw any definite conclusions, but the data again suggest that perhaps a two-box rather than a one-box kinetic model is needed. The need to split the data sets into two separate trendlines is supported by the very low (almost zero) correlation coefficient obtained if just one trendline is fitted to all of the data points. A similar trend was observed with the EWEW system, again suggesting that a two-box kinetic model is needed. The correlation coefficient for data points in the EWBP system was very low, and hence no conclusions can be drawn for this data set.

Figures 5.9-5.12 show the linearization procedure applied to ^{103}Ru adsorption data. When applied to ^{103}Ru sorption on to Botany Pond sediment, an apparently instantaneous reaction, followed by up to two further reactions is revealed. The correlation coefficients for the trendlines in both systems are reasonable, and are higher than those found if just one trendline is used. This suggests that ^{103}Ru sorption on to Botany Pond sediment will be best described by a two, or three-box kinetic model. Although the data for ^{103}Ru sorption on to Esthwaite Water sediment are noisy, the linearization procedure again revealed an apparently instantaneous reaction followed by two further reactions of similar timescales to those found for ^{103}Ru sorption on to Botany Pond sediment. Sorption of ^{103}Ru in the EWEW system gave slightly different results. Although the data set could again be split into two distinct components, both with reasonable correlation coefficients (the first process has a

Figure 5.9 Linearization of ^{103}Ru, BPBP sorption data; $[Md]_e$ = 700 Bq l^{-1}

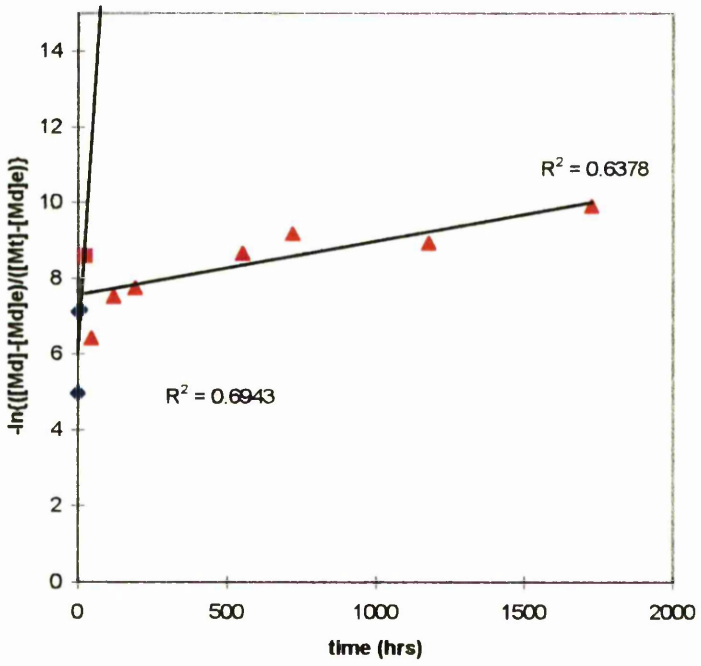

Figure 5.10 Linearization of ^{103}Ru, BPEW sorption data; $[Md]_e$ = 1000 Bq l^{-1}

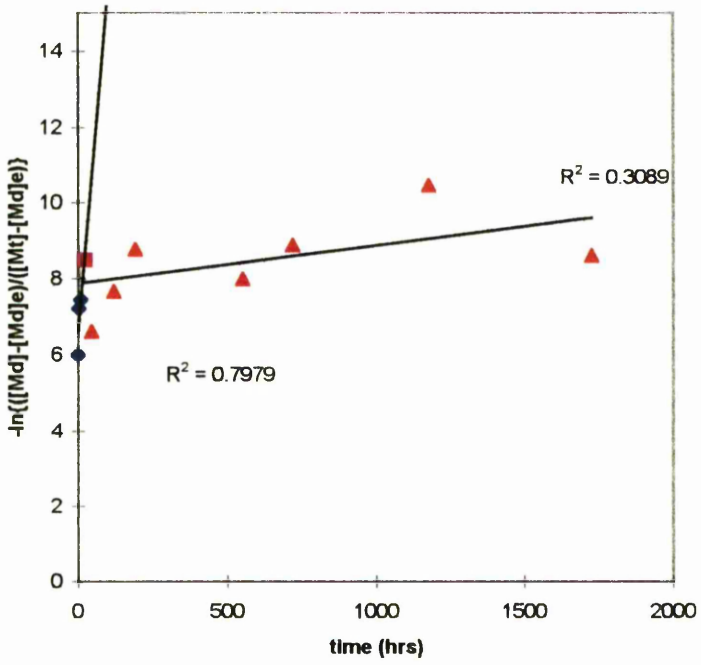

Figure 5.11 Linearization of ^{103}Ru, EWEW sorption data; $[Md]_e$ = 800 Bq l^{-1}

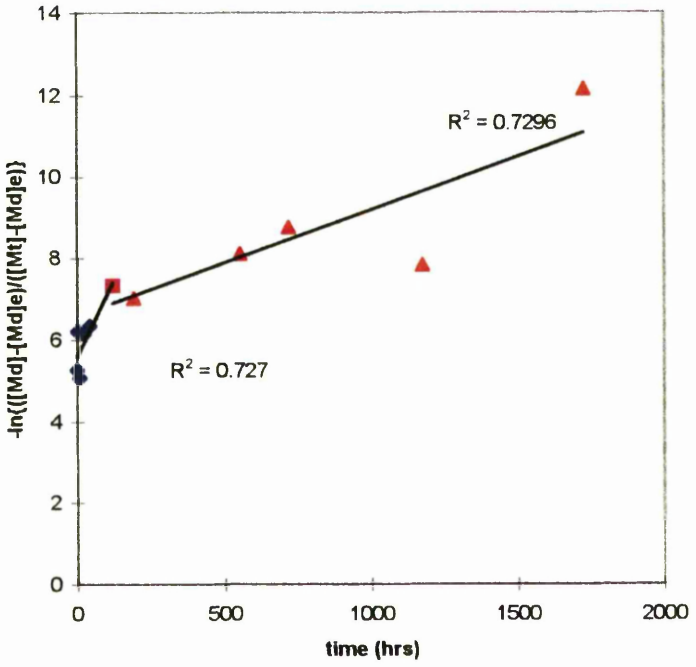

Figure 5.12 Linearization of ^{103}Ru, EWBP sorption data; $[Md]_e$ = 500 Bq l^{-1}

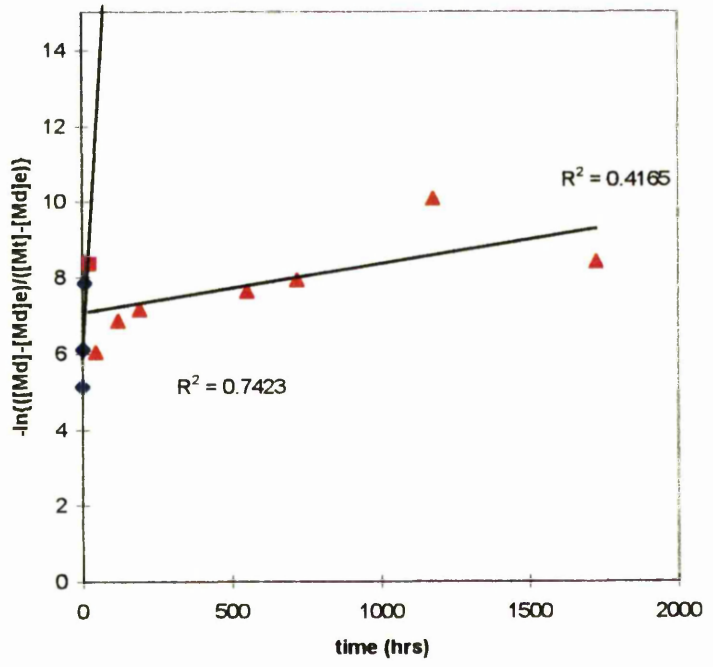

Figure 5.13 Linearization of ^{134}Cs, BPBP sorption data; $[Md]_e$ = 500 Bq l^{-1}

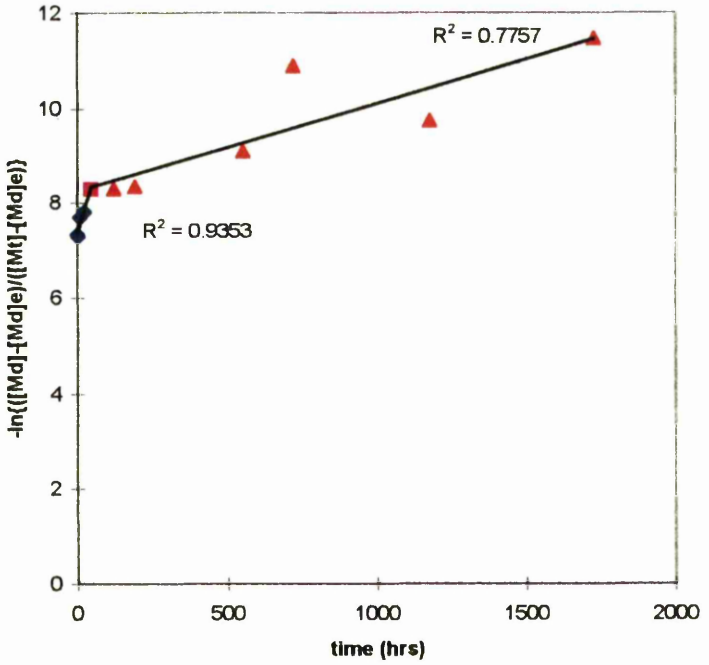

Figure 5.14 Linearization of ^{134}Cs, BPEW sorption data; $[Md]_e$ = 700 Bq l^{-1}

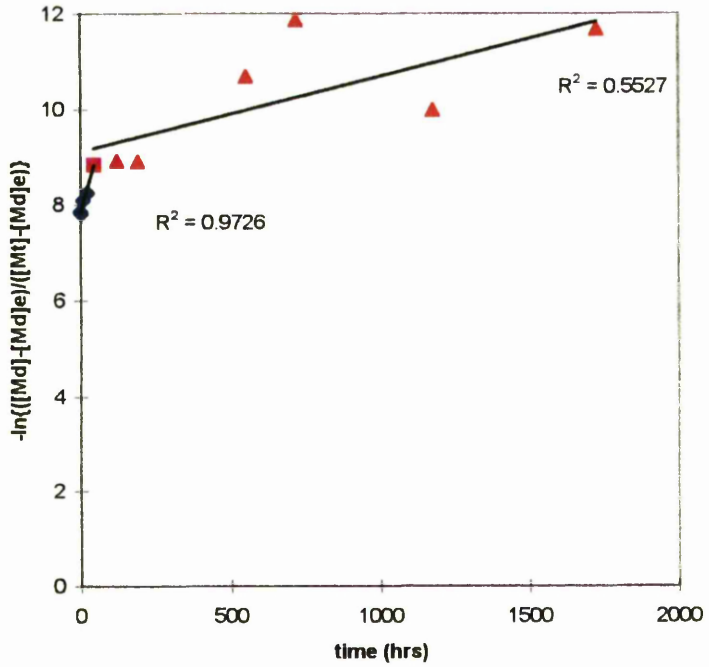

Figure 5.15 Linearization of ^{134}Cs, EWEW sorption data; $[Md]_e$ = 4000 Bq l^{-1}

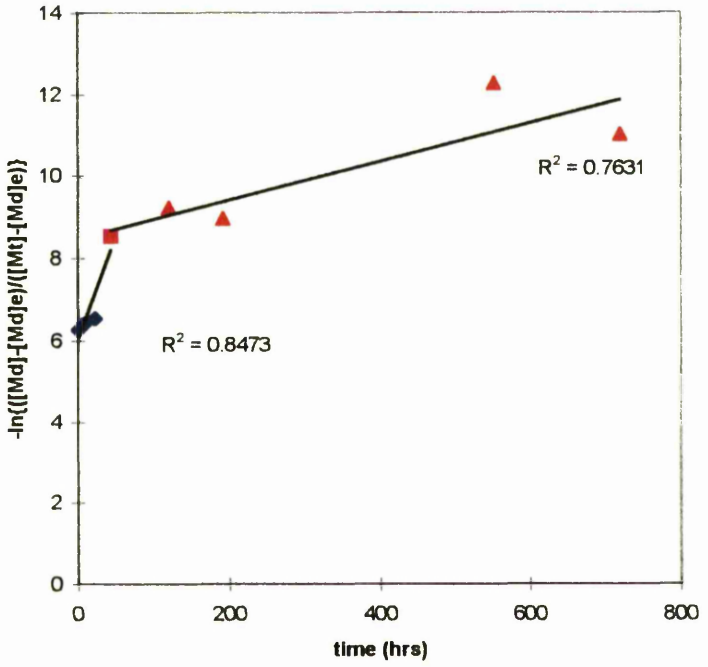

Figure 5.16 Linearization of ^{134}Cs, EWBP sorption data; $[Md]_e$ = 3000 Bq l^{-1}

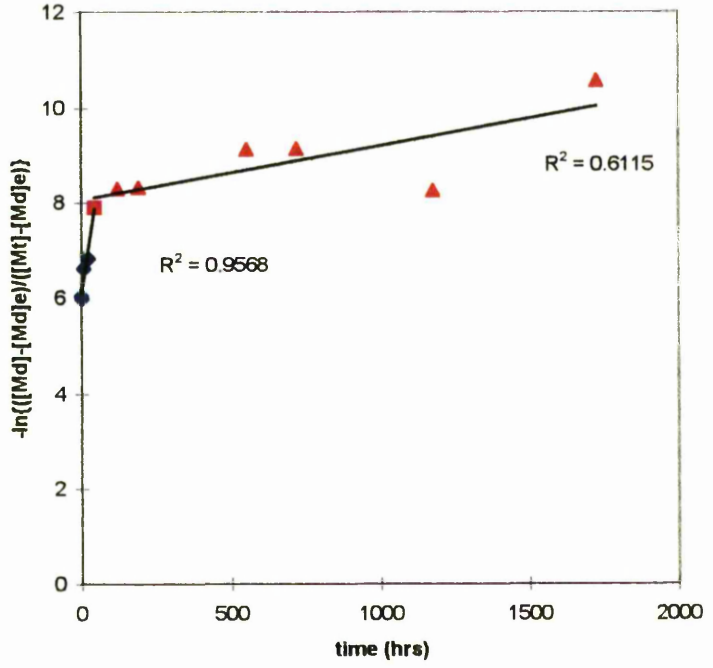

slightly longer timescale than was estimated for the other systems), a better correlation is observed ($r^2 = 0.8205$) when just one trendline runs through all of the data points.

Figures 5.13-5.16 show the linearization procedure applied to ^{134}Cs adsorption data. The procedure, when applied to ^{134}Cs sorption on to Botany Pond sediment, reveals an apparently instantaneous reaction possibly followed by two further processes. This suggests that a three-box kinetic model is needed to describe both sets of data adequately. When the linearization procedure is applied to ^{134}Cs sorption on to Esthwaite Water sediment the same trends are revealed. The last two data points in the EWEW system have again not been included because of the possibility of biological interference on this isotope within the system (cf. ^{57}Co sorption in this system). This is in good agreement with the linearization data of Comans and Hockley (1992) who applied the procedure to caesium sorption on both K- and Ca-saturated illite to reveal an apparently instantaneous reaction and two further processes. Timescales for the two further sorption processes observed for caesium sorption on to K-illite were in good agreement with the timescales found in this work (approximately 2 days). Timescales for caesium sorption on to Ca-illite were longer (approximately 5 days). Interestingly, when a further data set, which contained additional earlier time points was analysed, the apparently instantaneous reaction was divided into another two reactions (Comans and Hockley, 1992).

5.3 Kinetic box model

The kinetic box model has been used to describe the behaviour of a variety of radiotracers (but particularly radiocaesium) sorbing on to soils, sediments and clay minerals (Nyffeler et al, 1984; Jannasch et al, 1988; Comans and Hockley, 1992;

Madruga, 1993; Valcke, 1993; Wauters, 1994). The complexity of the model depends upon the number of boxes which the model contains, each box representing radiotracer sorbed on a specific range of sites. The simplest model is therefore the one-box model (discussed in Section 5.3.1), which assumes that all sorption is taking place by ion-exchange on to regular ion-exchange sites. Nyffeler et al (1984) found that this model could adequately describe the sorption of a variety of radiotracers, including strontium and caesium, on to marine sediments. Constant distribution coefficients were found for these two elements in adsorption experiments, even after only a few days. Cobalt, on the other hand, had an increasing distribution coefficient for the duration of the experiment (over 100 days) and it was found that a two-box model (discussed in Section 5.3.2) was needed to fit this behaviour. A two-box model is usually needed to describe caesium sorption on to most clays, soils and sediments (Comans and Hockley, 1992; Madruga, 1993; Valcke, 1993). Wauters (1994) found that an almost perfect fit was obtained when a parallel two-box model was applied to the experimental data. Interestingly, Comans and Hockley (1992) found that although the two-box model was adequate to describe caesium sorption on to K-saturated illite, a three-box model (discussed in Section 5.3.3) was needed to describe caesium sorption on to Ca-saturated illite.

An indication of the complexity of the box model which is needed to describe the data can be obtained both from looking at the experimental adsorption data itself, and also looking at the results of the linearization procedure (see Section 5.2.1). With the possible exception of ^{85}Sr, the data indicate that a number of different processes are occurring for the duration of the experiment, and a one-box model is not adequate to describe the data. For comparison though, each of the box models (one, two and three) has been applied to all of the adsorption data. The results are presented in

Section 5.4.

5.3.1 The one-box model

Figure 5.17 is a schematic representation of the 1-box model. Box V represents the concentration of radionuclide in the solution phase, and box W represents the concentration of radionuclide sorbed on to the solid phase (on the regular ion exchange sites). Sorption on to these sites occurs at a forward rate of K_f and at a backward rate K_b. Figures 5.18-5.23 show how the model curve alters as the parameters K_f and K_b are changed (all other conditions remain the same). As would be expected, as K_f decreases, sorption occurs at a slower rate and as K_b is decreased, a faster sorption rate is observed.

5.3.2 The two-box model

Figure 5.24 is a schematic representation of the two-box model. As before, box V represents the concentration of radionuclide in the solution phase and box W represents the concentration of radionuclide sorbed on easily accessible sites (ie. those on which regular ion exchange occurs). This reaction is assumed to have reached an effectively instantaneous equilibrium, and therefore can be described by the ratio, Kd (which can be referred to as the "exchangeable Kd"). Kd is simply the equilibrium value of a time varying sorption process. For any reaction which is at equilibrium, the ratio of Kf/Kb is equal to Kd. Sorption on to the less accessible sites occurs at a slower rate and this is represented by box Y. Sorption on to these sites occurs at a forward rate of K_1 and at a backward rate of K_{-1}. Figures 5.25-5.30 show how the model curve changes as the rate constants K_1 and K_{-1} are altered (all other conditions

Figure 5.17 Schematic representation and solution of 1-box model

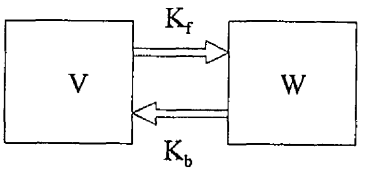

First order reaction:

$$\frac{dW(t)}{dt} = K_f V - K_b W$$

Mass balance:

$$V_0 + W_0 = V_{(t)} + W_{(t)}$$

Boundary conditions:

$$V_{(t=0)} = V_0$$

$$W_{(t=0)} = W_0 = 0$$

Solution:

$$[\text{solid}] = ((100K_f)/(K_f+K_b)).(1-\exp(-(K_f+K_b).t))$$

Parameters:

V(t) = concentration in solution phase (%).
W(t) = concentration on regular ion exchange sites (%).
K_f = forward rate constant (hr^{-1}).
K_b = backward rate constant (hr^{-1}).

Figure 5.18 1-box model curve; K_f=10; K_b=0.05

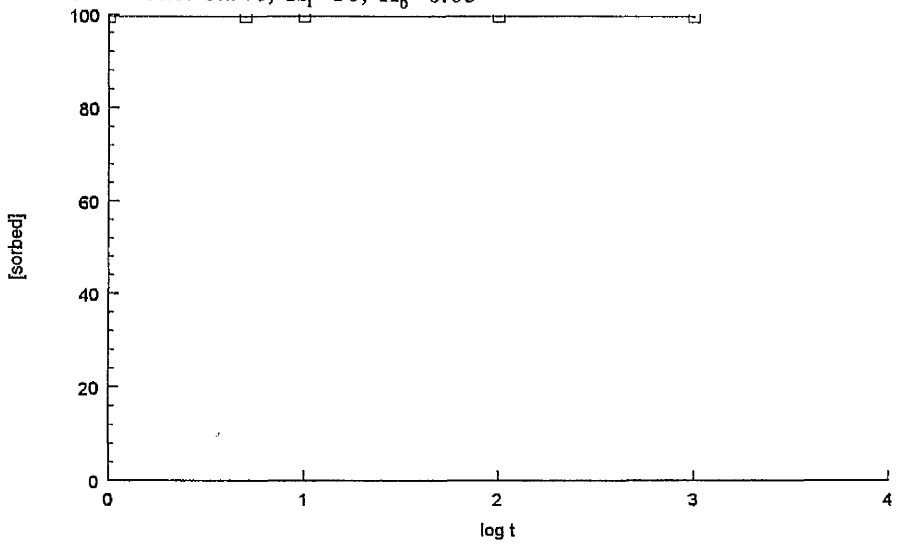

Figure 5.19 1-box model curve; K_f=1; K_b=0.05

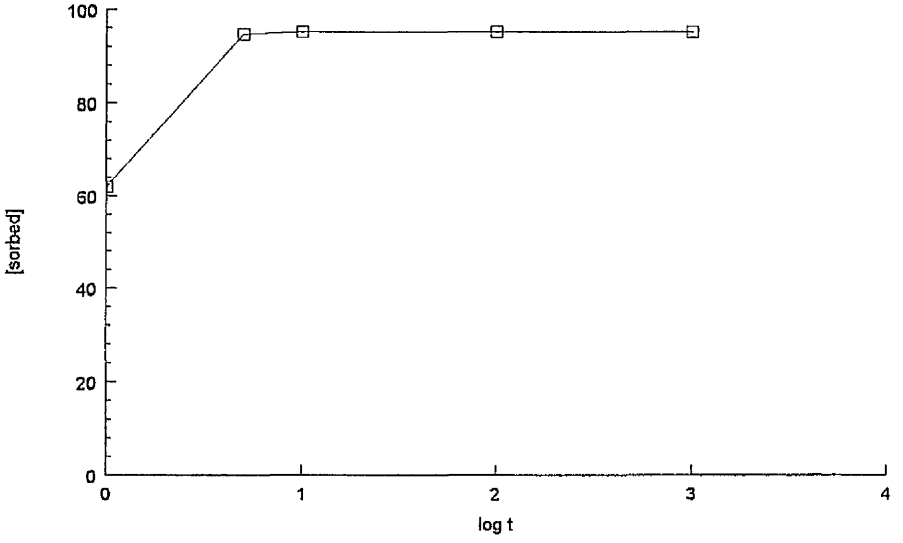

Figure 5.20 1-box model curve; K_f=0.1; K_b=0.05

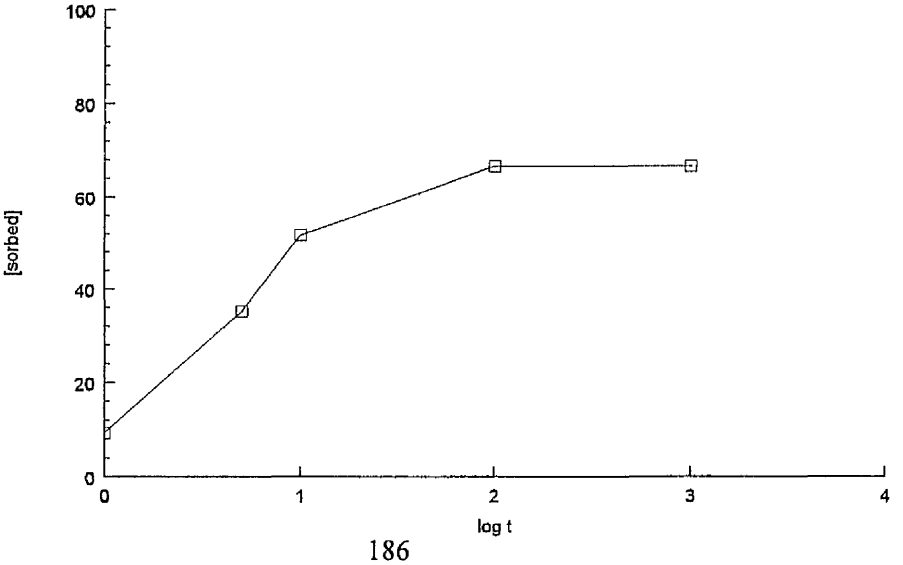

Figure 5.21 1-box model curve; K_f=1; K_b=0.1

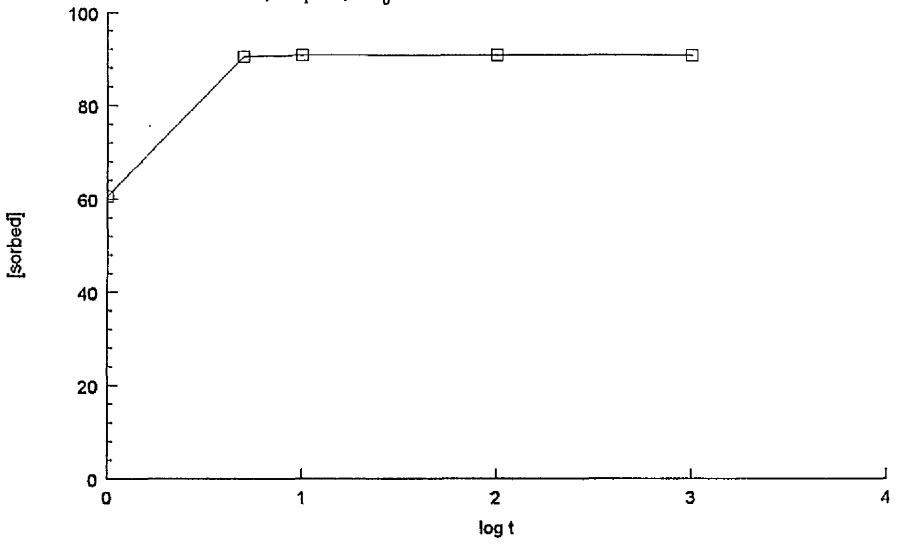

Figure 5.22 1-box model curve; K_f=1; K_b=0.01

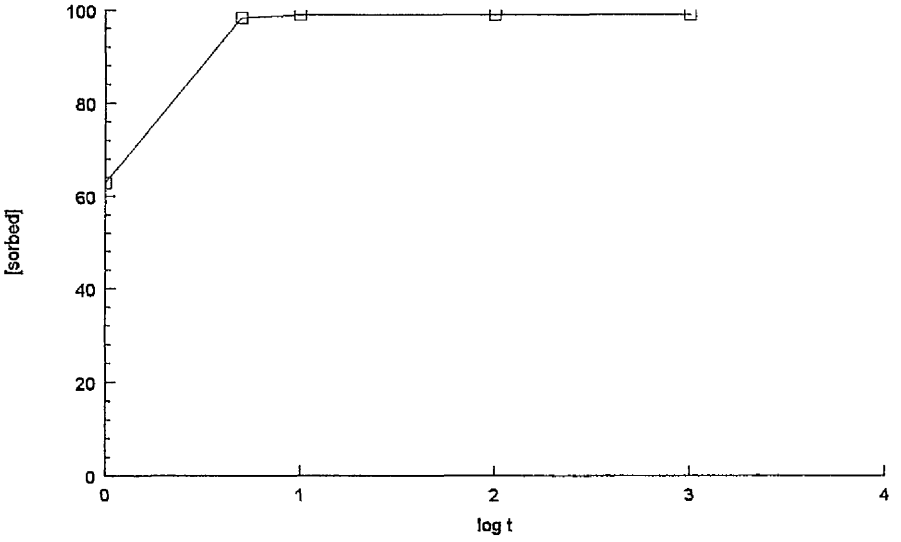

Figure 5.23 1-box model curve; K_f=1; K_b=0.005

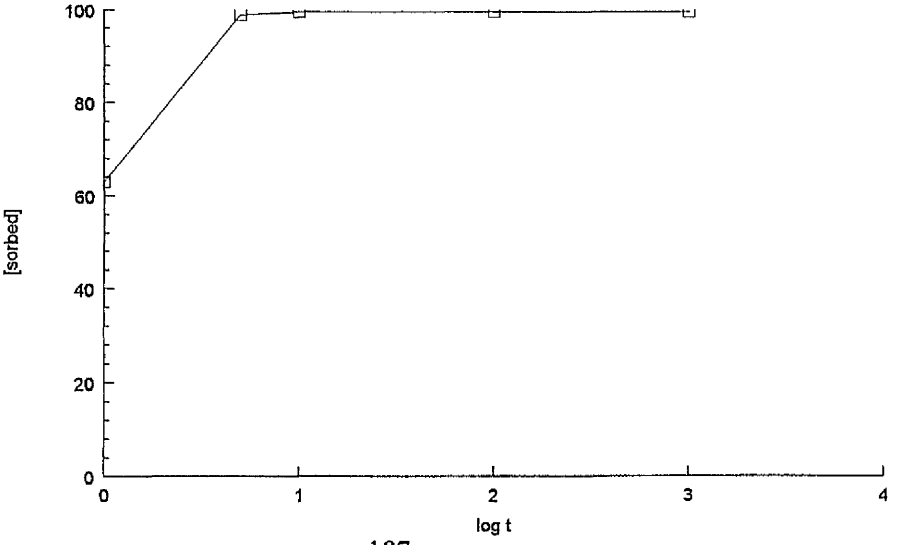

Figure 5.24 Schematic representation and solution of 2-box model

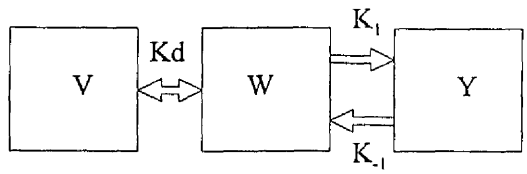

Instantaneous equilibrium equation:

$$W(t) = s.\ Kd.\ V(t)$$

First-order slow sorption reaction:

$$\frac{dY(t)}{dt} = K_1 W - K_{-1} Y$$

Mass balance:

$$V(t) + W(t) + Y(t) = V_0 + W_0 + Y_0$$

Boundary conditions:

$$V_{(t=0)} = V_0$$

$$W_{(t=0)} = W_0$$

$$Y_{(t=0)} = Y_0 = 0$$

Solution:

$$[solid] = (Y/(1+s.Kd))+s.Kd.V_0$$

in which,

$$\gamma = ((K_1.s.Kd)/(1+s.Kd))+K_{-1}$$

$$V_0 = 100/(1+s.Kd)$$

$$Y = ((K_1.Kd.s)/\gamma).V_0.(1-(\exp(-\gamma.t)))$$

Parameters:

V(t) = concentration in solution phase (%).
W(t) = concentration on equilibrium, regular ion-exchange sites (%).
Y(t) = concentration on less accessible exchange sites (%).
Kd = distribution coefficient for equilibrium sites (ml g^{-1}).
s = particle concentration (g ml^{-1}).
K_1 = forward rate constant for sorption on to less accessible exchange sites (hr^{-1}).
K_{-1} = backward rate constant for desorption from less accessible exchange sites (hr^{-1}).

Figure 5.25 2-box model curve; Kd=200; K_1=10; K_{-1}=0.05

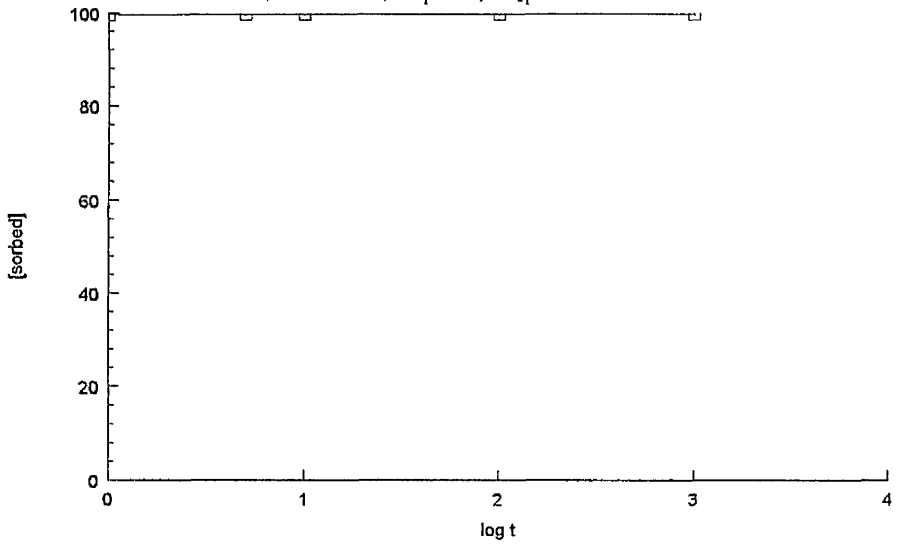

Figure 5.26 2-box model curve; Kd=200; K_1=1; K_{-1}=0.05

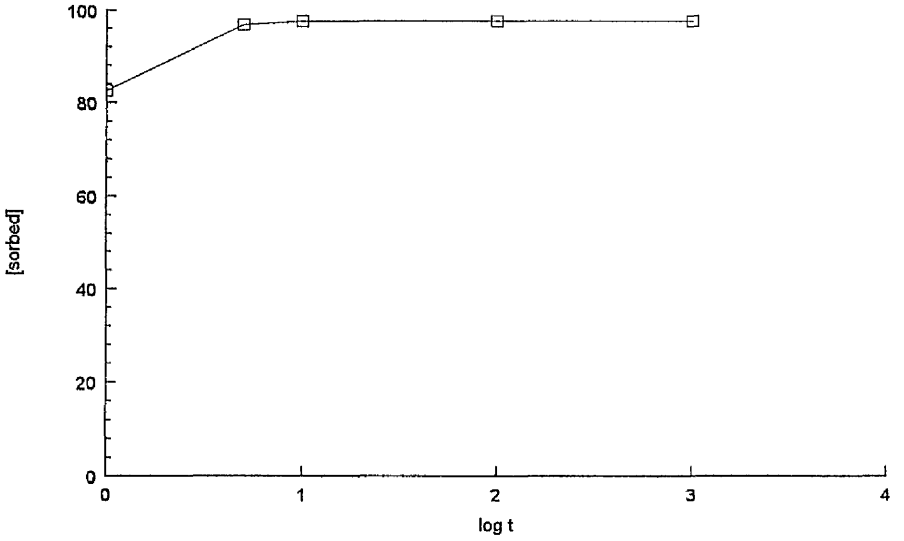

Figure 5.27 2-box model curve; Kd=200; K_1=0.1; K_{-1}=0.05

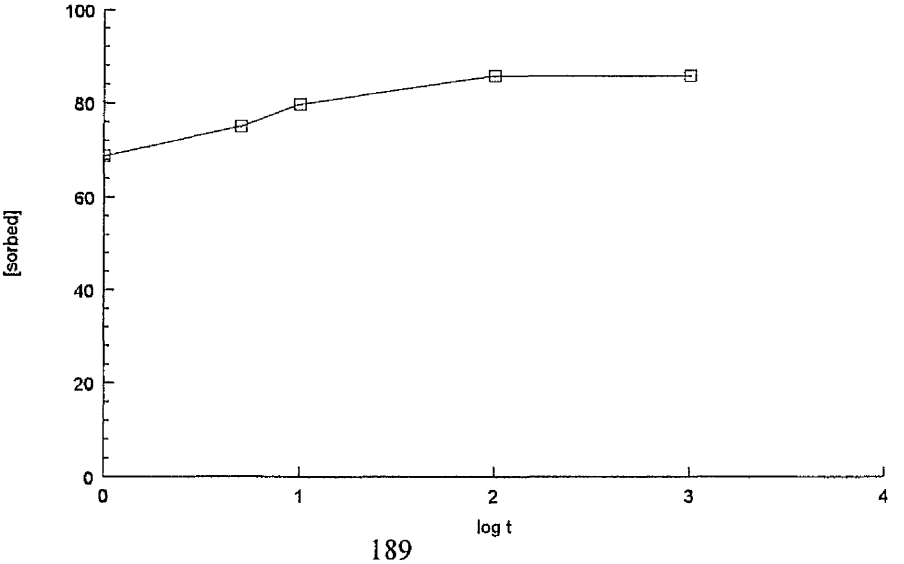

Figure 5.28 2-box model curve; Kd=200; K_1=1; K_{-1}=0.1

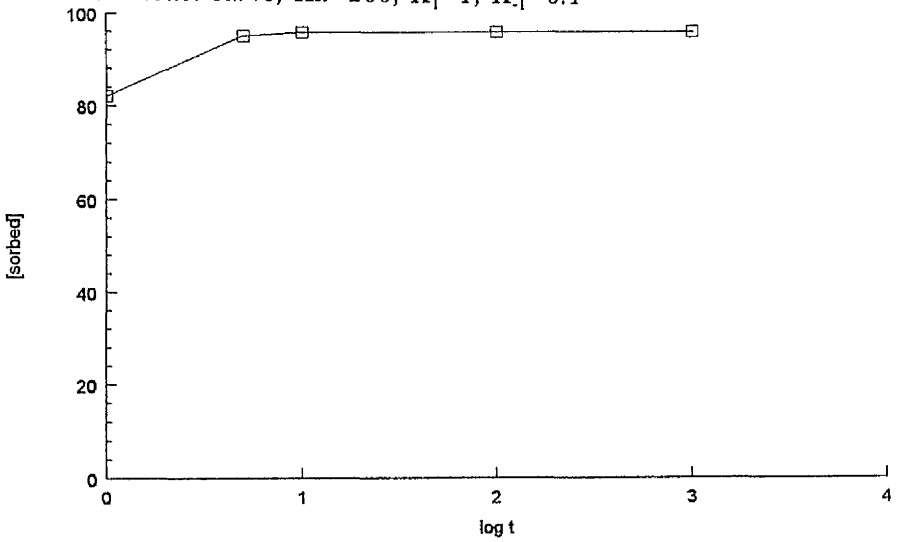

Figure 5.29 2-box model curve; Kd=200; K_1=1; K_{-1}=0.01

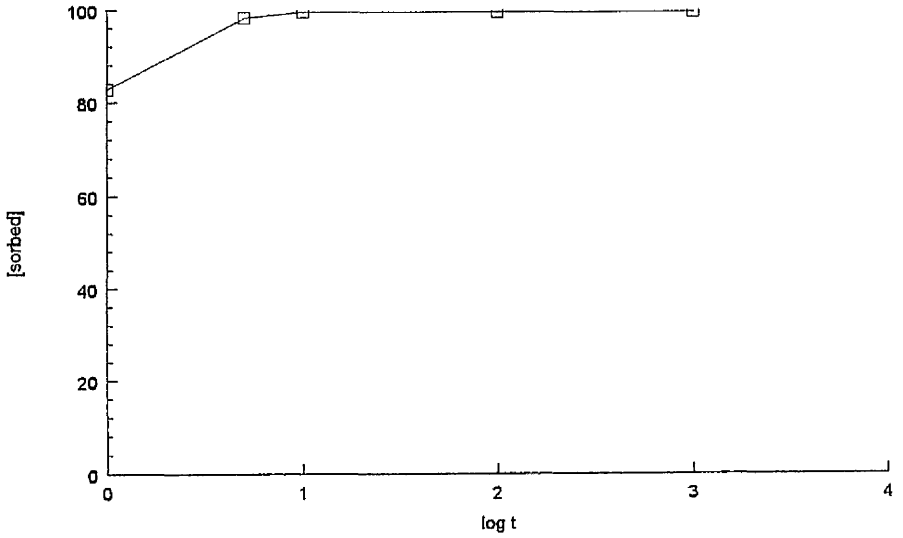

Figure 5.30 2-box model curve; Kd=200; K_1=1; K_{-1}=0.005

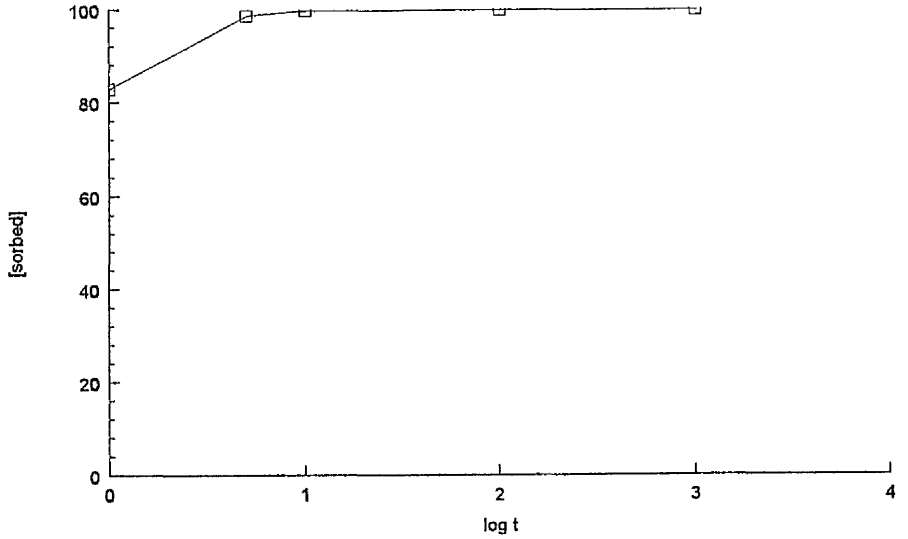

Figure 5.31 2-box model curve; Kd=1000; K_1=1; K_{-1}=0.1

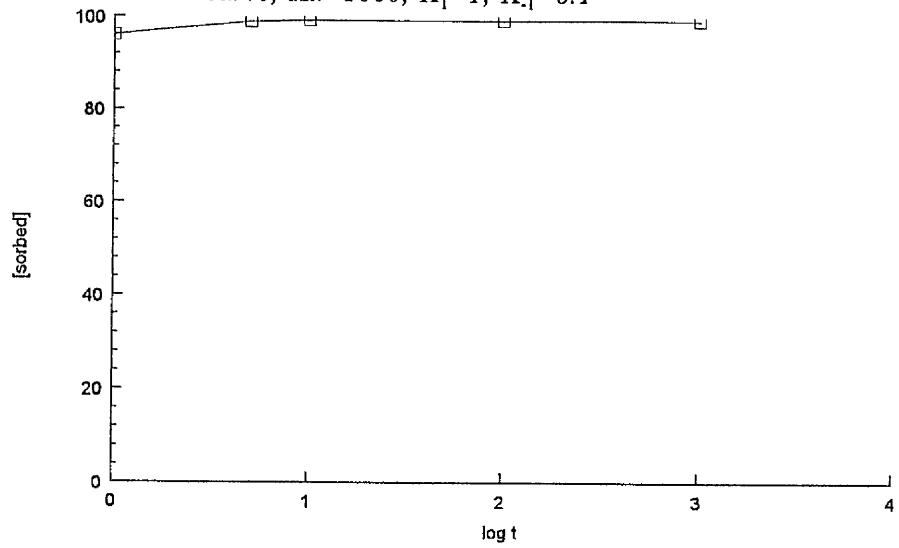

Figure 5.32 2-box model curve; Kd=500; K_1=1; K_{-1}=0.1

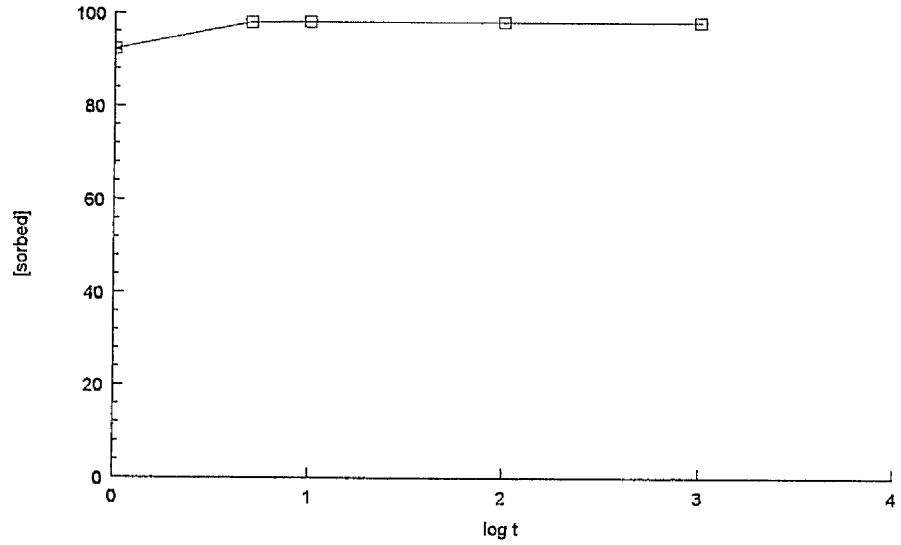

Figure 5.33 2-box model curve; Kd=10; K_1=1; K_{-1}=0.1

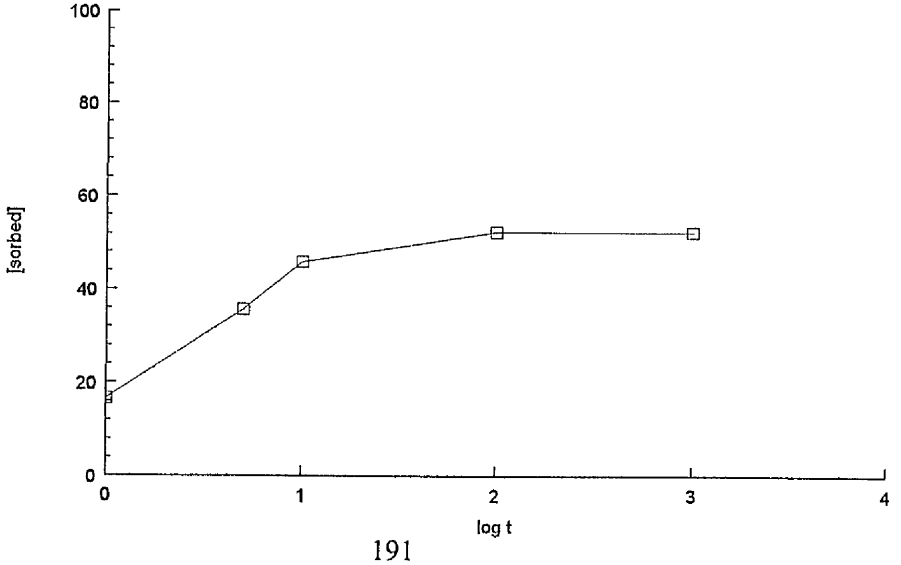

remain the same). As before, as K_1 is decreased sorption occurs at a much slower rate, and as K_{-1} is decreased the rate of sorption increases. Figures 5.31-5.33 show the effect of changing the parameter, Kd, with all other conditions remain constant. As would be expected, as Kd is decreased, sorption is reduced.

5.3.3 The three-box model

Figure 5.34 is a schematic representation of the three-box model. Again, box V represents the concentration of radionuclide in the solution phase and box W represents the concentration of radionuclide sorbed on regular ion exchange sites. This is assumed to occur effectively instantaneously and is represented by the distribution coefficient, Kd. As with the two-box model, the concentration of radionuclide sorbed on less accessible exchange sites is represented by box Y. Sorption on to these sites proceeds at a forward rate, K_1, and a backward rate, K_{-1}. Box Z however, represents the sites on to which sorption is kinetically controlled, i.e. those sites on to which sorption continues even after a period of weeks and months. Sorption proceeds on to these sites at a forward rate, K_2. A backward rate constant from these sites is not included as this would be unmeasurable in the timescale of this experiment. This means however that even after long adsorption times the model does not reach an equilibrium. Figures 5.35-5.40 show how the model curve changes as the rate constants, K_1 and K_{-1}, are changed (all other conditions remain constant). As before, as K_1 is decreased, sorption occurs at a slower rate, and as K_{-1} is decreased sorption occurs at a faster rate, although unlike the previous models an equilibrium is not established. Figures 5.41-5.43 show how the model curve changes as only the Kd is altered. Although, as the Kd is reduced, sorption initially occurs to a lesser extent, by the end almost 100% sorption has occurred in each system. Figures 5.44-5.46 show

Figure 5.34 Schematic representation and solution of 3-box model

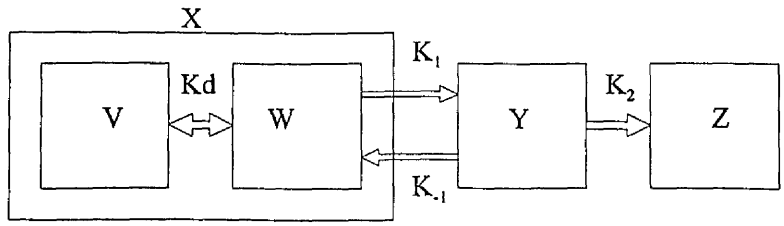

Instantaneous equilibrium equation: $W(t) = s.\ Kd.\ V(t)$

First-order equations:

$$\frac{dX}{dt} = -K_1X + K_{-1}Y$$

$$\frac{dY}{dt} = K_1X - (K_{-1} + K_2).\ Y$$

$$\frac{dZ}{dt} = K_2Y$$

Mass balance: $V(t) + W(t) + Y(t) + Z(t) = V_0 + W_0 + Y_0 + Z_0$

Boundary conditions: At $t = 0$, $X = X_0$, $Y = 0$, $Z = 0$.

Solution:

$$[solid] = (X.s.Kd)/(1+s.Kd)+Y+Z$$

in which,

$X = 100-Y-Z$

$Y = ((100K_1)/(a-b)).(\exp(a.t.)-\exp(b.t))$

$Z = 100(1-((1/a)-(1/b))^{-1}.((\exp(a.t))/a)-((\exp(b.t))/b)$

$a = (-c+(c^2-4g)^{1/2})/2$ $\quad$ $b = (-c-(c^2-4g)^{1/2})/2$

$c = K_1+K_{-1}+K_2$ $\quad$ $g = K_1.K_2$

Parameters:

$V(t)$ = concentration in solution phase (%).
$W(t)$ = concentration on equilibrium, regular ion-exchange sites (%).
$Y(t)$ = concentration on less accessible exchange sites (%).
$Z(t)$ = concentration on kinetically controlled sites (%).
Kd = distribution coefficient for equilibrium sites (ml g^{-1}).
s = particle concentration (g ml^{-1}).
K_1 = forward rate constant for sorption on to less accessible exchange sites (hr^{-1}).
K_{-1} = backward rate constant for desorption from less accessible exchange sites (hr^{-1}).
K_2 = forward rate constant for sorption on to kinetically controlled sites (hr^{-1}).

Figure 5.35 3-box model curve; Kd=200; K_1=10; K_{-1}=0.05; K_2=0.01

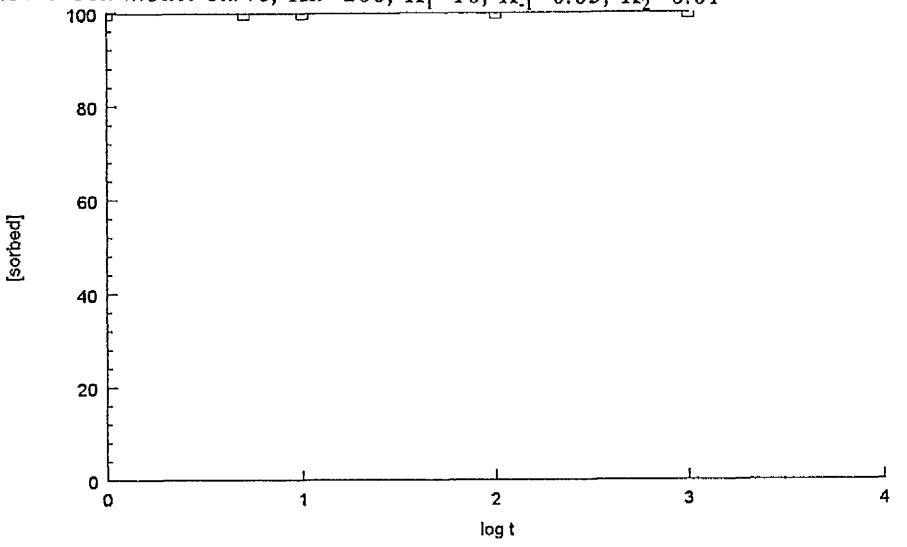

Figure 5.36 3-box model curve; Kd=200; K_1=1; K_{-1}=0.05; K_2=0.01

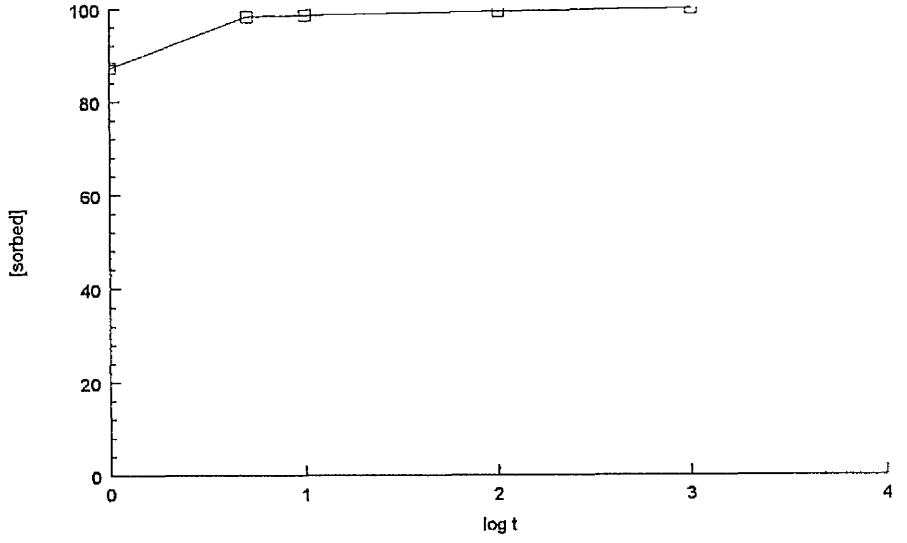

Figure 5.37 3-box model curve; Kd=200; K_1=0.1; K_{-1}=0.05; K_2=0.01

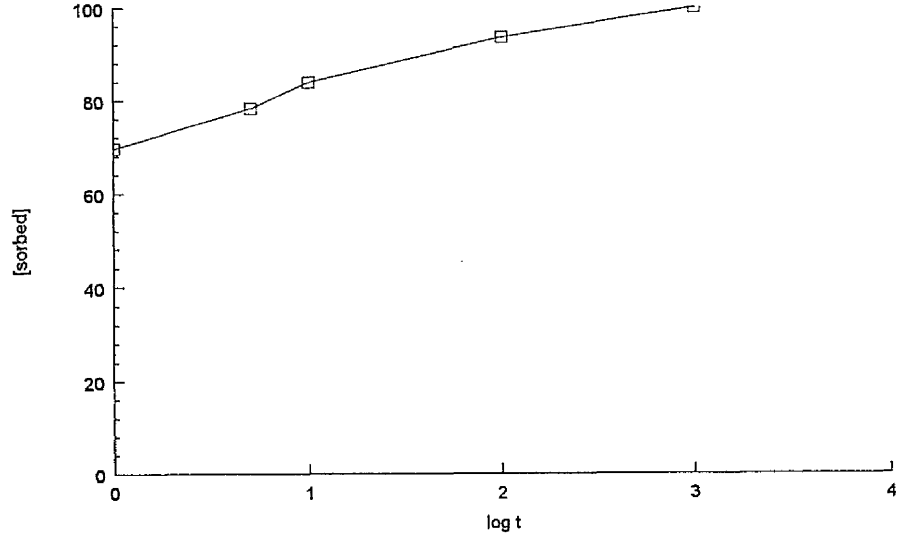

Figure 5.38 3-box model curve; Kd=200; K_1=1; K_{-1}=0.1; K_2=0.01

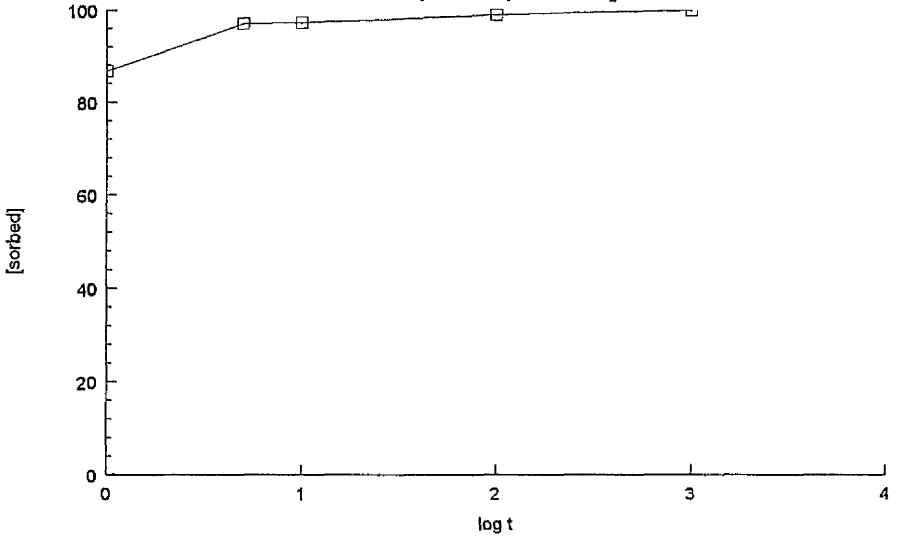

Figure 5.39 3-box model curve; Kd=200; K_1=1; K_{-1}=0.01; K_2=0.01

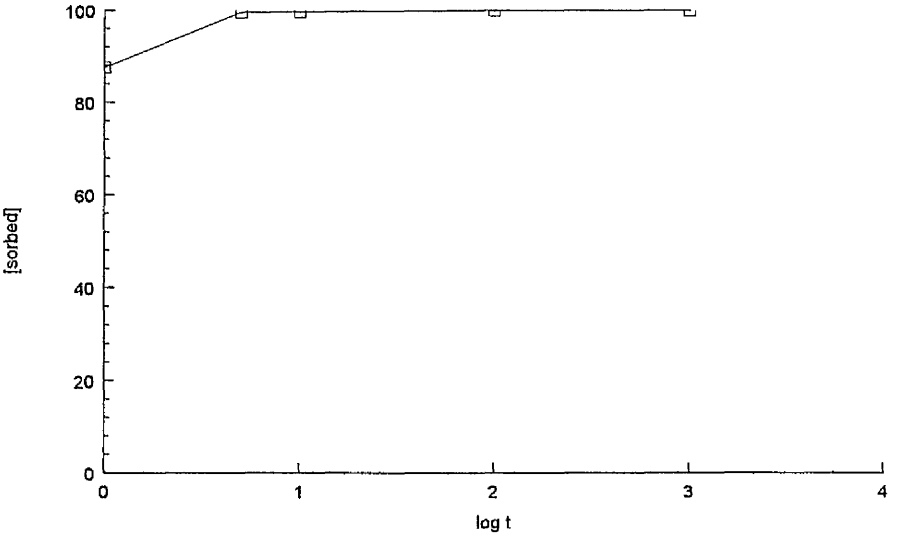

Figure 5.40 3-box model curve; Kd=200; K_1=1; K_{-1}=0.005; K_2=0.01

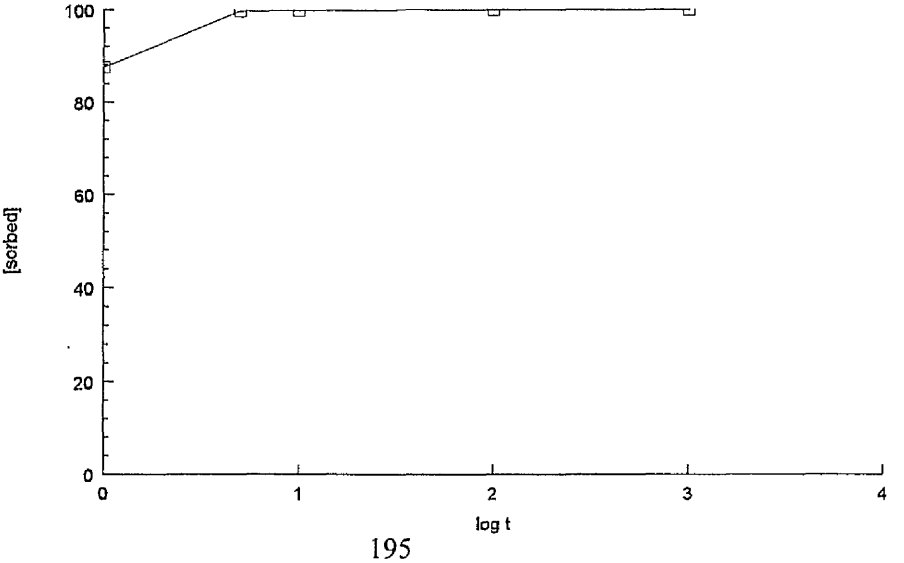

Figure 5.41 3-box model curve; Kd=1000; K_1=1; K_{-1}=0.1; K_2=0.01

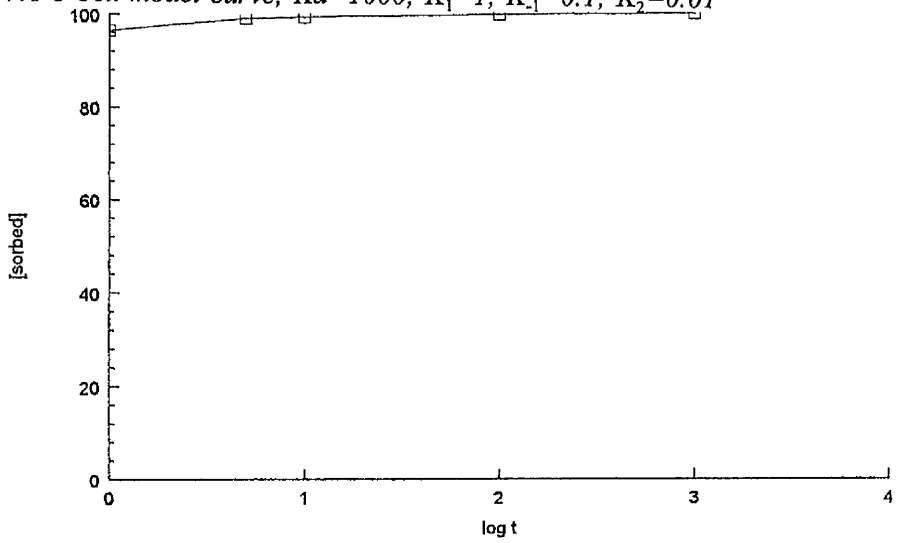

Figure 5.42 3-box model curve; Kd=500; K_1=1; K_{-1}=0.1; K_2=0.01

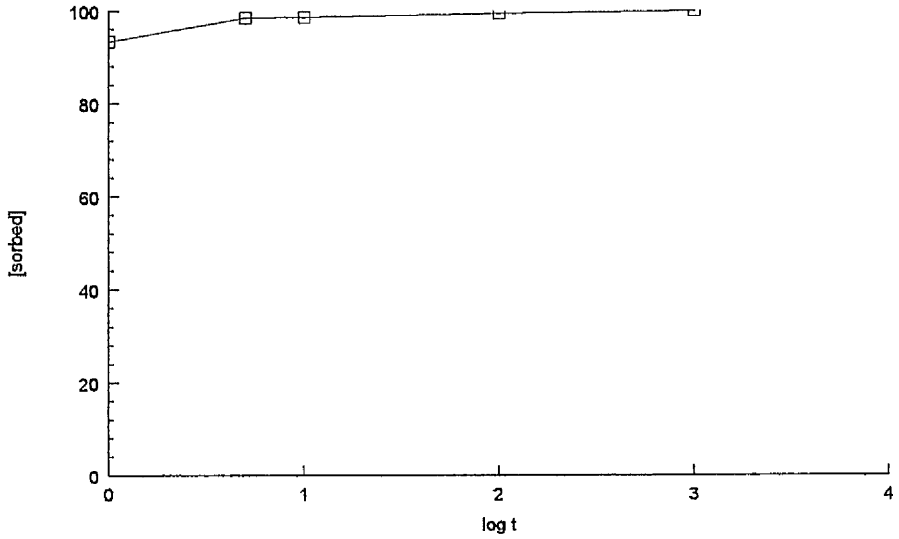

Figure 5.43 3-box model curve; Kd=10; K_1=1; K_{-1}=0.1; K_2=0.01

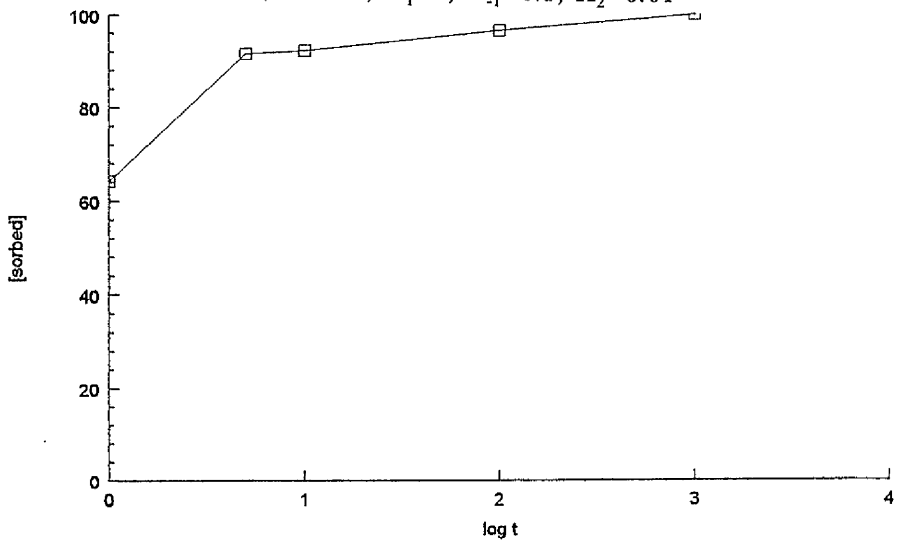

Figure 5.44 3-box model curve; Kd=200; K_1=1; K_{-1}=0.1; K_2=0.05

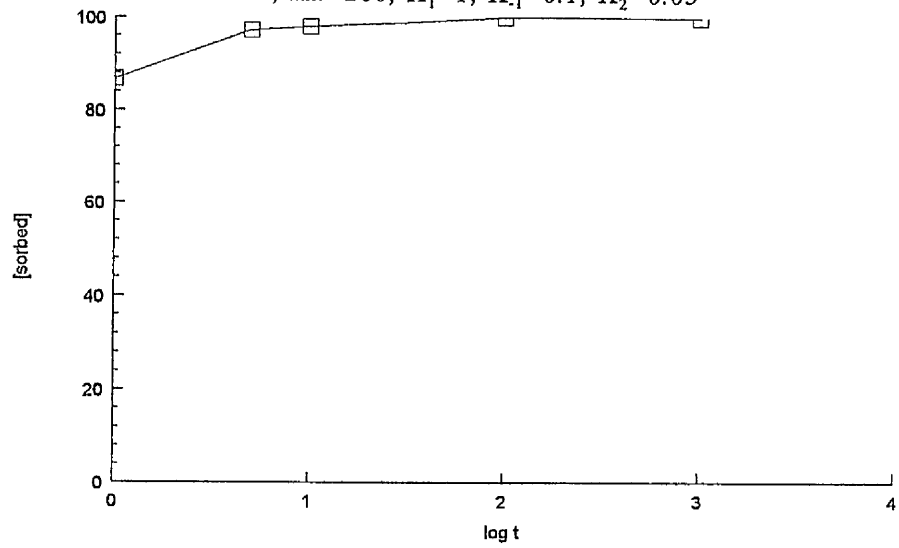

Figure 5.45 3-box model curve; Kd=200; K_1=1; K_{-1}=0.1; K_2=0.001

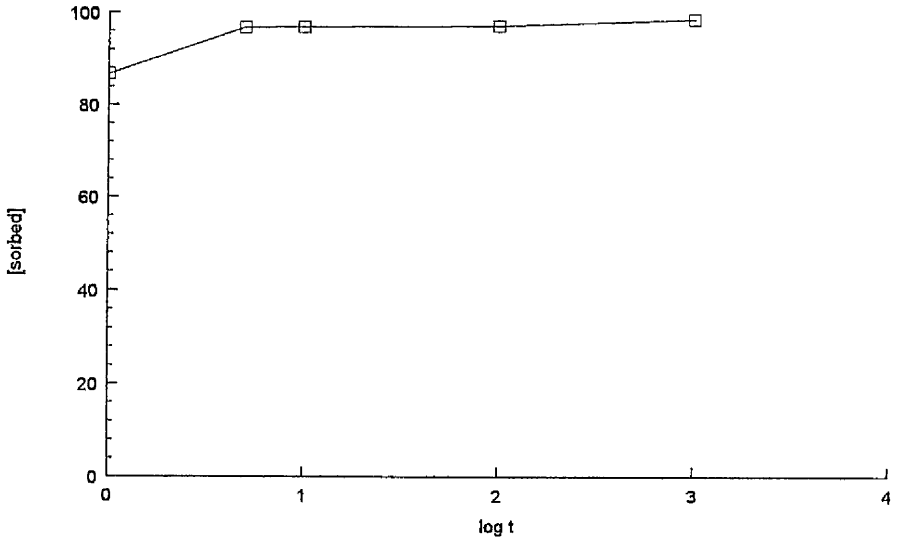

Figure 5.46 3-box model curve; Kd=200; K_1=1; K_{-1}=0.1; K_2=0.0001

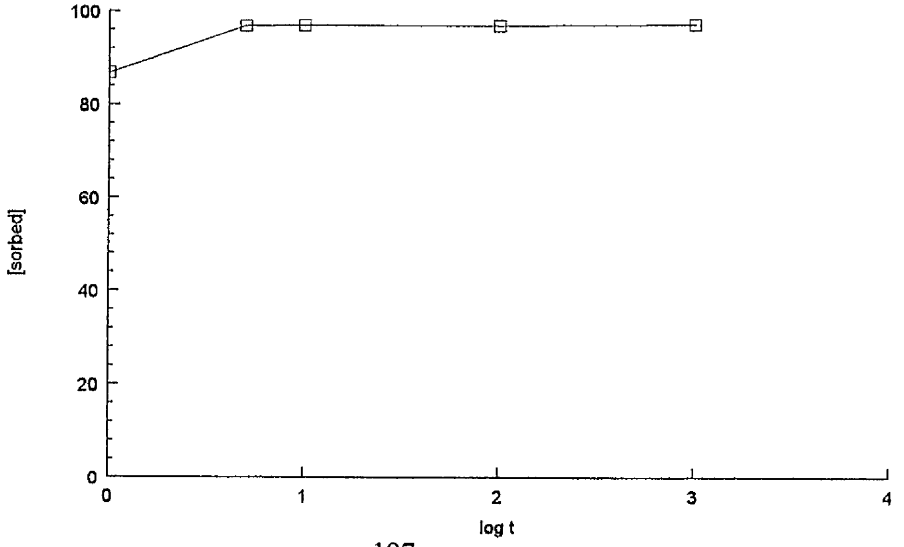

the effect of changing K_2 as the other parameters remain constant. As K_2 is decreased, the rate of sorption also decreases.

5.4 Application of the box model

Model solutions were found using a similar method to Nyffeler et al (1984). The different models were then fitted to the experimentally determined percentage sorbed data (for each radionuclide - freshwater system) using Sigmaplot Scientific Graphing System (Version 1.01). The model parameters ± 1 standard error are reported in Tables 5.1-5.15. It is important to remember however that these parameters, i.e. the distribution coefficients and rate constants, are highly dependent upon experimental conditions such as temperature, Eh, pH, sediment and solution composition. Whilst these were kept constant during this project, hence allowing an inter-comparison of these parameters between the radionuclides and freshwater systems used in this work, comparison with the results of other workers is much more difficult.

5.4.1 ^{57}Co

Figures 5.47-5.50 show the model predictions of ^{57}Co sorption in the four systems. Although the one-box model gives a reasonable fit for sorption on to Botany Pond sediment, the two-box model gives a much better description, as predicted by the linearization procedure. There is little difference in fit between the two and three-box models. Sorption of ^{57}Co on to Esthwaite Water sediment is slightly harder to fit because of the large decrease in the percentage sorbed at longer time periods. Despite this, the two and three-box models still give a better description of the experimental data than the one-box. This is in good agreement with Nyffeler et al (1984) who also

Figure 5.47 Model fit of ^{57}Co, BPBP sorption data

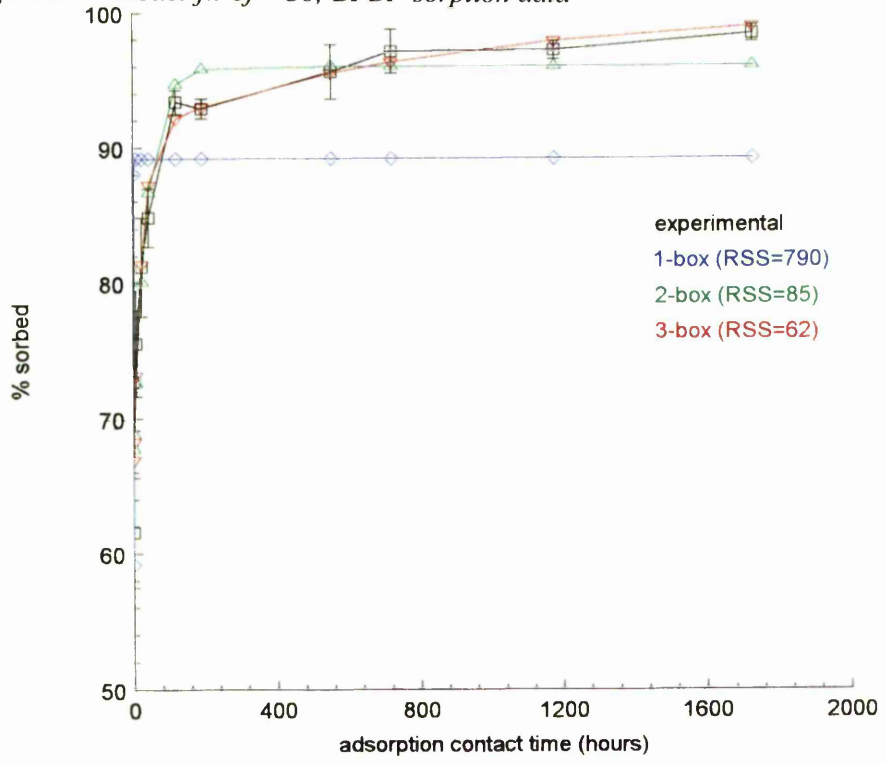

Figure 5.48 Model fit of ^{57}Co, BPEW sorption data

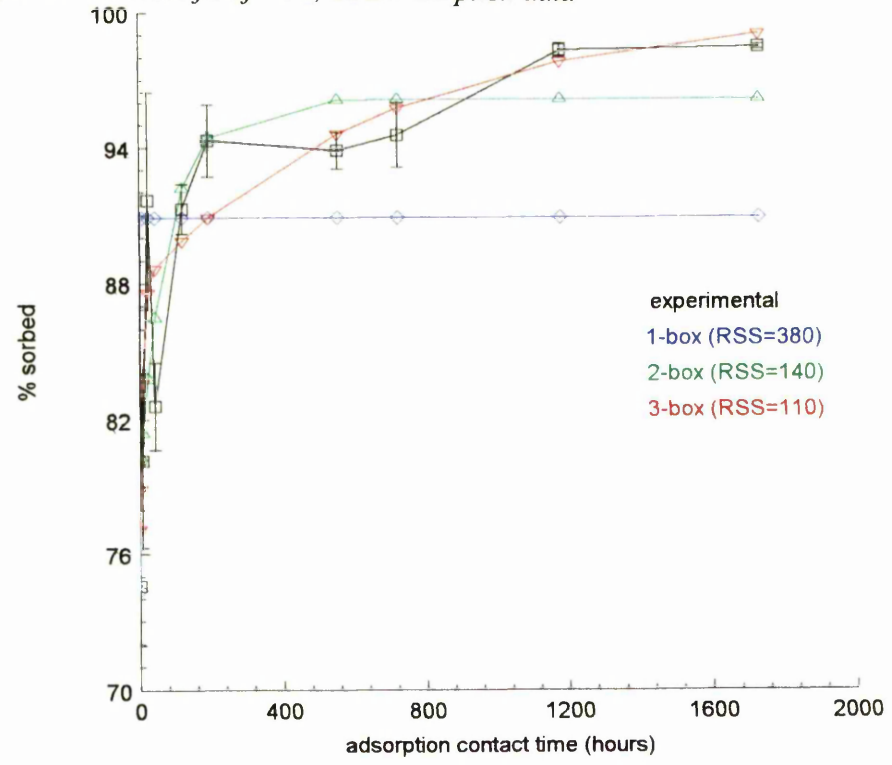

Figure 5.49 Model fit of ^{57}Co, EWEW sorption data

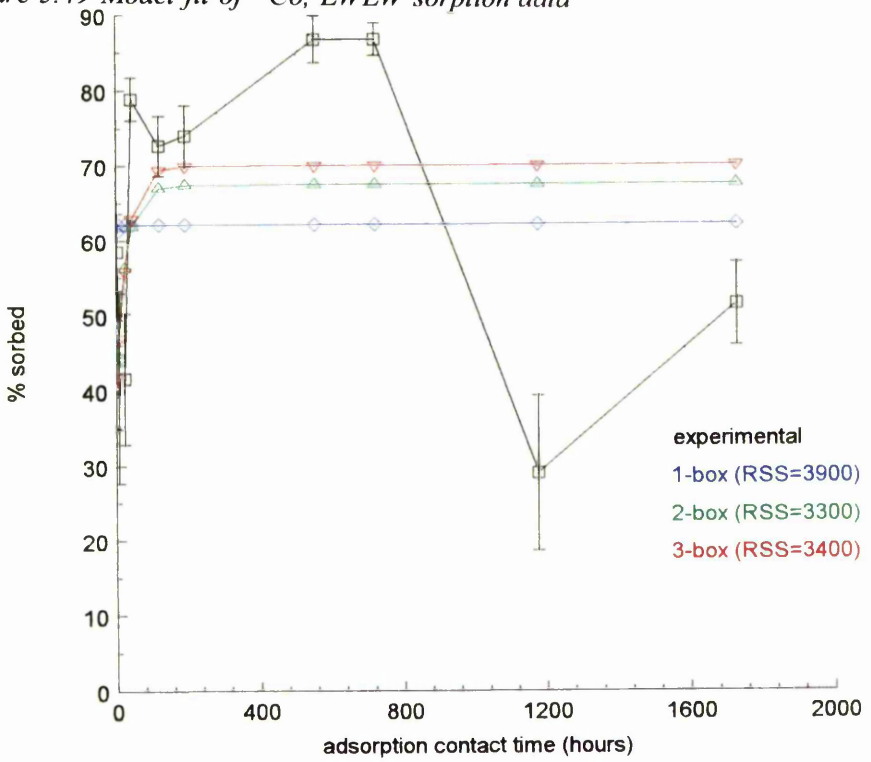

Figure 5.50 Model fit of ^{57}Co, EWBP sorption data

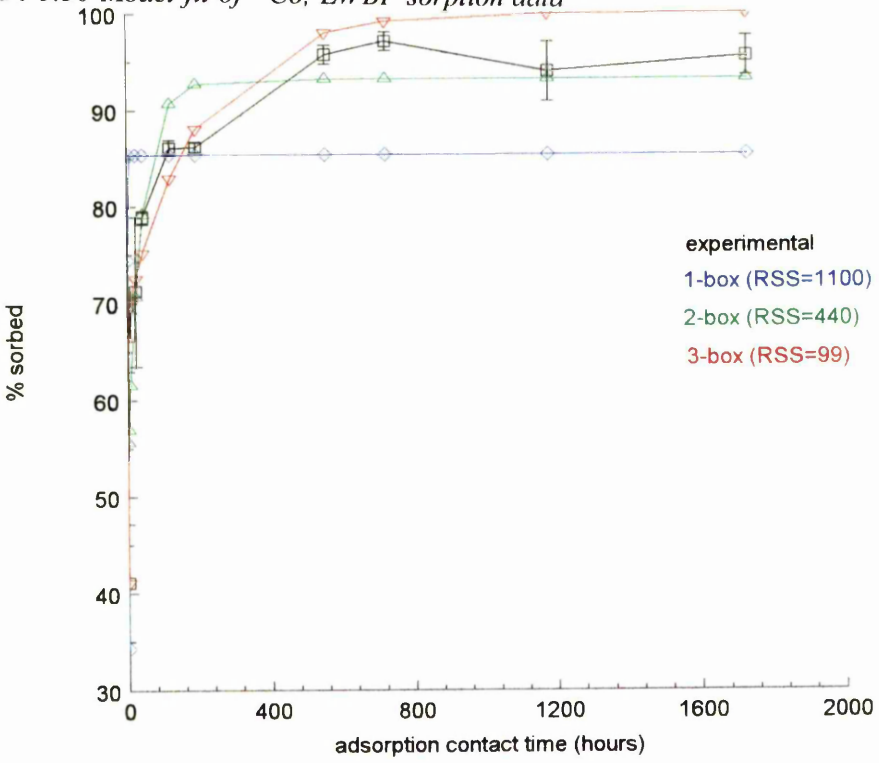

found that a two-box model was needed to describe adequately sorption of ^{57}Co on to marine sediments.

Comparison of the parameters in Table 5.1 indicate that, within error, K_f is approximately an order of magnitude larger than K_b. This is true for all of the systems, although the large errors for EWEW make it difficult to draw any conclusions. The rate constants are larger for ^{57}Co sorption on to Botany Pond sediment than Esthwaite Water sediment.

Table 5.1 Application of the one-box model to ^{57}Co sorption

SYSTEM	K_f (hr^{-1})	K_b (hr^{-1})
BPBP	1.94±0.56	0.24±0.11
BPEW	3.10±0.73	0.31±0.11
EWBP	0.88±0.28	0.15±0.07
EWEW	1.3±1.1	0.8±0.8

The Kd values reported in Table 5.2 are in reasonable agreement with the first distribution ratio measured experimentally after an adsorption time of 30 minutes, although the Kd values listed in Table 5.3 are in even better agreement (apart from the EWBP system).

Table 5.2 Application of the two-box model to ^{57}Co sorption

SYSTEM	Kd ($ml g^{-1}$)	K_1 (hr^{-1})	K_{-1} (hr^{-1})
BPBP	210±20	0.033±0.009	0.0031±0.0016
BPEW	400±60	0.012±0.007	0.0023±0.0021
EWBP	120±30	0.035±0.018	0.0034±0.0026
EWEW	80±50	0.03±0.08	0.02±0.04

Apart from the EWEW system in which the errors are too large to draw any conclusions, the forward rate constants, K_1, are again generally an order of magnitude larger than the backward rate constants, K_{-1}. The rate constants for sorption on to the sediments mixed with Botany Pond water are larger than those for sorption on to sediments which were mixed with Esthwaite water. The errors for the parameters listed in Table 5.3 are generally too large to draw any conclusions.

Table 5.3 Application of the three-box model to ^{57}Co sorption

SYSTEM	Kd ($ml g^{-1}$)	K_1 (hr^{-1})	K_{-1} (hr^{-1})	K_2 (hr^{-1})
BPBP	200±20	0.029±0.009	0.010±0.006	0.0016±0.0013
BPEW	330±70	0.06±0.07	0.06±0.07	0.0029±0.0023
EWBP	10±40	1.02±0.86	0.51±0.22	0.0074±0.0022
EWEW	70±40	0.02±0.03	0.02±0.04	$2x10^{-11}$±0.001

As the last two data points in both the EWBP and EWEW systems were excluded from the linearization procedure for reasons discussed previously (see Section 5.2.1), the model parameters were also re-evaluated using data sets for both systems from which the last two data points were excluded. The results of this can be seen in Tables 5.4 and 5.5. As might be expected, eliminating these last two data points has resulted in decreasing the residual sums of squares of the model curve fits. However, it can be seen that the two and three-box kinetic models continue to provide a better description of the data than the one-box model. Although there is little difference between the two and three-box models for ^{57}Co sorption in the EWEW system, the three-box model does provide a much better fit than the two-box for the EWBP system.

Generally speaking, excluding these two data points has had the effect of decreasing

the errors on the parameters. There has been little change to the parameter values in the EWBP experiments, but some change to the two and three-box rate constants in the EWEW system.

Table 5.4 New parameters for ^{57}Co sorption, EWBP system

BOX MODEL	RSS OF CURVE FIT	PARAMETER	REVISED VALUE
One-box	850	K_f (hr^{-1})	0.93±0.32
		K_b (hr^{-1})	0.20±0.09
Two-box	430	Kd (mlg^{-1})	120±30
		K_1 (hr^{-1})	0.040±0.024
		K_{-1} (hr^{-1})	0.005±0.005
Three-box	44	Kd (mlg^{-1})	8±30
		K_1 (hr^{-1})	1.05±0.72
		K_{-1} (hr^{-1})	0.52±0.18
		K_2 (hr^{-1})	0.0076±0.0018

Table 5.5 New parameters for ^{57}Co sorption, EWEW system

BOX MODEL	RSS OF CURVE FIT	PARAMETER	REVISED VALUE
One-box	2400	K_f (hr^{-1})	1.11±0.80
		K_b (hr^{-1})	0.53±0.43
Two-box	790	Kd (mlg^{-1})	81±23
		K_1 (hr^{-1})	0.019±0.014
		K_{-1} (hr^{-1})	0.003±0.004
Three-box	740	Kd (mlg^{-1})	77±26
		K_1 (hr^{-1})	0.01±0.02
		K_{-1} (hr^{-1})	0.01±0.02
		K_2 (hr^{-1})	0.002±0.005

5.4.2 ^{85}Sr

Figures 5.51-5.54 show the model predictions for ^{85}Sr sorption in the four freshwater systems. The linearization procedure predicted that a one or two-box kinetic model was needed to describe the data in each of the systems. Although the two-box model does fit the experimental data in all of the systems slightly better than the one and three-box models, the one-box model is generally adequate to describe the data. This is in agreement with Nyffeler et al (1984), who also found that a one-box model was sufficient to describe strontium sorption on to marine sediments, suggesting that strontium sorption occurs through ion-exchange reactions on to regular ion-exchange sites.

With the exception of the EWEW system, where the errors are too large to draw any definite conclusions, the forward rate constants in Table 5.6 are, within error, twice as large as the backward rate constants. Although errors are large, it appears that sorption on to the sediments from Esthwaite water gives larger rate constants than sorption from Botany Pond water. This could be due to the higher concentration of competing cations in Botany Pond water.

Table 5.6 Application of the one-box model to ^{85}Sr sorption

SYSTEM	K_f (hr^{-1})	K_b (hr^{-1})
BPBP	2.78±1.13	1.69±0.73
BPEW	7±20	3±9
EWBP	0.94±0.48	0.37±0.22
EWEW	50±3000	30±2000

The errors on the rate constants in Table 5.7 are too large to make any conclusions,

Figure 5.51 Model fit of ^{85}Sr, BPBP sorption data

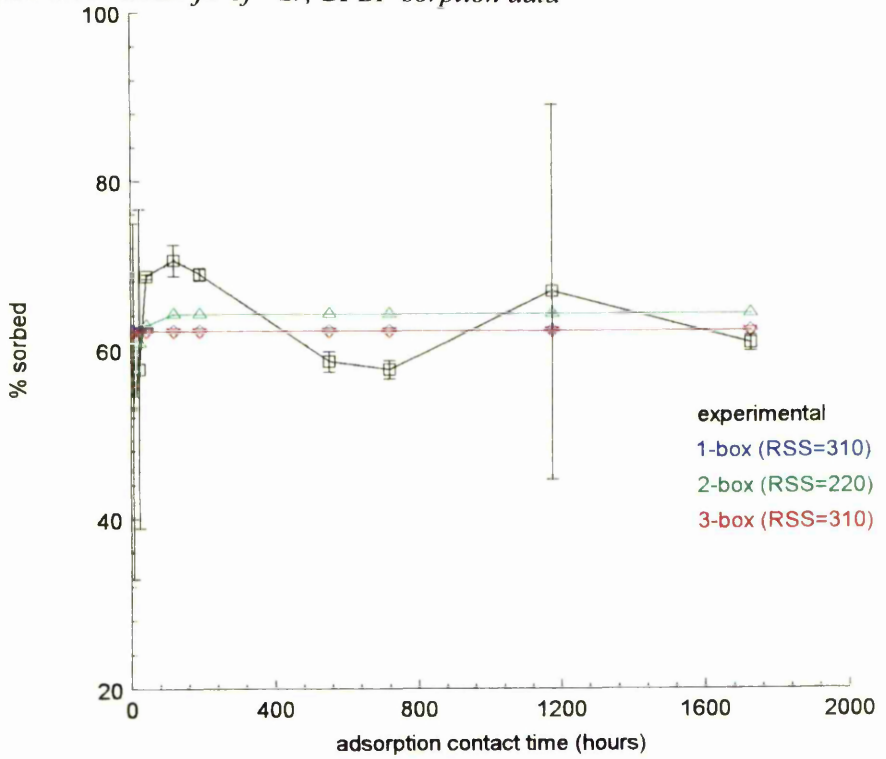

Figure 5.52 Model fit of ^{85}Sr, BPEW sorption data

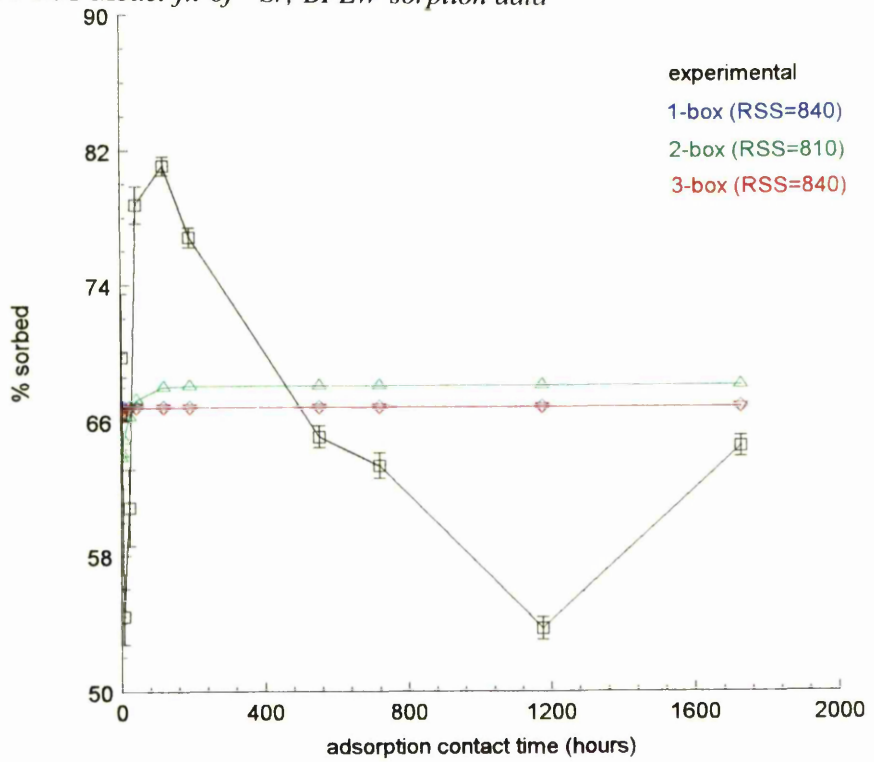

Figure 5.53 Model fit of ^{85}Sr, EWEW sorption data

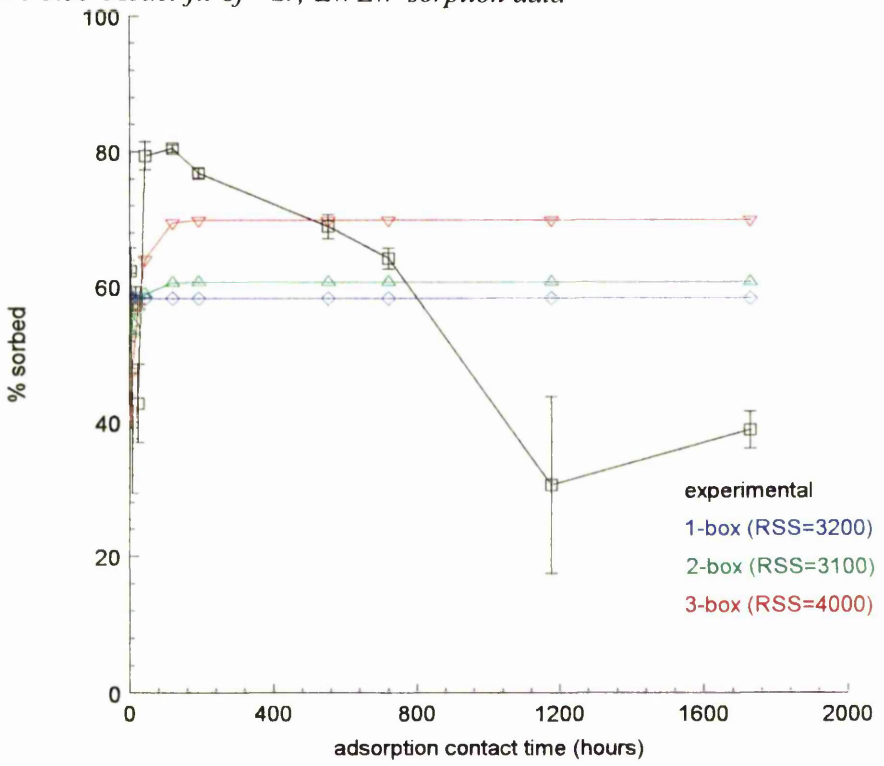

Figure 5.54 Model fit of ^{85}Sr, EWBP sorption data

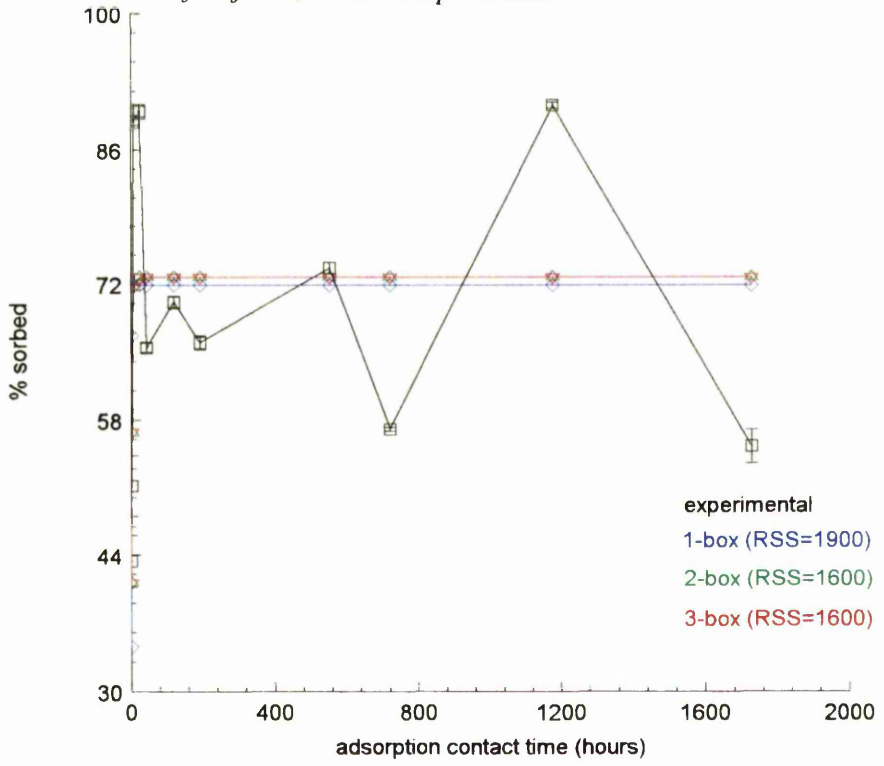

but the Kd values are in excellent agreement with the first distribution ratio measured experimentally after an adsorption time of 30 minutes.

Table 5.7 Application of the two-box model to ^{85}Sr sorption

SYSTEM	Kd (mlg^{-1})	K_1 (hr^{-1})	K_{-1} (hr^{-1})
BPBP	120±20	0.02±0.03	0.03±0.05
BPEW	180±60	0.01±0.05	0.03±0.20
EWBP	50±60	1±2	0.2±0.2
EWEW	110±60	0.01±0.08	0.03±0.20

As might be expected, the parameters in Table 5.8 show that the three-box model is unsuitable to describe ^{85}Sr sorption, as the error on some of the parameters is as much as eight to ten orders of magnitude larger than the parameter itself.

Table 5.8 Application of the three-box model to ^{85}Sr sorption

SYSTEM	Kd (mlg^{-1})	K_1 (hr^{-1})	K_{-1} (hr^{-1})	K_2 (hr^{-1})
BPBP	30±4000	2±100	2±9	$1x10^{-14}$±$2x10^{-4}$
BPEW	50±$5x10^7$	4±$2x10^6$	4±$7x10^5$	$4x10^{-12}$±$4x10^{-4}$
EWBP	50±60	0.3±0.5	0.2±0.3	$5x10^{-12}$±$6x10^{-4}$
EWEW	66±49	0.02±0.04	0.02±0.04	$3x10^{-11}$±$1x10^{-3}$

5.4.3 ^{103}Ru

The linearization procedure predicted that either a two or three-box model would best describe these data, and this was supported by the curve fits shown in Figures 5.55-5.58. Sorption of ^{103}Ru on to Botany Pond sediment is described adequately by all three models, although the three-box model describes the data best. Similarly for

Figure 5.55 Model fit of ^{103}Ru, BPBP sorption data

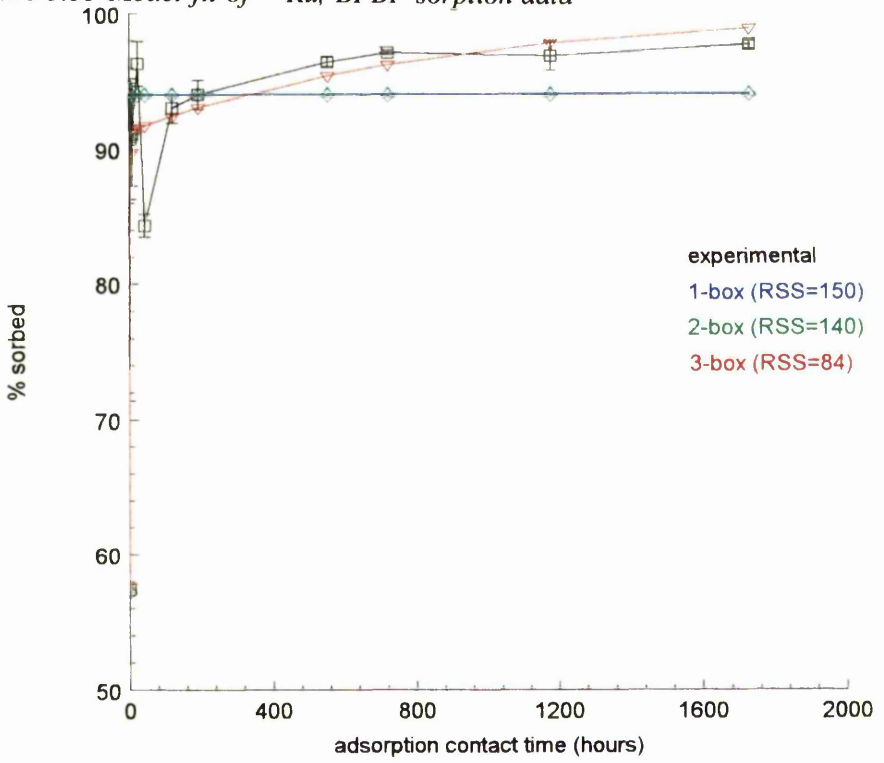

Figure 5.56 Model fit of ^{103}Ru, BPEW sorption data

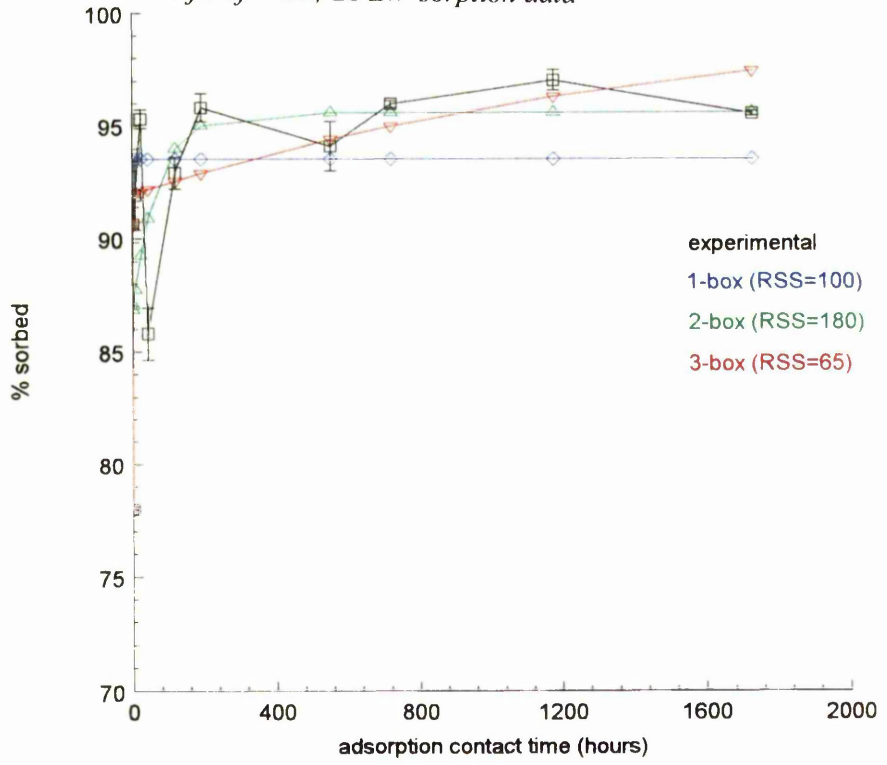

Figure 5.57 Model fit of ^{103}Ru, EWEW sorption data

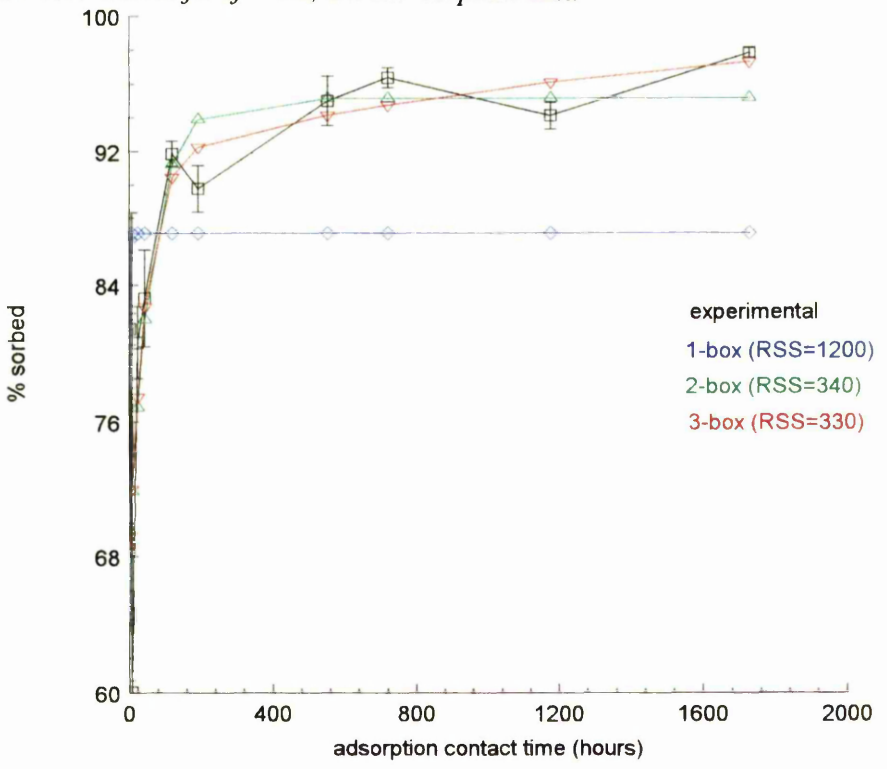

Figure 5.58 Model fit of ^{103}Ru, EWBP sorption data

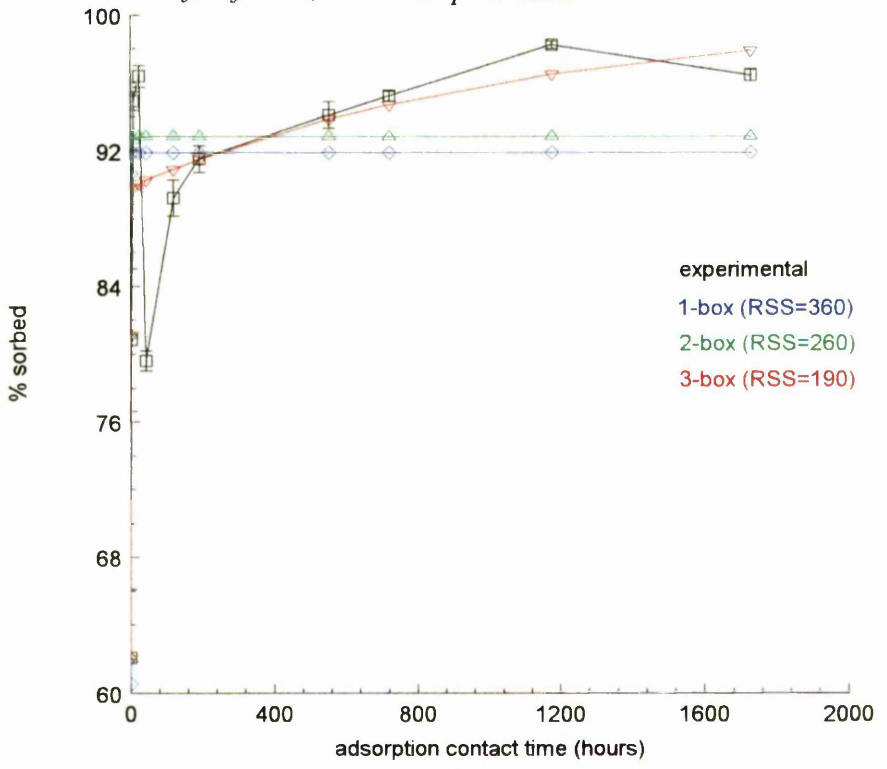

sorption on to Esthwaite Water sediment, the three-box model describes the data a little better than the one-box and two-box although all three models fit the Botany Pond data better than the Esthwaite Water.

Table 5.9 Application of the one-box model to ^{103}Ru sorption

SYSTEM	K_f (hr^{-1})	K_b (hr^{-1})
BPBP	1.76±0.20	0.11±0.03
BPEW	3.35±0.41	0.23±0.05
EWBP	1.98±0.37	0.18±0.06
EWEW	2.33±0.85	0.35±0.18

Within error, the forward rate constants shown in Table 5.9 are generally an order of magnitude larger than the backward rate constants. The systems which used Esthwaite water have somewhat larger rate constants than those which used Botany Pond water. This could be due to the lower ionic strength of Esthwaite water. The Kd values in Table 5.10 are in good agreement with the first distribution ratio measured experimentally after an adsorption time of 30 minutes, apart from the BPBP system, where the Kd found is lower than the experimental Rd value.

Table 5.10 Application of the two-box model to ^{103}Ru sorption

SYSTEM	Kd (mlg^{-1})	K_1 (hr^{-1})	K_{-1} (hr^{-1})
BPBP	10±50	10±40	0.108±0.037
BPEW	660±170	0.01±0.01	0.005±0.007
EWBP	100±50	1.1±0.9	0.093±0.048
EWEW	220±40	0.020±0.012	0.003±0.003

Although both of the Esthwaite Water sediment Kd values in Table 5.11 are also in

good agreement with the experimental values, again the BPBP system has a considerably lower value, as does the BPEW system. In Tables 5.10 and 5.11 the rate constants for sorption to sediments from Botany Pond water are larger than the rate constants from Esthwaite Water.

Table 5.11 Application of the three-box model to ^{103}Ru sorption

SYSTEM	Kd ($ml g^{-1}$)	K_1 (hr^{-1})	K_{-1} (hr^{-1})	K_2 (hr^{-1})
BPBP	$2x10^{-7}$±70	1.8±1.5	0.173±0.051	0.0013±$8x10^{-4}$
BPEW	160±170	1.2±1.5	0.328±0.185	$8x10^{-4}$±$6x10^{-4}$
EWBP	100±50	0.62±0.37	0.153±0.084	0.0011±0.0010
EWEW	220±50	0.016±0.012	0.005±0.009	$9x10^{-4}$± 0.002

5.4.4 ^{134}Cs

Figures 5.59-5.62 show the model predictions of ^{134}Cs sorption in the four freshwater systems. For sorption on to Botany Pond sediment a reasonable fit is obtained from the one-box model, but the two-box model gives a much better fit (RSS is less than 10). The three-box model gives an almost perfect fit to the data, as predicted by the linearization procedure (RSS is approximately 1).

Sorption of ^{134}Cs on to Esthwaite Water sediment was not as well described by the one-box model as the Botany Pond data. A good fit was obtained from the two-box model and there was little difference between the fit of the two and three-box models. This is in good agreement with the results of Comans and Hockley (1992), Madruga (1993), Valcke (1993) and Wauters (1994) who also found that a two-box model was adequate to describe caesium sorption. Comans and Hockley (1992) also found that for certain systems, a three-box model was needed, as has been observed here for the

Figure 5.59 Model fit of ^{134}Cs, BPBP sorption data

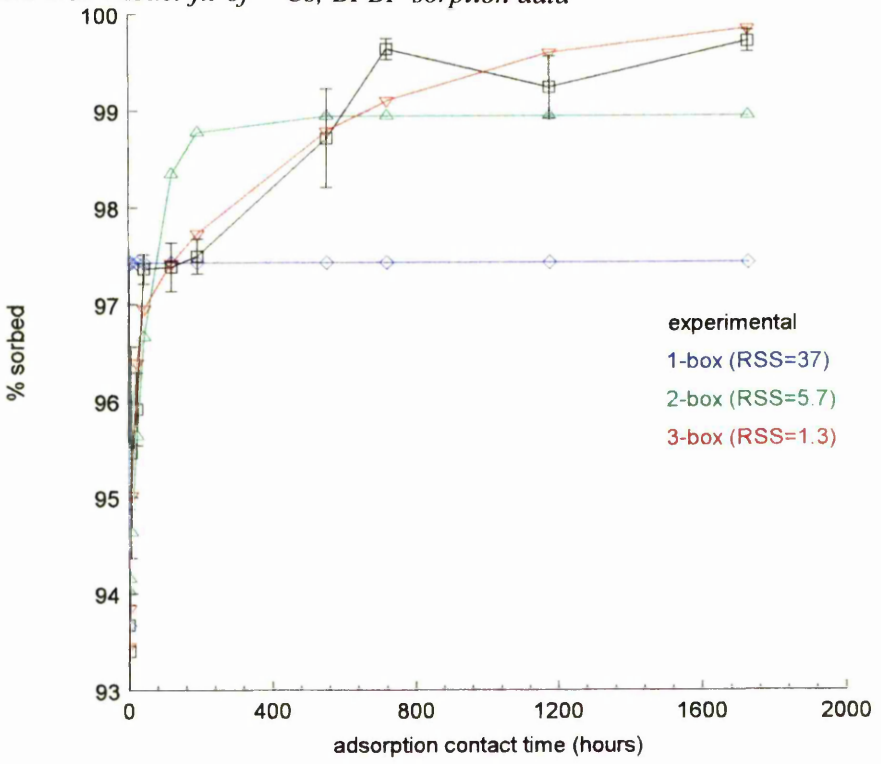

Figure 5.60 Model fit of ^{134}Cs, BPEW sorption data

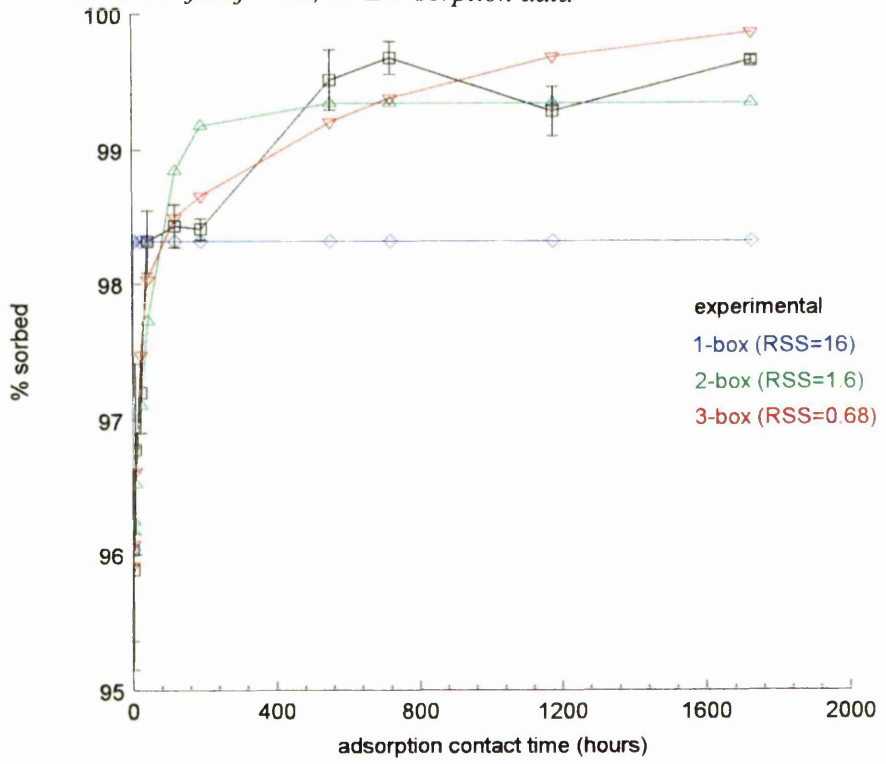

Figure 5.61 Model fit of ^{134}Cs, EWEW sorption data

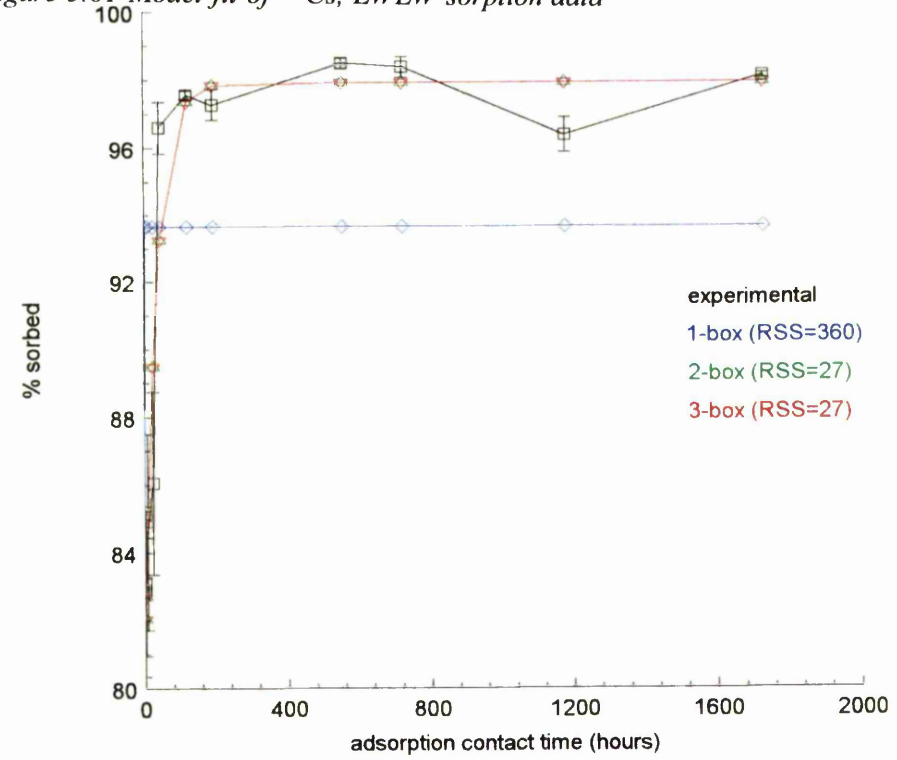

Figure 5.62 Model fit of ^{134}Cs, EWBP sorption data

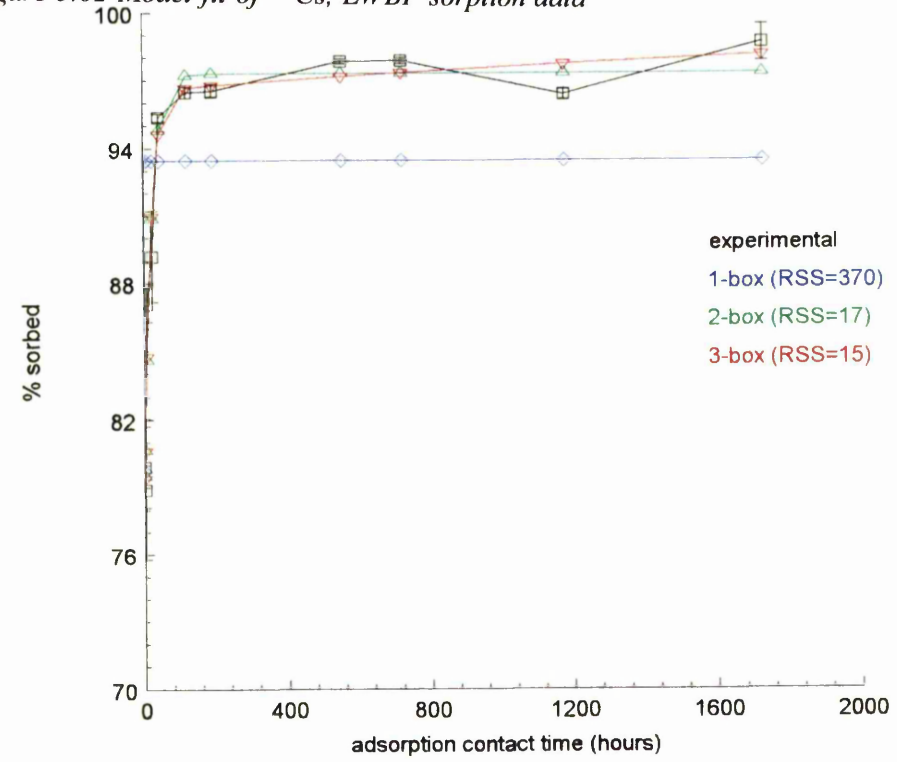

Botany Pond sediment. Although Nyffeler et al (1984) reported that a one-box model was sufficient to describe caesium sorption on to marine sediments, this could be because of a low clay content in the sediment which would mean that no caesium fixation was taking place. Although the two and three-box models do give better fits to the experimental data, the one-box model also gives a good fit and would be adequate to describe the data, particularly for sorption on to Botany Pond sediment. Model parameters for the two sediments are shown in Tables 5.12-5.14. Sorption to Botany Pond sediment gives higher forward rate constants (approximately double) than sorption to Esthwaite Water sediment, although backward rate constants for Botany Pond sediment are approximately half those for Esthwaite Water sediment. This is probably a reflection of the different clay mineralogy.

Table 5.12 Application of the one-box model to ^{134}Cs sorption

SYSTEM	K_f (hr^{-1})	K_b (hr^{-1})
BPBP	6.34±1.09	0.17±0.06
BPEW	7.41±1.17	0.13±0.04
EWBP	3.59±0.88	0.25±0.11
EWEW	4.03±1.09	0.27±0.13

Table 5.13 Application of the two-box model to ^{134}Cs sorption

SYSTEM	Kd (mlg^{-1})	K_1 (hr^{-1})	K_{-1} (hr^{-1})
BPBP	1600±150	0.016±0.006	0.0031±0.002
BPEW	2500±200	0.013±0.004	0.0026±0.001
EWBP	380±30	0.050±0.010	0.0059±0.002
EWEW	450±40	0.031±0.008	0.0033±0.002

The Kd values reported in Tables 5.13 and 5.14 agree well with the distribution ratios

measured experimentally after an adsorption time of 30 minutes. Rate constants in these tables are higher for sorption on to sediments from Botany Pond water than from Esthwaite water. The value of the rate constants, K_1 and K_{-1}, remains approximately the same (within error) for both the two and three-box models for sorption to Esthwaite Water sediment, and the value of K_2 is very small, indicating again perhaps that the two-box model is sufficient to describe ^{134}Cs sorption to this sediment. The K_2 value for ^{134}Cs sorption on to Botany Pond sediment is approximately an order of magnitude smaller than the K_1 value.

Table 5.14 Application of the three-box model to ^{134}Cs sorption

SYSTEM	Kd (mlg^{-1})	K_1 (hr^{-1})	K_{-1} (hr^{-1})	K_2 (hr^{-1})
BPBP	1400±90	0.043±0.016	0.036±0.018	0.003±0.001
BPEW	2300±140	0.027±0.010	0.019±0.010	0.003±0.001
EWBP	380±30	0.042±0.009	0.008±0.004	$4x10^{-4}$±$6x10^{-4}$
EWEW	450±40	0.025±0.007	0.003±0.003	$3x10^{-12}$±$8x10^{-4}$

Table 5.15 New parameters for ^{134}Cs sorption, EWEW system

BOX MODEL	RSS OF CURVE FIT	PARAMETER	REVISED VALUE
One-box	330	K_f (hr^{-1})	4.14±1.3
		K_b (hr^{-1})	0.32±0.17
Two-box	24	Kd (mlg^{-1})	450±40
		K_1 (hr^{-1})	0.030±0.009
		K_{-1} (hr^{-1})	0.0026±0.0021
Three-box	24	Kd (mlg^{-1})	450±50
		K_1 (hr^{-1})	0.024±0.009
		K_{-1} (hr^{-1})	0.003±0.004
		K_2 (hr^{-1})	$1x10^{-4}$±0.003

As the last two data points for the EWEW system have been excluded from the linearization procedure due to the possible biological interference on sorption which gave lower sorption yields, the model parameters for this system have been re-evaluated without taking the last two points into account. The results are shown in Table 5.15.

Excluding the last two data points for this system has improved the curve fits slightly, although there is still virtually no difference between the two and three-box models. The distribution coefficients remain approximately the same and the rate constants have changed slightly but the ratio K_1:K_{-1} still remains the same (approximately 10:1). Interestingly, the new value of K_2 is much larger and is now comparable to the value of K_2 for the EWBP system, suggesting that this new value is a more realistic estimate (although the error is still large).

5.5 Discussion

A one-box model was only adequate to describe the sorption of ^{85}Sr in these four freshwater systems. A two-box model was adequate to describe ^{57}Co, ^{103}Ru and ^{134}Cs sorption, although the three-box model did give better fits to the data of the last two radionuclides. An almost perfect fit was obtained when the three-box model was applied to ^{134}Cs sorption data.

Comparison of the rate constants found from the one-box model reveals that for all of the radionuclides, K_f was larger in the systems which contained Esthwaite water than in those containing Botany Pond water. This was most pronounced for ^{103}Ru sorption on to Botany Pond sediment, where K_f was approximately twice as large. The

largest K_f values were obtained for ^{134}Cs sorption.

Good agreement was generally obtained between the model Kd values and the first experimental Rd measured for all of the radionuclides. The highest Kd values were obtained for ^{134}Cs, as would be expected, and the lowest values were obtained for ^{85}Sr. K_1 and K_{-1} rate constant values calculated for ^{57}Co and ^{134}Cs sorption using the two-box model were comparable. When this model was applied to ^{85}Sr and ^{103}Ru sorption however, larger K_{-1} values were obtained.

5.6 Determination of the radionuclide content held in each model fraction

Using the equilibrium and rate constants reported in Tables 5.1-5.15, it is possible to predict the amount of radionuclide held in each model fraction (i.e. in each box) at a particular time. These predicted values can then be compared with the experimentally determined values of these fractions obtained from the desorption experiments and reported in Chapter 4. This comparison will provide a further indication of the realism with which this model describes radionuclide sorption in the four freshwater systems.

5.7 Comparison of predicted vs. experimental data

Predictions were made using the 2 and 3-box models for each of the radionuclides in all four freshwater systems. Three sorption times were used, 23, 192 and 1176 hours, corresponding to the adsorption times used for the ammonium acetate extractions since this extractant provided the best indication of the amount of radionuclide sorbed on the easily exchangeable sites (i.e. Box W; see Chapter 4). Ideally, the percentage of

radionuclide remaining on the sediment following ammonium extraction (refer to Section 4.7.3) should be equal to the amount of radionuclide predicted to be in Box Y (2-box model), and the sum of Box Y and Box Z (3-box model).

5.7.1 Cobalt

Comparisons between the predicted and observed fractions of ^{57}Co are shown in Tables 5.16 and 5.17.

Table 5.16 Comparison of predicted and observed behaviour of ^{57}Co (2-box model)

SYSTEM	TIME (hrs)	PREDICTED BOX Y (%)	OBSERVED BOX Y (%)
BPBP	23	38.9	65.8
	192	87.2	81.6
	1176	87.8	83.4
BPEW	23	19.3	81.5
	192	72.5	79.5
	1176	80.7	84.2
EWBP	23	34.3	42.4
	192	83.8	80.5
	1176	84.9	82.7
EWEW	23	21.4	4.96
	192	39.9	53.2
	1176	40.0	23.9

The 2-box and 3-box models gave comparable predictions of the amount of ^{57}Co remaining sorbed to the sediment following the extraction procedure (r^2 = 0.474 and 0.475 respectively). Better agreement between the observed and predicted data was obtained following longer sorption times (r^2 = 0.832 and 0.623 for 2 and 3-box

models). Interestingly, apart from the EWEW system, the predicted value was consistently lower than the observed value for the 23 hour sorption time, implying that more ^{57}Co was available in the exchangeable pool at this time than was actually measured. This could suggest that ammonium acetate is a poor extractant of ^{57}Co.

Since Box Y is most sensitive to the parameter, K_1, (see Sections 5.9.1 and 5.9.2), it is possible that poor agreement is being obtained between the predicted and observed fractions because of a poorly estimated value of this parameter. Using the value of K_1 ± the standard error gave a range of predicted values which were in slightly better agreement with the observed value. For example, a range of 18.5-46.9% was obtained for EWBP at 23 hours, 66.7-89.3% at 192 hours and 73.2-89.5% at 1176 hours. The observed values fell within all of these limits.

Table 5.17 Predicted behaviour of ^{57}Co (3-box model)

SYSTEM	TIME (hrs)	BOX Y (%)	BOX Z (%)	Y+Z (%)
BPBP	23	43.7	0.9	44.6
	192	60.8	18.2	79.1
	1176	18.4	75.2	93.7
BPEW	23	45.3	2.2	47.5
	192	38.0	23.1	61.1
	1176	9.3	81.2	90.5
EWBP	23	59.6	10.4	70.0
	192	25.9	61.0	87.0
	1176	0.2	99.7	99.9
EWEW	23	30.1	10^{-9}	30.1
	192	50.0	10^{-7}	50.0
	1176	50.0	10^{-6}	50.0

5.7.2 Strontium

Tables 5.18 and 5.19 show the predicted and observed amounts of ^{85}Sr remaining on the sediment following an extraction of the exchangeable pool with ammonium acetate. The 3-box model predictions are consistently high compared with the observed values. This is unsurprising, given the unsuitability of this model for the prediction of ^{85}Sr sorption in these systems (Section 5.4.2). Predictions made using the 2-box model are closer to the observed data ($r^2 = 0.671$ compared with 0.376 for the 3-box model) and generally appear to be slightly high. As was suggested in Section 5.4.2, this could imply that the simpler 1-box model is sufficient to describe ^{85}Sr sorption.

Table 5.18 Comparison of predicted and observed behaviour of ^{85}Sr (2-box model)

SYSTEM	TIME (hrs)	PREDICTED BOX Y (%)	OBSERVED BOX Y (%)
BPBP	23	16.3	0
	192	26.7	11.7
	1176	26.7	10.1
BPEW	23	10.0	0
	192	17.6	9.4
	1176	17.6	0
EWBP	23	62.5	63.2
	192	62.5	14.7
	1176	62.5	40.1
EWEW	23	8.3	0.7
	192	14.8	12.7
	1176	14.9	0

Table 5.19 Predicted behaviour of ^{85}Sr (3-box model)

SYSTEM	TIME (hrs)	BOX Y (%)	BOX Z (%)	Y+Z (%)
BPBP	23	50.0	10^{-11}	50.0
	192	50.0	10^{-11}	50.0
	1176	50.0	10^{-10}	50.0
BPEW	23	50.0	10^{-9}	50.0
	192	50.0	10^{-8}	50.0
	1176	50.0	10^{-7}	50.0
EWBP	23	60.0	10^{-9}	60.0
	192	60.0	10^{-8}	60.0
	1176	60.0	10^{-7}	60.0
EWEW	23	30.1	10^{-8}	30.1
	192	50.0	10^{-7}	50.0
	1176	50.0	10^{-6}	50.0

Large differences between the predicted and observed values for this radionuclide could also be due to the small amount of ^{85}Sr remaining on the sediment following ammonium extraction. Attempting to predict a small difference between two values (e.g. 100 - 88.3 for BPBP 192 hours) will lead to large errors. Where "observed" is greater (e.g. EWBP 23 and 1176 hours) better predictions are made.

5.7.3 Ruthenium

Tables 5.20 and 5.21 compare the predicted fractions of ^{103}Ru (using the 2 and 3-box models) with the experimentally measured value of this fraction.

Agreement between observed and calculated values is poorest for this element (r^2 = 0.038 and 0.167 for 2-box and 3-box models respectively) than for any other, and,

interestingly both models give a negative correlation coefficient. As with ^{57}Co, this suggests that ammonium acetate is an appropriate extractant of ^{103}Ru.

Using the value of K_1 ± the standard error makes little difference to the agreement between the predicted and observed values for this radionuclide.

Table 5.20 Comparison of predicted and observed behaviour of ^{103}Ru (2-box model)

SYSTEM	TIME (hrs)	PREDICTED BOX Y (%)	OBSERVED BOX Y(%)
BPBP	23	89.4	96.5
	192	89.4	89.6
	1176	89.4	79.8
BPEW	23	17.1	92.3
	192	58.9	91.1
	1176	63.5	80.8
EWBP	23	85.5	95.5
	192	85.5	93.5
	1176	85.5	86.7
EWEW	23	26.2	93.7
	192	78.8	92.1
	1176	82.1	78.3

Table 5.21 Predicted behaviour of ^{103}Ru (3-box model)

SYSTEM	TIME (hrs)	BOX Y (%)	BOX Z (%)	Y+Z (%)
BPBP	23	88.8	2.6	91.5
	192	72.7	20.3	93.0
	1176	22.6	75.2	97.8
BPEW	23	77.4	1.4	78.8
	192	69.6	11.3	81.0
	1176	37.5	52.2	89.7
EWBP	23	78.7	1.9	80.6
	192	67.8	15.5	83.3
	1176	28.5	64.5	93.0
EWEW	23	28.9	0.3	29.2
	192	67.0	9.4	76.4
	1176	35.1	53.5	88.6

5.7.4 Caesium

Comparisons of the predicted and observed fractions of ^{134}Cs are shown in Tables 5.22 and 5.23. Neither the 2-box model ($r^2 = 0.121$) nor the 3-box ($r^2 = 0.108$) appears to predict the amount of ^{134}Cs remaining sorbed to the sediment following the extraction procedure. Although the data set is small, in the case of sorption on to Botany Pond sediment, both models appear to overestimate the amount of ^{134}Cs contained within the exchangeable pool, whereas with Esthwaite Water sediment, the models seem to underestimate the fraction of ^{134}Cs which is measured in the exchangeable pool.

Using the value of $K_1 \pm$ the standard error led to slightly better agreement between the predicted and observed values.

Table 5.22 Comparison of predicted and observed behaviour of ^{134}Cs (2-box model)

SYSTEM	TIME (hrs)	PREDICTED BOX Y (%)	OBSERVED BOX Y (%)
BPBP	23	28.3	52.1
	192	80.4	81.7
	1176	82.9	78.4
BPEW	23	24.3	60.4
	192	78.2	86.5
	1176	82.8	83.2
EWBP	23	56.5	33.0
	192	87.0	51.6
	1176	87.0	48.5
EWEW	23	42.7	33.9
	192	88.1	54.5
	1176	88.5	50.3

Table 5.23 Predicted behaviour of ^{134}Cs (3-box model)

SYSTEM	TIME (hrs)	BOX Y (%)	BOX Z (%)	Y+Z (%)
BPBP	23	44.0	2.0	46.0
	192	40.1	25.0	65.1
	1176	8.3	84.5	92.8
BPEW	23	37.0	1.5	38.5
	192	42.6	25.3	68.0
	1176	7.9	86.2	94.1
EWBP	23	57.1	0.3	57.4
	192	79.2	5.6	84.8
	1176	56.9	32.2	89.1
EWEW	23	42.4	10^{-9}	42.4
	192	88.9	10^{-8}	88.9
	1176	89.3	10^{-7}	89.3

5.8 Discussion

Neither the 2-box nor the 3-box model gave particularly good predictions. Qualitatively, agreement between the predicted and observed values appears to be better for the longer sorption times and where desorption was relatively low. The discrepancies between the predicted and observed fractions could occur due to ammonium acetate actually being a poor extractant for the elements used here. It is also possible that disagreement between the predicted and observed values could be due to the use of a poorly estimated parameter in the prediction of the size of a fraction, especially given the considerable errors on certain of the parameters (see Sections 5.4.1-5.4.4).

With only three sorption times to compare, it is difficult to draw definite conclusions as to the ability of the box models to predict the amount of radionuclide sorbed in the different fractions at a particular time, especially given the variability of the experimental sorption data.

Although the ability of the box models to predict both the magnitude and time course of radionuclide sorption looks promising, they clearly do not predict speciation particularly well. This should be investigated further, in particular, comparing predicted and observed fractions at more sorption times, especially shorter ones. It might also be beneficial to use a range of extractants to suit all of the radionuclides, e.g. Mg^{2+} for Sr^{2+} and Mn^{2+} for Co^{2+}, instead of using just one general extractant (as was used in this work) which might not provide an accurate experimental estimate of the exchangeable pool for every radionuclide.

5.9 Model sensitivity

The sensitivity of the 2 and 3-box models to the parameters Kd, K_1, K_{-1} and K_2 (3-box) was tested by varying each of these parameters in turn by 10% whilst keeping all the others constant. Sorption data from the ^{134}Cs, BPBP system was used in this analysis.

5.9.1 Two-box model

The results of the sensitivity analysis are shown in Table 5.24.

Table 5.24 Sensitivity analysis of the 2-box model

PARAMETER	TIME (hrs)	[BOX Y] (%)	[SORBED] (%)
ORIGINAL DATA	23	28.3	95.6
	192	80.4	98.8
	1176	82.9	98.9
Kd +10% / -10%	23	28.4 / 28.1	96.0 / 95.2
	192	80.5 / 80.2	98.9 / 98.6
	1176	83.0 / 82.8	99.0 / 98.8
K_1 +10% / -10%	23	30.7 / 25.9	95.8 / 95.5
	192	82.3 / 78.1	98.9 / 98.6
	1176	84.2 / 81.4	99.0 / 98.9
K_{-1} +10% / -10%	23	28.2 / 28.4	95.7 / 95.7
	192	79.1 / 81.6	98.7 / 98.9
	1176	81.5 / 84.3	98.8 / 99.1

The model does not show a strong sensitivity towards any of the parameters (<10%

change in the original data). As might be expected, Box Y is most strongly influenced by changes in K_1, and the total percentage sorbed is most strongly influenced by changes in Kd.

5.9.2 Three-box model

Table 5.25 displays the results of the sensitivity analysis using the 3-box model.

Table 5.25 Sensitivity analysis of the 3-box model

PARAMETER	TIME (hrs)	[BOX Y] (%)	[BOX Z] (%)	[SORBED] (%)
ORIGINAL DATA	23	44.0	2.0	96.4
	192	40.1	25.0	97.7
	1176	8.3	84.5	99.6
Kd +10% / -10%	23	44.0 / 44.0	2.0 / 2.0	96.7 / 96.0
	192	40.1 / 40.1	25.0 / 25.0	97.6 / 97.5
	1176	8.3 / 8.3	84.5 / 84.5	99.6 / 99.6
K_1 +10% / -10%	23	46.7 / 41.1	2.1 / 1.8	96.6 / 96.2
	192	41.3 / 38.7	26.1 / 23.8	97.9 / 97.6
	1176	7.9 / 8.6	85.8 / 83.0	99.6 / 99.5
K_{-1} +10% / -10%	23	42.8 / 45.3	1.9 / 2.0	96.3 / 96.5
	192	38.8 / 41.5	24.1 / 26.0	97.6 / 97.9
	1176	8.6 / 7.9	83.2 / 85.8	99.5 / 99.7
K_2 +10% / -10%	23	43.9 / 44.2	2.2 / 1.8	96.4 / 96.4
	192	38.9 / 41.3	27.1 / 22.9	97.8 / 97.7
	1176	6.9 / 10.0	87.1 / 81.4	99.7 / 99.5

As with the 2-box model, a variation in Kd affects only the total percentage sorbed. A stronger sensitivity is displayed towards K_1 and K_{-1}, although varying this parameter

by 10% still only produces changes in the original data of <10%. The model is most sensitive to changes in K_2. Although changes in [sorbed] are minimal when this parameter is varied, changes in [Box Y] exceed 10% at longer sorption times and [Box Z] is changed by as much as 20% at shorter sorption times.

5.10 Summary

1. The linearization procedure was useful in providing an indication of the complexity of the box model needed to describe the experimental data.

2. The kinetic box model can be used successfully to describe the sorption of ^{57}Co, ^{85}Sr, ^{103}Ru and ^{134}Cs in freshwater systems.

3. Although the one-box kinetic model was adequate to describe ^{85}Sr sorption, at least a two-box model was needed for the remaining radionuclides.

4. A virtually perfect fit was obtained when the three-box kinetic model was applied to the ^{134}Cs Botany Pond sorption data (RSS is approximately 1).

5. Although the box model sometimes provided a reasonable prediction of the amount of radionuclide held in the exchangeable pool, further investigation is needed, perhaps because NH_4^+ is not always the most appropriate cation to use in desorption experiments.

6. A thorough evaluation of the sources and consequences of experimental errors should be undertaken.

CHAPTER 6 - CONCLUSIONS

CHAPTER 6 - CONCLUSIONS

6.1 Summary

To recap briefly, the objectives of the project were,

(1) to investigate and compare the sorption kinetics (short term and long term) of four radionuclides - ^{57}Co, ^{85}Sr, ^{103}Ru and ^{134}Cs - in four freshwater systems.

(2) to use the data in a kinetic box model in order to assess the suitability of this model for the description of radionuclide sorption in freshwater systems and, if successful, obtain rate parameters for the sorption reactions.

Investigation of the adsorption behaviour of the four radionuclides revealed very different sorption trends. Different behaviour was observed in each freshwater system, revealing the importance of sediment and solution composition in the adsorption process. Sorption was highly dependent upon adsorption time and for ^{57}Co, ^{103}Ru and ^{134}Cs it seemed that sorption in certain systems still had not finished even after 2 months.

Sorption at longer time points (after a few weeks) sometimes displayed unusual behaviour and this could be due to the effects of microbial activity, despite the precautions taken to keep this to a minimum. These unusual trends were particularly pronounced in sorption experiments using Esthwaite Water sediment. The presence of a "flyer" within a replicate data set was also occasionally observed which led to a large variation coefficient (sometimes greater than 100%). Although the cause of these

unusually high or low sorption values was not established, it was nonetheless identified as a real phenomenon.

It was necessary to use both the distribution ratio and the % sorbed on to the sediment to interpret the data. Use of the two parameters was necessary because of the sensitivity of the distribution ratio and the insensitivity of the % sorbed value. Even when the changes in percentage sorbed were small, the differences in Rd were magnified due to its being a ratio, sometimes wrongly implying that a significant change in sorption had occurred. It was sometimes difficult to identify the establishment of equilibrium from the % sorbed data. It was concluded therefore that both of these parameters should be used to characterise these systems.

The effect of adsorption time on the degree of radionuclide fixation on the sediment was established during the desorption procedures. A degree of fixation was observed for ^{57}Co, ^{103}Ru and ^{134}Cs, but ^{85}Sr was found to be held on readily exchangeable sites. An effect of the desorbing cation was also established, which further illustrates the different sorption mechanisms which are used by each radionuclide.

The sequential extraction procedure performed on the spiked sediment revealed the affinity which exists between the radionuclides and the different mineralogical components within the sediment. The radionuclides became increasingly harder to extract following an increase in adsorption time, indicating a degree of fixation was occurring, even with ^{85}Sr.

For each radionuclide - freshwater system the adsorption data was used successfully in the kinetic box model. The best results were obtained for ^{134}Cs sorption data. Using

the linearization procedure was useful in identifying the most suitable box model. Application of the box model allowed rate constants for the sorption mechanisms to be determined.

6.2 Recommendations for future research

The unusual trends in sorption which occurred in certain systems after adsorption times of a few weeks or more reveal the need for further work in this area. As sorption is rarely measured after a couple of weeks, this behaviour is not usually observed. As this behaviour has serious implications either in the interpretation of laboratory experiments or in real systems, the possibility that this effect is caused by biological activity needs to be investigated further.

Further work also needs to be carried out to find a general, more effective desorbent which will provide more informative data which could be used to model radionuclide desorption behaviour.

REFERENCES

REFERENCES

Abdel Gawad, A.S., Misak, N.Z., Sayah, T. and Abdel Malik, W.E.Y., 1977. Investigations on the behaviour of some radioisotopes in a laboratory-scale aquatic ecosystem. International Journal of Applied Radiation and Isotopes, 28, pp. 705-712.

Adams, S.N., Honeysett, J.L., Tiller, K.G. and Norrish, K., 1969. Factors controlling the increase of cobalt in plants following the addition of a cobalt fertilizer. Australian Journal of Soil Research, 7, pp. 29-42.

Alberts, J.J., Tilly, L.J. and Vigerstad, T.J., 1979. Seasonal cycling of Cs-137 in a reservoir. Science, 203, pp. 649-651.

Allen, S.E., 1989. Chemical analysis of ecological materials. 2nd Edition. Blackwell Scientific Publications.

Andersson, K.G. and Roed, J., 1994. The behaviour of Chernobyl Cs-137, Cs-134 and Ru-106 in undisturbed soils: Implications for external radiation. Journal of Environmental Radioactivity, 22, pp. 183-196.

Aston, S.R. and Duursma, E.K., 1973. Concentration effects on Cs-137, Zn-65, Co-60 and Ru-106 sorption by marine sediments, with geological implications. Netherlands Journal of Sea Research, 6, pp. 225-240.

Bachhuber, H., Bunzl, K. and Schimmack, W., 1986. Spatial variability of distribution coefficients of Cs-137, Zn-65, Sr-85, Co-57, Cd-109, Ce-141, Ru-103, Tc-95m and I-131 in a cultivated soil. Nuclear Technology, 2, pp. 359-371.

Benes, P., Lam Ramos, P. and Poliak, R., 1989. Factors affecting interaction of radiocaesium with freshwater solids (I) pH, composition of water and the solids. Journal of Radioanalytical and Nuclear Chemistry articles, 133, pp. 359-376.

Benes, P. and Poliak, R., 1990. Factors affecting the interaction of radiostrontium with river sediments. Journal of Radioanalytical and Nuclear Chemistry articles, 141, pp. 75-90.

Benes, P., Stamberg, K. and Stegmann, R., 1994. Study of the kinetics of the interaction of Cs-137 and Sr-85 with soils using a batch method: methodological problems. Radiochimica Acta, 66/67, pp. 315-321.

Berry, J.A., Bourke, P.J., Coates, H.A., Green, A., Jefferies, N.L., Littleboy, A.K. and Hooper, A.J., 1988. Sorption of radionuclides on sandstones and mudstones. Radiochimica Acta, 44/45, pp. 135-141.

Bird, G.A. and Evenden W.G., 1994. Effect of sediment type, temperature and colloids on the transfer of radionuclides from water to sediment. Journal of Environmental Radioactivity, 22, pp. 219-242.

Bolt, G.H., Sumner, M.E. and Kamphorst, A., 1963. A study of the equilibria between three categories of potassium in an illitic soil. Soil Science Society American Proceedings, 27, pp. 294-299.

Bunzl, K. and Schimmack, W., 1991. Kinetics of the sorption of Cs-137, Sr-85, Co-57, Zn-65 and Cd-109 by the organic horizons of a forest soil. Radiochimica Acta, 54, pp. 97-102.

Burns, R.G., 1976. The uptake of cobalt into ferromanganese nodules, soils and synthetic manganese (IV) oxides. Geochimica et Cosmochimica Acta, 40, pp. 95-102.

Cerling, T.E. and Spalding, B.P., 1981. A real distribution of Co-60, Cs-137 and Sr-90 in streambed gravels of White Oak Creek watershed, Oak Ridge, Tennessee. ORNL/TM-7318, Oak Ridge National Laboratory, Oak Ridge, Tennessee.

Cerling, T.E. and Turner, R.R., 1982. Formation of freshwater Fe-Mn coatings on gravel and the behaviour of Co-60, Sr-90 and Cs-137 in a small watershed. Geochimica et Cosmochimica Acta, 46, pp. 1333-1343.

Comans, R.N.J., Middelburg, J.J., Zonderhuis, J., Woittiez, J.R.W., De Lange, G.J., Das, H.A. and Van Der Weijden, C.H., 1989. Mobilization of radiocaesium in pore waters of lake sediment. Nature, 339, pp. 367-369.

Comans, R.N.J., Haller, M. and De Preter, P., 1991. Sorption of caesium on illite: non-equilibrium behaviour and reversibility. Geochimica et Cosmochimica Acta, 55, pp. 433-440.

Comans, R.N.J. and Hockley, D.E., 1992. Kinetics of caesium sorption on illite. Geochimica et Cosmochimica Acta, 56, pp. 1157-1164.

Cornell, R.M., 1993. Adsorption of caesium on minerals: a review. Journal of radioanalytical and nuclear chemistry, 171, pp. 483-500.

Cotton, F.A. and Wilkinson, G., 1988. Advanced inorganic chemistry. 5th Edition. John Wiley and Sons, New York.

Cremers, A., Elsen, A., De Preter, P and Maes, A., 1988. Quantitative analysis of radiocaesium in soils. Nature, 335, pp. 247-249.

Crerar, D.A., Cormick, R.K. and Barnes, H.L., 1972. Organic controls on the sedimentary geochemistry of manganese. Acta Mineral. Petrog. Szeged, xx/2, pp. 217-226.

Cronan, D.S. and Tooms, J.S., 1969. The geochemistry of manganese nodules and associated pelagic deposits from the Pacific and Indian Oceans. Deep-Sea Research, 16, pp. 335-359.

Das, H.A., 1992. Release of Cs-137 from anoxic lacustrine sediment measurement and formulation. Journal of Radioanalytical and Nuclear Chemistry articles, 156, pp. 129-149.

Davies, K.S. and Shaw, G., 1993. Fixation of Cs-137 by soils and sediments in the Esk Estuary, Cumbria, UK. Science of the Total Environment, 132, pp. 71-92.

Duursma, E.K. and Bosch, C.J., 1970. Theoretical, experimental and field studies

concerning diffusion of radioisotopes in sediments and suspended particles of the sea. Part B: Methods and experiments. Netherlands Journal of Sea Research, 4, pp. 395-469.

Duursma, E.K. and Gross, M.G., 1971. Marine sediments and radioactivity. In Radioactivity in Marine Environment. US National Academy of Science, Washington D.C., pp. 147-160.

Elprince, A.M., Rich, C.I. and Martens, D.C., 1977. Effect of temperature and hydroxy aluminium interlayers on the adsorption of trace radioactive caesium by sediments near water-cooled nuclear reactors. Water Resources Research, 13, pp. 375-380.

Erel, Y., Morgan, J.J. and Patterson, C.C., 1991. Natural levels of Pb and Cd in a remote mountain stream. Geochimica et Cosmochimica Acta, 55, pp. 707-719.

Erten, H.N., Aksoyoglu, S., Hatipoglu, S. and Gokturk, H., 1988. Sorption of caesium and strontium on montmorillonite and kaolinite. Radiochimica Acta, 44/45, pp. 147-151.

Essington, E., Nishita, H. and Wallace, A., 1963. Effect of chelating agents on the uptake of Y-91, Ce-144, Ru-106 and Pm-147 by beans grown in a calcareous soil. Soil Science, 95, pp. 331-337.

Evans, D.W., Alberts, J.J. and Clark, R.A., 1983. Reversible ion-exchange fixation of Cs-137 leading to mobilization from reservoir sediments. Geochimica et Cosmochimica Acta, 47, pp. 1041-1049.

Evans, R.D., Andrews, D. and Cornett, R.J., 1988. Chemical fractionation and bioavailability of Co-60 to benthic deposit-feeders. Canadian Journal of Fisheries and Aquatic Science, 45, pp. 228-236.

Fahad, A.A., Ali, A.W. and Shihab, R.M., 1989. Mobilization and fractionation of Cs-137 in calcareous soils. Journal of Radioanalytical and Nuclear Chemistry articles, 130, pp. 195-201.

Francis, C.W. and Brinkley, F.S., 1976. Preferential adsorption of Cs-137 to micaceous minerals in contaminated freshwater sediment. Nature, 260, pp. 511- 513.

Fukui, M., 1990. Desorption kinetics and mobility of some radionuclides in sediments. Health Physics, 59, pp. 879-889.

Garder, K. and Skulberg, O., 1964. Sorption phenomena of radionuclides to clay particles in river water. International Journal of Air and Water Pollution, 8, pp. 229-241.

Goldberg, E.D., 1954. Marine geochemistry I. Chemical scavengers of the sea. Journal of Geology, 62, pp. 249-265.

Greenland, D.J. and Hayes, M.H.B., 1981. The chemistry of soil processes. John Wiley and Sons, UK.

Grutter, A., von Gunten, H.R., Rossler, E. and Keil, R., 1994. Sorption of nickel and cobalt on a size-fraction of unconsolidated glaciofluvial deposits and on clay minerals. Radiochimica Acta, 65, pp. 181-187.

Gutierrez, M. and Fuentes, H.R., 1991. Competitive adsorption of caesium, cobalt and strontium in conditioned clayey soil suspensions. Journal of Environmental Radioactivity, 13, pp. 271-282.

Heaney, S.I., 1976. Temporal and spatial distribution of the dinoflagellate "Ceratuim hirundinella" O.F. Muller within a small productive lake. Freshwater Biology, 6, pp. 531-542.

Hird, A.B., Rimmer, D.L. and Livens, F.R., 1996. Factors affecting the sorption and fixation of caesium in acid organic soil. European Journal of Soil Science, 47, pp. 97-104.

Hodgson, J.F., 1963. Chemistry of the micronutrient elements in soils. Advanced Agronomy, 15, pp. 119-159.

Hsu, C. and Chang, K., 1995. Study of factors dominating sorption/desorption of Cs in soil. Radiochimica Acta, 68, pp. 129-133.

Jacobs, D.G. and Tamura, T., 1960. The mechanism of ion fixation using radio-isotope techniques. Trans. 7th Int. Congr. Soil Sci., Madison, 2, pp. 206-214.

Jannasch, H.W., Honeyman, B.D., Balistrieri, L.S. and Murray, J.W., 1988. Kinetics of trace element uptake by marine particles. Geochimica et Cosmochimica Acta, 52, pp. 567-577.

Jenne, E.A. and Wahlberg, J.S., 1965. Manganese and iron oxide scavenging of Co-60 in White Oak Creek sediment, Oak Ridge, Tennessee (abs.). Transactions American Geophysical Union, 46, pp. 170.

Jenne, E.A., 1968. Controls on Mn, Fe, Co, Ni, Cu and Zn concentrations in soils and water. The significant role of hydrous Mn and Fe oxides. In: Trace Inorganics in Water. Advances in Chemistry Series, 73. American Chemical Society, pp. 337-387.

Jones, R.F., 1960. The accumulation of nitrosyl ruthenium by fine particles and marine organisms. Limnology and Oceanography, 5, pp. 312-325.

Keren, R. and O'Connor, G.A., 1983. Strontium adsorption by non-calcareous soils - exchangeable ions and solution effects. Soil Science, 135, pp. 308-315.

Kharkar, D.P., Turekian, K.K. and Bertine, K.K., 1968. Stream supply of dissolved silver, molybdenum, antimony, selenium, chromium, cobalt, rubidium and caesium to the ocean. Geochimica et Cosmochimica Acta, 32, pp. 285-298.

Kinniburgh, D.G., Syers, J.K. and Jackson, M.L., 1975. Specific adsorption of trace amounts of calcium and strontium by hydrous oxides of iron and aluminium. Soil Science Society American Proceedings, 39, pp. 464-470.

Krauskopf, K.B., 1956. Factors controlling the concentration of thirteen rare metals in seawater. Geochimica et Cosmochimica Acta, 9, pp. 1-32.

Krauskopf, K.B., 1979. Introduction to geochemistry. 2nd Edition. McGraw-Hill, London.

Li, Y.H., Burkhardt, L., Buchholtz, M., O'Hara, P. and Santschi, P.H., 1984. Partition of radiotracers between suspended particles and seawater. Geochimica et Cosmochimica Acta, 48, pp. 2011-2019.

Libby, W.F., 1958. Beneficiation of soils contaminated with Sr-90: beneficial effects of potassium. Science, 128, pp. 1134-1135.

Lima, M.F. and Mazzilli, B.P., 1994. Determination of the distribution coefficients for Cs-134, Co-60 and Th-234 in the Pinheiros river sediment-water. Journal of Radioanalytical and Nuclear Chemistry articles, 177, pp. 139-147.

Livens, F.R. and Baxter, M.S., 1988. Chemical associations of artificial radionuclides in Cumbrian soils. Journal of Environmental Radioactivity, 7, pp. 75-86.

Loganathan, P. and Burau, R.G., 1973. Sorption of heavy metal ions by a hydrous manganese oxide. Geochimica et Cosmochimica Acta, 37, pp. 1277-1293.

Madruga, M.J., 1993. Adsorption-desorption behaviour of radiocaesium and radiostrontium in sediments. PhD Thesis. K.U. Leuven.

Marshall, C.E. and Garcia, G., 1959. Exchange equilibria in a carboxylic resin and in Attapulgite clay. Journal of Physical Chemistry, 63, pp. 1663-1666.

Martin, R.P., Newbold, P. and Russell, R.S., 1957. Discrimination between strontium and calcium in plants and soils. UNESCO/NS/RIC/175, International conference on radioisotopes in scientific research.

McBride, M.B., 1979. Chemisorption and precipitation of Mn^{2+} at $CaCO_3$ surfaces. Journal of Soil Science Society of America, 43, pp. 693-698.

McClaren, R.G., Lawson, D.M. and Swift, R.S., 1986. Sorption and desorption of cobalt by soils and soil components. Journal of Soil Science, 37, pp. 413-426.

McKenzie, R.M., 1967. The sorption of cobalt by manganese minerals in soils. Australian Journal of Soil Research., 5, pp. 235-246.

McKenzie, R.M., 1970. The reaction of cobalt with manganese dioxide minerals. Australian Journal of Soil Research., 8, pp. 97-106.

McKinley, I.G. and Alexander, W.R., 1992. Constraints on the applicability of in-situ distribution coefficient values. Journal of Environmental Radioactivity, 15, pp. 19-34.

Means, J.L., Crerar, D.A., Borcsik, M.P. and Duguid, J.O., 1978a. Adsorption of cobalt and selected actinides by Mn and Fe oxides in soils and sediments. Geochimica et Cosmochimica Acta, 42, pp. 1763-1773.

Means, J.L., Crerar, D.A. and Duguid, J.O., 1978b. Migration of radioactive wastes: radionuclide mobilization by complexing agents. Science, 200, pp. 1477-1481.

Meece, D.E. and Benninger, L.K., 1993. The coprecipitation of plutonium and other radionuclides with calcium carbonate. Geochimica et Cosmochimica Acta, 57, pp. 1447-1458.

Meier, H., Zimmerhackl, E., Zeitler, G. and Menge, P., 1994. Parameter studies of radionuclide sorption in site-specific sediment/groundwater systems. Radiochimica Acta, 66/67, pp. 277-284.

Morganstein, M., 1973. Editor. The origin and distribution of manganese nodules in the Pacific and prospects for exploitation. NSF-IDOE Publ.

Morris, H.W., Livens, F.R., Nolan, L. and Hilton, J., 1994. Determination of thorium-234/uranium-238 disequilibrium in freshwater systems. Analyst, 119, pp. 2403-2406.

Mortimer, C.H., 1941. The exchange of dissolved substances between mud and water in lakes. Journal of Ecology, 29, pp. 280-329.

Mortimer, C.H., 1942. The exchange of dissolved substances between mud and water in lakes. Journal of Ecology, 30, pp. 147-201.

Moyes, L., 1996. Personal communication.

Murray, J.W., 1973. The interaction of metal ions at the hydrous manganese dioxide - solution interface. PhD Thesis. MIT-WHOI.

Murray, J.W., 1975a. The interaction of metal ions at the manganese dioxide-solution interface. Geochimica et Cosmochimica Acta, 39, pp. 505-519.

Murray, J.W., 1975b. The interaction of cobalt with hydrous manganese dioxide. Geochimica Cosmochimica Acta, 39, pp. 635-647.

Nishita, H., Kowalewsky, B.W., Steen, A.J. and Larson, K.H., 1956. Fixation and extractability of fission products contaminating various soils and clays, I: Sr-90, Y-91, Ru-106, Cs-137, Ce-144. Soil Science, 81, pp. 317-326.

Nishita, H. and Essington, E.H., 1967. Effect of chelating agents on the movement of fission products in soils. Soil Science, 103, pp. 168-176.

Nyffeler, U.P., Li, Y.H. and Santschi, P.H., 1984. A kinetic approach to describe trace-element distribution between particles and solution in natural aquatic systems. Geochimica et Cosmochimica Acta, 48, pp. 1513-1522.

Ohnuki, T., 1994. Sorption characteristics of strontium on sandy soils and their components. Radiochimica Acta, 64, pp. 237-245.

Olsen, C.R., Lowry, P.D., Lee, S.Y., Larsen, I.L. and Cutshall, N.H., 1986. Geochemical and environmental processes affecting radionuclide migration from a

formerly used seepage trench. Geochimica et Cosmochimica Acta, 50, pp. 593-607.

Pardue, J.H., DeLaune, R.D., Patrick Jr, W.H. and Whitcomb, J.H., 1989. Effect of redox potential on the fixation of Cs-137 in lake sediment. Health Physics, 57, pp. 781-789.

Patel, B., Patel, S. and Pawar, S., 1978. Desorption of radioactivity from nearshore sediment. Estuarine and Coastal Marine Science, 7, pp. 49-58.

Pillai, K.C., Dey, N.N., Mathew, E. and Kothari, B.U., 1975. Behaviour of discharged radionuclides from fuel reprocessing operations in the aquatic environment of Bombay harbour bay. In Impacts of Nuclear Releases into the Aquatic Environment. IAEA, Vienna, STI/PUB/406, pp. 277-300.

Polar, E. and Bayulgen, N., 1991. Differences in the availability of Cs-134, 137 and Ru-106 from a Chernobyl contaminated soil to a water plant, duckweed and to the terrestrial plants, bean and lettuce. Journal of Environmental Radioactivity, 13, pp. 251-259.

Robbins, J.A., Linder, G., Pfeiffer, W., Kleiner, J., Stabel, H.H. and Frenzel, P., 1992. Epilimnetic scavenging of Chernobyl radionuclides in Lake Constance. Geochimica et Cosmochimica Acta, 56, pp. 2339-2361.

Rose, A.W., Hawkes, H.E. and Webb, J.S., 1979. Geochemistry in mineral exploration. 2nd Edition. Academic Press, London.

Santschi, P.H. and Honeyman, B.D., 1989. Radionuclides in aquatic environments. Radiation Physics and Chemistry, 34, pp. 213-240.

Santschi, P.H., Bajo, C., Mantovani, M., Orciuolo, D., Cranston, R.E. and Bruno, J., 1988a. Uranium in pore waters from North Atlantic (GME and Southern Nares Abyssal Plain) sediments. Nature, 331, pp. 155-157.

Santschi, P.H., Bollhalder, S., Farrenkothe, K., Luck, A., Zingg, S and Sturm, M., 1988b. Chernobyl radionuclides in the environment: Tracers for the tight coupling of atmospheric, terrestrial and aquatic geochemical processes. Environmental Science and Technology, 22, pp. 510-516.

Sawhney, B.L., 1969. Caesium uptake by layer silicates: effect on interlayer collapse and cation exchange capacity. Proceedings International Clay Conference, Tokyo, 1, pp. 605-611. Israel Universities Press.

Sawhney, B.L., 1970. Potassium and caesium ion selectivity in relation to clay mineral structure. Clays and Clay Minerals, 18, pp. 47-52.

Sawhney, B.L., 1972. Selective sorption and fixation of cations by clay minerals: a review. Clays and Clay Minerals, 20, pp. 93-100.

Schell, W.R., Sibley, T.H., Sanchez, A. and Clayton, J.R. Jr, 1980. Distribution coefficients for radionuclides in aquatic environments. III. Adsorption and desorption of Ru-106, Cs-137, Am-241, Sr-85 and Pu-237 in marine and freshwater systems.

NUREG/CR-0803, Nuclear Regulatory Commission.

Schulz, R.K., Overstreet, R. and Barshad, I., 1960. On the soil chemistry of Cs-137. Soil Science, 89, pp. 16-27.

Schulz, R.K. and Riedel, H.H., 1960. Effect of aging on the fixation of Sr-90 by soils. Soil Science, 91, pp. 262-264.

Schulz, R.K., 1965. Soil chemistry of radionuclides. Health Physics, 11, pp. 1317-1324.

Sharpe, A.G., 1986. Inorganic Chemistry. 2nd Edition. Longman Scientific and Technical, UK.

Shiao, S.Y., Rafferty, P., Pilleyer, R.E. and Rogers, W.J., 1979. Ion-exchange equilibria between montmorillonite and solutions of moderate to high ionic strength. In: S. Fried (editor), Radioactive Waste in Geologic Storage. American Chemical Society, Symposium Ser., 100, pp. 297-324.

Sholkovitz, E.R. and Copland, D., 1982. The chemistry of suspended matter in Esthwaite Water, a biologically productive lake with seasonally anoxic hypolimnion. Geochimica et Cosmochimica Acta, 46, pp. 393-410.

Sholkovitz, E.R., Cochran, J.K. and Carey, A.E., 1983. Laboratory studies of diagenesis and mobility of Pu-239, 240 and Cs-137 in nearshore sediments. Geochimica et Cosmochimica Acta, 47, pp. 1369-1379.

Singh, O.V. and Tandon, S.N., 1977. Studies on adsorption of caesium and strontium radionuclides on hydrated manganese oxide. International Journal of Applied Radiation and Isotopes, 28, pp. 701-704.

Smith, J.T. and Comans, R.N.J., 1996. Modelling the diffusive transport and remobilisation of Cs-137 in sediments: The effects of sorption kinetics and reversibility. Geochimica et Cosmochimica Acta, 60, pp. 995-1004.

Spalding, B.P. and Cerling, T.E., 1979. Association of radionuclides with stream bed sediments in White Oak Creek watershed. ORNL/TM-6895. Oak Ridge National Laboratory, Oak Ridge, Tennessee.

Staunton, S., 1994. Adsorption of radiocaesium on various soils: interpretation and consequences of the effects of soil:solution ratio and solution composition on the distribution coefficient. European Journal of Soil Science, 45, pp. 409-418.

Tamura, T., 1965. Reactions of Cs-137 and Sr-90 with soil minerals and sequioxides. Transactions of the 8th International Congress of Soil Science, pp. 465-478. Academy of the Republic of Romania, Bucharest, Romania.

Taylor, R.M. and McKenzie, R.M., 1966. The association of trace elements with manganese minerals in Australian soils. Australian Journal of Soil Research, 4, pp. 29-39.

Taylor, R.M., 1968. The association of manganese and cobalt in soil - further observations. Journal of Soil Science, 19, pp. 77-80.

Tessier, A., Campbell, P.G.C. and Bisson, M., 1979. Sequential extraction procedure for the speciation of particulate trace metals. Analytical Chemistry, 51, pp. 844-851.

Tewari, P.H., Campbell, A.B. and Lee, W., 1972. Adsorption of Co^{2+} by oxides from aqueous solution. Canadian Journal of Chemistry, 50, pp. 1642-1648.

Tewari, P.H. and Lee, W., 1975. Adsorption of Co(II) at the oxide-water interface. Journal of Colloid and Interface Science, 52, pp. 77-88.

Tiller, K.G., Honeysett, J.L. and Hallsworth, E.G., 1969. The isotopically exchangeable form of native and applied cobalt in soils. Australian Journal of Soil Research, 7, pp. 43-56.

Torstenfelt, B., Andersson, K. and Allard, B., 1982. Sorption of strontium and caesium on rocks and minerals. Chemical Geology, 36, pp. 123-137.

Valcke, E., 1993. The behaviour dynamics of radiocaesium and radiostrontium in soils rich in organic matter. PhD thesis. K.U. Leuven.

Wauters, J., 1994. Radiocaesium in aquatic sediments: sorption, remobilization and fixation. PhD thesis. K.U. Leuven.

West, J.M., Haigh, D.G., Hooker, P.J. and Rowe, E.J., 1991. Microbial influence on the sorption of Cs-137 onto materials relevant to the geological disposal of radioactive waste. Experimentia, 47, pp. 549-552.

Wiklander, L., 1950. Fixation of potassium by clays saturated with different cations. Soil Science, 69, pp. 261-268.

Wiklander, L., 1964. Uptake, adsorption and leaching of radiostrontium in a lysimeter experiment. Soil Science, 97, pp. 168-172.

APPENDICES

APPENDIX 1 - ADSORPTION DATA					
(1a) Adsorption data for Co-57 BPBP system					
time(hrs)	mass(g)	ac,sol(Bq)	ac,sed(Bq)	Rd(ml/g)	%sorbed
0.5	0.3016	396.957	724.681	181.59058	64.60917
	0.3008	393.935	727.703	184.23537	64.878597
	0.2995	438.012	683.626	156.33528	60.948898
	0.3022	421.945	699.693	164.61844	62.381357
	0.2994	505.819	615.819	121.99089	54.903543
2	0.2975	302.196	819.442	273.4411	73.057618
	0.3	256.205	865.433	337.78927	77.15796
	0.3014	308.649	812.989	262.17894	72.482298
	0.2996	367.685	753.953	205.32782	67.218924
	0.2996	297.13	824.508	277.86114	73.509278
8	0.3022	317.422	804.216	251.51418	71.700139
	0.2997	259.931	861.707	331.84559	76.825767
	0.299	206.096	915.542	445.71657	81.625444
	0.2986	296.344	825.294	279.79761	73.579354
	0.3023	293.309	828.329	280.25966	73.849941
23	0.3	142.717	978.921	685.91759	87.27602
	0.2985	249.455	872.183	351.39237	77.759758
	0.3001	226.527	895.111	395.01372	79.803912
	0.2989	227.302	894.336	394.90515	79.734816
	0.299	208.48	913.158	439.47239	81.412898
44	0.2996	138.314	983.324	711.88517	87.66857
	0.3	177.91	943.728	530.45248	84.138376
	0.3004	176.614	945.024	534.36627	84.253921
	0.3013	155.895	965.743	616.81014	86.101131
	0.2997	201.897	919.741	456.00562	81.999807
120	0.3009	72.754	1048.884	1437.3736	93.513594
	0.2994	79.654	1041.984	1310.7592	92.898422
	0.301	65.031	1056.607	1619.3764	94.20214
	0.2976	88.671	1032.967	1174.3381	92.094508
	0.2999	66.054	1055.584	1598.5951	94.110934
192	0.2998	89.747	1031.891	1150.5447	91.998577
	0.2991	87.111	1034.527	1191.1698	92.233591
	0.2996	75.835	1045.803	1380.8918	93.238906
	0.298	74.642	1046.996	1412.1042	93.345268
	0.2975	71.425	1050.213	1482.7278	93.632081
552	0.3014	30.704	1090.934	3536.564	97.262575
	0.3008	76.468	1045.17	1363.1719	93.182471
	0.2981	63.024	1058.614	1690.4057	94.381075
	0.3003	54.483	1067.155	1956.7368	95.14255
	0.2978	22.31	1099.328	4963.9144	98.010945
720	0.2991	64.67	1056.968	1639.3203	94.234325
	0.2995	28.568	1093.07	3832.5918	97.453011
	0.3025	26.225	1095.413	4142.4595	97.661902
	0.3019	23.493	1098.145	4644.9319	97.905474

	0.2995	19.527	1102.111	5653.4589	98.259064
1176	0.3003	29.02	1092.618	3761.2904	97.412712
	0.2987	34.833	1086.805	3133.6232	96.894453
	0.2986	42.822	1078.816	2531.115	96.182191
	0.2995	24.059	1097.579	4569.6469	97.855012
	0.2983	28.203	1093.435	3899.1116	97.485552
1728	0.2999	28.392	1093.246	3851.8263	97.468702
	0.2998	11.544	1110.094	9622.614	98.970791
	0.302	16.513	1105.125	6648.1335	98.527778
	0.2999	21.111	1100.527	5214.7883	98.117842
	0.2989	13.029	1108.609	8540.0941	98.838395
(1b) Adsorption data for Co-57 BPEW system					
time(hrs)	mass(g)	ac,sol(Bq)	ac,sed(Bq)	Rd(ml/g)	%sorbed
0.5	0.2988	282.555	839.083	298.15534	74.808717
	0.2992	312.13	809.508	260.04308	72.171949
	0.3019	257.916	863.722	332.77741	77.005415
	0.3018	255.394	866.244	337.15652	77.230265
	0.3009	318.321	803.317	251.60585	71.619988
2	0.3018	174.67	946.968	538.91343	84.427239
	0.3025	189.961	931.677	486.40362	83.063965
	0.3005	191.002	930.636	486.42816	82.971155
	0.3019	191.746	929.892	481.90823	82.904823
	0.2985	177.772	943.866	533.60993	84.15068
8	0.3017	171.191	950.447	552.06844	84.737411
	0.3025	194.962	926.676	471.3829	82.6181
	0.2991	210.497	911.141	434.15471	81.233072
	0.2976	269.545	852.093	318.6721	75.968628
	0.3016	265.896	855.742	320.12601	76.293956
23	0.2982	63.474	1058.164	1677.1455	94.340955
	0.2986	189.055	932.583	495.59941	83.14474
	0.299	81.476	1040.162	1280.9181	92.735981
	0.2977	67.552	1054.086	1572.4623	93.97738
	0.298	65.767	1055.871	1616.2473	94.136522
44	0.3007	183.386	938.252	510.43582	83.650162
	0.2995	177.78	943.858	531.79982	84.149966
	0.3	190.427	931.211	489.01206	83.022419
	0.2996	191.873	929.765	485.22009	82.8935
	0.3006	232.59	889.048	381.47532	79.263363
120	0.2999	106.515	1015.123	953.35069	90.503621
	0.3019	99.551	1022.087	1020.2354	91.124498
	0.3001	99.132	1022.506	1031.1154	91.161854
	0.301	107.831	1013.807	937.05787	90.386292
	0.3013	76.782	1044.856	1354.9371	93.154476
192	0.3023	50.38	1071.258	2110.1777	95.508355
	0.3025	57.01	1064.628	1852.0074	94.917255
	0.2992	64.763	1056.875	1636.2751	94.226034
	0.2977	52.629	1069.009	2046.9096	95.307844

	0.3014	94.41	1027.228	1082.996	91.582846
552	0.2989	67.511	1054.127	1567.1614	93.981035
	0.2996	57.15	1064.488	1865.108	94.904773
	0.3009	75.153	1046.485	1388.3078	93.29971
	0.3011	65.317	1056.321	1611.314	94.176642
	0.3017	80.279	1041.359	1289.8656	92.8427
720	0.2988	36.383	1085.255	2994.8422	96.756262
	0.2992	64.899	1056.739	1632.6361	94.213909
	0.3026	73.079	1048.559	1422.5011	93.484618
	0.3019	76.34	1045.298	1360.649	93.193883
	0.3023	55.722	1065.916	1898.3636	95.032087
1176	0.2992	20.619	1101.019	5354.105	98.161706
	0.3005	22.206	1099.432	4942.8202	98.020217
	0.3007	14.572	1107.066	7579.5283	98.700829
	0.2981	15.758	1105.88	7062.6256	98.59509
	0.2985	21.431	1100.207	5159.5151	98.089312
1728	0.3015	17.108	1104.53	6424.0988	98.474731
	0.3001	17.192	1104.446	6422.045	98.467242
	0.3017	16.033	1105.605	6856.9526	98.570573
	0.2995	19.144	1102.494	5768.5675	98.29321
	0.2981	17.567	1104.071	6324.9731	98.433808
(1c) Adsorption data for Co-57 EWBP system					
time (hrs)	mass(g)	ac,sol(Bq)	ac,sed(Bq)	Rd(ml/g)	%sorbed
0.5	0.3014	608.989	512.649	83.789321	45.705388
	0.3014	711.704	409.934	57.331399	36.547799
	0.3012	756.499	365.139	48.074652	32.554086
	0.3012	610.647	510.991	83.346873	45.557568
	0.3007	617.459	504.179	81.46376	44.950242
2	0.2999	359.182	762.456	212.34645	67.977012
	0.2996	417.188	704.45	169.08217	62.805468
	0.298	360.819	760.819	212.27407	67.831065
	0.2994	316.756	804.882	254.6108	71.759516
	0.3015	414.343	707.295	169.85351	63.059115
8	0.2981	375.298	746.34	200.13348	66.540185
	0.3007	342.923	778.715	226.55297	69.426589
	0.2996	361.693	759.945	210.38826	67.753143
	0.2975	352.282	769.356	220.22731	68.592184
	0.2977	373.763	747.875	201.63928	66.677038
23	0.3007	452.676	668.962	147.43541	59.641524
	0.3006	336.15	785.488	233.20546	70.030438
	0.299	325.081	796.557	245.8529	71.017298
	0.2988	285.541	836.097	293.98749	74.542499
	0.3013	215.148	906.49	419.51532	80.81841
44	0.2986	226.638	895	396.75441	79.794016
	0.2998	237.19	884.448	373.13463	78.853249
	0.2998	239.253	882.385	369.05437	78.669321
	0.3001	248.769	872.869	350.75839	77.820919

	0.2992	235.264	886.374	377.76455	79.024962
120	0.3001	141.573	980.065	692.03762	87.378013
	0.298	166.393	955.245	577.94261	85.165178
	0.3018	154.901	966.737	620.37764	86.189751
	0.298	159.097	962.541	609.06303	85.815655
	0.2992	157.08	964.558	615.69712	85.995482
192	0.2981	148.675	972.963	658.59383	86.744832
	0.3017	160.604	961.034	595.01558	85.681298
	0.2998	148.697	972.941	654.74761	86.742871
	0.3004	156.423	965.215	616.23275	86.054057
	0.301	160.324	961.314	597.615	85.706262
552	0.3021	35.96	1085.678	2998.1398	96.793975
	0.302	38.637	1083.001	2784.4522	96.555306
	0.3011	62.672	1058.966	1683.5226	94.412457
	0.2989	51.873	1069.765	2069.8666	95.375246
	0.3009	49.605	1072.033	2154.675	95.57745
720	0.2991	13.5	1108.138	8233.129	98.796403
	0.3021	35.583	1086.055	3030.9571	96.827586
	0.2999	37.193	1084.445	2916.6956	96.684046
	0.2983	36.128	1085.51	3021.7457	96.778996
	0.3017	41.265	1080.373	2603.3815	96.321006
1176	0.2984	89.387	1032.251	1161.0031	92.030673
	0.2997	83.072	1038.566	1251.4513	92.593689
	0.299	88.957	1032.681	1164.7591	92.06901
	0.2988	67.619	1054.019	1565.0217	93.971406
	0.298	9.158	1112.48	12229.158	99.183516
1728	0.2985	48.634	1073.004	2217.3705	95.66402
	0.3015	57.761	1063.877	1832.6969	94.850299
	0.2996	11.95	1109.688	9298.49	98.934594
	0.2983	70.836	1050.802	1491.8833	93.684593
	0.3012	60.402	1061.236	1749.9552	94.61484
(1d) Adsorption data for Co-57 EWEW system					
time(hrs)	mass(g)	ac,sol(Bq)	ac,sed(Bq)	Rd(ml/g)	%sorbed
0.5	0.3014	703.178	418.46	59.233403	37.307937
	0.3009	639.784	481.854	75.089837	42.95985
	0.3014	576.852	544.786	94.00253	48.570573
	0.3002	681.399	440.239	64.565064	39.249651
	0.3007	740.742	380.896	51.30117	33.958907
2	0.3011	531.118	590.52	110.77815	52.648002
	0.3014	412.126	709.512	171.35932	63.256773
	0.3002	422.838	698.8	165.15414	62.301741
	0.2977	526.066	595.572	114.08708	53.098415
	0.301	437.678	683.96	155.75096	60.978676
8	0.2988	641.311	480.327	75.198464	42.82371
	0.299	592.701	528.937	89.540261	47.15755
	0.2987	589.94	531.698	90.519723	47.403708
	0.2997	602.297	519.341	86.313042	46.302015

	0.2998	920.182	201.456	21.907665	17.960875
23	0.2992	751.043	370.595	49.475981	33.040518
	0.3	590.575	531.063	89.923041	47.347094
	0.3011	578.8	542.838	93.444172	48.396898
	0.3017	583.896	537.742	91.576576	47.942563
	0.2997	773.457	348.181	45.061268	31.04219
44	0.2991	214.325	907.313	424.60895	80.891785
	0.2983	289.609	832.029	288.93118	74.179816
	0.2993	245.562	876.076	357.59806	78.10684
	0.3006	213.238	908.4	425.15256	80.988697
	0.3007	223.348	898.29	401.25672	80.087337
120	0.2996	357.144	764.494	214.34343	68.158711
	0.3024	251.312	870.326	343.56443	77.594197
	0.2987	347.841	773.797	223.42528	68.988123
	0.2993	280.143	841.495	301.08305	75.02376
	0.2984	298.712	822.926	276.96861	73.368235
192	0.3011	214.384	907.254	421.64506	80.886525
	0.2993	309.049	812.589	263.54703	72.446636
	0.2996	331.828	789.81	238.33567	70.415767
	0.3005	291.849	829.789	283.84826	73.980108
	0.2988	314.258	807.38	257.94808	71.982226
552	0.2998	149.195	972.443	652.22811	86.698471
	0.298	118.957	1002.681	848.55066	89.39435
	0.2992	113.527	1008.111	890.36659	89.878463
	0.3011	166.978	954.66	569.63933	85.113022
	0.3025	197.965	923.673	462.72793	82.350366
720	0.2999	128.034	993.604	776.30576	88.585087
	0.2986	129.914	991.724	766.94871	88.417475
	0.3006	181.627	940.011	516.51722	83.806986
	0.3011	141.312	980.326	691.19721	87.401283
	0.3005	166.668	954.97	572.02404	85.14066
1176	0.2995	986.363	135.275	13.737421	12.060487
	0.3018	764.311	357.327	46.472683	31.857605
	0.2997	670.344	451.294	67.390138	40.235263
	0.3022	795.148	326.49	40.761364	29.108322
	0.2998	769.582	352.056	45.77691	31.387667
1728	0.3009	513.787	607.851	117.95411	54.193153
	0.3022	586.005	535.633	90.738751	47.754534
	0.3009	451.047	670.591	148.22962	59.786758
	0.3003	593.777	527.861	88.810053	47.061619
	0.3002	582.338	539.3	92.547748	48.081467
(2a) Adsorption data for Sr-85 BPBP system					
time(hrs)	mass(g)	ac,sol(Bq)	ac,sed(Bq)	Rd(ml/g)	%sorbed
0.5	0.3016	436.443	547.565	124.79525	55.646397
	0.3008	446.574	537.434	120.02594	54.616832
	0.2995	472.736	511.272	108.33225	51.958114

	0.3022	428.806	555.202	128.53369	56.422509
	0.2994	402.287	581.721	144.89327	59.117507
2	0.2975	418.637	565.371	136.18529	57.455935
	0.3	412.157	571.851	138.74591	58.114467
	0.3014	399.418	584.59	145.68061	59.40907
	0.2996	405.597	578.411	142.79771	58.781128
	0.2996	407.754	576.254	141.51262	58.561922
8	0.3022	601.82	382.188	63.043051	38.839928
	0.2997	502.894	481.114	95.764832	48.893302
	0.299	89.398	894.61	1004.0516	90.914911
	0.2986	529.037	454.971	86.403059	46.236514
	0.3023	544.784	439.224	80.010102	44.636222
23	0.3	506.846	477.162	94.143389	48.491679
	0.2985	499.942	484.066	97.310987	49.193299
	0.3001	83.964	900.044	1071.5832	91.467143
	0.2989	488.136	495.872	101.95865	50.393086
	0.299	501.866	482.142	96.391171	48.997772
44	0.2996	305.969	678.039	221.89969	68.905842
	0.3	312.333	671.675	215.05092	68.2591
	0.3004	308.656	675.352	218.51276	68.632775
	0.3013	310.98	673.028	215.48785	68.396598
	0.2997	308.209	675.799	219.48596	68.678202
120	0.3009	288.04	695.968	240.8993	70.72788
	0.2994	290.187	693.821	239.57359	70.509691
	0.301	272.647	711.361	260.04235	72.292197
	0.2976	320.975	663.033	208.2343	67.380855
	0.2999	279.829	704.179	251.73009	71.562325
192	0.2998	310.956	673.052	216.59045	68.399037
	0.2991	299.721	684.287	228.99498	69.540796
	0.2996	298.118	685.89	230.3805	69.703702
	0.298	313.139	670.869	215.67785	68.17719
	0.2975	311.302	672.706	217.91026	68.363875
552	0.3014	409.43	574.578	139.68422	58.391598
	0.3008	400.496	583.512	145.30984	59.299518
	0.2981	421.017	562.991	134.57398	57.214067
	0.3003	416.633	567.375	136.04496	57.659592
	0.2978	391.952	592.056	152.1691	60.167804
720	0.2991	408.032	575.976	141.58427	58.53367
	0.2995	417.475	566.533	135.9312	57.574024
	0.3025	422.855	561.153	131.60903	57.02728
	0.3019	406.729	577.279	141.03885	58.666088
	0.2995	431.354	552.654	128.33465	56.163568
1176	0.3003	476.505	507.503	106.39888	51.575089
	0.2987	86.226	897.782	1045.7279	91.237266
	0.2986	498.728	485.28	97.759752	49.316672
	0.2995	482.953	501.055	103.92139	50.91981
	0.2983	88.704	895.304	1015.0684	90.985439
1728	0.2999	393.984	590.024	149.8083	59.961301

	0.2998	379.473	604.535	159.41537	61.435984
	0.302	387.929	596.079	152.63913	60.576642
	0.2999	397.419	586.589	147.64885	59.612219
	0.2989	376.581	607.427	161.8941	61.729884
(2b) Adsorption data for Sr-85 BPEW system					
time(hrs)	mass(g)	ac,sol(Bq)	ac,sed(Bq)	Rd(ml/g)	%sorbed
0.5	0.2988	306.033	677.975	222.42627	68.899338
	0.2992	323.539	660.469	204.68474	67.120288
	0.3019	340.392	643.616	187.89085	65.407598
	0.3018	320.731	663.277	205.56824	67.405651
	0.3009	359.841	624.167	172.93752	63.43109
2	0.3018	283.177	700.831	246.0126	71.222084
	0.3025	316.995	667.013	208.67853	67.785323
	0.3005	347.334	636.674	182.99811	64.702116
	0.3019	290.892	693.116	236.77306	70.438045
	0.2985	249.969	734.039	295.12765	74.596853
8	0.3017	445.843	538.165	120.02714	54.69112
	0.3025	452.034	531.974	116.71191	54.061959
	0.2991	474.848	509.16	107.54854	51.743482
	0.2976	432.866	551.142	128.35074	56.00991
	0.3016	438.833	545.175	123.57385	55.403513
23	0.2982	365.606	618.402	170.16537	62.845221
	0.2986	419.481	564.527	135.20846	57.370164
	0.299	387.554	596.454	154.41689	60.614751
	0.2977	388.534	595.474	154.44583	60.515158
	0.298	364.239	619.769	171.29646	62.984142
44	0.3007	203.145	780.863	383.4922	79.355351
	0.2995	200.118	783.89	392.36784	79.66297
	0.3	200.416	783.592	390.98276	79.632686
	0.2996	218.226	765.782	351.38086	77.822741
	0.3006	223.03	760.978	340.5188	77.334534
120	0.2999	188.307	795.701	422.69609	80.863265
	0.3019	191.308	792.7	411.75025	80.558288
	0.3001	189.141	794.867	420.11099	80.77851
	0.301	184.849	799.159	430.8944	81.214685
	0.3013	177.832	806.176	451.37975	81.927789
192	0.3023	234.238	749.77	317.65362	76.195519
	0.3025	227.813	756.195	329.19344	76.848461
	0.2992	232.643	751.365	323.83265	76.357611
	0.2977	219.611	764.397	350.75777	77.68199
	0.3014	225.524	758.484	334.75854	77.081081
552	0.2989	345.464	638.544	185.51685	64.892155
	0.2996	353.362	630.646	178.70852	64.08952
	0.3009	336.651	647.357	191.71805	65.787778
	0.3011	341.965	642.043	187.06518	65.247742
	0.3017	341.173	642.835	187.35738	65.328229
720	0.2988	369.68	614.328	166.8457	62.4312

	0.2992	352.211	631.797	179.85988	64.20649
	0.3026	354.043	629.965	176.40575	64.020313
	0.3019	361.534	622.474	171.0922	63.259039
	0.3023	366.08	617.928	167.51164	62.79705
1176	0.2992	445.627	538.381	121.1373	54.713071
	0.3005	463.127	520.881	112.28331	52.934631
	0.3007	454.976	529.032	116.00622	53.762978
	0.2981	458.214	525.794	115.47994	53.433915
	0.2985	458.944	525.064	114.9819	53.359729
1728	0.3015	348.059	635.949	181.80397	64.628438
	0.3001	354.667	629.341	177.38648	63.956899
	0.3017	357.32	626.688	174.3974	63.687287
	0.2995	342.885	641.123	187.29117	65.154247
	0.2981	345.621	638.387	185.88451	64.8762
(2c) Adsorption data for Sr-85 EWBP system					
time(hrs)	mass(g)	ac,sol(Bq)	ac,sed(Bq)	Rd(ml/g)	%sorbed
0.5	0.3014	547.245	436.763	79.440514	44.386123
	0.3014	586.58	397.428	67.438704	40.388696
	0.3012	584.101	399.907	68.192615	40.640625
	0.3012	530.528	453.48	85.136563	46.084991
	0.3007	537.604	446.404	82.842541	45.365891
2	0.2999	474.605	509.403	107.36778	51.768177
	0.2996	517.701	466.307	90.192905	47.388537
	0.298	472.854	511.154	108.82525	51.946122
	0.2994	436.191	547.817	125.84277	55.672007
	0.3015	499.448	484.56	96.536427	49.243502
8	0.2981	114.975	869.033	760.66271	88.315644
	0.3007	106.828	877.18	819.20284	89.143584
	0.2996	107.734	876.274	814.45405	89.051512
	0.2975	109.281	874.727	807.16469	88.894298
	0.2977	109.217	874.791	807.15415	88.900802
23	0.3007	111.069	872.939	784.11337	88.712592
	0.3006	99.077	884.931	891.39222	89.931281
	0.299	95.408	888.6	934.48338	90.304144
	0.2988	93.94	890.068	951.29079	90.45333
	0.3013	95.921	888.087	921.85781	90.25201
44	0.2986	342.456	641.552	188.21686	65.197844
	0.2998	346.695	637.313	183.9479	64.767055
	0.2998	341.225	642.783	188.50079	65.322945
	0.3001	336.308	647.7	192.52714	65.822636
	0.2992	335.595	648.413	193.72956	65.895094
120	0.3001	292.414	691.594	236.43312	70.283372
	0.298	305.382	678.626	223.71343	68.965496
	0.3018	293.747	690.261	233.58337	70.147905
	0.298	293.187	690.821	237.20608	70.204815
	0.2992	287.96	696.048	242.36321	70.73601
192	0.2981	337.989	646.019	192.35435	65.651804

	0.3017	326.071	657.937	200.64026	66.862973
	0.2998	335.109	648.899	193.76737	65.944484
	0.3004	345.071	638.937	184.91447	64.932094
	0.301	334.652	649.356	193.39453	65.990927
552	0.3021	266.056	717.952	267.97414	72.962008
	0.302	259.39	724.618	277.50461	73.639442
	0.3011	253.727	730.281	286.77007	74.214945
	0.2989	264.11	719.898	273.57818	73.159771
	0.3009	253.936	730.072	286.64244	74.193706
720	0.2991	422.484	561.524	133.31005	57.064983
	0.3021	424.976	559.032	130.62996	56.811733
	0.2999	419.271	564.737	134.7399	57.391505
	0.2983	423.568	560.44	133.06811	56.954822
	0.3017	422.776	561.232	132.00125	57.035309
1176	0.2984	93.26	890.748	960.24462	90.522435
	0.2997	95.968	888.04	926.27639	90.247234
	0.299	90.339	893.669	992.54791	90.819282
	0.2988	88.169	895.839	1020.1281	91.039809
	0.298	94.315	889.693	949.6518	90.41522
1728	0.2985	456.841	527.167	115.97385	53.573447
	0.3015	421.174	562.834	132.96971	57.198112
	0.2996	448.314	535.694	119.65034	54.440005
	0.2983	451.429	532.579	118.64859	54.123442
	0.3012	420.976	563.032	133.2116	57.218234
(2d) Adsorption data for Sr-85 EWEW system					
time(hrs)	mass(g)	ac,sol(Bq)	ac,sed(Bq)	Rd(ml/g)	%sorbed
0.5	0.3014	420.467	563.541	133.40485	57.269961
	0.3009	389.826	594.182	151.96646	60.383859
	0.3014	358.575	625.433	173.61162	63.559747
	0.3002	410.072	573.936	139.86657	58.326355
	0.3007	426.019	557.989	130.67259	56.705738
2	0.3011	416.308	567.7	135.8672	57.69262
	0.3014	340.68	643.328	187.9593	65.37833
	0.3002	341.619	642.389	187.91725	65.282904
	0.2977	395.804	588.204	149.75806	59.776343
	0.301	359.709	624.299	172.98008	63.444505
8	0.2988	599.162	384.846	64.488664	39.110048
	0.299	557.789	426.219	76.667787	43.314587
	0.2987	553.141	430.867	78.233618	43.786941
	0.2997	563.881	420.127	74.580904	42.695486
	0.2998	761.441	222.567	29.24921	22.618414
23	0.2992	617.429	366.579	59.530595	37.253661
	0.3	526.618	457.39	86.854228	46.482346
	0.3011	517.097	466.911	89.964793	47.449919
	0.3017	521.748	462.26	88.099099	46.97726
	0.2997	633.851	350.157	55.298092	35.584772
44	0.2991	195.869	788.139	403.59145	80.094776

	0.2983	235.334	748.674	319.94555	76.084138
	0.2993	207.766	776.242	374.48739	78.885741
	0.3006	183.471	800.537	435.45799	81.354725
	0.3007	191.764	792.244	412.17316	80.511947
120	0.2996	201.344	782.664	389.23879	79.538378
	0.3024	191.843	792.165	409.64642	80.503919
	0.2987	193.197	790.811	411.1103	80.366318
	0.2993	187.829	796.179	424.8764	80.911842
	0.2984	188.717	795.291	423.67953	80.821599
192	0.3011	227.085	756.923	332.10373	76.922444
	0.2993	219.719	764.289	348.66193	77.671015
	0.2996	231.706	752.302	325.11303	76.452834
	0.3005	224.798	759.21	337.16793	77.154861
	0.2988	239.561	744.447	312.00268	75.654568
552	0.2998	332.301	651.707	196.25032	66.229848
	0.298	311.262	672.746	217.58553	68.36794
	0.2992	291.21	692.798	238.53934	70.405728
	0.3011	289.539	694.469	238.9771	70.575544
	0.3025	307.021	676.987	218.67953	68.798933
720	0.2999	348.904	635.104	182.08899	64.542565
	0.2986	332.993	651.015	196.42074	66.159523
	0.3006	361.131	622.877	172.13525	63.299993
	0.3011	347.223	636.785	182.72368	64.713397
	0.3005	372.856	611.152	163.63827	62.108438
1176	0.2995	665.307	318.701	47.982819	32.38805
	0.3018	594.326	389.682	65.17599	39.601507
	0.2997	540.243	443.765	82.223964	45.097702
	0.3022	868.368	115.64	13.219988	11.751937
	0.2998	747.728	236.28	31.620807	24.012
1728	0.3009	575.939	408.069	70.640893	41.47009
	0.3022	624.445	359.563	57.162024	36.540658
	0.3009	570.699	413.309	72.204924	42.002606
	0.3003	618.338	365.67	59.078481	37.161283
	0.3002	623.349	360.659	57.819732	36.652039
(3a) Adsorption data for Ru-103 BPBP system					
time(hrs)	mass(g)	ac,sol(Bq)	ac,sed(Bq)	Rd(ml/g)	%sorbed
0.5	0.3016	511.08	599.937	116.76339	53.998904
	0.3008	499.881	611.136	121.93115	55.006899
	0.2995	698.065	412.952	59.255428	37.168828
	0.3022	356.201	754.816	210.36465	67.939194
	0.2994	300.31	810.707	270.49771	72.969811
2	0.2975	136.782	974.235	718.23913	87.688577
	0.3	132.548	978.469	738.19975	88.06967
	0.3014	147.374	963.643	650.83861	86.735216
	0.2996	46.137	1064.88	2311.164	95.847318
	0.2996	51.449	1059.568	2062.2027	95.369198

8	0.3022	154.506	956.511	614.57008	86.093282
	0.2997	89.525	1021.492	1142.1553	91.942067
	0.299	37.38	1073.637	2881.8292	96.635515
	0.2986	106.023	1004.994	952.34615	90.457122
	0.3023	107.096	1003.921	930.27081	90.360544
23	0.3	66.644	1044.373	1567.0923	94.001532
	0.2985	48.48	1062.537	2202.7153	95.63643
	0.3001	16.442	1094.575	6654.9706	98.520095
	0.2989	38.926	1072.091	2764.313	96.496363
	0.299	34.712	1076.305	3111.0414	96.875655
44	0.2996	163.362	947.655	580.86962	85.296175
	0.3	177.459	933.558	526.06968	84.027337
	0.3004	185.24	925.777	499.10617	83.326988
	0.3013	165.484	945.533	568.909	85.105178
	0.2997	179.102	931.915	520.84725	83.879455
120	0.3009	71.546	1039.471	1448.5253	93.560315
	0.2994	77.502	1033.515	1336.2057	93.024229
	0.301	63.28	1047.737	1650.2151	94.304318
	0.2976	81.476	1029.541	1273.803	92.666539
	0.2999	95.007	1016.01	1069.762	91.448646
192	0.2998	82.138	1028.879	1253.4581	92.606954
	0.2991	49.382	1061.635	2156.311	95.555244
	0.2996	63.517	1047.5	1651.3666	94.282986
	0.298	71.872	1039.145	1455.5308	93.530972
	0.2975	66.052	1044.965	1595.3283	94.054816
552	0.3014	45.094	1065.923	2352.8004	95.941196
	0.3008	41.796	1069.221	2551.3861	96.238041
	0.2981	35.134	1075.883	3081.7452	96.837672
	0.3003	38.687	1072.33	2769.0406	96.517875
	0.2978	38.069	1072.948	2839.2509	96.5735
720	0.2991	31.792	1079.225	3404.8579	97.138478
	0.2995	33.029	1077.988	3269.2108	97.027138
	0.3025	34.523	1076.494	3092.4235	96.892667
	0.3019	31.447	1079.57	3411.3771	97.16953
	0.2995	29.835	1081.182	3629.9212	97.314623
1176	0.3003	40.275	1070.742	2655.9214	96.374943
	0.2987	20.748	1090.269	5277.6849	98.132522
	0.2986	47.754	1063.263	2236.9815	95.701776
	0.2995	42.25	1068.767	2533.8491	96.197178
	0.2983	25.528	1085.489	4276.3834	97.702285
1728	0.2999	32.228	1078.789	3348.4818	97.099234
	0.2998	24.431	1086.586	4450.5377	97.801024
	0.302	26.787	1084.23	4020.7924	97.588966
	0.2999	24.982	1086.035	4348.7196	97.75143
	0.2989	23.521	1087.496	4640.5262	97.882931
(3b) Adsorption data for Ru-103 BPEW system					
time(hrs)	mass(g)	ac,sol(Bq)	ac,sed(Bq)	Rd(ml/g)	%sorbed

0.5	0.2988	60.198	1050.819	1752.615	94.581721
	0.2992	133.642	977.375	733.29365	87.971201
	0.3019	315.548	795.469	250.50475	71.598274
	0.3018	344.247	766.77	221.40987	69.015146
	0.3009	368.487	742.53	200.90507	66.833361
2	0.3018	111.164	999.853	894.07512	89.994393
	0.3025	111.168	999.849	891.97052	89.994032
	0.3005	96.171	1014.846	1053.4958	91.343877
	0.3019	108.67	1002.347	916.57197	90.218872
	0.2985	93.247	1017.77	1096.9623	91.607059
8	0.3017	67.918	1043.099	1527.1672	93.886862
	0.3025	88.627	1022.39	1144.0537	92.022894
	0.2991	91.888	1019.129	1112.4364	91.729379
	0.2976	115.386	995.631	869.82847	89.61438
	0.3016	84.52	1026.497	1208.0589	92.392556
23	0.2982	56.301	1054.716	1884.6601	94.932481
	0.2986	57.181	1053.836	1851.6237	94.853274
	0.299	48.769	1062.248	2185.406	95.610418
	0.2977	50.897	1060.12	2098.9653	95.418882
	0.298	46.851	1064.166	2286.6279	95.783053
44	0.3007	161.281	949.736	587.49952	85.48348
	0.2995	139.423	971.594	698.03119	87.450867
	0.3	163.758	947.259	578.45052	85.260532
	0.2996	151.81	959.207	632.69063	86.335943
	0.3006	172.787	938.23	541.9142	84.447853
120	0.2999	80.984	1030.033	1272.321	92.710823
	0.3019	90.113	1020.904	1125.7854	91.889143
	0.3001	78.427	1032.59	1316.1869	92.940972
	0.301	75.648	1035.369	1364.1197	93.191103
	0.3013	68.928	1042.089	1505.3284	93.795955
192	0.3023	36.182	1074.835	2948.033	96.743344
	0.3025	53.233	1057.784	1970.661	95.208624
	0.2992	47.186	1063.831	2260.5762	95.7529
	0.2977	43.816	1067.201	2454.4598	96.056226
	0.3014	52.043	1058.974	2025.3542	95.315733
552	0.2989	61.936	1049.081	1700.0481	94.425288
	0.2996	54.594	1056.423	1937.6368	95.086124
	0.3009	82.64	1028.377	1240.6838	92.56177
	0.3011	55.056	1055.961	1910.9694	95.04454
	0.3017	73.192	1037.825	1409.9589	93.412162
720	0.2988	46.599	1064.418	2293.3813	95.805735
	0.2992	45.544	1065.473	2345.6918	95.900693
	0.3026	42.123	1068.894	2515.7511	96.208609
	0.3019	45.504	1065.513	2326.8443	95.904293
	0.3023	44.627	1066.39	2371.3818	95.98323
1176	0.2992	32.351	1078.666	3343.1737	97.088163
	0.3005	31.821	1079.196	3385.8154	97.135867
	0.3007	41.251	1069.766	2587.2723	96.287096

	0.2981	27.393	1083.624	3981.0561	97.534421
	0.2985	32.593	1078.424	3325.3865	97.066382
1728	0.3015	48.703	1062.314	2170.3568	95.616359
	0.3001	48.407	1062.61	2194.4262	95.643001
	0.3017	49.094	1061.923	2150.8521	95.581166
	0.2995	50.025	1060.992	2124.4643	95.497369
	0.2981	51.329	1059.688	2077.6601	95.379999
(3c) Adsorption data for Ru-103 EWBP system					
time(hrs)	mass(g)	ac,sol(Bq)	ac,sed(Bq)	Rd(ml/g)	%sorbed
0.5	0.3014	370.083	740.934	199.27756	66.689709
	0.3014	485.483	625.534	128.24927	56.302829
	0.3012	391.782	719.235	182.84901	64.736633
	0.3012	420.965	690.052	163.26839	62.109941
	0.3007	437.728	673.289	153.4564	60.601143
2	0.2999	149.372	961.645	644.00668	86.555381
	0.2996	249.672	861.345	345.45123	77.527617
	0.298	208.597	902.42	435.51753	81.22468
	0.2994	190.998	920.019	482.6557	82.808724
	0.3015	265.98	845.037	316.12634	76.059772
8	0.2981	50.358	1060.659	2119.6619	95.467396
	0.3007	50.298	1060.719	2103.9599	95.472797
	0.2996	56.813	1054.204	1858.0457	94.886397
	0.2975	63.969	1047.048	1650.56	94.242302
	0.2977	60.909	1050.108	1737.3804	94.517726
23	0.3007	47.591	1063.426	2229.309	95.716447
	0.3006	45.62	1065.397	2330.7112	95.893852
	0.299	40.715	1070.302	2637.5577	96.33534
	0.2988	37.617	1073.4	2864.9569	96.614183
	0.3013	29.915	1081.102	3598.32	97.307422
44	0.2986	225.905	885.112	393.64418	79.666828
	0.2998	232.704	878.313	377.68965	79.054866
	0.2998	234.073	876.944	374.89545	78.931646
	0.3001	222.372	888.645	399.48774	79.984825
	0.2992	218.817	892.2	408.82818	80.304802
120	0.3001	101.858	1009.159	990.42071	90.832003
	0.298	117.866	993.151	848.26535	89.391161
	0.3018	131.859	979.158	738.15067	88.131685
	0.298	128.16	982.857	772.04538	88.464623
	0.2992	120.081	990.936	827.42945	89.191795
192	0.2981	101.61	1009.407	999.74477	90.854325
	0.3017	100.019	1010.998	1005.1103	90.997527
	0.2998	99.393	1011.624	1018.481	91.053872
	0.3004	81.095	1029.922	1268.328	92.700832
	0.301	90.099	1020.918	1129.3424	91.890403
552	0.3021	64.604	1046.413	1608.4747	94.185147
	0.302	55.904	1055.113	1874.8667	94.968214
	0.3011	76.715	1034.302	1343.3141	93.095065

	0.2989	58.986	1052.031	1790.0903	94.69081
	0.3009	71.806	1039.211	1442.9194	93.536913
720	0.2991	48.943	1062.074	2176.5519	95.594757
	0.3021	52.191	1058.826	2014.6495	95.302412
	0.2999	56.407	1054.61	1870.2673	94.92294
	0.2983	52.637	1058.38	2022.1739	95.262269
	0.3017	56.42	1054.597	1858.6576	94.92177
1176	0.2984	21.531	1089.486	5087.2126	98.062046
	0.2997	16.955	1094.062	6459.1988	98.473921
	0.299	22.552	1088.465	4842.6098	97.970148
	0.2988	19.671	1091.346	5570.2756	98.22946
	0.298	17.313	1093.704	6359.639	98.441698
1728	0.2985	40.891	1070.126	2630.1717	96.319498
	0.3015	38.095	1072.922	2802.4257	96.57116
	0.2996	38.139	1072.878	2816.829	96.567199
	0.2983	45.559	1065.458	2351.9612	95.899343
	0.3012	35.035	1075.982	3058.9274	96.846583
(3d) Adsorption data for Ru-103 EWEW system					
time(hrs)	mass(g)	ac,sol(Bq)	ac,sed(Bq)	Rd (ml/g)	%sorbed
0.5	0.3014	415.635	695.382	166.5288	62.589681
	0.3009	332.155	778.862	233.78615	70.103518
	0.3014	369.199	741.818	199.99303	66.769275
	0.3002	403.695	707.322	175.09525	63.664372
	0.3007	444.122	666.895	149.81076	60.025634
2	0.3011	214.456	896.561	416.53562	80.697325
	0.3014	196.863	914.154	462.20354	82.280829
	0.3002	195.087	915.93	469.18543	82.440683
	0.2977	206.828	904.189	440.54706	81.383903
	0.301	217.265	893.752	409.99826	80.444494
8	0.2988	305.146	805.871	265.1542	72.534534
	0.299	303.661	807.356	266.76333	72.668195
	0.2987	312.256	798.761	256.91656	71.894579
	0.2997	292.893	818.124	279.60482	73.637397
	0.2998	1006.211	104.806	10.422855	9.433339
23	0.2992	242.529	868.488	359.05403	78.170541
	0.3	205.651	905.366	440.24391	81.489842
	0.3011	208.493	902.524	431.29833	81.234041
	0.3017	184.246	926.771	500.17308	83.416455
	0.2997	233.518	877.499	376.14975	78.9816
44	0.2991	147.397	963.62	655.72539	86.733146
	0.2983	228.566	882.451	388.28175	79.427317
	0.2993	205.307	905.71	442.18086	81.520805
	0.3006	175.216	935.801	533.01818	84.229224
	0.3007	173.482	937.535	539.16401	84.385297
120	0.2996	93.392	1017.625	1091.0824	91.594008
	0.3024	95.317	1015.7	1057.145	91.420743
	0.2987	99.248	1011.769	1023.8719	91.066923

	0.2993	79.16	1031.857	1306.5567	92.874997
	0.2984	84.82	1026.197	1216.3398	92.365553
192	0.3011	90.557	1020.46	1122.7536	91.84918
	0.2993	107.27	1003.747	937.9086	90.344882
	0.2996	131.458	979.559	746.14464	88.167778
	0.3005	118.894	992.123	833.07165	89.298634
	0.2988	121.026	989.991	821.28375	89.106737
552	0.2998	47.266	1063.751	2252.0641	95.7457
	0.298	44.825	1066.192	2394.5291	95.965408
	0.2992	44.697	1066.32	2392.0422	95.976929
	0.3011	58.311	1052.706	1798.7347	94.751565
	0.3025	82.679	1028.338	1233.4926	92.55826
720	0.2999	33.749	1077.268	3193.0641	96.962333
	0.2986	42.669	1068.348	2515.5429	96.159465
	0.3006	49.191	1061.826	2154.2693	95.572435
	0.3011	43.427	1067.59	2449.3744	96.091239
	0.3005	34.214	1076.803	3142.0217	96.920479
1176	0.2995	59.293	1051.724	1776.7355	94.663178
	0.3018	78.05	1032.967	1315.5748	92.974905
	0.2997	67.266	1043.751	1553.2302	93.945547
	0.3022	55.264	1055.753	1896.4736	95.025819
	0.2998	67.726	1043.291	1541.4863	93.904144
1728	0.3009	25.744	1085.273	4203.0256	97.682844
	0.3022	23.995	1087.022	4497.2225	97.840267
	0.3009	20.136	1090.881	5401.3615	98.187606
	0.3003	24.423	1086.594	4444.6157	97.801744
	0.3002	28.552	1082.465	3788.6797	97.430102
(4a) Adsorption data for Cs-134 BPBP system					
time(hrs)	mass(g)	ac,sol(Bq)	ac,sed(Bq)	Rd(ml/g)	%sorbed
0.5	0.3016	584.507	7517.587	1279.3185	92.785729
	0.3008	529.529	7572.565	1426.2534	93.464295
	0.2995	626.382	7475.712	1195.4674	92.268888
	0.3022	408.703	7693.391	1868.6879	94.955588
	0.2994	416.442	7685.652	1849.2501	94.86007
2	0.2975	543.674	7558.42	1401.9313	93.28971
	0.3	484.664	7617.43	1571.693	94.01804
	0.3014	507.296	7594.798	1490.1596	93.738705
	0.2996	559.274	7542.82	1350.4813	93.097167
	0.2996	579.339	7522.755	1300.2402	92.849515
8	0.3022	512.68	7589.414	1469.5645	93.672253
	0.2997	293.709	7808.385	2661.2059	96.3749
	0.299	319.531	7782.563	2443.7665	96.056192
	0.2986	392.963	7709.131	1970.9936	95.149859
	0.3023	320.221	7781.873	2411.6675	96.047676
23	0.3	311.406	7790.688	2501.7784	96.156475
	0.2985	375.155	7726.939	2070.0158	95.369654

	0.3001	352.089	7750.005	2200.416	95.654346
	0.2989	306.723	7795.371	2550.8551	96.214275
	0.299	310.152	7791.942	2520.7002	96.171953
44	0.2996	196.536	7905.558	4027.8182	97.574257
	0.3	223.782	7878.312	3520.5298	97.237973
	0.3004	210.947	7891.147	3735.8386	97.396389
	0.3013	210.911	7891.183	3725.3322	97.396833
	0.2997	227.761	7874.333	3460.7396	97.188863
120	0.3009	216.423	7885.671	3632.7399	97.328802
	0.2994	226.476	7875.618	3484.4314	97.204723
	0.301	188.223	7913.871	4190.5501	97.67686
	0.2976	194.667	7907.427	4094.7857	97.597325
	0.2999	234.39	7867.704	3357.7915	97.107044
192	0.2998	221.582	7880.512	3558.8492	97.265127
	0.2991	184.634	7917.46	4301.0951	97.721157
	0.2996	203.155	7898.939	3893.3253	97.492562
	0.298	214.355	7887.739	3704.4514	97.354326
	0.2975	193.723	7908.371	4116.6139	97.608976
552	0.3014	112.211	7989.883	7087.3355	98.615037
	0.3008	130.158	7971.936	6108.5251	98.393526
	0.2981	91.956	8010.138	8766.3581	98.865034
	0.3003	147.841	7954.253	5374.9005	98.175274
	0.2978	39.86	8062.234	20375.8	99.508028
720	0.2991	24.204	8077.89	33474.618	99.701262
	0.2995	20.344	8081.75	39791.792	99.748904
	0.3025	42.435	8059.659	18835.985	99.476247
	0.3019	33.87	8068.224	23671.234	99.58196
	0.2995	29.098	8072.996	27790.479	99.640858
1176	0.3003	45.157	8056.937	17824.231	99.44265
	0.2987	88.096	8013.998	9136.4835	98.912676
	0.2986	43.981	8058.113	18407.708	99.457165
	0.2995	40.642	8061.452	19868.388	99.498377
	0.2983	92.646	8009.448	8694.486	98.856518
1728	0.2999	29.39	8072.704	27476.678	99.637254
	0.2998	16.986	8085.108	47630.411	99.79035
	0.302	18.674	8083.42	43000.361	99.769516
	0.2999	36.68	8065.414	21995.92	99.547278
	0.2989	15.441	8086.653	52564.038	99.80942
(4b) Adsorption data for Cs-134 BPEW system					
time(hrs)	mass(g)	ac,sol(Bq)	ac,sed(Bq)	Rd(ml/g)	%sorbed
0.5	0.2988	270.407	7831.687	2907.8905	96.662505
	0.2992	320.82	7781.274	2431.9181	96.040283
	0.3019	274.788	7827.306	2830.5621	96.608432
	0.3018	331.461	7770.633	2330.3759	95.908947
	0.3009	407.133	7694.961	1884.383	94.974966
2	0.3018	391.519	7710.575	1957.654	95.167681
	0.3025	350.527	7751.567	2193.1276	95.673625

	0.3005	356.805	7745.289	2167.1226	95.596138
	0.3019	334.654	7767.44	2306.4287	95.869537
	0.2985	231.923	7870.171	3410.4938	97.137493
8	0.3017	196.513	7905.581	4000.2621	97.574541
	0.3025	254.011	7848.083	3064.1283	96.864872
	0.2991	311.123	7790.971	2511.68	96.159968
	0.2976	313.066	7789.028	2508.0471	96.135987
	0.3016	229.316	7872.778	3414.9438	97.16967
23	0.2982	241.17	7860.924	3279.17	97.023362
	0.2986	254.901	7847.193	3092.9596	96.853887
	0.299	234.841	7867.253	3361.238	97.101478
	0.2977	217.535	7884.559	3652.5039	97.315077
	0.298	184.839	7917.255	4312.0721	97.718627
44	0.3007	129.119	7972.975	6160.53	98.40635
	0.2995	129.579	7972.515	6162.9004	98.400673
	0.3	122.632	7979.462	6506.8351	98.486416
	0.2996	169.166	7932.928	4695.695	97.912071
	0.3006	132.649	7969.445	5995.9275	98.362781
120	0.2999	120.15	7981.944	6645.531	98.51705
	0.3019	132.398	7969.696	5981.6152	98.365879
	0.3001	128.66	7973.434	6195.2255	98.412015
	0.301	144.754	7957.34	5478.8839	98.213375
	0.3013	110.546	7991.548	7197.9695	98.635587
192	0.3023	118.232	7983.862	6701.3314	98.540723
	0.3025	128.401	7973.693	6158.6707	98.415212
	0.2992	135.494	7966.6	5895.391	98.327667
	0.2977	131.255	7970.839	6119.7066	98.379987
	0.3014	132.498	7969.596	5986.9412	98.364645
552	0.2989	57.984	8044.11	13924.037	99.284333
	0.2996	15.772	8086.322	51338.563	99.805334
	0.3009	51.213	8050.881	15673.365	99.367904
	0.3011	25.603	8076.491	31429.853	99.683995
	0.3017	46.336	8055.758	17287.565	99.428098
720	0.2988	20.92	8081.174	38784.075	99.741795
	0.2992	19.424	8082.67	41723.03	99.76026
	0.3026	17.839	8084.255	44928.491	99.779822
	0.3019	36.134	8065.96	22181.87	99.554017
	0.3023	38.944	8063.15	20546.946	99.519334
1176	0.2992	69.6	8032.494	11571.798	99.140963
	0.3005	66.848	8035.246	12000.174	99.174929
	0.3007	55.431	8046.663	14482.746	99.315844
	0.2981	37.633	8064.461	21565.81	99.535515
	0.2985	61.846	8040.248	13065.762	99.236666
1728	0.3015	25.28	8076.814	31790.47	99.687982
	0.3001	26.828	8075.266	30090.112	99.668876
	0.3017	26.36	8075.734	30463.693	99.674652
	0.2995	29.52	8072.574	27391.771	99.63565
	0.2981	31.342	8070.752	25914.723	99.613162

(4c) Adsorption data for Cs-134 EWBP system					
time(hrs)	mass(g)	ac,sol(Bq)	ac,sed(Bq)	Rd(ml/g)	%sorbed
0.5	0.3014	1473.014	6629.08	447.94469	81.819342
	0.3014	1803.703	6298.391	347.57025	77.737817
	0.3012	1742.966	6359.128	363.39165	78.487463
	0.3012	1495.547	6606.547	439.98792	81.541229
	0.3007	1621.415	6480.679	398.76235	79.987704
2	0.2999	1601.052	6501.042	406.18354	80.239035
	0.2996	2044.944	6057.15	296.59673	74.760303
	0.298	1689.91	6412.184	381.98595	79.142306
	0.2994	1370.87	6731.224	492.00241	83.080053
	0.3015	1838.354	6263.74	339.0303	77.310137
8	0.2981	1124.259	6977.835	624.61671	86.123847
	0.3007	971.945	7130.149	731.88819	88.00378
	0.2996	1006.262	7095.832	706.10892	87.580223
	0.2975	1051.704	7050.39	676.01121	87.019356
	0.2977	1089.924	7012.17	648.33377	86.547626
23	0.3007	1158.207	6943.887	598.14198	85.704844
	0.3006	868.806	7233.288	830.89324	89.276772
	0.299	808.577	7293.517	905.03564	90.020148
	0.2988	743.94	7358.154	993.05116	90.817929
	0.3013	798.577	7303.517	910.62039	90.143573
44	0.2986	380.372	7721.722	2039.5628	95.305263
	0.2998	364.023	7738.071	2127.1274	95.50705
	0.2998	386.347	7715.747	1998.4352	95.231517
	0.3001	391.728	7710.366	1967.64	95.165102
	0.2992	360.095	7741.999	2155.7366	95.555532
120	0.3001	270.862	7831.232	2890.2624	96.656889
	0.298	309.535	7792.559	2534.401	96.179568
	0.3018	269.048	7833.046	2894.0293	96.679278
	0.298	304.532	7797.562	2577.6912	96.241317
	0.2992	277.856	7824.238	2823.4619	96.570566
192	0.2981	267.201	7834.893	2950.8985	96.702075
	0.3017	294.413	7807.681	2637.0054	96.366211
	0.2998	257.32	7844.774	3050.6791	96.824031
	0.3004	270.721	7831.373	2888.9318	96.658629
	0.301	314.755	7787.339	2465.8758	96.11514
552	0.3021	181.321	7920.773	4338.0044	97.762048
	0.302	161.629	7940.465	4880.2375	98.005096
	0.3011	174.866	7927.228	4516.7544	97.841718
	0.2989	180.596	7921.498	4402.451	97.770996
	0.3009	184.22	7917.874	4285.1978	97.726267
720	0.2991	164.321	7937.773	4845.1859	97.97187
	0.3021	172.992	7929.102	4551.6464	97.864848
	0.2999	184.279	7917.815	4298.078	97.725539
	0.2983	166.61	7935.484	4790.0534	97.943618
	0.3017	188.618	7913.476	4171.8636	97.671985

1176	0.2984	278.08	7824.014	2828.6701	96.567801
	0.2997	301.45	7800.644	2590.2977	96.279357
	0.299	320.458	7781.636	2436.4071	96.044751
	0.2988	276.857	7825.237	2837.8057	96.582896
	0.298	298.016	7804.078	2636.2525	96.321741
1728	0.2985	42.635	8059.459	18998.379	99.473778
	0.3015	171.429	7930.665	4603.1937	97.88414
	0.2996	63.868	8038.226	12602.489	99.21171
	0.2983	85.725	8016.369	9404.5541	98.94194
	0.3012	189.653	7912.441	4155.4404	97.65921
(4d) Adsorption data for Cs-134 EWEW system					
time(hrs)	mass(g)	ac,sol(Bq)	ac,sed(Bq)	Rd(ml/g)	%sorbed
0.5	0.3014	1388.3	6713.794	481.3519	82.864924
	0.3009	1396.565	6705.529	478.7083	82.762913
	0.3014	1099.031	7003.063	634.24361	86.435223
	0.3002	1385.281	6716.813	484.54704	82.902186
	0.3007	1676.922	6425.172	382.26076	79.30261
2	0.3011	1630.647	6471.447	395.41391	79.873759
	0.3014	1179.104	6922.99	584.41264	85.446923
	0.3002	1253.571	6848.523	545.95714	84.527815
	0.2977	1423.017	6679.077	472.98654	82.436429
	0.301	1360.192	6741.902	494.01141	83.211846
8	0.2988	1261.602	6840.492	544.38435	84.428692
	0.299	1111.587	6990.507	630.97955	86.280251
	0.2987	1092.579	7009.515	644.34899	86.514857
	0.2997	1119.038	6983.056	624.64778	86.188287
	0.2998	1650.178	6451.916	391.24386	79.632697
23	0.2992	1366.525	6735.569	494.21551	83.133681
	0.3	1004.583	7097.511	706.51315	87.600946
	0.3011	955.462	7146.632	745.24402	88.207221
	0.3017	954.195	7147.899	744.88155	88.222859
	0.2997	1368.572	6733.522	492.5033	83.108416
44	0.2991	221.267	7880.827	3572.3992	97.269015
	0.2983	375.022	7727.072	2072.174	95.371295
	0.2993	291.056	7811.038	2689.9656	96.407645
	0.3006	252.909	7849.185	3097.3662	96.878474
	0.3007	236.288	7865.806	3321.1569	97.083618
120	0.2996	194.821	7907.273	4064.1564	97.595424
	0.3024	183.891	7918.203	4271.748	97.730327
	0.2987	212.234	7889.86	3733.7082	97.380504
	0.2993	200.723	7901.371	3945.6618	97.522579
	0.2984	200.914	7901.18	3953.7044	97.520221
192	0.3011	209.185	7892.909	3759.3872	97.418137
	0.2993	171.302	7930.792	4640.5415	97.885707
	0.2996	270.962	7831.132	2893.9805	96.655655
	0.3005	223.096	7878.998	3525.7863	97.24644
	0.2988	231.644	7870.45	3411.2942	97.140937

552	0.2998	123.853	7978.241	6445.9992	98.471346
	0.298	134.496	7967.598	5963.7995	98.339985
	0.2992	114.826	7987.268	6974.574	98.582761
	0.3011	110.216	7991.878	7224.6148	98.63966
	0.3025	135.347	7966.747	5837.5185	98.329481
720	0.2999	169.767	7932.327	4674.0368	97.904653
	0.2986	137.278	7964.816	5829.1637	98.305648
	0.3006	127.671	7974.423	6233.6051	98.424222
	0.3011	127.03	7975.064	6255.1594	98.432134
	0.3005	103.752	7998.342	7696.2696	98.719442
1176	0.2995	288.336	7813.758	2714.4729	96.441216
	0.3018	322.973	7779.121	2394.2325	96.01371
	0.2997	342.541	7759.553	2267.5593	95.772192
	0.3022	234.601	7867.493	3329.1495	97.10444
	0.2998	286.064	7816.03	2734.0889	96.469258
1728	0.3009	155.365	7946.729	5099.5785	98.082409
	0.3022	157.648	7944.446	5002.671	98.054231
	0.3009	145.531	7956.563	5450.9106	98.203785
	0.3003	157.763	7944.331	5030.5804	98.052812
	0.3002	160.512	7941.582	4944.36	98.018883

APPENDIX 2 - SUPPLEMENTARY ADSORPTION EXPTS					
PHASE SEPARATION					
(a) Phase separation data for Co-57					
system	separation	mass(g)	ac,sol(Bq)	ac,sed(Bq)	Rd(ml/g)
BPBP	cent	0.2971	176.402	537.477	307.663
		0.3011	170.016	543.863	318.721
		0.2998	192.746	521.133	270.553
		0.3018	111.022	602.857	539.768
		0.3008	117.05	596.829	508.536
	cent+fil	0.2971	124.162	589.717	479.594
		0.3011	100.939	612.94	605.02
		0.2998	75.766	638.113	842.777
		0.3018	95.118	618.761	646.64
		0.3008	97.337	616.542	631.725
BPEW	cent	0.3021	122.519	591.36	479.313
		0.3002	119.693	594.186	496.094
		0.2988	140.755	573.124	408.814
		0.2987	134.447	579.432	432.85
		0.2994	171.006	542.873	318.095
	cent+fil	0.299	103.451	610.428	592.038
		0.3016	121.022	592.857	487.277
		0.3023	102.884	610.995	589.35
		0.2982	156.079	557.8	359.54
		0.3015	208.68	505.199	240.888
EWBP	cent	0.3016	211.837	502.042	235.737
		0.2976	203.388	510.491	253.018
		0.3014	200.32	513.559	255.178
		0.2983	200.003	513.876	258.398
		0.3	202.761	511.118	252.079
	cent+fil	0.2975	196.464	517.415	265.577
		0.2979	209.797	504.082	241.965
		0.2991	200.258	513.621	257.251
		0.2985	192.25	521.629	272.692
		0.3003	180.93	532.949	294.267
EWEW	cent	0.3029	529.074	184.805	34.5955
		0.2978	458.465	255.414	56.1222
		0.3007	464.239	249.64	53.6488
		0.3027	407.263	306.616	74.6154
		0.2985	457.329	256.55	56.3794
	cent+fil	0.2985	435.11	278.769	64.3906
		0.3	421.555	292.324	69.3442
		0.3	454.885	258.994	56.9361
		0.3008	468.262	245.617	52.3134
		0.3001	451.124	262.755	58.2251
(b) Phase separation data for Sr-85					
system	separation	mass(g)	ac,sol(Bq)	ac,sed(Bq)	Rd(ml/g)

BPBP	cent	0.3014	634.481	525.519	82.4419
		0.2995	638.178	521.822	81.904
		0.2982	668.287	491.713	74.0223
		0.3004	514.705	645.295	125.205
		0.2997	521.518	638.482	122.55
	cent+fil	0.2971	523.764	636.236	122.66
		0.3011	505.382	654.618	129.056
		0.2998	502.517	657.483	130.925
		0.3018	544.761	615.239	112.264
		0.3008	517.413	642.587	123.862
BPEW	cent	0.3021	595.229	564.771	94.2234
		0.3002	589.698	570.302	96.6464
		0.2988	588.424	571.576	97.5269
		0.2987	586.209	573.791	98.3076
		0.2994	610.535	549.465	90.1777
	cent+fil	0.299	546.911	613.089	112.475
		0.3016	584.426	575.574	97.9629
		0.3023	544.83	615.17	112.051
		0.2982	548.127	611.873	112.304
		0.3015	570.191	589.809	102.926
EWBP	cent	0.3016	696.919	463.081	66.0944
		0.2976	673.583	486.417	72.7957
		0.3014	667.021	492.979	73.5643
		0.2983	658.096	501.904	76.7007
		0.3	672.438	487.562	72.5066
	cent+fil	0.2975	653.454	506.546	78.1696
		0.2979	679.318	480.682	71.2583
		0.2991	648.742	511.258	79.0447
		0.2985	659.445	500.555	76.2869
		0.3003	657.876	502.124	76.2488
EWEW	cent	0.3029	873.37	286.63	32.5046
		0.2978	847.987	312.013	37.0664
		0.3007	820.491	339.509	41.2824
		0.3027	766.808	393.192	50.8191
		0.2985	824.035	335.965	40.9756
	cent+fil	0.2985	786.543	373.457	47.7194
		0.3	762.448	397.552	52.1415
		0.3	823.588	336.412	40.8471
		0.3008	816.364	343.636	41.9815
		0.3001	819.696	340.304	41.502
(c) Phase separation data for Ru-103					
system	separation	mass(g)	ac,sol(Bq)	ac,sed(Bq)	Rd(ml/g)
BPEW	cent	0.3021	25.645	451.419	1748.03
		0.3002	30.093	446.971	1484.31
		0.2988	31.881	445.183	1402
		0.2987	31.572	445.492	1417.18
		0.2994	38.267	438.797	1148.97

	cent+fil	0.299	22.09	454.974	2066.53
		0.3016	23.771	453.293	1896.8
		0.3023	21.784	455.28	2074.07
		0.2982	26.969	450.095	1679.01
		0.3015	29.513	447.551	1508.91
EWBP	cent	0.3016	45.227	431.837	949.756
		0.2976	47.159	429.905	918.959
		0.3014	48.411	428.653	881.333
		0.2983	41.602	435.462	1052.7
		0.3	44.804	432.26	964.78
	cent+fil	0.2975	47.037	430.027	921.914
		0.2979	41.428	435.636	1058.96
		0.2991	39.913	437.151	1098.56
		0.2985	44.531	432.533	976.189
		0.3003	40.547	436.517	1075.49
EWEW	cent	0.3029	223.516	253.548	112.35
		0.2978	220.382	256.682	117.332
		0.3007	217.379	259.685	119.184
		0.3027	191.966	285.098	147.19
		0.2985	211.643	265.421	126.04
	cent+fil	0.2985	194.282	282.782	146.284
		0.3	182.282	294.782	161.718
		0.3	201.229	275.835	137.075
		0.3008	217.766	259.298	118.755
		0.3001	203.771	273.293	134.073
(d) Phase separation data for Cs-134					
system	separation	mass(g)	ac,sol(Bq)	ac,sed(Bq)	Rd(ml/g)
BPBP	cent	0.3014	443.652	9345.962	2096.81
		0.2995	468.063	9321.551	1994.84
		0.2982	548.149	9241.465	1696.12
		0.3004	330.678	9458.936	2856.66
		0.2997	334.233	9455.381	2831.81
	cent+fil	0.2971	170.865	9618.749	5684.39
		0.3011	137.758	9651.856	6980.79
		0.2998	143.109	9646.505	6745.17
		0.3018	181.656	9607.958	5257.55
		0.3008	183.344	9606.27	5225.54
BPEW	cent	0.3021	223.851	9565.763	4243.57
		0.3002	279.46	9510.154	3400.78
		0.2988	344.255	9445.359	2754.73
		0.2987	277.899	9511.715	3437.62
		0.2994	322.124	9467.49	2944.97
	cent+fil	0.299	179.204	9610.41	5380.77
		0.3016	133.385	9656.229	7200.96
		0.3023	112.005	9677.609	8574.6
		0.2982	104.929	9684.685	9285.46
		0.3015	106.746	9682.868	9025.81

EWBP	cent	0.3016	940.246	8849.368	936.183
		0.2976	883.46	8906.154	1016.23
		0.3014	891.796	8897.818	993.107
		0.2983	796.636	8992.978	1135.3
		0.3	918.32	8871.294	966.035
	cent+fil	0.2975	402.37	9387.244	2352.59
		0.2979	547.646	9241.968	1699.48
		0.2991	397.157	9392.457	2372.04
		0.2985	379.965	9409.649	2488.9
		0.3003	397.823	9391.791	2358.44
EWEW	cent	0.3029	1597.645	8191.969	507.844
		0.2978	1351.912	8437.702	628.742
		0.3007	1423.919	8365.695	586.144
		0.3027	1369.295	8420.319	609.453
		0.2985	1414.764	8374.85	594.936
	cent+fil	0.2985	255.087	9534.527	3756.54
		0.3	467.337	9322.277	1994.77
		0.3	741.994	9047.62	1219.37
		0.3008	938.741	8850.873	940.337
		0.3001	661.829	9127.785	1378.72

REPRODUCIBILITY					
Repeat adsorption data for Cs-134 BPBP system					
time(hrs)	mass(g)	ac,sol(Bq)	ac,sed(Bq)	Rd(ml/g)	mean Rd
8	0.2999	386.648	7715.446	1996.136	1948.408
	0.2999	412.05	7690.044	1866.911	
	0.3019	381.606	7720.488	2010.424	
	0.301	420.35	7681.744	1821.392	
	0.3004	376.858	7725.236	2047.177	
120	0.3017	106.096	7995.998	7494.102	3460.739
	0.299	311.774	7790.32	2507.064	
	0.2999	310.447	7791.647	2510.652	
	0.3014	325.203	7776.891	2380.288	
	0.2978	324.876	7777.218	2411.589	
192	0.2992	164.083	7938.011	4850.738	4763.287
	0.2999	165.138	7936.956	4807.859	
	0.2994	173.008	7929.086	4592.259	
	0.2994	166.405	7935.689	4778.457	
	0.2977	167.039	7935.055	4787.122	

STERILISATION					
(a) Adsorption data for sterilised samples, Co-57					
time(hrs)	mass(g)	ac,sol(Bq)	ac,sed(Bq)	Rd(ml/g)	%sorbed
1104	0.3012	52.434	679.091	1289.975	92.83223
	0.2971	56.428	675.097	1208.065	92.28625
	0.2976	56.119	675.406	1213.23	92.32849
	0.3013	54.312	677.213	1241.514	92.57551
	0.3024	56.336	675.189	1188.992	92.29883
1176	0.2987	63.609	667.916	1054.604	91.3046
	0.2971	54.408	677.117	1256.665	92.56239
	0.3008	60.803	670.722	1100.173	91.68819
	0.3003	50.565	680.96	1345.357	93.08773
	0.2988	59.245	672.28	1139.303	91.90117
1320	0.3025	61.415	670.11	1082.1	91.60452
	0.2996	64.307	667.218	1038.936	91.20919
	0.2984	72.085	659.44	919.714	90.14593
	0.2971	58.746	672.779	1156.412	91.96938
	0.3023	65.33	666.195	1011.98	91.06934
1680	0.3025	59.238	672.287	1125.512	91.90212
	0.2996	58.751	672.774	1146.657	91.9687
	0.3015	67.172	664.353	984.1121	90.81754
	0.298	40.214	691.311	1730.618	94.50272
	0.3006	46.496	685.029	1470.367	93.64396
(b) Adsorption data for sterilised samples, Cs-134					
time(hrs)	mass(g)	ac,sol(Bq)	ac,sed(Bq)	Rd(ml/g)	%sorbed
1104	0.3012	177.452	9439.887	5298.491	98.15487
	0.2971	172.367	9444.972	5533.057	98.20775
	0.2976	177.001	9440.338	5376.506	98.15956
	0.3013	182.935	9434.404	5134.992	98.09786
	0.3024	202.768	9414.571	4606.177	97.89164
1176	0.2987	375.236	9242.103	2473.73	96.09834
	0.2971	177.359	9439.98	5374.48	98.15584
	0.3008	174.632	9442.707	5392.822	98.1842
	0.3003	223.301	9394.038	4202.692	97.67814
	0.2988	198.445	9418.894	4765.412	97.93659
1320	0.3025	202.097	9415.242	4620.271	97.89862
	0.2996	289.714	9327.625	3223.896	96.98759
	0.2984	282.997	9334.342	3316.075	97.05743
	0.2971	190.075	9427.264	5008.172	98.02362
	0.3023	206.15	9411.189	4530.48	97.85648
1680	0.3025	204.206	9413.133	4571.53	97.87669
	0.2996	168.436	9448.903	5617.278	98.24862
	0.3015	178.749	9438.59	5254.089	98.14139
	0.298	125.443	9491.896	7617.484	98.69566
	0.3006	128.071	9489.268	7394.592	98.66833

APPENDIX 3 - DESORPTION DATA					
FRESH LAKE WATER DESORPTION					
(1a) Desorption data for Co-57 BPBP system					
time(hrs)	ac,sol(Bq)	ac,sed(Bq)	act,des(Bq)	%desorbed	mean%
	(following adsorption)				
0.5	396.957	724.681	38.095	5.2567957	6.09534
	393.935	727.703	35.315	4.8529414	
	438.012	683.626	35.544	5.1993341	
	421.945	699.693	49.202	7.0319412	
	505.819	615.819	50.101	8.1356697	
2	302.196	819.442	35.02	4.2736399	4.1657
	256.205	865.433	33.081	3.8224796	
	308.649	812.989	31.768	3.9075559	
	367.685	753.953	34.957	4.6364959	
	297.13	824.508	34.533	4.1883159	
8	317.422	804.216	38.335	4.7667542	4.53215
	259.931	861.707	36.284	4.210712	
	206.096	915.542	40.716	4.4472018	
	296.344	825.294	38.409	4.6539779	
	293.309	828.329	37.955	4.5821165	
23	142.717	978.921	17.172	1.7541763	2.88872
	249.455	872.183	30.01	3.4407917	
	226.527	895.111	29.863	3.3362343	
	227.302	894.336	27.532	3.078485	
	208.48	913.158	25.878	2.8339017	
44	138.314	983.324	31.932	3.2473529	2.62646
	177.91	943.728	25.257	2.6763008	
	176.614	945.024	26.143	2.7663848	
	155.895	965.743	21.852	2.2627138	
	201.897	919.741	20.046	2.1795266	
120	72.754	1048.884	13.005	1.2398893	2.10007
	79.654	1041.984	27.202	2.6105967	
	65.031	1056.607	18.36	1.7376376	
	88.671	1032.967	21.623	2.0932905	
	66.054	1055.584	29.756	2.8189135	
192	89.747	1031.891	21.909	2.1231894	1.83905
	87.111	1034.527	27.784	2.6856718	
	75.835	1045.803	18.628	1.781215	
	74.642	1046.996	13.92	1.329518	
	71.425	1050.213	13.397	1.275646	
552	30.704	1090.934	10.034	0.9197623	1.50439
	76.468	1045.17	24.414	2.3358879	
	63.024	1058.614	18.681	1.7646659	
	54.483	1067.155	14.537	1.3622201	
	22.31	1099.328	12.526	1.1394234	
720	64.67	1056.968	21.868	2.0689368	1.30266
	28.568	1093.07	11.973	1.0953553	

	26.225	1095.413	14.722	1.343968	
	23.493	1098.145	10.773	0.981018	
	19.527	1102.111	11.286	1.0240348	
1176	29.02	1092.618	8.572	0.7845377	0.88501
	34.833	1086.805	8.669	0.7976592	
	42.822	1078.816	12.203	1.1311475	
	24.059	1097.579	8.919	0.8126067	
	28.203	1093.435	9.831	0.8990932	
1728	28.392	1093.246	14.576	1.3332772	1.03659
	11.544	1110.094	8.124	0.7318299	
	16.513	1105.125	11.651	1.0542699	
	21.111	1100.527	9.005	0.8182444	
	13.029	1108.609	13.806	1.2453444	
(1b) Desorption data for Co-57 BPEW system					
time(hrs)	ac,sol(Bq)	ac,sed(Bq)	act,des(Bq)	%desorbed	mean%
	(following adsorption)				
0.5	282.555	839.083	32.665	3.8929403	3.65474
	312.13	809.508	35.838	4.4271335	
	257.916	863.722	28.056	3.2482674	
	255.394	866.244	27.35	3.157309	
	318.321	803.317	28.502	3.5480389	
2	174.67	946.968	23.322	2.4628076	2.72662
	189.961	931.677	29.164	3.1302694	
	191.002	930.636	23.262	2.4995809	
	191.746	929.892	24.457	2.6300904	
	177.772	943.866	27.47	2.9103708	
8	171.191	950.447	27.721	2.9166276	3.12854
	194.962	926.676	25.98	2.8035689	
	210.497	911.141	24.548	2.6942043	
	269.545	852.093	30.681	3.6006633	
	265.896	855.742	31.043	3.6276121	
23	63.474	1058.164	7.695	0.727203	1.13286
	189.055	932.583	20.789	2.229185	
	81.476	1040.162	10.467	1.0062856	
	67.552	1054.086	8.721	0.8273518	
	65.767	1055.871	9.231	0.8742545	
44	183.386	938.252	20.757	2.2123054	1.95392
	177.78	943.858	17.913	1.897849	
	190.427	931.211	17.251	1.852534	
	191.873	929.765	18.76	2.0177142	
	232.59	889.048	15.907	1.7892172	
120	106.515	1015.123	19.729	1.9435083	1.87959
	99.551	1022.087	18.617	1.8214692	
	99.132	1022.506	20.382	1.9933379	
	107.831	1013.807	21.29	2.1000052	
	76.782	1044.856	16.087	1.539638	
192	50.38	1071.258	16.824	1.57049	1.54655

	57.01	1064.628	9.869	0.9269905	
	64.763	1056.875	20.245	1.9155529	
	52.629	1069.009	15.735	1.471924	
	94.41	1027.228	18.981	1.8477884	
552	67.511	1054.127	6.038	0.5727963	0.78493
	57.15	1064.488	6.848	0.643314	
	75.153	1046.485	8.77	0.8380435	
	65.317	1056.321	6.528	0.617994	
	80.279	1041.359	13.043	1.2524979	
720	36.383	1085.255	7.413	0.6830653	1.35647
	64.899	1056.739	14.615	1.3830284	
	73.079	1048.559	22.077	2.1054609	
	76.34	1045.298	19.622	1.877168	
	55.722	1065.916	7.82	0.7336413	
1176	20.619	1101.019	3.555	0.3228827	0.46767
	22.206	1099.432	5.334	0.4851596	
	14.572	1107.066	4.283	0.3868785	
	15.758	1105.88	6.44	0.5823417	
	21.431	1100.207	6.173	0.5610762	
1728	17.108	1104.53	5.502	0.4981304	0.71937
	17.192	1104.446	7.958	0.7205422	
	16.033	1105.605	8.776	0.7937735	
	19.144	1102.494	7.485	0.6789153	
	17.567	1104.071	9.997	0.9054671	
(1c) Desorption data for Co-57 EWBP system					
time(hrs)	ac,sol(Bq)	ac,sed(Bq)	act,des(Bq)	%desorbed	mean%
	(following adsorption)				
0.5	608.989	512.649	47.414	9.2488233	11.4154
	711.704	409.934	48.374	11.800436	
	756.499	365.139	50.204	13.749285	
	610.647	510.991	62.191	12.170664	
	617.459	504.179	50.961	10.10772	
2	359.182	762.456	36.532	4.7913585	5.1836
	417.188	704.45	33.315	4.7292214	
	360.819	760.819	39.551	5.1984769	
	316.756	804.882	41.754	5.1875927	
	414.343	707.295	42.518	6.0113531	
8	375.298	746.34	45.082	6.0404105	6.1927
	342.923	778.715	49.094	6.3044888	
	361.693	759.945	50.627	6.6619295	
	352.282	769.356	45.058	5.8565865	
	373.763	747.875	45.621	6.1000836	
23	452.676	668.962	64.557	9.6503239	7.22997
	336.15	785.488	79.419	10.110785	
	325.081	796.557	76.186	9.5644128	
	285.541	836.097	31.116	3.7215778	
	215.148	906.49	28.126	3.1027369	

44	226.638	895	41.085	4.5905028	4.62466
	237.19	884.448	42.106	4.7607095	
	239.253	882.385	41.877	4.7458876	
	248.769	872.869	39.627	4.5398565	
	235.264	886.374	39.766	4.4863681	
120	141.573	980.065	38.674	3.9460648	4.01183
	166.393	955.245	39.458	4.130668	
	154.901	966.737	52.008	5.3797465	
	159.097	962.541	32.17	3.3421953	
	157.08	964.558	31.449	3.2604571	
192	148.675	972.963	26.612	2.7351503	2.66112
	160.604	961.034	25.875	2.6924125	
	148.697	972.941	28.03	2.8809558	
	156.423	965.215	23.878	2.473853	
	160.324	961.314	24.256	2.523213	
552	35.96	1085.678	16.958	1.5619733	1.42678
	38.637	1083.001	18.888	1.7440427	
	62.672	1058.966	5.043	0.4762193	
	51.873	1069.765	18.389	1.7189757	
	49.605	1072.033	17.503	1.6326923	
720	13.5	1108.138	4.107	0.3706217	1.29585
	35.583	1086.055	12.863	1.1843783	
	37.193	1084.445	16.318	1.5047328	
	36.128	1085.51	17.681	1.6288196	
	41.265	1080.373	19.346	1.7906778	
1176	89.387	1032.251	16.473	1.5958328	1.27026
	83.072	1038.566	15.506	1.4930202	
	88.957	1032.681	18.194	1.7618219	
	67.619	1054.019	14.352	1.3616453	
	9.158	1112.48	1.546	0.1389688	
1728	48.634	1073.004	8.093	0.7542376	1.50805
	57.761	1063.877	25.129	2.3620212	
	11.95	1109.688	4.871	0.4389522	
	70.836	1050.802	20.811	1.9804873	
	60.402	1061.236	21.273	2.0045494	
(1d) Desorption data for Co-57 EWEW system					
time(hrs)	ac,sol(Bq)	ac,sed(Bq)	act,des(Bq)	%desorbed	mean%
	(following adsorption)				
0.5	703.178	418.46	73.533	17.572289	16.8482
	639.784	481.854	78.419	16.274432	
	576.852	544.786	77.523	14.229991	
	681.399	440.239	77.2	17.535929	
	740.742	380.896	70.954	18.628182	
2	531.118	590.52	45.157	7.6469891	7.72313
	412.126	709.512	62.996	8.8787787	
	422.838	698.8	50.004	7.1556955	
	526.066	595.572	47.45	7.9671308	

	437.678	683.96	47.652	6.9670741	
8	641.311	480.327	53.486	11.135331	14.2056
	592.701	528.937	61.379	11.604218	
	589.94	531.698	59.893	11.264477	
	602.297	519.341	61.482	11.838465	
	920.182	201.456	50.738	25.185648	
23	751.043	370.595	134.027	36.165356	27.2648
	590.575	531.063	14.363	2.7045755	
	578.8	542.838	135.884	25.032146	
	583.896	537.742	197.099	36.653079	
	773.457	348.181	124.54	35.768752	
44	214.325	907.313	79.04	8.711437	9.87142
	289.609	832.029	94.004	11.298164	
	245.562	876.076	85.915	9.8067976	
	213.238	908.4	88.324	9.7230295	
	223.348	898.29	88.191	9.8176535	
120	357.144	764.494	61.651	8.0642883	8.0214
	251.312	870.326	65.476	7.523158	
	347.841	773.797	60.738	7.8493455	
	280.143	841.495	81.996	9.7440864	
	298.712	822.926	56.997	6.9261392	
192	214.384	907.254	79.98	8.8156128	11.4109
	309.049	812.589	86.066	10.591578	
	331.828	789.81	102.02	12.917031	
	291.849	829.789	102.8	12.388692	
	314.258	807.38	99.644	12.341648	
552	149.195	972.443	85.686	8.8114162	9.02157
	118.957	1002.681	98.228	9.7965355	
	113.527	1008.111	66.703	6.6166325	
	166.978	954.66	91.299	9.5635095	
	197.965	923.673	95.321	10.319778	
720	128.034	993.604	43.854	4.4136296	5.44304
	129.914	991.724	48.617	4.9022712	
	181.627	940.011	62.131	6.6096035	
	141.312	980.326	48.469	4.9441716	
	166.668	954.97	60.598	6.3455397	
1176	986.363	135.275	53.357	39.443356	25.2476
	764.311	357.327	63.81	17.857593	
	670.344	451.294	65.351	14.480804	
	795.148	326.49	95.168	29.148825	
	769.582	352.056	89.096	25.307337	
1728	513.787	607.851	70.071	11.527661	11.7621
	586.005	535.633	65.948	12.312161	
	451.047	670.591	56.917	8.4875878	
	593.777	527.861	73.775	13.976217	
	582.338	539.3	67.449	12.506768	

(2a) Desorption data for Sr-85 BPBP system					
time(hrs)	ac,sol(Bq)	ac,sed(Bq)	act,des(Bq)	%desorbed	mean%
	(following adsorption)				
0.5	436.443	547.565	144.594	26.406728	24.8427
	446.574	537.434	131.132	24.399647	
	472.736	511.272	123.059	24.069184	
	428.806	555.202	137.477	24.761618	
	402.287	581.721	142.967	24.576558	
2	418.637	565.371	129.346	22.878075	22.537
	412.157	571.851	132.447	23.161103	
	399.418	584.59	127.661	21.837698	
	405.597	578.411	125.608	21.716046	
	407.754	576.254	133.07	23.092248	
8	601.82	382.188	179.514	46.970078	33.8445
	502.894	481.114	211.074	43.871931	
	89.398	894.61	225.711	25.2301	
	529.037	454.971	204.833	45.021111	
	544.784	439.224	35.705	8.1291095	
23	506.846	477.162	178.773	37.465892	25.0002
	499.942	484.066	182.642	37.730805	
	83.964	900.044	34.702	3.8555893	
	488.136	495.872	188.631	38.04026	
	501.866	482.142	38.129	7.9082511	
44	305.969	678.039	130.391	19.230605	18.1838
	312.333	671.675	122.506	18.23888	
	308.656	675.352	117.778	17.439498	
	310.98	673.028	110.124	16.362469	
	308.209	675.799	132.779	19.647706	
120	288.04	695.968	158.713	22.80464	22.9857
	290.187	693.821	157.442	22.69202	
	272.647	711.361	165.994	23.334706	
	320.975	663.033	153.13	23.095381	
	279.829	704.179	161.975	23.001964	
192	310.956	673.052	168.794	25.078894	25.1838
	299.721	684.287	169.83	24.818534	
	298.118	685.89	170.743	24.893642	
	313.139	670.869	173.166	25.812193	
	311.302	672.706	170.301	25.315814	
552	409.43	574.578	221.696	38.584143	39.1764
	400.496	583.512	225.696	38.678896	
	421.017	562.991	226.001	40.142915	
	416.633	567.375	229.863	40.513417	
	391.952	592.056	224.761	37.962794	
720	408.032	575.976	227.802	39.550606	40.1685
	417.475	566.533	230.275	40.646352	
	422.855	561.153	229.965	40.980802	
	406.729	577.279	221.142	38.307647	
	431.354	552.654	228.561	41.356979	

1176	476.505	507.503	207.11	40.809611	26.9067
	86.226	897.782	198.846	22.148584	
	498.728	485.28	36.964	7.6170458	
	482.953	501.055	208.805	41.67307	
	88.704	895.304	199.52	22.285168	
1728	393.984	590.024	429.552	72.802462	71.0149
	379.473	604.535	428.116	70.817405	
	387.929	596.079	410.063	68.793398	
	397.419	586.589	418.386	71.325238	
	376.581	607.427	433.313	71.335815	
(2b) Desorption data for Sr-85 BPEW system					
time(hrs)	ac,sol(Bq)	ac,sed(Bq)	act,des(Bq)	%desorbed	mean%
	(following adsorption)				
0.5	306.033	677.975	78.758	11.616653	11.3626
	323.539	660.469	73.762	11.168124	
	340.392	643.616	73.279	11.385516	
	320.731	663.277	73.384	11.063854	
	359.841	624.167	72.27	11.578632	
2	283.177	700.831	72.288	10.314612	10.5306
	316.995	667.013	63.241	9.4812245	
	347.334	636.674	83.537	13.120844	
	290.892	693.116	64.927	9.3674075	
	249.969	734.039	76.113	10.369068	
8	445.843	538.165	117.777	21.884924	20.5233
	452.034	531.974	109.225	20.532018	
	474.848	509.16	99.638	19.569094	
	432.866	551.142	111.426	20.217294	
	438.833	545.175	111.287	20.413078	
23	365.606	618.402	111.563	18.04053	17.8012
	419.481	564.527	98.868	17.513423	
	387.554	596.454	108.069	18.118581	
	388.534	595.474	104.4	17.532252	
	364.239	619.769	110.325	17.800987	
44	203.145	780.863	77.549	9.9311915	8.61364
	200.118	783.89	68.885	8.787585	
	200.416	783.592	65.672	8.3808921	
	218.226	765.782	63.579	8.3024934	
	223.03	760.978	58.337	7.666056	
120	188.307	795.701	92.493	11.62409	11.8754
	191.308	792.7	95.571	12.05639	
	189.141	794.867	96.547	12.146309	
	184.849	799.159	98.07	12.271651	
	177.832	806.176	90.925	11.278555	
192	234.238	749.77	121.435	16.1963	15.1125
	227.813	756.195	118.073	15.614094	
	232.643	751.365	109.557	14.581062	
	219.611	764.397	114.941	15.03682	

	225.524	758.484	107.206	14.134247	
552	345.464	638.544	125.136	19.597083	20.3779
	353.362	630.646	135.411	21.471792	
	336.651	647.357	131.129	20.256057	
	341.965	642.043	132.687	20.666373	
	341.173	642.835	127.913	19.898263	
720	369.68	614.328	128.627	20.937838	20.1639
	352.211	631.797	130.114	20.594273	
	354.043	629.965	122.75	19.485209	
	361.534	622.474	124.43	19.98959	
	366.08	617.928	122.427	19.812502	
1176	445.627	538.381	109.705	20.376834	21.2293
	463.127	520.881	116.212	22.310662	
	454.976	529.032	114.767	21.693773	
	458.214	525.794	110.027	20.925876	
	458.944	525.064	109.419	20.839174	
1728	348.059	635.949	187.373	29.463526	31.065
	354.667	629.341	199.497	31.699349	
	357.32	626.688	194.177	30.984637	
	342.885	641.123	197.665	30.831057	
	345.621	638.387	206.494	32.34621	
(2c) Desorption data for Sr-85 EWBP system					
time(hrs)	ac,sol(Bq)	ac,sed(Bq)	act,des(Bq)	%desorbed	mean%
	(following adsorption)				
0.5	547.245	436.763	109.317	25.028906	25.5216
	586.58	397.428	104.339	26.25356	
	584.101	399.907	95.567	23.897306	
	530.528	453.48	119.908	26.441739	
	537.604	446.404	116.005	25.98655	
2	474.605	509.403	115.609	22.694998	22.7148
	517.701	466.307	99.923	21.428587	
	472.854	511.154	114.791	22.457224	
	436.191	547.817	127.509	23.275838	
	499.448	484.56	114.925	23.717393	
8	114.975	869.033	31.776	3.6564779	3.85567
	106.828	877.18	32.449	3.6992407	
	107.734	876.274	33.357	3.806686	
	109.281	874.727	35.532	4.0620674	
	109.217	874.791	35.463	4.0538826	
23	111.069	872.939	29.818	3.4158171	3.7792
	99.077	884.931	34.183	3.862787	
	95.408	888.6	34.463	3.878348	
	93.94	890.068	34.814	3.9113865	
	95.921	888.087	33.993	3.8276655	
44	342.456	641.552	133.536	20.814525	20.1022
	346.695	637.313	124.216	19.49058	
	341.225	642.783	121.242	18.862042	

	336.308	647.7	130.837	20.200247	
	335.595	648.413	137.098	21.143623	
120	292.414	691.594	158.852	22.968967	23.8077
	305.382	678.626	165.658	24.410795	
	293.747	690.261	169.533	24.56071	
	293.187	690.821	162.189	23.477717	
	287.96	696.048	164.407	23.620066	
192	337.989	646.019	186.74	28.906271	28.74
	326.071	657.937	187.818	28.546502	
	335.109	648.899	185.599	28.60214	
	345.071	638.937	185.345	29.008337	
	334.652	649.356	185.953	28.636526	
552	266.056	717.952	266.056	37.057631	35.8135
	259.39	724.618	259.39	35.796792	
	253.727	730.281	253.727	34.743749	
	264.11	719.898	264.11	36.687142	
	253.936	730.072	253.936	34.782323	
720	422.484	561.524	247.397	44.058135	44.1897
	424.976	559.032	252.097	45.095272	
	419.271	564.737	240.874	42.652421	
	423.568	560.44	250.606	44.715937	
	422.776	561.232	249.336	44.426547	
1176	93.26	890.748	39.03	4.3817107	4.29891
	95.968	888.04	37.218	4.1910274	
	90.339	893.669	40.028	4.4790633	
	88.169	895.839	38.244	4.2690707	
	94.315	889.693	37.133	4.1736869	
1728	456.841	527.167	415.3	78.77959	79.2252
	421.174	562.834	449.081	79.789245	
	448.314	535.694	418.81	78.180827	
	451.429	532.579	435.498	81.771531	
	420.976	563.032	436.94	77.604825	
(2d) Desorption data for Sr-85 EWEW system					
time(hrs)	ac,sol(Bq)	ac,sed(Bq)	act,des(Bq)	%desorbed	mean%
	(following adsorption)				
0.5	420.467	563.541	73.687	13.075712	13.4612
	389.826	594.182	80.293	13.5132	
	358.575	625.433	83.986	13.428457	
	410.072	573.936	83.051	14.470429	
	426.019	557.989	71.525	12.818353	
2	416.308	567.7	62.756	11.05443	11.2927
	340.68	643.328	75.524	11.739579	
	341.619	642.389	71.736	11.167065	
	395.804	588.204	66.671	11.334673	
	359.709	624.299	69.721	11.167886	
8	599.162	384.846	85.988	22.343483	24.365
	557.789	426.219	95.9	22.50017	

	553.141	430.867	95.963	22.27207	
	563.881	420.127	92.947	22.123548	
	761.441	222.567	72.525	32.585693	
23	617.429	366.579	99.881	27.246787	27.1507
	526.618	457.39	113.523	24.819738	
	517.097	466.911	111.523	23.88528	
	521.748	462.26	139.233	30.120062	
	633.851	350.157	103.933	29.681828	
44	195.869	788.139	104.362	13.241573	13.4074
	235.334	748.674	106.431	14.215934	
	207.766	776.242	103.568	13.342231	
	183.471	800.537	105.514	13.180403	
	191.764	792.244	103.441	13.05671	
120	201.344	782.664	100.039	12.781858	12.7361
	191.843	792.165	99.694	12.585004	
	193.197	790.811	98.074	12.401699	
	187.829	796.179	104.494	13.124436	
	188.717	795.291	101.696	12.787269	
192	227.085	756.923	160.79	21.242583	20.9546
	219.719	764.289	166.989	21.848934	
	231.706	752.302	151.919	20.193885	
	224.798	759.21	147.719	19.456935	
	239.561	744.447	164.006	22.030581	
552	332.301	651.707	180.798	27.742222	28.2965
	311.262	672.746	209.561	31.150092	
	291.21	692.798	176.893	25.533128	
	289.539	694.469	193.323	27.837528	
	307.021	676.987	197.811	29.21932	
720	348.904	635.104	128.875	20.291952	20.8514
	332.993	651.015	132.613	20.370191	
	361.131	622.877	135.566	21.76449	
	347.223	636.785	125.015	19.632215	
	372.856	611.152	135.664	22.198078	
1176	665.307	318.701	120.327	37.755451	55.6108
	594.326	389.682	143.097	36.721481	
	540.243	443.765	159.178	35.869886	
	868.368	115.64	136.956	118.43307	
	747.728	236.28	116.425	49.274166	
1728	575.939	408.069	211.903	51.928228	50.9892
	624.445	359.563	185.101	51.479435	
	570.699	413.309	185.042	44.770862	
	618.338	365.67	200.379	54.797768	
	623.349	360.659	187.434	51.969866	
(3a) Desorption data for Ru-103 BPBP system					
time(hrs)	ac,sol(Bq)	ac,sed(Bq)	act,des(Bq)	%desorbed	mean%
	(following adsorption)				

0.5	511.08	599.937	20.288	3.3816884	4.79502
	499.881	611.136	27.705	4.5333608	
	698.065	412.952	43.477	10.528342	
	356.201	754.816	24.362	3.2275415	
	300.31	810.707	18.68	2.3041617	
2	136.782	974.235	11.41	1.1711753	0.95948
	132.548	978.469	8.161	0.8340581	
	147.374	963.643	15.12	1.5690458	
	46.137	1064.88	8.311	0.7804635	
	51.449	1059.568	4.69	0.4426332	
8	154.506	956.511	17.498	1.8293569	1.10909
	89.525	1021.492	9.433	0.9234531	
	37.38	1073.637	11.648	1.0849104	
	106.023	1004.994	11.708	1.1649821	
	107.096	1003.921	5.449	0.5427718	
23	66.644	1044.373	6.357	0.6086906	0.32531
	48.48	1062.537	4.357	0.4100563	
	16.442	1094.575	1.981	0.1809835	
	38.926	1072.091	3.296	0.3074366	
	34.712	1076.305	1.285	0.1193899	
44	163.362	947.655	11.3	1.1924171	0.99885
	177.459	933.558	8.689	0.9307402	
	185.24	925.777	9.463	1.0221684	
	165.484	945.533	8.241	0.8715719	
	179.102	931.915	9.108	0.9773424	
120	71.546	1039.471	15.4	1.4815228	1.78775
	77.502	1033.515	18.366	1.7770424	
	63.28	1047.737	19.012	1.8145775	
	81.476	1029.541	18.113	1.7593277	
	95.007	1016.01	21.4	2.1062785	
192	82.138	1028.879	10.44	1.0146966	1.14489
	49.382	1061.635	8.197	0.7721109	
	63.517	1047.5	13.275	1.2673031	
	71.872	1039.145	12.723	1.224372	
	66.052	1044.965	15.11	1.4459814	
552	45.094	1065.923	9.921	0.9307427	0.98773
	41.796	1069.221	13.142	1.2291191	
	35.134	1075.883	8.277	0.7693216	
	38.687	1072.33	9.647	0.8996298	
	38.069	1072.948	11.908	1.1098394	
720	31.792	1079.225	21.072	1.9525122	2.18506
	33.029	1077.988	29.754	2.760142	
	34.523	1076.494	20.572	1.9110185	
	31.447	1079.57	22.264	2.0623026	
	29.835	1081.182	24.211	2.2393085	
1176	40.275	1070.742	20.601	1.9239929	1.8842
	20.748	1090.269	17.167	1.5745655	
	47.754	1063.263	11.524	1.0838334	

	42.25	1068.767	24.309	2.2744901	
	25.528	1085.489	27.833	2.5640978	
1728	32.228	1078.789	44.655	4.1393637	3.44291
	24.431	1086.586	32.416	2.9832889	
	26.787	1084.23	40.764	3.7597189	
	24.982	1086.035	32.122	2.9577316	
	23.521	1087.496	36.697	3.3744492	
(3b) Desorption data for Ru-103 BPEW system					
time(hrs)	ac,sol(Bq)	ac,sed(Bq)	act,des(Bq)	%desorbed	mean%
	(following adsorption)				
0.5	60.198	1050.819	6.765	0.6437836	3.12525
	133.642	977.375	15.014	1.5361555	
	315.548	795.469	40.667	5.11233	
	344.247	766.77	21.06	2.7465863	
	368.487	742.53	41.488	5.5873837	
2	111.164	999.853	26.685	2.6688923	2.70041
	111.168	999.849	55.372	5.5380362	
	96.171	1014.846	21.84	2.1520507	
	108.67	1002.347	12.677	1.2647317	
	93.247	1017.77	19.117	1.8783222	
8	67.918	1043.099	18.96	1.8176606	1.64284
	88.627	1022.39	16.168	1.5813926	
	91.888	1019.129	13.963	1.3700915	
	115.386	995.631	19.459	1.9544389	
	84.52	1026.497	15.301	1.4906035	
23	56.301	1054.716	4.432	0.4202079	0.82278
	57.181	1053.836	9.977	0.9467317	
	48.769	1062.248	11.165	1.0510728	
	50.897	1060.12	10.529	0.9931895	
	46.851	1064.166	7.478	0.7027099	
44	161.281	949.736	9.987	1.0515554	0.94573
	139.423	971.594	9.282	0.9553373	
	163.758	947.259	7.971	0.8414805	
	151.81	959.207	10.586	1.10362	
	172.787	938.23	7.287	0.7766752	
120	80.984	1030.033	24.516	2.3801179	1.72506
	90.113	1020.904	15.585	1.5265882	
	78.427	1032.59	19.727	1.9104388	
	75.648	1035.369	16.562	1.5996229	
	68.928	1042.089	12.594	1.208534	
192	36.182	1074.835	16.017	1.4901822	1.21101
	53.233	1057.784	11.622	1.098712	
	47.186	1063.831	12.136	1.1407827	
	43.816	1067.201	12.466	1.1681024	
	52.043	1058.974	12.255	1.1572522	
552	61.936	1049.081	12.283	1.1708343	1.20414
	54.594	1056.423	12.414	1.1750975	

	82.64	1028.377	11.434	1.1118491	
	55.056	1055.961	11.27	1.0672743	
	73.192	1037.825	15.522	1.4956279	
720	46.599	1064.418	28.358	2.6641789	3.81983
	45.544	1065.473	38.413	3.6052533	
	42.123	1068.894	54.522	5.1007864	
	45.504	1065.513	39.533	3.7102316	
	44.627	1066.39	42.855	4.0186986	
1176	32.351	1078.666	15.846	1.4690368	1.72879
	31.821	1079.196	16.609	1.5390161	
	41.251	1069.766	19.349	1.8087133	
	27.393	1083.624	20.962	1.9344348	
	32.593	1078.424	20.412	1.892762	
1728	48.703	1062.314	48.98	4.6106895	5.34959
	48.407	1062.61	61.178	5.7573334	
	49.094	1061.923	65.62	6.1793558	
	50.025	1060.992	51.287	4.8338725	
	51.329	1059.688	56.87	5.366674	
(3c) Desorption data for Ru-103 EWBP system					
time(hrs)	ac,sol(Bq)	ac,sed(Bq)	act,des(Bq)	%desorbed	mean%
	(following adsorption)				
0.5	370.083	740.934	10.45	1.410382	2.09594
	485.483	625.534	13.46	2.1517615	
	391.782	719.235	15.429	2.1451959	
	420.965	690.052	19.395	2.8106577	
	437.728	673.289	13.208	1.9617133	
2	149.372	961.645	17.06	1.7740434	2.425
	249.672	861.345	17.777	2.0638652	
	208.597	902.42	20.331	2.2529421	
	190.998	920.019	26.407	2.8702668	
	265.98	845.037	26.736	3.1638851	
8	50.358	1060.659	8.593	0.8101567	0.82609
	50.298	1060.719	11	1.0370324	
	56.813	1054.204	9.449	0.8963161	
	63.969	1047.048	6.675	0.6375066	
	60.909	1050.108	7.87	0.7494467	
23	47.591	1063.426	4.402	0.4139451	0.28718
	45.62	1065.397	3.868	0.3630572	
	40.715	1070.302	3.579	0.3343916	
	37.617	1073.4	1.321	0.1230669	
	29.915	1081.102	2.178	0.2014611	
44	225.905	885.112	19.811	2.2382478	2.1954
	232.704	878.313	20.309	2.3122736	
	234.073	876.944	24.578	2.8026875	
	222.372	888.645	17.321	1.9491473	
	218.817	892.2	14.941	1.6746245	
120	101.858	1009.159	22.379	2.2175891	2.09433

	117.866	993.151	11.845	1.1926686	
	131.859	979.158	29.911	3.0547675	
	128.16	982.857	23.757	2.417137	
	120.081	990.936	15.751	1.5895073	
192	101.61	1009.407	11.162	1.1057978	1.09961
	100.019	1010.998	11.286	1.1163227	
	99.393	1011.624	14.387	1.4221687	
	81.095	1029.922	8.738	0.8484138	
	90.099	1020.918	10.264	1.0053697	
552	64.604	1046.413	11.482	1.0972723	7.44071
	55.904	1055.113	99.709	9.4500779	
	76.715	1034.302	113.293	10.953571	
	58.986	1052.031	74.214	7.0543549	
	71.806	1039.211	89.874	8.6482918	
720	48.943	1062.074	25.259	2.3782712	2.53408
	52.191	1058.826	26.634	2.5154275	
	56.407	1054.61	27.973	2.6524497	
	52.637	1058.38	23.732	2.2422948	
	56.42	1054.597	30.393	2.881954	
1176	21.531	1089.486	8.824	0.8099232	0.80371
	16.955	1094.062	9.156	0.8368813	
	22.552	1088.465	10.273	0.9438062	
	19.671	1091.346	8.497	0.7785798	
	17.313	1093.704	7.102	0.649353	
1728	40.891	1070.126	46.152	4.3127632	3.85667
	38.095	1072.922	45.776	4.2664798	
	38.139	1072.878	53.486	4.9852826	
	45.559	1065.458	29.015	2.723242	
	35.035	1075.982	32.232	2.9955891	
(3d) Desorption data for Ru-103 EWEW system					
time(hrs)	ac,sol(Bq)	ac,sed(Bq)	act,des(Bq)	%desorbed	mean%
	(following adsorption)				
0.5	415.635	695.382	16.196	2.3290796	2.37255
	332.155	778.862	14.18	1.8206049	
	369.199	741.818	16.978	2.2887015	
	403.695	707.322	13.56	1.9170901	
	444.122	666.895	23.39	3.5072988	
2	214.456	896.561	13.395	1.4940422	1.63952
	196.863	914.154	24.787	2.7114687	
	195.087	915.93	10.883	1.1881912	
	206.828	904.189	12.934	1.4304531	
	217.265	893.752	12.275	1.3734235	
8	305.146	805.871	17.579	2.1813665	5.70153
	303.661	807.356	17.271	2.139205	
	312.256	798.761	19.97	2.5001221	
	292.893	818.124	19.595	2.3951137	
	1006.211	104.806	20.219	19.291834	

23	242.529	868.488	6.09	0.7012187	1.18126
	205.651	905.366	5.956	0.6578555	
	208.493	902.524	11.41	1.2642323	
	184.246	926.771	14.383	1.5519476	
	233.518	877.499	15.19	1.7310561	
44	147.397	963.62	126.834	13.162242	4.6007
	228.566	882.451	27.796	3.1498633	
	205.307	905.71	21.501	2.3739387	
	175.216	935.801	20.406	2.1805918	
	173.482	937.535	20.034	2.1368802	
120	93.392	1017.625	6.244	0.6135856	1.49938
	95.317	1015.7	11.496	1.1318303	
	99.248	1011.769	9.239	0.9131531	
	79.16	1031.857	18.815	1.8234116	
	84.82	1026.197	30.939	3.0149182	
192	90.557	1020.46	71.654	7.0217353	2.62702
	107.27	1003.747	18.102	1.8034425	
	131.458	979.559	13.772	1.4059388	
	118.894	992.123	15.782	1.5907302	
	121.026	989.991	13.001	1.3132443	
552	47.266	1063.751	10.711	1.0069086	1.36838
	44.825	1066.192	13.514	1.2675015	
	44.697	1066.32	15.986	1.4991747	
	58.311	1052.706	15.531	1.4753407	
	82.679	1028.338	16.381	1.5929587	
720	33.749	1077.268	20.552	1.907789	2.78895
	42.669	1068.348	32.588	3.0503169	
	49.191	1061.826	35.336	3.3278522	
	43.427	1067.59	34.513	3.2327954	
	34.214	1076.803	26.123	2.4259776	
1176	59.293	1051.724	33.773	3.2112037	3.15672
	78.05	1032.967	39.961	3.868565	
	67.266	1043.751	31.79	3.0457456	
	55.264	1055.753	33.202	3.1448644	
	67.726	1043.291	26.22	2.513201	
1728	25.744	1085.273	44.356	4.0870822	5.21923
	23.995	1087.022	39.124	3.5991912	
	20.136	1090.881	40.2	3.6850949	
	24.423	1086.594	111.924	10.300443	
	28.552	1082.465	47.892	4.4243463	
(4a) Desorption data for Cs-134 BPBP system					
time(hrs)	ac,sol(Bq)	ac,sed(Bq)	act,des(Bq)	%desorbed	mean%
	(following adsorption)				
0.5	584.507	7517.587	87.445	1.1632057	1.40682
	529.529	7572.565	103.935	1.3725204	
	626.382	7475.712	122.398	1.6372755	

	408.703	7693.391	115.087	1.4959203	
	416.442	7685.652	104.922	1.3651672	
2	543.674	7558.42	130.401	1.7252415	1.55467
	484.664	7617.43	104.936	1.3775775	
	507.296	7594.798	121.028	1.5935644	
	559.274	7542.82	124.446	1.6498604	
	579.339	7522.755	107.356	1.4270836	
8	512.68	7589.414	123.426	1.6262916	1.49195
	293.709	7808.385	106.789	1.3676196	
	319.531	7782.563	110.557	1.4205731	
	392.963	7709.131	110.752	1.436634	
	320.221	7781.873	125.18	1.6086102	
23	311.406	7790.688	137.104	1.7598446	1.83694
	375.155	7726.939	138.774	1.7959764	
	352.089	7750.005	161.366	2.0821406	
	306.723	7795.371	137.049	1.7580818	
	310.152	7791.942	139.37	1.7886427	
44	196.536	7905.558	114.033	1.4424409	1.19932
	223.782	7878.312	89.118	1.1311814	
	210.947	7891.147	104.378	1.3227228	
	210.911	7891.183	82.011	1.0392738	
	227.761	7874.333	83.546	1.0609915	
120	216.423	7885.671	76.379	0.9685796	1.0162
	226.476	7875.618	79.532	1.0098509	
	188.223	7913.871	91.638	1.1579415	
	194.667	7907.427	76.923	0.9727943	
	234.39	7867.704	76.46	0.971821	
192	221.582	7880.512	77.331	0.9812941	1.03307
	184.634	7917.46	91.181	1.1516446	
	203.155	7898.939	85.297	1.0798539	
	214.355	7887.739	70.223	0.8902805	
	193.723	7908.371	84.007	1.0622542	
552	112.211	7989.883	14.461	0.1809914	0.30031
	130.158	7971.936	37.711	0.4730469	
	91.956	8010.138	14.962	0.1867883	
	147.841	7954.253	28.244	0.3550805	
	39.86	8062.234	24.641	0.3056349	
720	24.204	8077.89	29.503	0.3652315	0.30479
	20.344	8081.75	20.056	0.2481641	
	42.435	8059.659	21.622	0.2682744	
	33.87	8068.224	32.152	0.3985016	
	29.098	8072.996	19.681	0.2437881	
1176	45.157	8056.937	27.282	0.338615	0.40626
	88.096	8013.998	20.841	0.2600575	
	43.981	8058.113	51.299	0.6366131	
	40.642	8061.452	34.592	0.4291038	
	92.646	8009.448	29.387	0.3669042	
1728	29.39	8072.704	40.93	0.5070172	0.36384

	16.986	8085.108	18.402	0.2276036	
	18.674	8083.42	38.48	0.4760361	
	36.68	8065.414	20.731	0.2570358	
	15.441	8086.653	28.425	0.3515051	
(4b) Desorption data for Cs-134 BPEW system					
time(hrs)	ac,sol(Bq)	ac,sed(Bq)	act,des(Bq)	%desorbed	mean%
	(following adsorption)				
0.5	270.407	7831.687	67.868	0.8665821	1.00459
	320.82	7781.274	83.753	1.0763405	
	274.788	7827.306	87.594	1.1190824	
	331.461	7770.633	64.187	0.8260202	
	407.133	7694.961	87.332	1.1349245	
2	391.519	7710.575	102.518	1.3295766	1.39292
	350.527	7751.567	173.403	2.2370058	
	356.805	7745.289	102.516	1.3235917	
	334.654	7767.44	66.238	0.8527649	
	231.923	7870.171	96.145	1.221638	
8	196.513	7905.581	84.762	1.0721793	1.02831
	254.011	7848.083	85.418	1.0883932	
	311.123	7790.971	67.926	0.8718554	
	313.066	7789.028	85.234	1.0942829	
	229.316	7872.778	79.898	1.0148641	
23	241.17	7860.924	77.852	0.990367	1.2209
	254.901	7847.193	113.245	1.4431275	
	234.841	7867.253	100.716	1.2801927	
	217.535	7884.559	99.584	1.2630256	
	184.839	7917.255	89.291	1.1278025	
44	129.119	7972.975	50.789	0.6370144	0.64375
	129.579	7972.515	55.082	0.6908987	
	122.632	7979.462	48.808	0.6116703	
	169.166	7932.928	55.253	0.696502	
	132.649	7969.445	46.437	0.582688	
120	120.15	7981.944	52.903	0.6627834	0.62186
	132.398	7969.696	49.49	0.6209773	
	128.66	7973.434	56.324	0.7063958	
	144.754	7957.34	48.846	0.6138483	
	110.546	7991.548	40.379	0.5052713	
192	118.232	7983.862	60.954	0.7634651	0.6868
	128.401	7973.693	45.348	0.5687202	
	135.494	7966.6	60.424	0.7584666	
	131.255	7970.839	50.801	0.6373357	
	132.498	7969.596	56.265	0.7059956	
552	57.984	8044.11	10.902	0.1355277	0.1765
	15.772	8086.322	13.147	0.1625832	
	51.213	8050.881	16.706	0.2075052	
	25.603	8076.491	11.792	0.146004	
	46.336	8055.758	18.6	0.2308907	

720	20.92	8081.174	13.71	0.1696536	0.26992
	19.424	8082.67	22.869	0.2829387	
	17.839	8084.255	29.602	0.3661686	
	36.134	8065.96	20.464	0.2537082	
	38.944	8063.15	22.345	0.2771249	
1176	69.6	8032.494	18.131	0.2257207	0.33556
	66.848	8035.246	31.016	0.3859994	
	55.431	8046.663	22.325	0.2774442	
	37.633	8064.461	33.544	0.4159484	
	61.846	8040.248	29.965	0.3726875	
1728	25.28	8076.814	13.464	0.1666994	0.26844
	26.828	8075.266	19.286	0.238828	
	26.36	8075.734	28.429	0.3520299	
	29.52	8072.574	23.007	0.285002	
	31.342	8070.752	24.182	0.2996251	
(4c) Desorption data for Cs-134 EWBP system					
time(hrs)	ac,sol(Bq)	ac,sed(Bq)	act,des(Bq)	%desorbed	mean%
	(following adsorption)				
0.5	1473.014	6629.08	100.347	1.5137395	1.70074
	1803.703	6298.391	103.221	1.6388471	
	1742.966	6359.128	115.938	1.8231745	
	1495.547	6606.547	129.028	1.9530323	
	1621.415	6480.679	102.065	1.5749121	
2	1601.052	6501.042	135.732	2.0878499	2.52449
	2044.944	6057.15	155.994	2.5753696	
	1689.91	6412.184	162.496	2.5341756	
	1370.87	6731.224	166.279	2.470264	
	1838.354	6263.74	185.081	2.9548002	
8	1124.259	6977.835	168.364	2.4128401	2.32861
	971.945	7130.149	181	2.5385164	
	1006.262	7095.832	167.249	2.3570034	
	1051.704	7050.39	145.12	2.0583259	
	1089.924	7012.17	159.621	2.2763424	
23	1158.207	6943.887	208.987	3.0096544	2.79582
	868.806	7233.288	207.72	2.8717231	
	808.577	7293.517	198.105	2.7161793	
	743.94	7358.154	168.615	2.2915394	
	798.577	7303.517	225.678	3.0899908	
44	380.372	7721.722	147.13	1.905404	1.97742
	364.023	7738.071	154.408	1.9954327	
	386.347	7715.747	161.62	2.0946773	
	391.728	7710.366	156.966	2.0357788	
	360.095	7741.999	143.677	1.8558127	
120	270.862	7831.232	153.337	1.9580189	1.98422
	309.535	7792.559	152.226	1.953479	
	269.048	7833.046	200.333	2.5575364	
	304.532	7797.562	140.68	1.8041537	

	277.856	7824.238	128.935	1.6478921	
192	267.201	7834.893	127.428	1.6264166	1.60881
	294.413	7807.681	122.135	1.5642929	
	257.32	7844.774	130.091	1.6583142	
	270.721	7831.373	122.575	1.5651789	
	314.755	7787.339	126.921	1.6298379	
552	181.321	7920.773	100.782	1.2723758	1.21737
	161.629	7940.465	101.673	1.2804414	
	174.866	7927.228	95.911	1.2098933	
	180.596	7921.498	91.536	1.155539	
	184.22	7917.874	92.527	1.1685839	
720	164.321	7937.773	80.044	1.0083937	1.04041
	172.992	7929.102	81.505	1.0279222	
	184.279	7917.815	85.335	1.0777595	
	166.61	7935.484	80.71	1.0170772	
	188.618	7913.476	84.745	1.0708948	
1176	278.08	7824.014	87.132	1.1136483	1.27225
	301.45	7800.644	110.749	1.4197418	
	320.458	7781.636	110.05	1.414227	
	276.857	7825.237	95.903	1.2255603	
	298.016	7804.078	92.719	1.188084	
1728	42.635	8059.459	31.963	0.3965899	0.41829
	171.429	7930.665	37.354	0.4710072	
	63.868	8038.226	25.319	0.3149824	
	85.725	8016.369	20.781	0.2592321	
	189.653	7912.441	51.402	0.6496352	
(4d) Desorption data for Cs-134 EWEW system					
time(hrs)	ac,sol(Bq)	ac,sed(Bq)	act,des(Bq)	%desorbed	mean%
	(following adsorption)				
0.5	1388.3	6713.794	85.406	1.2720974	1.18233
	1396.565	6705.529	74.066	1.1045512	
	1099.031	7003.063	74.859	1.0689465	
	1385.281	6716.813	63.842	0.9504805	
	1676.922	6425.172	97.379	1.5155859	
2	1630.647	6471.447	88.275	1.364069	1.53793
	1179.104	6922.99	166.595	2.4064024	
	1253.571	6848.523	81.623	1.1918336	
	1423.017	6679.077	93.418	1.3986663	
	1360.192	6741.902	89.579	1.3286903	
8	1261.602	6840.492	106.428	1.555853	1.54084
	1111.587	6990.507	100.394	1.4361476	
	1092.579	7009.515	123.037	1.7552855	
	1119.038	6983.056	112.586	1.6122741	
	1650.178	6451.916	86.754	1.3446238	
23	1366.525	6735.569	125.369	1.8612978	1.81312
	1004.583	7097.511	74.516	1.0498892	
	955.462	7146.632	145.309	2.0332515	

	954.195	7147.899	131.723	1.8428212	
	1368.572	6733.522	153.411	2.2783174	
44	221.267	7880.827	77.049	0.9776766	1.19099
	375.022	7727.072	106.288	1.3755275	
	291.056	7811.038	89.71	1.1485029	
	252.909	7849.185	104.245	1.3280997	
	236.288	7865.806	88.501	1.1251358	
120	194.821	7907.273	67.357	0.851836	1.2289
	183.891	7918.203	71.108	0.898032	
	212.234	7889.86	85.481	1.0834286	
	200.723	7901.371	114.247	1.4459136	
	200.914	7901.18	147.381	1.8653037	
192	209.185	7892.909	101.188	1.2820115	1.32062
	171.302	7930.792	127.017	1.6015677	
	270.962	7831.132	94.317	1.2043853	
	223.096	7878.998	106.846	1.3560861	
	231.644	7870.45	91.222	1.1590443	
552	123.853	7978.241	75.918	0.9515631	0.95743
	134.496	7967.598	74.258	0.9319998	
	114.826	7987.268	83.06	1.039905	
	110.216	7991.878	76.464	0.9567714	
	135.347	7966.747	72.252	0.9069197	
720	169.767	7932.327	53.577	0.675426	0.68676
	137.278	7964.816	66.533	0.8353363	
	127.671	7974.423	53.888	0.6757605	
	127.03	7975.064	51.759	0.6490105	
	103.752	7998.342	47.851	0.5982615	
1176	288.336	7813.758	76.191	0.9750878	1.04401
	322.973	7779.121	85.361	1.0973091	
	342.541	7759.553	89.442	1.1526695	
	234.601	7867.493	90.299	1.1477481	
	286.064	7816.03	66.219	0.8472204	
1728	155.365	7946.729	38.575	0.4854199	0.5485
	157.648	7944.446	48.978	0.6165062	
	145.531	7956.563	32.583	0.409511	
	157.763	7944.331	51.252	0.6451393	
	160.512	7941.582	46.533	0.5859412	

LAKE WATER DESORPTION OF STERILISED SAMPLES					
(a) Desorption data for sterilised samples, Co-57					
time(hrs)	ac,sol(Bq)	ac,sed(Bq)	act,des(Bq)	%desorbed	mean%
	(following adsorption)				
1104	52.434	679.091	21.382	3.1486207	2.67574
	56.428	675.097	15.346	2.2731548	
	56.119	675.406	17.865	2.6450757	
	54.312	677.213	18.432	2.7217434	
	56.336	675.189	17.488	2.5900896	
1176	63.609	667.916	23.382	3.5007396	3.4717
	54.408	677.117	19.414	2.8671559	
	60.803	670.722	26.622	3.9691556	
	50.565	680.96	23.624	3.4692199	
	59.245	672.28	23.881	3.5522401	
1320	61.415	670.11	22.443	3.3491516	3.67014
	64.307	667.218	25.553	3.8297828	
	72.085	659.44	27.561	4.1794553	
	58.746	672.779	23.851	3.5451463	
	65.33	666.195	22.965	3.4471889	
1680	59.238	672.287	25.922	3.8557937	3.44446
	58.751	672.774	22.016	3.2724213	
	67.172	664.353	23.515	3.539534	
	40.214	691.311	17.972	2.5996983	
	46.496	685.029	27.092	3.9548691	
(b) Desorption data for sterilised samples, Cs-134					
time(hrs)	ac,sol(Bq)	ac,sed(Bq)	act,des(Bq)	%desorbed	mean%
	(following adsorption)				
1104	177.452	9439.887	128.917	1.3656625	0.92911
	172.367	9444.972	68.227	0.7223632	
	177.001	9440.338	79.815	0.8454676	
	182.935	9434.404	74.404	0.7886455	
	202.768	9414.571	86.937	0.9234303	
1176	375.236	9242.103	123.553	1.3368494	1.23782
	177.359	9439.98	88.931	0.9420677	
	174.632	9442.707	132.12	1.399175	
	223.301	9394.038	123.475	1.3143975	
	198.445	9418.894	112.707	1.1966055	
1320	202.097	9415.242	97.619	1.0368188	1.29871
	289.714	9327.625	172.02	1.8441994	
	282.997	9334.342	133.34	1.4284885	
	190.075	9427.264	93.599	0.9928543	
	206.15	9411.189	112.104	1.1911779	
1680	204.206	9413.133	135.078	1.4349951	1.09064
	168.436	9448.903	93.456	0.9890672	
	178.749	9438.59	75.756	0.8026199	
	125.443	9491.896	99.85	1.05195	
	128.071	9489.268	111.457	1.1745585	

AMMONIUM ACETATE EXTRACTIONS

(a) ammonium acetate extraction data for Co-57

system	time(hrs)	ac,sed(Bq)	ext1(Bq)	ext2(Bq)	ext3(Bq)	ext,tot(Bq)	act,sed(Bq)	%sed	mean%
BPBP	23	902.193	170.574	66.746	63.034	300.354	601.839	66.708	65.808
		924.974	176.561	88.13	53.368	318.059	606.915	65.614	
		939.036	184.265	79.013	64.447	327.725	611.311	65.1	
	192	1053.8	118.664	54.667	38.004	211.335	842.465	79.945	81.558
		1062.311	139.191	50.16	33.326	222.677	839.634	79.038	
		1064.431	89.493	36.881	25.939	152.313	912.118	85.691	
	1176	1101.19	56.341	78.128	51.662	186.131	915.059	83.097	83.369
		1091.019	90.352	67.978	41.862	200.192	890.827	81.651	
		1106.498	49.67	62.428	49.892	161.99	944.508	85.36	
BPEW	23	953.372	126.346	96.728	26.135	249.209	704.163	73.86	81.525
		1050.629	88.153	39.797	28.257	156.207	894.422	85.132	
		1065.102	87.237	43.018	23.302	153.557	911.545	85.583	
	192	1088.082	114.719	67.626	45.126	227.471	860.611	79.094	79.493
		1084.744	114.459	54.093	36.553	205.105	879.639	81.092	
		1046.209	147.337	49.158	30.594	227.089	819.12	78.294	
	1176	1104.574	45.959	72.556	50.664	169.179	935.395	84.684	84.184
		1104.766	51.565	71.522	53.475	176.562	928.204	84.018	
		1111.349	34.09	85.863	59.526	179.479	931.87	83.85	
EWBP	23	733.519	311.523	52.236	63.617	427.376	306.143	41.736	42.358
		864.907	375.171	56.363	73.315	504.849	360.058	41.63	
		872.743	349.399	59.5	82.382	491.281	381.462	43.708	
	192	999.575	117.256	41.888	36.198	195.342	804.233	80.457	80.475
		1000.971	114.652	45.13	37.356	197.138	803.833	80.305	
		985.57	108.201	48.356	34.041	190.598	794.972	80.661	
	1176	1048.724	88.347	60.515	38.735	187.597	861.127	82.112	82.68
		1050.875	91.749	52.861	39.266	183.876	866.999	82.503	
		1068.371	78.062	60.242	38.775	177.079	891.292	83.425	
EWEW	23	545.426	388.926	55.133	36.724	480.783	64.643	11.852	4.9562
		578.722	451.592	73.527	55.136	580.255	-1.533	-0.265	
		594.841	455.46	65.403	54.458	575.321	19.52	3.2815	
	192	898.655	317.03	51.659	34.688	403.377	495.278	55.113	53.169
		932.589	353.846	48.822	36.795	439.463	493.126	52.877	
		907.024	351.726	52.137	35.902	439.765	467.259	51.516	
	1176	421.137	227.192	30.845	17.302	275.339	145.798	34.62	23.91
		421.658	301.27	29.605	17.679	348.554	73.104	17.337	
		441.152	302.763	31.95	19.205	353.918	87.234	19.774	

(b) ammonium acetate extraction data for Sr-85

system	time(hrs)	ac,sed(Bq)	ext1(Bq)	ext2(Bq)	ext3(Bq)	ext,tot(Bq)	act,sed(Bq)	%sed	mean%
BPBP	23	566.699	552.077	20.316	0	572.393	-5.694	-1.005	-0.272
		594.495	562.53	28.079	0	590.609	3.886	0.6537	
		520.263	477.191	45.492	0	522.683	-2.42	-0.465	
	192	856.625	667.312	68.886	14.768	750.966	105.659	12.334	11.681
		844.027	655.283	62.216	27.201	744.7	99.327	11.768	
		842.999	654.009	63.043	33.72	750.772	92.227	10.94	
	1176	1096.62	845.598	94.932	0	940.53	156.09	14.234	10.052
		522.236	434.744	90.429	0	525.173	-2.937	-0.562	
		1094.816	819.109	95.229	0	914.338	180.478	16.485	
BPEW	23	663.387	588.861	64.185	0	653.046	10.341	1.5588	0.1127
		704.515	644.34	66.736	0	711.076	-6.561	-0.931	
		730.086	658.485	73.715	0	732.2	-2.114	-0.29	
	192	860.914	676.651	81.657	20.329	778.637	82.277	9.5569	9.3577
		879.33	692.665	86.647	23.115	802.427	76.903	8.7456	
		865.682	672.479	88.818	19.803	781.1	84.582	9.7706	
	1176	648.078	617.306	34.655	0	651.961	-3.883	-0.599	-0.277
		637.085	605.052	32.499	0	637.551	-0.466	-0.073	
		635.813	609.682	27.133	0	636.815	-1.002	-0.158	
EWBP	23	923.055	223.283	75.559	39.074	337.916	585.139	63.392	63.229

		924.874	227.362	73.328	39.683	340.373	584.501	63.198	
		922.072	224.495	75.463	40.312	340.27	581.802	63.097	
	192	832.751	621.961	60.826	26.743	709.53	123.221	14.797	14.665
		834.49	627.745	59.611	27.641	714.997	119.493	14.319	
		824.274	623.833	60.6	17.189	701.622	122.652	14.88	
	1176	929.77	415.602	94.748	43.27	553.62	376.15	40.456	40.086
		925.25	423.561	90.248	44.054	557.863	367.387	39.707	
		926.818	429.429	84.182	41.586	555.197	371.621	40.096	
EWEW	23	570.905	530.586	40.448	0	571.034	-0.129	-0.023	0.6586
		578.426	548.571	40.101	0	588.672	-10.246	-1.771	
		621.233	560.79	37.024	0	597.814	23.419	3.7698	
	192	931.27	708.394	79.583	33.585	821.562	109.708	11.78	12.667
		904.213	663.41	90.058	33.079	786.547	117.666	13.013	
		906.921	674.137	79.777	33.219	787.133	119.788	13.208	
	1176	399.02	379.72	21.366	0	401.086	-2.066	-0.518	-0.098
		452.771	436.342	16.322	0	452.664	0.107	0.0236	
		513.935	479.384	33.527	0	512.911	1.024	0.1992	
(c) ammonium acetate extraction data for Ru-103									
system	time(hrs)	ac,sed(Bq)	ext1(Bq)	ext2(Bq)	ext3(Bq)	ext,tot(Bq)	act,sed(Bq)	%sed	mean%
BPBP	23	1096.556	13.445	13.285	9.788	36.518	1060.038	96.67	96.506
		1075.387	17.024	10.616	11.889	39.529	1035.858	96.324	
		1077.59	11.838	15.547	10.066	37.451	1040.139	96.525	
	192	1060.775	58.22	26.102	24.566	108.888	951.887	89.735	89.588
		1051.868	53.757	30.619	24.727	109.103	942.765	89.628	
		1060.075	57.804	32.405	22.156	112.365	947.71	89.4	
	1176	1091.343	104.756	81.88	36.802	223.438	867.905	79.526	79.837
		1107.436	93.923	84.153	34.135	212.211	895.225	80.838	
		1093.076	109.231	79.394	39.307	227.932	865.144	79.148	
BPEW	23	1073.413	42.858	20.577	22.414	85.849	987.564	92.002	92.335
		1070.649	37.468	21.469	21.256	80.193	990.456	92.51	
		1071.644	34.668	24.893	20.887	80.448	991.196	92.493	
	192	1090.852	50.581	27.431	18.815	96.827	994.025	91.124	91.07
		1079.667	50.967	26.656	20.055	97.678	981.989	90.953	
		1071.229	48.183	27.424	19.363	94.97	976.259	91.134	
	1176	1089.115	90.52	81.758	34.161	206.439	882.676	81.045	80.777
		1104.586	93.003	83.339	35.894	212.236	892.35	80.786	
		1098.836	89.678	85.239	39.374	214.291	884.545	80.498	
EWBP	23	1067.828	19.133	12.539	16.63	48.302	1019.526	95.477	95.5
		1069.265	13.593	9.169	18.751	41.513	1027.752	96.118	
		1073.881	19.865	13.145	21.688	54.698	1019.183	94.907	
	192	1020.569	33.13	14.734	17.2	65.064	955.505	93.625	93.537
		1022.284	35.537	16.014	16.847	68.398	953.886	93.309	
		1031.182	32.656	18.788	13.746	65.19	965.992	93.678	
	1176	1098.31	48.702	64.48	30.729	143.911	954.399	86.897	86.653
		1103.218	47.64	66.99	31.224	145.854	957.364	86.779	
		1098.738	53.165	57.852	39.714	150.731	948.007	86.281	
EWEW	23	874.578	21.057	14.154	18.572	53.783	820.795	93.85	93.733
		911.322	21.882	15.375	17.619	54.876	856.446	93.978	
		913.934	30.738	12.218	17.626	60.582	853.352	93.371	
	192	1021.849	51.772	12.691	17.449	81.912	939.937	91.984	92.11
		1007.905	42.324	18.14	14.448	74.912	932.993	92.568	
		1002.992	42.298	18.516	21.648	82.462	920.53	91.778	
	1176	1075.541	120.624	78.306	34.116	233.046	842.495	78.332	78.28
		1088.955	126.758	86.284	34.878	247.92	841.035	77.233	
		1069.511	107.763	79.697	34.193	221.653	847.858	79.275	
(d) ammonium acetate extraction data for Cs-134									
system	time(hrs)	ac,sed(Bq)	ext1(Bq)	ext2(Bq)	ext3(Bq)	ext,tot(Bq)	act,sed(Bq)	%sed	mean%
BPBP	23	7911.371	3209.732	418.922	167.262	3795.916	4115.455	52.019	52.107
		7932.42	3114.117	409.671	171.412	3695.2	4237.22	53.416	
		7931.312	3266.389	458.976	170.071	3895.436	4035.876	50.885	

	192	7984.236	1096.431	266.716	88.098	1451.245	6532.991	81.824	81.714
		7957.962	1080.128	293.128	98.891	1472.147	6485.815	81.501	
		7992.378	1082.696	272.733	97.851	1453.28	6539.098	81.817	
	1176	8084.219	1251.51	399.131	64.578	1715.219	6369	78.783	78.352
		8034.839	1356.744	380.213	58.992	1795.949	6238.89	77.648	
		8096.044	1314.413	358.243	57.798	1730.454	6365.59	78.626	
BPEW	23	7938.776	2645.837	374.107	149.298	3169.242	4769.534	60.079	60.378
		7960.438	2600.365	372.719	153.149	3126.233	4834.205	60.728	
		7967.969	2671.916	341.458	147.642	3161.016	4806.953	60.328	
	192	8044.816	789.319	229.309	68.894	1087.522	6957.294	86.482	86.506
		8019.041	750.243	223.101	106.505	1079.849	6939.192	86.534	
		8027.024	792.487	223.753	67.142	1083.382	6943.642	86.503	
	1176	8050.625	972.178	299.792	57.302	1329.272	6721.353	83.489	83.154
		8066.262	1021.371	274.998	58.928	1355.297	6710.965	83.198	
		8098.005	1038.012	301.654	55.063	1394.729	6703.276	82.777	
EWBP	23	7152.874	3196.335	883.062	688.93	4768.327	2384.547	33.337	33.011
		7441.008	3204.699	972.764	796.31	4973.773	2467.235	33.157	
		7491.622	3293.995	991.134	768.79	5053.919	2437.703	32.539	
	192	7962.321	2492.548	1056.868	291.93	3841.346	4120.975	51.756	51.634
		7929.816	2504.321	1038.113	284.072	3826.506	4103.31	51.745	
		7974.865	2570.476	1015.794	289.509	3875.779	4099.086	51.4	
	1176	7911.146	2548.827	1215.042	144.209	3908.078	4003.068	50.6	48.482
		7911.393	2758.488	1189.373	143.681	4091.542	3819.851	48.283	
		7896.797	2900.615	1187.454	131.739	4219.808	3676.989	46.563	
EWEW	23	6860.938	3192.166	805.26	557.656	4555.082	2305.856	33.608	33.944
		7291.941	3348.854	896.712	592.715	4838.281	2453.66	33.649	
		6886.933	3239.125	770.414	496.174	4505.713	2381.22	34.576	
	192	8057.809	2527.991	946.636	231.199	3705.826	4351.983	54.01	54.481
		7925.449	2413.45	951.336	238.254	3603.04	4322.409	54.538	
		7985.844	2423.685	932.441	245.797	3601.923	4383.921	54.896	
	1176	7889.949	2945.191	850.072	88.83	3884.093	4005.856	50.772	50.31
		7864.482	2872.785	922.4	107.225	3902.41	3962.072	50.379	
		7882.249	2921.653	928.006	108.869	3958.528	3923.721	49.779	

SUCCESSIVE DESORPTION

(a) Successive desorption data following an adsorption time of 0.5 hours

Total desorption time(hrs)			0.5	2.5	74.5	170.5	362.5	698.5		
isotope	water	ac,sed(Bq)	des1(Bq)	des2(Bq)	des3(Bq)	des4(Bq)	des5(Bq)	des6(Bq)		
Co57	BP	952.493	15.841	7.381	0	1.396	1.569	1.943		
		940.126	14.328	12.336	5.602	3.017	0	3.613		
		930.949	16.192	14.331	4.187	0	0	0		
	EW	977.237	14.021	3.534	2.096	4.434	0	1.391		
		945.695	12.282	8.758	2.535	3.865	3.222	0		
		947.235	12.176	17.604	6.556	5.955	1.224	1.206		
Sr85	BP	530.778	146.191	114.113	87.819	80.618	61.501	87.553		
		488.818	159.899	117.664	86.109	79.447	68.702	86.326		
		579.941	171.044	125.329	94.532	92.238	61.089	92.931		
	EW	713.912	95.836	78.654	90.019	85.661	95.208	103.939		
		658.261	89.114	69.601	86.424	83.343	84.707	100.812		
		732.913	98.061	84.644	89.497	87.894	91.775	98.26		
Cs134	BP	9171.571	112.065	74.609	74.485	89.769	49.916	71.903		
		9157.132	150.46	96.691	85.607	73.465	60.142	81.356		
		9191.96	113.629	83.021	73.374	80	57.013	78.039		
	EW	9208.125	155.678	93.061	83.547	60.549	51.665	23.306		
		9116.946	139.113	128.749	80.311	65.875	46.631	18.413		
		9140.945	148.316	149.896	80.964	58.575	54.464	25.799		

(b) Successive desorption data for adsorption time of 264 hours

Total desorption time(hrs)			0.5	2.5	10.5	34.5	82.5	178.5	442.5	730.5
isotope	water	ac,sed(Bq)	des1(Bq)	des2(Bq)	des3(Bq)	des4(Bq)	des5(Bq)	des6(Bq)	des7(Bq)	des8(Bq)
Co57	BP	980.227	13.784	10.469	13.483	17.934	10.407	7.866	14.615	5.39
		994.731	11.958	18.513	13.444	5.533	3.47	4.907	64.319	3.252
		974.596	12.788	14.253	22.345	10.703	14.662	12.552	18.534	32.584
	EW	978.791	9.069	8.318	8.96	5.561	6.971	4.127	12.742	8.329
		965.793	10.073	11.653	7.513	24.253	4.588	11.879	31.154	4.866
		977.058	9.266	10.324	24.756	7.79	6.135	6.991	12.7	46.697
Sr85	BP	590.613	201.202	163.203	115.658	78.553	77.984	52.158	36.21	43.919
		586.194	211.016	154.011	114.613	89.765	66.667	49.382	51.693	30.16
		582.517	208.083	162.258	112.024	78.757	78.827	51.647	34.699	44.76
	EW	686.06	94.761	93.901	85.879	72.929	76.491	77.655	80.152	55.442
		681.808	91.899	92.894	84.217	75.025	75.684	78.135	79.378	58.528
		686.205	93.789	94.801	83.452	76.144	78.898	80.447	81.954	58.966
Cs134	BP	9272.845	84.453	46.354	66.262	34.764	14.993	35.876	71.369	25.03
		9274.453	75.4	38.243	44.763	22.201	50.123	34.336	85.223	20.729
		9205.575	85.953	57.556	32.147	29.697	34.899	65.148	75.711	85.705
	EW	9336.903	47.7	38.892	34.403	25.02	20.649	70.712	73.641	40.506
		9307.484	53.772	40.715	35.421	34.936	22.662	29.669	117.342	17.957
		9331.732	46.456	48.12	50.885	30.194	14.804	37.764	68.221	30.578

APPENDIX 4 - TESSIER EXTRACTION DATA						
(a) Tessier extraction data for Co-57						
time(hrs)	system	ac,sed(Bq)	ext1(Bq)	ext2(Bq)	ext3(Bq)	ext4(Bq)
168	BPBP	1115.086	195.044	338.816	367.35	72.569
		1118.459	200.028	360.67	411.264	79.178
		1112.816	277.161	336.278	390.524	79.686
	EWEW	1061.128	371.044	135.932	309.554	64.112
		1062.827	376.118	153.902	303.288	68.386
		1051.286	449.689	168.678	347.518	75.662
816	BPBP	1140.597	89.684	214.611	335.818	77.491
		1143.433	96.058	235.914	385.67	87.775
		1138.722	108.863	244.191	403.356	94.804
	EWEW	1121.667	277.997	160.496	392.859	111.142
		1127.51	263.367	132.75	335.925	91.7
		1129.971	284.539	152.618	376.61	103.529
1488	BPBP	1144.246	87.448	160.815	389.343	90.347
		1141.958	96.572	96.389	435.889	100.54
		1138.867	115.515	106.454	487.209	102.572
	EWEW	1140.864	215.169	102.653	277.547	118.867
		1137.17	213.372	110.505	315.32	132.004
		1126.494	216.863	117.203	317.293	148.063
(b) Tessier extraction data for Sr-85						
time(hrs)	system	ac,sed(Bq)	ext1(Bq)	ext2(Bq)	ext3(Bq)	ext4(Bq)
168	BPBP	861.067	559.954	275.645	89.54	15.81
		875.797	534.941	271.578	100.024	22.621
		848.507	642.767	264.017	91.368	10.228
	EWEW	905.343	554.55	185.163	189.366	24.213
		917.153	535.682	184.434	177.082	30.617
		897.835	621.104	210.597	208.281	21.908
816	BPBP	953.372	291.59	187.333	97.992	17.662
		957.131	276.602	184.697	143.994	54.044
		959.865	280.545	176.469	95.858	12.466
	EWEW	985.917	361.075	140.819	140.606	20.254
		985.967	350.833	132.42	131.321	60.247
		988.681	391.154	147.752	139.975	15.173
1488	BPBP	982.4	249.215	148.029	96.056	22.991
		946.809	275.13	151.017	141.921	37.241
		972.742	259.978	128.425	126.572	23.772
	EWEW	996.84	411.121	129.875	134.369	26.306
		975.676	350.204	133.309	190.7	41.733
		957.651	381.696	146.837	144.556	27.956
(c) Tessier extraction data for Cs-134						
time(hrs)	system	ac,sed(Bq)	ext1(Bq)	ext2(Bq)	ext3(Bq)	ext4(Bq)
168	BPBP	10062.83	172.877	119.789	784.712	280.706
		10064.537	147.923	103.202	788.791	289.394
		10066.797	119.088	84.055	743.399	289.044
	EWEW	10037.44	108.717	165.733	1879.65	545.573

		10048.081	277.47	226.219	1998.53	518.249
		10041.938	253.918	212.073	2134.02	545.947
816	BPBP	10088.846	66.722	85.508	800.178	275.325
		10077.622	81.281	91.519	792.551	272.704
		10078.864	93.296	94.036	835.406	301.991
	EWEW	10051.698	95.889	154.945	1967.79	566.013
		10050.062	108.389	159.364	2033.17	571.821
		10047.62	95.923	161.543	2128.41	580.21
1488	BPBP	10090.752	65.154	93.921	711.106	315.872
		10073.797	75.833	97.234	761.912	312.768
		10066.883	69.389	99.028	782.49	281.786
	EWEW	10058.216	88.731	141.235	1542.28	772.425
		10027.794	85.516	142.575	1626.88	718.791
		10030.589	80.912	151.035	1631.4	780.692